Proceedings of the Joint Nordic Spring meeting '92. Extended abstracts

Lindgård, Per-Anker

Publication date:
1992

Document Version
Publisher's PDF, also known as Version of record

RISØ

Risø-R-628(EN)

Proceedings of the Joint Nordic Spring Meeting '92

Edited by Per-Anker Lindgård

JOINT NORDIC SPRING MEETING

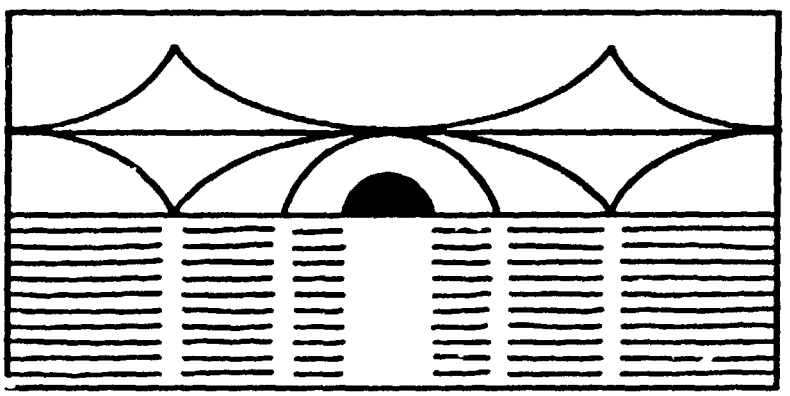

7-10 MAY 1992
Nyborg Strand, Denmark

Risø National Laboratory, Roskilde, Denmark
May 1992

Proceedings of the Joint Nordic Spring Meeting '92

Risø-R-628(EN)

Edited by Per-Anker Lindgård

Risø National Laboratory, Roskilde, Denmark
May 1992

Abstract

Proceedings in the form of extended abstracts of the Joint Nordic Spring Meeting '92 including the 3rd Nordic Conference on Surface Science, the Nordic Symposium on Computer Simulation, and 3rd Nordic Symposium on Superconductivity. In addition there are contributions from workshops on the Physics of Small Clusters, on Soft Condensed Matter Physics and from an Electronic Properties Workshop. The proceedings contain over 300 contributions on the mentioned subjects. Further, there are several contributions on general solid state subjects, magnetism, semiconductors etc.

ISBN 87-550-1810-6
ISSN 0106-2840

Grafisk Service Risø, 1992

Risø-R-628(EN)

THE SOLID STATE SECTIONS OF THE NORDIC PHYSICAL SOCIETIES
in cooperation with the
3rd NORDIC CONFERENCE ON SURFACE SCIENCE
6th NORDIC SYMPOSIUM ON COMPUTER SIMULATION
3rd NORDIC SYMPOSIUM ON SUPERCONDUCTIVITY

JOINT NORDIC SPRING MEETING
7-10 MAY 1992
Nyborg Strand, Denmark

Sponsors:
NorFa
The Danish Natural Science Research Council
NORDITA
NOVOs Fond
Thomas B.Thrige's Fond
Kraks Fond
Knud Højgaards Fond
Danish Ministry of Research and Education
The Materials Development Program (MUP) on:
High-Tc Superconducting Thin Film Components
The Materials Development Program on:
Synchroton Radiation Studies of Surfaces

ORGANIZING COMMITTEES:

Plenum Scientific Committee:
Per-Anker Lindgård, Risø, Denmark
(chairman)
Henrik Jeldtoft Jensen, NBI, Denmark
(secretary)
Jens Onsgaard, Odense, Denmark
Ole.G. Mouritsen, DTH, Denmark
Niels Hessel Andersen, Risø, Denamrk

Advisory Committee:
Bengt Lundquist, Göteborg, Sweden
Risto Nieminen, Espoo, Finland
Olav Steinsvoll, Oslo, Norway

Local Organizing Committee:
J. Onsgaard and S. Tougaard, Odense, Denmark
Lajla Frederiksen (secretary), Risø , Denmark

SYMPOSIA COMMITTEES:

Symposium A
J. Onsgaard, Odense, Denmark
(chairman)
M. Lindroos, Tampere, Finland
J.K. Grepstad, Trondheim, Norway
L. Johansson, Linköping, Sweden
I. Lindau, Lund, Sweden
N. Mårtensson, Uppsala, Sweden
I. Chorkendorff, DTH, Denmark
I. Stensgaard, Århus, Denmark

Symposium B
O.G. Mouritsen, DTH, Denamrk
(chairman)
K. Kaski, Tampere, Finland
A. Hansen, Oslo, Noway
B. Jönsson, Lund, Sweden
S. Toxværd, Copenhagen, Denmark
E. Præstgård, Roskilde, Denmark

Symposium C
N. H. Andersen, Risø, Denmark
(chairman)
J.T. Eriksson, Tampere, Finland
A.J. Kallio, Oulun Yliopisto, Finland
T. Sigfusson, Reykjavik, Island
H. Fjellvåg, Oslo, Norway
K. Fossheim, Trondheim, Norway
K.V. Rao, Stockholm, Sweden
G. Wendin, Göteborg, Sweden

Symposium D
Plenum and Advisory
Scientific Committees

Preface

The idea for the present Joint Nordic Spring Meeting stems partly from a conversation at one of the bars at the 1989 APS meeting in Anaheim, California. A group of Scandinavians had traveled a quarter of the circumference of the earth in order to take part in this gigantic confluence of scientific exchange in which about 7000 people from all over the world participate. This meeting provides a (very) general overview of the current activities on a world wide scale and is certainly inspiring.

We thought that the idea of holding a similar meeting on a Nordic level would be interesting. First of all, it seems irrational to have to travel to America in order to discover what our neighbouring colleagues are doing. Secondly, because a larger Nordic meeting, in contrast to individual national meetings, would more easily be able to finance and attract key-investigators from outside the Nordic countries. Finally, it is clear that the more we collaborate and join forces in areas of common interest, the more powerful will science in the Nordic countries become. The collective effect of a lively exchange of ideas is synergetic. The total outcome is greater than the sum of the individual inputs.

Inspired by the APS meeting, we took steps to revive the Joint Nordic Meetings which have been held at intervals of about 10 years, but this time to organize it in the form of symposia and workshops in order to preserve the intimacy of a small symposium, yet simultanously to open for broader contacts. We were very lucky that three Nordic Symposia on very timely subjects were due to be held in Denmark in 1992. It was encouraging that the Nordic Physical Societies warmly supported the idea. A large number of fondations, mentioned on the front cover, have backed the project financially, which has enabled us to invite several international key speakers and also to support the participation of many students who wish to present their work for a large audience - as well as a number of other participants. This support is gratefully acknowledged.

The increasing integration and collaboration in Europe does not render Nordic collaboration superfluous. On the contrary, we need to develop and strengthen the scientific community in our countries to make sure that we maintain the highest international level. Science in the Nordic countries should continue as an integrated and lively part of the international activity. This is only possible as long as we have an active scientific environment which can attract fellow scientist from outside the Nordic countries and which enables us to make interesting contributions abroad.

The proceedings of the JOINT NORDIC SPRING MEETING '92 are printed in the Risø-R-Report series, which is widely distributed and published via library networks. The contributions in the form of extended abstracts constitute a brief status of the physics going on in the Nordic countries in the selected areas. We have encouraged the contributors to provide references to more complete accounts, as well as to give full addresses and other contact information. A main purpose of these proceedings is to function as a key for increased contact and collaboration. Of course, physics is not regional and therefore it is a special pleasure that the topics of the meeting have attracted contributors from a broad range of countries. The crucial point is to open up contacts between related fields of physics. It is the hope the meeting will contribute to this.

Per-Anker Lindgård

CONTENTS

A: POSTER

JOINT NORDIC SPRING MEETING '92

Plel

Two-Dimensional Physics: From Theorists' Dreams to Real Surface Physics

Jacques Villain

D.R.F.M.C./S.P.S.M.S./M.D.N
C.E.N.G., 85 X, 38041 Grenoble Cédex, France, Tel.: (33) 76 88 31 44, Telex ENERGAT GRENO N° 320-323, Telefax (33) 76 88 51 09, Bitnet "Villain @ FRDRFG01"

Two-dimensional physics became popular in 1944, when Onsager derived an exact solution of the two-dimensional Ising model. An equally spectacular breakthrough took place in 1966 and 1967 as it was realized that the two-dimensional *XY*-model has a strange low-temperature phase with infinite susceptibility, but no long range order. In the beginning of the seventies the nature of the transition was elucidated, mainly by Kosterlitz and Thouless, and the critical exponents determined: $\gamma = \nu = -\alpha = \infty, \beta = 0, \eta = 1/4$.

More or less at the same time, surface physics became accessible to experimentation. It was realized that the Kosterlitz-Thouless transition was equivalent or similar to many transitions which do occur on surfaces: in particular, melting of incommensurate adsorbed layers, and roughening transitions.

The precise check of theoretical predictions is still a difficult matter. One of the reasons is the very weak (logarithmic) divergence of the height-height correlation function on a rough surface as a function of distance. Recent predictions that a growing surface may have a much more spectacular roughness are therefore extremely exciting. A few experimental results are already available, but there is no clear agreement with theoretical predictions, probably because theoretical models do not always correspond to reality.

The talk will emphasize some contributions which are not so well known, as well as the problems which are not well understood yet, at least by the speaker.

Ple2

Fluctuations in First-Order Phase Transitions

Martin Grant

Physics Department, McGill University,
Montreal PQ H3A 2T8, Canada
[Fax: 514--398--3733],
[E--mail: grant@nazgul.physics.mcgill.ca]

If a system is prepared at a high temperature in a disordered state, then rapidly cooled to a low temperature where it is ordered in equilibrium, it orders kinetically. Small domains of ordered phase of size R(t) form and grow to macroscopic size as time t goes on. In this talk, I will discuss the main ideas in the field. Namely, that patteren formation during first-order transitions is determined by interface dynamics and scaling of lengths to R(t). I will also discuss some new work: Emilio Hernandez-Garcia and I have recently introduced analogies between large fluctuations in the scaling regime of the kinetics of first-order transitions, and equilibrium fluctuations in systems with quenched disorder such as spin glasses. The sensitive dependence on initial conditions in the former problem has been treated by us in the same manner as quenched disorder in the latter case. We have calculated time-dependent overlap functions, and found them to be directly related to the order parameter for the transition. Finally, I shall discuss methods to test our results experimentally.

Ple3

Superconductivity in Alkali Intercalated C_{60}

R. M. Fleming
AT&T Bell Laboratories, Murray Hill, NJ 07974, USA

The fullerenes, including C_{60} and larger carbon spheroids, were first observed in the gas phase in 1985.[1] In 1990 the discovery of a synthetic method based on spark erosion[2] led to the production of macroscopic quantities of C_{60} and stimulated numerous other studies of the structure and properties of these fascinating materials. By far, the most actively investigated fullerene has been C_{60}. It is produced in the largest quantity, and with its "soccer ball" structure (a truncated icosahedron) it has the highest symmetry. To first order, C_{60} can be thought of as a nearly spherical, inert building block from which one can construct a variety of van der Waals bonded crystal structures. In its pristine form, C_{60} forms a face-centered cubic (FCC) structure with the molecules freely rotating at room temperature. At about 250 K, the molecules order rotationaly to form a primitive cubic structure.[3] Like intercalated graphite, C_{60} can form ionic solids by intercalating alkali atoms to form a series of compounds, A_xC_{60} with x = 2,3,4 and 6. For x = 2 or 3, the alkali atoms are incorporated into the interstices of the FCC lattice. For x = 4 and 6 the C_{60} molecules are displaced to from a body-centered tetragonal (BCT) and a body-centered cubic (BCC) lattice respectively. The free rotation of C_{60} observed in the pristine material does not occur in the intercalated compounds, although molecular reorientations between symmetry-related positions do occur.

Most of the interest in C_{60} compounds has been with the superconducting series A_3C_{60} where A = K, Rb, Na_2Cs or combinations of K, Rb and Cs.[4-7] The superconducting compositions form an FCC isostructural series with the highest transition temperatures ($\simeq$ 33 K) surpassed only by the copper oxides. The A_3C_{60} structure shown in Fig. 1 is formed by placing alkali atoms on two types of sites in the FCC host lattice, tetrahedral (two per cell, radius $\simeq$ 2.1 Å) and octahedral (one per cell, radius $\simeq$ 1.1 Å). For the mixed alkalis there is no ordering of the alkali atoms between the two sites, but there is in all materials a scaling of the size of the unit cell with the average size of the intercalant atom.

Conductivity in A_3C_{60} occurs because of the half filling of bands derived from unoccupied t_{1u} and t_{1g} molecular orbitals of C_{60}. Unlike other molecular compounds (e.g. the organic charge transfer salts), C_{60} is isotropic and the usual Peierls transition to an insulating state at low temperatures is suppressed and the compounds remain metallic at low temperatures. Of particular significance is the coupling of the density of states to the size of the unit cell. The change in the density of states alone is sufficient to account for the change in the superconducting transition temperature among all members of the isostructural series.[8] A plot of the experimentally observed lattice parameters against the superconducting transition temperature is shown in Fig 2. The scaling of the superconducting temperature with the lattice constant has also been extended to smaller cells by applying pressure to K_3C_{60} and Rb_3C_{60}.[9]

Within a conventional BCS description of superconductivity, the observation that the variation in the transition temperature can be accounted for by only a change in the unit cell implies that the alkali phonon modes are not important in mediating the electron-phonon coupling. Instead, the superconductivity is thought to arise because of coupling of purely in-

tramolecular C_{60} modes. The change in T_c is driven by a decrease in the bandwidth and an increase in the density of states as the C_{60} molecules are moved farther apart. This is supported by calculations[10,11] indicating coupling to intramolecular modes in the range 1000-2000K and by Raman[12] and inelastic neutron scattering measurements[13] that indicate that the predicted modes (predominately of H_g symmetry) are observable in C_{60} and A_6C_{60} but not in A_3C_{60}. Further support of electron-phonon mediated superconductivity and involvement of C_{60} modes is ^{13}C isotope effect experiments that show a decrease in T_c with α in the range 0.30 - 0.32.[14,15] One difficulty that remains is reconciling various measurements of the density of states in A_3C_{60}. For example, using the McMillan equation with a constant V and μ, the 40% change in the density of states between K_3C_{60} and Rb_3C_{60} derived from NMR measurements[16] predicts a prefactor of 300K, a number much smaller than the 1000-2000K expected from coupling to intramolecular modes. Measurements of the bandwidth vary among the various experimental techniques leading to difficulty in determining the severity of this discrepancy.

The maximum and minimum T_c in A_3C_{60} is limited by the structure. Larger FCC unit cells (e.g. FCC Cs_3C_{60}) do not form. T_c's lower than 10K are observed under pressure[9], but attempts to make smaller unit cells using smaller intercalants (e.g. Na_3C_{60}) result in non-cubic structures at low temperature and no superconductivity.

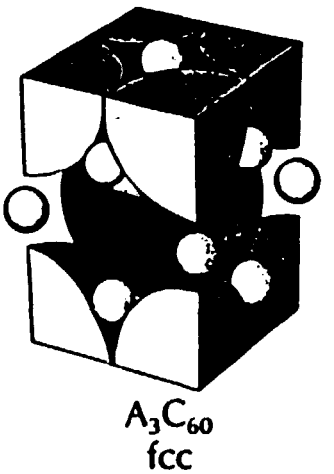

Fig 1: Structure of A_3C_{60}. The large spheres are C_{60}, the small spheres are alkali atoms.

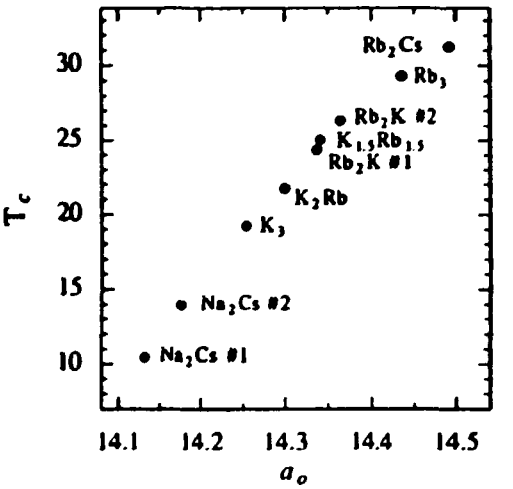

Fig 2: T_c versus unit cell size of A_3C_{60}.

[1] H. W. Kroto, et al. Nature 318, 162 (1985).
[2] W. Kratschmer, Nature 347, 354 (1990).
[3] P. A. Heiney, et al. Phys. Rev. Lett. 66, 2911 (1991).
[4] A. F. Hebard, et al. Nature 350, 600 (1991).
[5] K. Holczer, et al. Science 252, 1154 (1991).
[6] P. W. Stephens, et al. Nature 351, 632 (1991).
[7] M. J. Rosseinsky, et al. Phys. Rev. Lett. 66, 2830 (1991).
[8] R. M. Fleming, et al. Nature 352, 787 (1991).
[9] O. Zhou, et al. preprint.
[10] M. A. Schluter, et al. Phys. Rev. Lett., in press.
[11] C. M. Varma, et al. Science 254, 989 (1991).
[12] S. J. Duclos, et al. Science 254, 1625 (1991).
[13] K. Prassides, et al. Nature 354, 462 (1991).
[14] A. Ramirez, et al. Phys. Rev. Lett. in press.
[15] C.-C. Chen and C. M. Lieber, preprint.
[16] R. Tycko, et al. Phys. Rev. Lett., in press.

Ple4

Structures of Two-Dimensional Soft Condensed Matter

J.Als-Nielsen

Risø National Laboratory, DK 4000 Roskilde, Phone: 4542371212, Fax: 45 42370115

Amphiphilic molecules may form two-dimensional model systems of soft condensed matter ona water surface, so called Langmuir films. The polar head part of the molecule, e.g. carboxyl acid COOH or alcohol, is attracted to water (hydrophilic) whereas the hydro-carbon tail part is repelled by water (hydrophobic). In a Langmuir trough one can apply and measure a two-dimensional pressure, Π, and the temperature, T, is of course also variable. The molecular structure of the film depends on Π and T but also on the pH of the water subphase (a polar head as COOH may for example become charged COO^- at high pH) and on the concentration of counter-ions in the subphase. In addition there are rich possibilites for altering the chemistry in different parts of the amphiphilic molecule, so the parameter space in which different structures occur is truly multi-dimensional. The Langmuir film may be drawn and stacked onto a solid substrate - a Langmuir-Blodgett film. These have many interesting technological applications [1].

Structure on a *mesoscopic* scale may be obtained by fluorescent microscopy: a dye-molecule introduced into the film may be soluble in the 2-d liquid phase but not in the 2-d solid phase, so by exciting the dye by laser light and subsequently observing the fluorescent light in a microscope, one may distinguish the two phases and study the morphology [2].

Structure on a *microscopic* scale can be obtained by X-ray reflectivity and diffraction methods. The scattering volume of a monomolecular film is of course minute, and furthermore it is a polycrystalline 2-d powder within the irradiated area. Nevertheless, by taking advantage of the enormous gain in intensity from synchrotron sources compared to conventional X-ray sources, it is possible to derive the structures down to atomic length scale precision. We present the X-ray methodology [3] and give several examples of structures[4] determined in this way.

---

[1]See e.g. Advanced Materials, Vol. 3 (January) 1991

[2]An interesting example of this technique for studying 2 dimensional crystal growth is published in Phys.Rev. Lett., vol 67, p. 2489 (1991).

[3]For recent reviews see e.g. J.Als-Nielsen, "X-Ray Refelctivity Studies of Liquid Surfaces" Handbook of Synchrotron Radiation, Vol. 3, ed. G.Brown and D.E.Moncton, Elsevier Science Publishers B.V. 1991 and *ibid.* J.Als-Nielsen and H.Møhwald, vol. 4

[4]See Ang.Chemie, vol 104,p.134 (March 1992) and references therein

Ple6

Membranes, Random Surfaces, and Self-Assembly

S. Leibler

CEA Service de Physique Théorique de Saclay, 91191 Gif-Sur-Yvette CEDEX, France
Telephone: (1)69088117, Telex: ENERG 604641 F, E-mail LEIBLER@FRASACII

A : 3RD NORDIC CONFERENCE ON SURFACE SCIENCE

AlFr1

Energetics and Dynamics of Surfaces and Clusters.

Karsten W. Jacobsen

Laboratory of Applied Physics, Technical University of Denmark,
DK-2800 Lyngby, Denmark.

At the basis of the understanding of many surface phenomena is a fundamental knowledge about the nature of the interatomic interactions at surfaces and the first part of the talk will give a short overview of some of the theoretical methods available today for the treatment of energetics at surfaces. The advantages and disadvantages of the different methods will be discussed in terms of reliability, computational efficiency (which is very important for dynamical studies), and to what extent the results can be analyzed in a physically transparent way. The methods range from complete *ab initio* approaches (Car-Parinello, LMTO) well suited for accurate structural studies to more approximate schemes (Effective Medium) which allow for dynamical or Monte Carlo simulations.

The methods will be illustrated by a number of examples covering aspects of the following topics: Surface and defect energies, surface structures and reconstructions due to interactions with adsorbates (alkali-metal atoms or ligth gas atoms), molecule-surface interactions, and surface diffusion.

The last part of the talk will be concerned with finite temperature properties of small and medium size clusters. In particular a dynamical simulation based on effective medium interatomic potentials of a 17000 atom copper cluster in free space will be discussed. The simulation has been performed on the CM-200 parallel computer at UNI-C. The cluster exhibits interesting behavior near the melting point where a coexistence between a solid nucleus at the center of the cluster and a surrounding shell of copper in the liquid phase can be observed. The nature of the melting process will be discussed and illustrated by a movie.

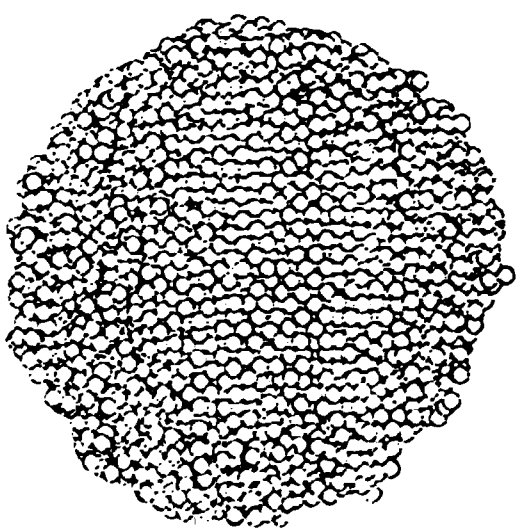

A snapshot of a partly melted copper cluster with a diameter of 70 Å. The figure shows a cut trough the center of the cluster. The coexistence between a solid nucleus at the center and a melted shell around it is clearly seen. The simulation has been performed by a group at DTH (O. H. Nielsen, P. Stoltze, J. Sethna, J. K. Nørskov, and K. W. Jacobsen)

AIFr2

Molecular Beam Studies of Elementary Gas-Surface Reactions: Dissociation and Formation of Hydrogen at a Cu(111) Surface

Charles T. Rettner, Daniel J. Auerbach and Hope A. Michelsen

IBM Almaden Research Center, K33/801, 650 Harry Road, San Jose, CA 95120-6099, USA. (Fax.(408)927-2433). (e-mail RETTNER at ALMADEN, BITNET).

The interaction of hydrogen with copper has been the focus of a large number of dynamical studies.[1,2] Thus Lennard-Jones used the H_2/Cu interaction as a model in discussing the origin of the potential energy barrier to dissociative chemisorption, and this system was the subject of the first molecular beam study of the dynamics of surface reactions. It has since been the focus of a large number of experimental and theoretical studies of the dynamics of dissociative chemisorption and the related process of recombinative desorption. In fact it has become an important testing ground for ideas and techniques and for the comparison of theory with experiment.

It has long been accepted that the dissociation of hydrogen on copper surfaces is inhibited by a sizable activation barrier. Molecular beam studies by Hayden and Lamont and by Rendulic and coworkers have recently shown that this can be overcome by both kinetic energy and vibrational energy.[1] This is consistent via detailed balance with earlier studies of the reverse process of recombinative desorption. These showed that desorbing molecules leave the surface with both high kinetic energy and high vibrational energy. These studies will be reviewed and our own more recent measurements on a Cu(111) surface will be presented. Four different studies will be described:

1. Desorption dynamics

We have measured the angular distributions of H_2, HD, and D_2 desorbing from Cu(111) for surface temperatures in the range 370 K to 800 K. These are strongly peaked and symmetric about the surface normal in every case. Results for all three isotopes are indistinguishable, being close to a $\cos^{12}\theta_f$ distribution at 600 K, slightly narrower at 400 K, and slightly broader at 800 K. Results will be discussed in terms of other previous desorption measurements and related to adsorption data via detailed balance. We will also report on progress towards measuring the velocity distributions of molecules desorbing in specific quantum states.

2. Dissociation dynamics

We have determined the adsorption probability, S_0, of H_2 and D_2 on Cu(111) for wide range of kinetic energies, E_i, and incidence angles, θ_i, for molecular beams with different vibrational temperatures. The data span over 5 orders of magnitude. Using a quantitative model analysis we have been able to determine S_0 as a function of translational energy for each specific vibrational state of these two molecules. Results for D_2 are summarized in Figure 1. This is the first time such detailed dynamical information has been obtained for any system. Most recently, we have been able to estimate the effect of surface temperature on these probabilities, by comparing these observations with those based on aspects of the reverse process of recombinative desorption.

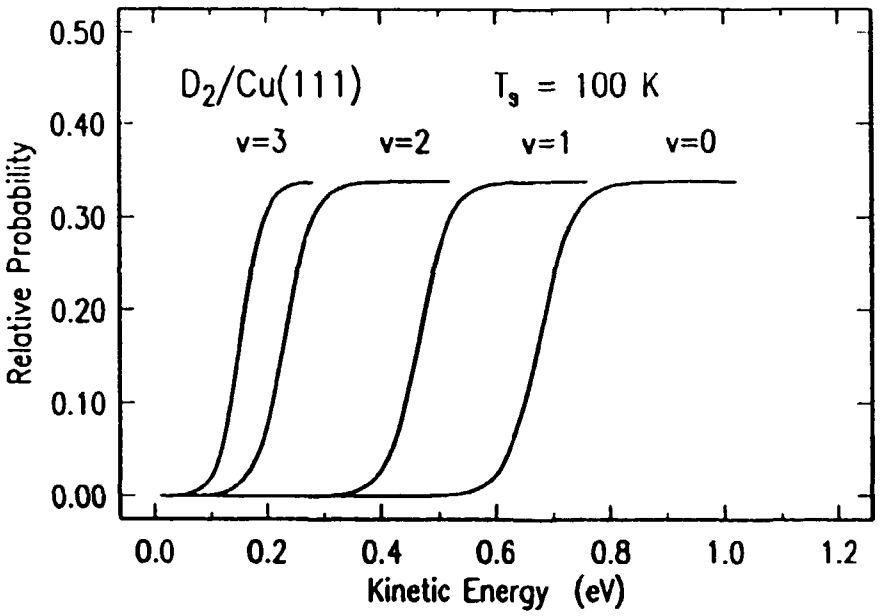

Figure 1 Adsorption function deduced for the D_2/Cu(111) system from systematic measurements of the adsorption probability as a function of kinetic energy and the molecular beam source temperature. The adsorption functions for D_2 molecules in specific vibrational states are indicated.

3. Observation of direct vibrational excitation

The above studies have been complemented by laser experiments in which we have made the first direct measurements of the energy dependence of the dissociation probability of a molecule in a specific quantum state. We have been able to determine the dissociation function for both H_2 and D_2 on Cu(111) for molecules in the $v = 0$ and $v = 1$ state. A surprising aspect of this study was the observation of direct vibrational excitation in this system. The dynamical origin of this excitation appears to be different from any previous study.

4. Direct reaction of an atomic hydrogen beam with adsorbed hydrogen atom

Reactions between two accommodated adsorbates are well known and are said to proceed by a Langmuir-Hinschelwood (L-H) mechanism. In the case of highly reactive systems, there is speculation that reaction may occur directly between a gas-phase species and an adsorbate, in a so-called Eley-Rideal (E-R) mechanism. However, instances in which this later mechanism is invoked are far rarer and the evidence for the assigned mechanism is generally weak. We have observed just such a process for the case of H and D atoms incident on D and H covered Cu(111) surfaces at 100 K. Angular distributions of the nascent HD product are different for incident H and D atoms and display a slight sensitivity to the incidence energy. Product molecules are found to leave the surface with very high velocities, with a mean kinetic energy of close to 1 eV.

---

1. For a recent review, see: B. E. Hayden, "The Dynamics of Hydrogen Adsorption and Desorption on Copper Surfaces," in "Dynamics of Gas-Surface Interactions," C.T. Rettner and M.N.R. Ashfold Eds., (Royal Society of Chemistry, London, 1991).
2. H. A. Michelsen and D. J. Auerbach, *J. Chem. Phys.*, **94**, 7502 (1991), and references therein.

ACFr3

Diffusion Anomaly near Structural Phase Transitions

T. Ala - Nissilä*, W. K. Han‡, and S. C. Ying‡

*Research Institute for Theoretical Physics, University of Helsinki,
Siltavuorenpenger 20 C, SF - 00170 Helsinki, Finland.

‡Department of Physics, Brown University,
Box 1843, Providence R.I. 02912, U.S.A.

Sudden changes in diffusion coefficients of adatoms on surfaces have regularly been interpreted as indicating possible phase transitions which may occur either on the adsorbate overlayer, or on the substrate itself[1]. In this work, we consider the latter possibility using a recently developed microscopic theory of diffusion[2,3]. We first argue that the properties of single adatom diffusion are determined by the behavior of the dynamical structure function associated with the substrate. Using a combination of analytic methods and computer simulations, we calculate this quantity for a model of the $(1 \times 1) \rightarrow c(2 \times 2)$ reconstruction of the $W(100)$ surface. The dynamical behavior of the surface is dominated by a central peak, which diverges at the transition temperature[4]. We show how such a diverging central peak generally leads to an *anomalous vanishing* of the diffusion coefficient D at the vicinity of the transition. For the model of the $W(100)$ surface, we calculate in detail the anomalous behavior of D as a function of temperature, and study its finite size dependence.

1. R. Gomer, Rep. Prog. Phys. **53**, 917 (1990).

2. S. C. Ying, Phys. Rev. B. **41**, 7068 (1990).

3. T. Ala - Nissilä and S. C. Ying, Phys. Rev. Lett. **65**, 879 (1990).

4. W. K. Han and S. C. Ying, Phys. Rev. B **41**, 9163 (1990).

ACFr4

Inelastic Scattering and Chemisorption of CO on a Cu(111) Surface

Lichang Wang, Qingfeng Ge and Gert D. Billing

Chem. Lab. III, H.C. Ørsted Institute
University of Copenhagen, DK-2100 Copenhagen, Denmark

The molecule-surface interaction is of interest for both theoretical and experimental studies of catalysis and surface science. Here, a semiclassical model[1, 2, 3, 4] is used to calculate energy transfer in collisions between CO and a Cu(111) surface. An analytical potential surface was constructed to characterize CO-Cu(111) interaction by fitting the experimental strenching frequency and binding energy at equilibrium configuration. According to the previous study[2], fairly large 'crystal' sizes were used in the calculation. The properties calculated are scattering angles, energy accommodation, sticking probabilities, dissociation probabilities, rotational/vibrational excitation of the diatom, the effect of the surface temperature and coupling to phonon modes.

[1] G.D. Billing, Comp. Phys. Rep. 12 383,1990
[2] G.D. Billing, Chem. Phys. 86 349, 1984
[3] G.D. Billing, Chem. Phys. 74 143, 1983
[4] G.D. Billing, Chem. Phys. 70 223, 1982

AIFr5

Thermodynamic and Kinetic Effects in the Growth of Thin Metal Films

R.J. Behm

Institut für Kristallographi und Mineralogie, Universität

Thermodynamic and Kinetic Effects in the Growth of Thin Metal Films

R.J. Behm, Dept. Surface Chemistry and Catalysis, Univ. Ulm, Fed. Rep. Germany

Epitaxial growth of thin metal films vapor-deposited on metallic substrates has been studied by a variety of techniques over many years [1]. Detailed theories predicting the growth mode of these films have been developed based on the thermodynamic properties of the respective materials [2,3]. They give a correct description of the growth process if this is determined by the thermodynamic properties, i.e if the film is able to reach its thermodynamical stable configuration. In all other cases the growth process will be controlled by kinetic effects, which can lead to vastly different film morphologies as compared to that expected from the (thermodynamic) growth mode. These growth processes have been investigated by scanning tunneling microscopy (STM). Due to the local nature of the measurement this method can provide direct information on the film morphology, which is particularly informative for the understanding of the respective growth processes. This will be demonstrated in different examples.

In the range of kinetic limitations nucleation and growth phenomena dominate the growth process. On sufficiently large terraces condensation of metal adatoms at step edges can be neglected and two-dimensional (2D) islands are formed by homogeneous nucleation. The nucleation process as well as the subsequent 2D growth of these islands can be characterized, which allows direct comparisons with theoretical predictions [4,5]. Systematic investigations of the functional dependence of the island density on flux rate and deposition temperature allow conclusions on the critical cluster size and on the mobility of metal adatoms to be drawn [4,6]. The shape of the growing 2D island is of similar interest. In the initial stages of thin Au films on Ru(0001) at 300 K the islands exhibit a strongly dendritic shape [7]. This is consistent with the diffusion limited aggregation model of Witten and Sander and implies a reduced mobility of Au atoms along the edges of the islands [5,7]. The 2D growth of these islands with increasing coverage and the collapse of their dendritic shape upon annealing could also be observed by STM. The latter behavior demonstrates that the dendritic island forms represent metastable configurations, which at sufficiently high temperatures convert into the thermodynamically stable compact forms.

The transition from 2D to 3D growth is initiated by the nucleation of second layer islands on top of first layer areas. STM measurements on Au/Ru(0001) show characteristic variations in the spatial distribution of higher layer islands on these areas, which reveal significant effects of the step edges on the adatom mobility [8]. They can either act as repulsive, partly reflecting barriers for diffusing higher layer adatoms or they can allow these adatoms to cross the step edge and fall down on the lower level terrace, in which case they get trapped at the lower terrace side of the step. These general effects are in good agreement with earlier results from field ion microscopy and He scattering studies [9,10]. The onset of second and higher layer nucleation was also found to depend strongly on the deposition temperature. Higher layer islands can be removed by annealing. Upon deposition at room temperature several Au layers coexist in films above 1-2 monolayers nominal coverage, while upon deposition at higher temperatures or after annealing the film was found to grow in a layer-by-layer fashion up to two layers thickness [8]. At higher coverages formation of 3D clusters was observed under these conditions. These observations demonstrate that the coexistence of several Au layers at nominal coverages above 1-2 monolayers results from kinetic effects and that under thermodynamically controlled conditions Au films grow in a Stranski-Krastanov mode with a critical thickness of two layers on this substrate.

These and other examples demonstrate how STM studies provide detailed information on the microscopic processes that occur during deposition of thin metal films on metallic substrates.

References

1] E. Bauer, Applic. Surface Sci. 11/12, 479 (1982).

2] E. Bauer, Z. Krist. 110, 372 (1958).

3] J.A. Venables, G.D.T. Spiller, and M. Hanbücken, Rep. Prog. Phys. 47, 399 (1984).

4] T.A. Witten and L.M. Sander, Phys. Rev. B27, 5686 (1983).

5] S. Günther, E. Kopatzki, and R.J. Behm, to be publ.

6] R.Q. Hwang, J. Schröder, C. Günther, and R.J. Behm, Phys. Rev. Lett. 67, 3279 (1991).

7] S. Stoyanov and I. Markov, Surface Sci. 116, 313 (1982).

8] R.Q. Hwang, C. Günther, J. Schröder, S. Günther, E. Kopatzki, and R.J. Behm, J. Vac. Sci. Technol. A, in press.

9] G. Ehrlich, Surface Sci. 246, 1 (1991).

10] R.V. Kunkel, B. Poelsema, L.K. Verheij, and G. Comsa, Phys. Rev. Lett. 65, 733 (1990).

ACFr6

The Dynamics of Oxygen-Induced Restructuring of Ni (110) Studied by Scanning Tunneling Microscopy

F. Besenbacher, L. Eierdal, I. Stensgaard, and E. Lægsgaard
Institute of Physics, Aarhus University, DK-8000 Aarhus C, Denmark
[Fax:+45 86 12 07 40] [E-mail:fbe@dfi.aau.dk]

By means of scanning tunneling microscopy (STM), we have been able to visualize in real time and space the dynamics of the oxygen-(O)-induced reconstruction of the Ni(110) surface in the form of *STM movies*. Atomically resolved STM images of the clean and the O-covered Ni(110) surface were achieved. It is found that O adsorption at room temperature initiates the nucleation of two different reaction channels/structures. For low oxygen exposures, O induces an intermediate structure consisting of strings directed along the [1$\bar{1}$0] direction, growing either out from [001] step edges or in troughs created on large flat terraces. It can be concluded that this phase is indeed a reconstructed one consisting of Ni [1$\bar{1}$0] strings, with O atoms probably located along at the threefold coordinated rudimentary (111) face of the strings rather than a disordered phase with O adsorbed on a unreconstructed surface, as previously suggested in the literature.

At higher oxygen exposures, this structure is dissolved, and the O induces three different reconstruction structures, a (3x1), a (2x1), and a (3x1) structure corresponding to O coverages, of 1/3, 1/2 and 2/3 ML, respectively. These reconstructions are all stabilized by -Ni-O- rows running along the [001] direction. From the nucleation and growth of these reconstruction phases, we can conclude that they are of the added-row rather than the missing-row type. From a comparison of the present results with results for oxygen-induced reconstructions on Cu and Ag surfaces a simple physical picture evolves for the oxygen-induced reconstructions of the transition metals.

At higher oxygen exposures, a (9x4) suboxide and finally a NiO(001) oxide are formed. The nucleation and growth of these will be discussed.

ACFr7

Scanning tunneling microscopy studies of hydrogen exposure of In covered Si(111) surfaces

Fredrik Owman and Per Mårtensson

Department of Physics, Linköping University
S-581 83 Linköping, Fax: +46 13 137568

An earlier photoemission study[1] has shown that it is possible to create an ideal, hydrogen-terminated Si(111)1x1 surface from the clean Si(111)7x7 surface in a two stage process. First the 7x7 reconstruction is removed by evaporation of In and subsequent annealing, resulting in a $\sqrt{3}x\sqrt{3}$ overlayer of In adatoms on an unreconstructed Si(111) surface. In the second stage the In overlayer is exposed to atomic hydrogen, whereby the bonds between Si and In are broken such that each Si-In bond is replaced with a Si-H bond, resulting in a H-terminated Si(111)1x1 surface. The In atoms diffuse on the surface and gather in metallic islands. If the sample is heated the H atoms desorb and the In islands flow out, which restores the ordered In overlayer.

We have performed STM measurements in order to investigate the size and distribution of the In islands as well as the occurrence of defects on the hydrogen-terminated surface. Below, two top views are shown (the topography is encoded such that the light areas are higher than the dark areas). In the left image the distribution of metallic In islands can clearly be seen. Between the In islands the surface is relatively flat, with many small defect structures. The right image, recorded at much higher magnification, shows the details of the hydrogen-terminated 1x1 surface. We interpret the defects as originating from the extra Si atoms already present in the ordered In overlayer due to the fact that the initial Si(111)7x7 surface contains 8 % of a monolayer more Si atoms than the ideal 1x1 surface. Our studies have also shown that it is possible to completely eliminate the indium from the surface by performing the hydrogen exposure at a slightly higher temperature. The small defect structures are present to the same extent also in this case.

Additionally, we have irradiated the hydrogen-terminated Si(111)1x1 surface with a large dose of electrons, field emitted from the tunneling tip[2]. This causes the H atoms to desorb and the In islands to flow out restoring the ordered In overlayer ($\sqrt{3}x\sqrt{3}$). If the amount of indium present is not enough to cover the entire surface, the parts not covered reconstruct to 2x1, the same structure as found on the cleaved Si surface[2].

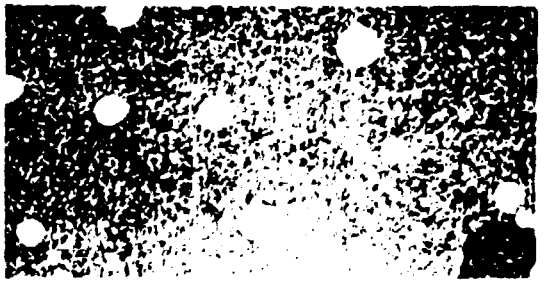

400 Å black to white: 33 Å

25 Å black to white: 3.3 Å

[1] E. Landemark, C.J. Karlsson, and R.I.G. Uhrberg, Phys. Rev. B **44**, 1950 (1991)
[2] R.S. Becker, G.S. Higashi, and A.J. Becker, Phys. Rev. Lett. **65**, 1917 (1990)

ACFr8

STM Observation of Organic Molecules Adsorbed on Graphite

Lars L. Madsen
Danish Institute of Fundamental Metrology
Lundtoftevej 100, Build. 307 DK-2800 Lyngby
Fax: +45 45 93 11 37, E-mail: DFMLLM @ VM.UNI-C.DK
and
Centre for Interdisciplinary Studies of Molecular Interactions
Blegdamsvej 21, DK-2100 Copenhagen Ø

Using STM to investigate molecular materials requires either that the material itself is conductive or that it forms a very thin layer on a conductor. Images of molecular material of the latter kind are considered here.

Two different molecules have been studied, didodecylbenzene $H_{25}C_{12}(C_6H_4)C_{12}H_{25}$ (DDB) [1] and dioctadecyldisulphite $H_{37}C_{18}S_2C_{18}H_{37}$ dissolved in octylbenzene. A drop of the almost saturated solution was applied to graphite and the tunnelling tip immersed into the droplet.

It is seen that both molecules form well ordered self-assembled monolayers when adsorbed from the solution in octylbenzene onto graphite. This monolayer was observed in-situ by the STM and the dynamic of the domain boundaries was observed.

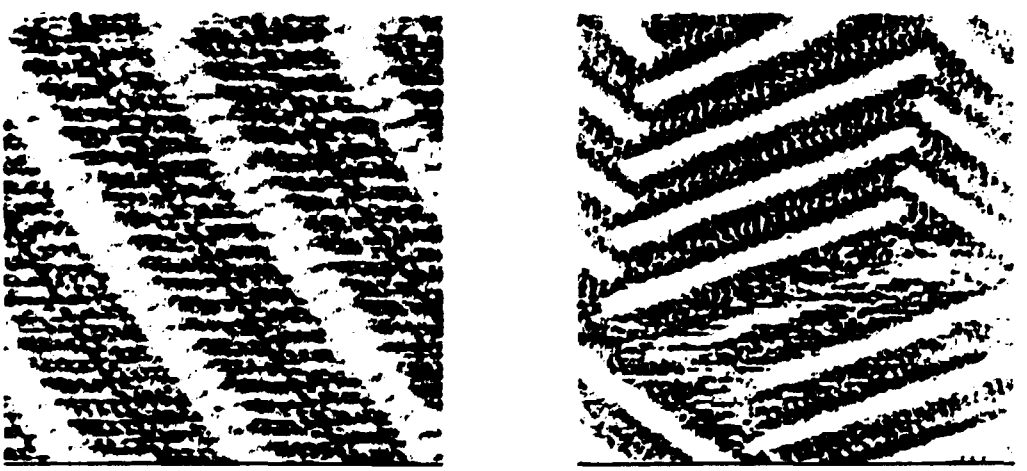

The left hand picture shows a 10nm by 10nm STM image of DDB. The molecules align themselves side by side to form long lamellea of which 4 are seen in the image. The brightest regions, corresponding to maximum tunnelling probability at a given distance, correspond to the position of the benzene rings. The alkyl side chains are seen as. bright almost horizontal extensions to both side of these regions.

The right hand picture is a 20nm by 20nm scan of DDB showing molecular sharp domain boundaries. In such areas the dynamics of reorganisation of the molecules can be shown in real time, recorded on a video tape.

[1] First seen by STM by J. Rape *et al. Phys. Rev. Lett.* 1991,66:2096-99

ACFr9

GROWTH STRUCTURE OF Au AND Ag ON Ni(111) AND Si(111) DETERMINED BY INELASTIC PEAK SHAPE ANALYSIS.

H.S. Hansen[1], C. Jansson[2], and S. Tougaard[2]

1) Radiofysisk Laboratorium, Odense University Hospital, DK- 5000 Odense C.
2) Fysisk Institut, Odense Universitet, DK- 5230 Odense M, Denmark.

The structure of 0-15 nm of Au and Ag evaporated on Ni(111) and Si(111) was studied. The amounts of deposits were monitored by a Quartz Crystal Microbalance (QCM). The geometrical structure of the overlayer was determined by analysis of the detailed peak shape of X-ray excited core level peaks from the substrate and overlayer atoms. Au and Ag grown on Ni(111) as well as Ag grown on Si(111) was found to form a layer-by-layer plus island (Stranski-Krastanov) structure. The total amount of evaporated material determined by the peak shape analysis method was found to be proportional to the observed QCM frequency shift to within ~ 10 % and slightly larger for the highest amounts of evaporated adsorbate.

The applied method for structure determination by peak shape analysis has been developed at Odense University over the past few years. The basic idea is that the electrons during transport out of the solid will lose energy and thereby cause a distortion of the original energy distribution. The amount of distortion depends on the path length travelled by the electrons. Thus using a quantitative model for electron transport, the in depth concentration profile can be determined through analysis of the observed energy distribution of emitted electrons.

AlFr10

New Scanning Probe Microscopies of Surface and Subsurface Structure

W. J. Kaiser, S. J. Manion, A. M. Milliken,
L. D. Bell, and M. H. Hecht

Center for Space Microelectronics Technology
Jet Propulsion Laboratory, California Institute of Technology
Pasadena, California 91109

New scanning probe microscopies have been developed for imaging and spectroscopic characterization of surface and subsurface structure. These techniques are based on Ballistic-Electron-Emission Microscopy (BEEM). BEEM is a unique characterization method with capabilities for imaging subsurface interface electronic structure at nanometer-scale spatial resolution. BEEM employs scanning tunneling microscopy in a novel way, to inject low-energy, ballistic carriers into a semiconductor device structure. This enables the first local, direct measurement of Schottky barrier height, conduction and valence band offset, and interface bandstructure for subsurface interfaces. BEEM methods have been developed for injection and control of both electrons and holes and the first direct spectroscopy of carrier scattering. In this presentation new BEEM methods for direct spectroscopic investigation of subsurface semiconductor interfaces will be presented.

A new microscopy, also based on ballistic electron transport, has been developed for direct imaging and spectroscopic investigation of material properties. This method, tunneling transmission microscopy (TTM), employs scanning tunneling microscopy instrumentation to position a tunneling tip over a sample surface. Electron tunneling from the tip to the sample deposits electrons into the conduction band of the sample. For TTM the sample is a free-standing conducting film of thickness ranging up to 100 nm, supported only by a grid structure. As in BEEM, electrons injected by tunneling may propagate ballistically through the entire thickness of the sample until reaching the vacuum interface. For tip-sample bias greater than the sample surface work function, a fraction of the electrons reaching the vacuum interface will be emitted into vacuum. TTM includes methods to then resolve the angle and energy dependent emitted electron distribution.

A wide range of unique experimental investigations may be implemented by TTM. First, by simply scanning the tunnel tip over the sample surface, a transmission microscopy of the sample subsurface properties may be obtained. This is complementary to conventional transmission electron microscopy, since in TTM the electron energy is low and the energy (and the energy-dependent electron mean-free-path) may be adjusted over a large range. A second set of TTM investigations involves spectroscopy of transmitted carriers. For example, the electron emission yield for TTM may be measured as a function of injected electron energy to provide the first direct, local measure of work function. In addition, the electron emission distribution may be analyzed to provide new information on carrier scattering.

This presentation will describe the experimental methods of TTM. Also, the first TTM results including nanometer resolution images and electron spectroscopy, will be discussed. Finally, the variety of exciting TTM applications will be addressed.

* Research supported by ONR and SDIO/IST.

AIFr11

Surface Chemistry on Silicon- Turning Reactions on and off*

J.T. Yates, Jr., C.C. Cheng, Q. Gao, H. Gutleben, M.L. Colaianni, P. Chen**, and W.J. Choyke**

Surface Science Center, Department of Chemistry, University of Pittsburg, Pittsburg, PA 15260 USA

(412)624-8320, FAX(412)624-6003

The ability to manipulate the surface chemistry of semiconductors has wide practical technological impact. In addition, the new kinds of surface chemistries which occur on covalently bonded solids are of significant intellectual importance and form an exciting new area for detailed investigation using surface science methods.

In the lecture several examples wll be given of the rich surface chemistry which exists on silicon single crystals.

HALOGEN SURFACE CHEMISTRY

The bonding of chlorine to Si(100) has been studied by ESDIAD and HREELS methods. The directionality of the Si-Cl bonds has been determined, and the dynamical behavior of these bonds has been measured as a function of increasing temperature. Comparison of Cl_2 and HCl as adsorbing species indicates that a site exclusion process exists for HCl in which only alternate Si_2 dimer sites can adsorb HCl. It has also been shown that atomic hydrogen collision with the Si-Cl bond results in efficient bond cleavage, producing HCl(g) by an Eley-Rideal process.

METHYL SURFACE CHEMISTRY

The bonding and thermal stability of adsorbed methyl (CH_3(a)) on Si(100) has been measured by HREELS. In addition,it has been shown that CH_3(a) can be removed by atomic hydrogen exposure, but the methyl extraction process does not proceed by an Eley-Rideal mechanism. The mechanism of CH_3(a) removal occurs by an etching process, producing CH_3SiH(g).

NH_3 AND PH_3 SURFACE CHEMISTRY

The adsorption of NH_3 and PH_3 on both Si(100)-(2 x 1) and Si(111)-(7 x 7) has been studied using ESDIAD, temperature programmed desorption, and HREELS. It has been shown that the dissociative chemistry of these two group III hydrides differs significantly on the two surfaces because of the involvement of Si backbond strain. In the case of Si adatoms on Si(111)-(7 x 7) efficient N-H(a) and P-H(a) formation takes place as strained Si backbonds are broken in the presence of $Si-NH_2$ or $Si-PH_2$ adsorbate species.

DOPING EFFECTS IN CONTROLLING Si SURFACE CHEMISTRY

The surface chemistry of the Si(111)- (7 x 7) surface is strongly influenced by B doping into a subsurface site beneath a Si adatom. Thus, both the surface chemistry of NH_3 and of atomic hydrogen can be turned off by the B dopant as it removes an electron from the adatom dangling bond.

---

* Work supported by the Office of Naval Research and the Air Force Office of Scientific Research.

** Department of Physics, University of Pittsburgh

ACFr12

Limitations of a Central Force Model of Vibrational Phase Relaxation

M. Persson[a], K. Burke[b], D. Langreth[c] and Z. Y. Zhang[d]

[a]Institute of Theoretical Physics,
Chalmers University of Technology S-412 96 Göteborg, Sweden,
[Fax: +46-31-416984], [E-mail: tfymp@fy.chalmers.se]

[b]Department of Physics and Materials Research Institute,
Indiana University, Bloomington, IN 47405, USA

[c]Department of Physics and Astronomy,
Rutgers University, Piscataway, NJ 08855-0849, USA

[d]Department of Chemistry,
UC Santa Barbara, CA 93106, USA

For many adsorbate-covered surfaces, the temperature-dependent linewidth of the adsorbate-substrate stretch absorption line in the infra-red spectrum is dominated by vibrational dephasing .[1] The central force model is frequently employed to interpret experiments on these systems [2]. In this work, we point out a previously unreported renormalization of the effective coupling constants which has a dramatic impact on the interpretation of lineshape data. We consider the localized vibration of an adsorbate bound directly above a substrate surface atom in the high stretch frequency limit, and emphasize two important consequences. Firstly, for atomic adsorbates (*e.g.* H/Si(111) [3]), the observed linewidth is due to non-central forces. Secondly, in the case of molecular adsorbates (*e.g.* CO/Pt(111)[4]), if the linewidth is dominated by a central force, the details of that force are irrelevant for dephasing. In particular, this coupling constant renormalization explains why the large dephasing linewidths and the strong Fermi resonance effects suggested by a central force model never have been observed for CO adsorbed on a variety of metal surfaces.

[1] Y. Chabal, Surf. Sci. Reports 8, 211 (1988).
[2] D.C. Langreth and M. Persson, Phys. Rev. B43, 1353 (1991)
[3] P. Dumas, Y. Chabal and G. S. Higashi, Phys. Rev. Lett.65. 1124 (1990).
[4] R. Ryberg in em Vibrations at Surfaces 1990, ed. Y. Chabal, F.M. Hoffmann, and G.P Williams (Elsevier, New York, 1990).

ACFr13

Dissociation of H_2 on Al(110)

B. Hammer, K.W. Jacobsen and J.K. Norskov
Laboratory of Applied Physics, Technical University of Denmark
DK 2800 Lyngby, Denmark
Fax: (+45) 45 93 23 99, E-mail: hammer@ltf.dth.dk

By means of the pseudopotential method the total energy of a system consisting of an Al(110) slab and a dissociating H_2-molecule has been calculated. The adiabatic dissociation path is found by fixing one degree of freedom for the incoming molecule and minimize the total energy with respect to the other degrees of freedom in the molecule. The energy barrier for dissociation comes readily as the largest excess energy along this adiabatic path. The work is aiming at a parametrization of the potential seen by the dissociating H_2-molecule. The parametrized potential will subsequently serve as input for dynamical studies.

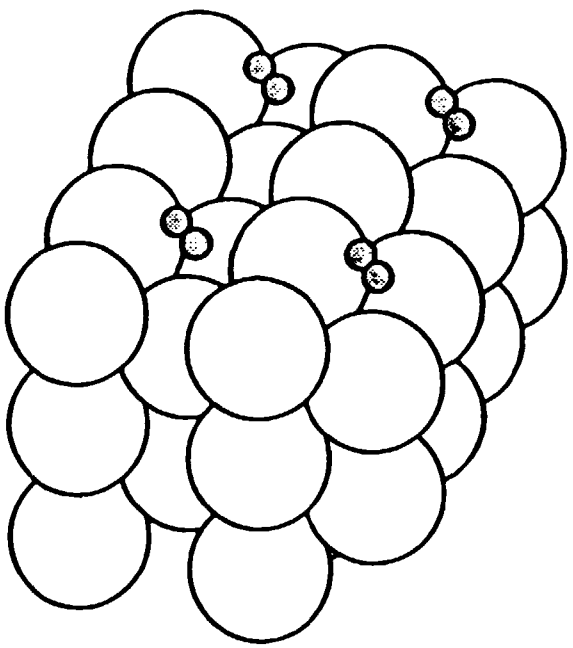

AISa1

Recent Developments at MAX-LAB.

Ralf Nyholm

MAX-LAB, Lund University, Box 118, S - 221 00 Lund, Sweden
and
Department of Synchrotron Radiation Research, Institute of Physics, Lund University, Sölvegatan 14, S-223 62 Lund, Sweden.
[Fax: 46-46 104710], [e-mail: RALF.NYHOLM@MAXLAB.LUSE]

The MAX I storage ring has been in operation since 1986 and several experimental stations for research in atomic and molecular physics, solid state physics, surface physics, chemistry, physical chemistry and biochemistry have been developed. Today six beamlines are in operation and another three are under commissioning or under construction. In this report we will focus on the present and future possibilities for surface physics experiments.

The MAX I storage ring is operated at an electron energy of 500 MeV with fillings of typically 250 mA circulating current. The beam life-time is around 3 h at 200 mA and increases to about 5 h at 100 mA. The main source of synchrotron radiation are the bending magnets with a critical energy of 230 eV. In practice this means that the usable photon energy range extends to about 1 keV (depending on the particular beamline and the type of experiment). The storage ring is also equipped with two undulators with useful photon energies of 12 to 150 eV and 50 to 600 eV, respectively; the first undulator will be used for spectromicroscopy with surface physics applications and the second mainly for atomic and molecular physics.

At MAX-LAB the main experimental technique used for surface physics experiments is photoelectron spectroscopy, with or without angular resolution. Other techniques that have become increasingly important are X-ray absorption spectroscopy (mainly NEXAFS) and soft X-ray fluorescence spectroscopy. In the future we can also foresee experiments utilizing scanning spectromicroscopy and infra-red absorption techniques.

Research programs are carried out on a large variety of material systems: clean and adsorbate covered metal and semi-conductor surfaces, compound semi-conductors grown by *in situ* molecular beam epitaxy, clean and adsorbate covered high temperature super-conductors, metal-metal and metal-semiconductor surface compounds and interfaces etc.

The table below summarizes the present and planned beamlines useful for surface physics experiments.

	BEAMLINE CHARACTERISTICS			
BEAM PORT	ENERGY RANGE (eV)	ENERGY RESOLU-TION (E/ΔE)	EXPERIMENTAL EQUIPMENT	TYPE OF EXPERIMENTS
22	20 - 1000	1000 - 4000	Hemispherical electron energy analyser. Partial electron yield detector.	Photoelectron spectroscopy; core levels. X-ray absorption spectroscopy (NEXAFS).
31 [1]	12 - 150 undulator	500 - 1000	Hemispherical electron energy analyser. [2] Partial electron yield detector.	Scanning spectromicroscopy with 1 μm lateral resolution. Photoelectron spectroscopy on selected spots. Imaging by partial e^- yield detection.
33 [3]	10 - 200	2000 - 10000	Angle resolved hemispherical electron energy analyser. [3]	Photoelectron spectroscopy; bandstructure and core levels.
41	15 - 200	500 - 1000	Angle resolved hemispherical electron energy analyser. MBE station for III-V compounds.	Photoelectron spectroscopy; bandstructure and core levels.
52	5 - 30	1000 - 2000	Angle resolved hemispherical electron energy analyser. [4]	Photoelectron spectroscopy; bandstructure.
53	white beam	--- [5]	Soft X-ray spectrometer.	Soft X-ray fluorescence spectroscopy; adsorbate systems. [6]
73 [1]	1000 - 10 cm^{-1}	≥ 0.003 cm^{-1}	High resolution FTIR spectrometer. [7]	Reflectance and absorption spectroscopy on adsorbates.

1. Under commissioning.
2. Planned.
3. Under construction.
4. Planned. This beamline is mainly used for atomic & molecular physics.
5. A medium resolution monochromator ($E/\Delta E \approx 100$) is planned.
6. Surface sensitivity is obtained by gracing incidence of the exciting photons.
7. This FTIR spectrometer has been chosen for high resolution experiments on mainly gases and liquids. For surface applications a simpler FTIR spectrometer with lower resolution will probably be more efficient.

AISa2

CORE LEVEL SPECTROSCOPY OF ADSORBATES

Anders Nilsson
Department of Physics, Uppsala University, Box 530
S-751 21 Uppsala, Sweden

Core level spectroscopy provides a local probe of the electronic and geometric structure since it selects one atomic species at a time. This is particularly useful for studies of adsorbates on surfaces where it is possible to isolate from the substrate both the information from the adsorbate itself but also between different atoms within an adsorbed molecule.

In the present contribution various core level spectroscopies will be applied to different adsorbate systems ranging from weak (physisorption) to strong (chemisorption) interaction. In the primary process, core holes are created by either photoionization where the electron becomes completely free or by photoabsorption where the core electron is excited to a bound state or a continuum resonance. The secondary process corresponds to the subsequent de-excitation of the core hole into various valence hole states by Auger like decay or x-ray emission.

Using X-ray Photoelectron Spectroscopy (XPS), the ionization process of an adsorbate can be studied. In the case of the chemisorption where the adsorbate and substrate orbitals overlap, metallic screening takes place through charge transfer from the substrate allowing for the lowest possible core hole state to be observed. Chemical shifts for different surroundings in an adsorbate can be seen. Different adsorption sites can be distinguished in the case of CO adsorption on Ni(100). For physisorbed molecules the ionized final state is screened by the creation of an image potential in the substrate. This is demonstrated for O_2 adsorbed on graphite where the paramagnetic splitting in the final state of the free molecule is preserved. The localization of the core hole within a homonuclear adsorbed molecule in a perpendicular geometry on the surface is shown in the case of N_2 chemisorbed on Ni(100) and O_2 physisorbed in the ζ phase on graphite. Core level photoionization is a complex dynamical process and this is reflexted in the satellite structure. These shake-up satellites can be viewed upon as local valence excitations on the adsorbate in the presence of the core hole. For physisorbed molecules the satellite spectra resemble the free molecule whereas in chemisorbed molecules new strong satellites appear which are related to the adsorbate-substrate chemical bond formation.

In X-ray Absorption Spectroscopy (XAS) or Near Edge X-ray Absorption Fine Structure (NEXAFS) the empty states of an adsorbate are studied. The localized nature of the core hole and the dipole selection rules make it possible to probe the atomic

population as well as the symmetry of the various unoccupied orbitals. In chemisorbed systems, the Fermi level position for the unoccupied density of states in a XA spectrum can be derived from the corresponding XPS binding energy. In the case of physisorption where the adsorbate and substrate are electronically isolated, there is no charge transfer from the substrate to screen the core hole and therefore no simple relationship between the XAS and XPS processes. This will be exemplified for Ar adsorbed on graphite and Ag(110) and for N_2 adsorbed on graphite and Ni(100).

In the Autoionization and Auger decay, the adsorbate core hole state is filled from a valence level while another valence electron is emitted. If the core hole state is ionic (XPS final state), the final de-excited state will contain two valence holes and the process is denoted Auger decay. If the core hole state is neutral (XAS final state) the decay is by autoionization. The latter process may be divided in two different types. In the participator decay, the core excited electron participates in the decay and a single valence hole state is created similar to a valence photoemission final state. In the spectator decay, the core excited remains in the excited orbital as a spectator resulting in a two hole-one particle final state. In chemisorbed systems, the excited state is delocalized due to the hybridization with substrate and its presence as a spectator or participator is negligible. The autoionization and the Auger decay become very similar. This is demonstrated for CO adsorbed on Ni(100) and Ar on Ag(110). For physisorbed systems the excited electron remains localized on the adsorbate and the autoionization and Auger decay will be different. For Ar physisorbed on graphite the presence of a spectator in the autoionization shifts the corresponding Auger transition by 3.6 eV towards lower kinetic energies. In N_2 physisorbed on graphite an interesting phenomenon occurs in the decay spectra. The Auger spectrum shows decay from both an ionic and neutral intermediate state. The neutral state is created by charge transfer from the substrate after the photoionization process but prior to the core hole decay.

In Soft X-ray Emission Spectroscopy (SXES) the core hole state is de-excited by the emission of x-ray photons. The final state of the x-ray emission process is simpler than the corresponding Auger final state since it involves only a single valence hole, as in valence photoemission. The localized nature of the initial core hole state of the x-ray transition, along with the dipole selction rules, makes it possible both to separate the emission from different atomic sites in a system and to separate between various orbital symmetries in the valence region. K emission from adsorbed oxygen and nitrogen on Ni(100) and Cu(100) will be presented. The observed spectral feaures correspond to the occupied 2p partial density of states of the adsorbate.

ACSa3

Na Adsorption on Al(111) and Al(100): A SEXAFS Study

S. Aminpirooz[1], A. Schmalz[1], L. Becker[1], J. Haase[1], D. R. Batchelor[1], M. Nielsen[1], D. L. Adams[1] and E. Bøgh[1]

[1]Fritz-Haber-Institut der Max-Planck-Gesellschaft, Faradayweg 4 - 6, D-1000 Berlin 33, Germany, [Fax: 30-8305520]

[1]Institute of Physics, University of Aarhus, D-8000 Aarhus C, Denmark, [Fax: 86-12 740]

The adsorption of alkali metals involves a greater diversity of phenomena than hitherto suspected. Among these are unusual chemisorption sites[1] and surface alloy formation.[2] SEXAFS studies on Al(111)-(√3x√3)R30°-Na, where a quasi-substitutional 6-fold coordinated site had been suggested, greatly stimulated further experiments in this area.

Here we present the results of SEXAFS measurements on Na adsorption on Al(111) and Al(100) surfaces. The following ordered overlayers have been studied by taking data at normal ($\theta = 90°$; E vector parallel to the surface) and near-grazing X-ray incidence: Al(111)-(4x4)-Na, Al(111)-(√3x√3)R30°-Na, Al(111)-(2x2)-Na and Al(100)-c(2x2)-Na. With the exception of the (4x4) structure which we obtained by Na adsorption at 120 K, all other structures were formed at room temperature.

Each of these structures shows a very distinct adsorption phenomenon. For Al(111)-(4x4)-Na we find a "normal" (on-surface) adsorption with Na atoms forming a quasi-close-packed hexagonal structure which is in registry with the substrate. As already mentioned, in Al(111)-(√3x√3)R30°-Na surface Al atoms are displaced from their equilibrium positions which are occupied by Na atoms of the sixfold-coordinated hole so created. Additional Na adsorption results in a (2x2) structure which can only be explained by a double Na layer with first-layer Na atoms still in a sixfold site. Room-temperature Na adsorption on Al(100), finally, leads to the formation of a surface alloy with Na atoms being "sub-surface" with respect to a completely rearranged Al surface layer. The latter result is consistent with the interpretation of the recent core-level shift data.[2]

[1]A. Schmalz, S. Aminpirooz, L. Becker, J. Haase, J. Neugebauer, M. Scheffler, D. R. Batchelor, D. L. Adams and E. Bøgh, Phys. Rev. Lett. 67, 2163 (1991).

[2]J. N. Andersen, M. Qvarford, R. Nyholm, J. F. van Acker and E. Lundgren, Phys. Rev. Lett. 68, 94 (1992); J. N. Andersen, E. Lundgren, R. Nyholm and M. Qvarford, to be published

ACSa4

Some Electronic Properties of Si(100)/Na: Interface Metallization. Surface Photovoltage and Na Quantum Well States

A. Hamawi and L Wallidén
Physics Department, Chalmers University of Technology
S-412 96 Göteborg, Sweden, [Fax: 46 31 165176]

Angle resolved photoemission at low photon energies ($h\nu < 6$ eV) is used to study Si(100)/Na for adsorbed amounts ranging from small monolayer coverages to several atomic layers of Na. If the substrate holder is cooled by LN_2 or He the overlayer-substrate interface and the overlayer thickness is well defined enough for quantum well type overlayer states and resonances to be observed via the photoemission spectra. The states are formed by Na valence electrons, which propagate back and forth between the vacuum barrier and the overlayer-substrate interface, when the phase condition $\Phi_B+\Phi_C+2\Phi_D = 2\pi m$, $m = 0, 1, 2....$ is satisfied. Φ_B, Φ_C and Φ_C are the phase shifts at the vacuum barrier, the substrate adsorbate interface and across the interior of the overlayer respectively. Here we use the phase condition and measured energies to estimate the film thickness. Of main present interest is however the strong monolayer coverage dependence of the surface photovoltage (SPV) which is monitored as a rigid shift of the spectra induced by the light source used for photoemission. This source which produces an SPV of few mV at RT nearly eliminates the band bending (0.5 eV) at low temperature. This has been observed previously and is ascribed to a slower relaxation rate at low temperature. Here we find that upon adsorption of monolayer amounts of Na the light sensitivity of the SPV is drastically reduced with the main change occurring in the Na coverage range where, judged from the

ACSa5

Simple and Reconstructed Adsorption Structures for Al(111)-K-($\sqrt{3}$x$\sqrt{3}$)R30°

J. Burchhardt[§], M. Nielsen[§], D. L. Adams[§], C. Stampfl[‡] and M. Scheffler[‡]

[§]Institute of Physics, Aarhus University, DK-8000 Aarhus C, Denmark.
Fax: 45-86-120740, E-mail: dla@dfi.aau.dk
[‡]Fritz-Haber-Institute der Max-Planck-Gesellschaft, D-1000 Berlin 33, Germany.
Fax: 49-30-8305520, E-mail: mxs@DGAIPP1S.bitnet

The adsorption of alkali metals on metal surfaces has been widely supposed to lead to the formation of simple (ie. unreconstructed) adsorption structures. Recent SEXAFS measurements and total energy calculations[1] for Na adsorption on Al(111) have shown, however, that a reconstruction of the substrate occurs for this system and have thereby stimulated an interest in further structural studies.

In the present LEED study[2], the Al(111)-K-($\sqrt{3}$x$\sqrt{3}$)R30° structures formed by adsorption of K at 90K and at 300K are shown to be *two different* structures resulting from simple and reconstructive adsorption, respectively. These conclusions are consistent with the interpretation of measurements of core-electron binding-energy shifts for this system[3].

LEED intensity-energy spectra for a total of 17 beams have been measured at 90K in the energy range 50 - 450eV and at normal incidence for the Al(111)-K-($\sqrt{3}$x$\sqrt{3}$)R30° structures formed by adsorption of K at 90K and 300K, respectively, using a newly-developed video-LEED system[4]. The observation of large differences between the sets of spectra measured after adsorption at 90K and 300K leads immediately and unambiguously to the conclusion that the two structures are quite different. Furthermore, intensity-energy spectra measured after adsorption at 90K and warming to 300K are found to be identical to those measured after adsorption at 300K alone, indicating that an irreversible phase transition occurs on warming from 90K to 300K.

A quantitative analysis of the experimental spectra, involving calculations[5] of LEED intensities using the layer-doubling method of the dynamical theory of LEED, shows that adsorption of K at 90K leads to the formation of a simple adsorption structure with K atoms located on the on-top sites and with a K - Al interlayer spacing of 3.0Å. The structure formed by K adsorption at 300K, however, is shown to involve a reconstruction of the substrate, with K atoms located in quasi-substitutional sites of 6-fold symmetry formed by removal of 1/3 monolayer of Al atoms, precisely as found by SEXAFS for the Al(111)-Na-($\sqrt{3}$x$\sqrt{3}$)R30° structure. The K - Al interlayer spacing is found to be 2.15Å.

---

[1] A. Schmalz, S. Aminpirooz, L. Becker, J. Haase, J. Neugebauer, M. Scheffler, D. R. Batchelor, D. L. Adams and E, Bøgh, Phys. Rev. Lett. 67, 2163 (1991)

[2]Support of this work by the Danish Natural Science Research Council is gratefully acknowledged

[3]J. N. Andersen, private communication

[4]D. L. Adams, S. P. Andersen and J. Burchhardt, in The Structure of Surfaces III (S. Y. Tong, M. A. Van Hove, K. Takayanagi and X. D. Xie, eds) Springer, Berlin (1991) p. 123

[5]We are grateful to W. Moritz for supplying the computer programs used in the calculations.

AISa6

The question of referencing core-levels in photoelectron spectroscopy[1]

Steinar Raaen

Institutt for fysikk, Univ. i Trondheim, NTH, N-7034 Trondheim, Norway,
[Fax: -47-7-593628], [E-mail: sraaen@phys.unit.no]

Important physical insights on the solid state may be obtained from analysis of peak positions and linewidths in photoelectron spectroscopy. Examples may range from adsorption studies to systems of strongly correlated electrons. Information on the initial state of the system in question is commonly sought, and hence initial and final state effects in photoemission have been extensively studied in the literature. In metallic systems, core-level binding energies are measured with respect to the Fermi level, and are insensitive to changes in the system work function. However, in overlayer systems that incorporate insulating or poorly conducting layers, or poorly conducting substrates, the question of charge equilibrium has to be considered. For such systems charge transfer between the overlayer and substrate may be insufficient to equilibrate Fermi levels. Core levels will be referenced to the analyzer Fermi level if overlayer and substrate Fermi levels are equilibrated. If this is not the case, overlayer core levels will be referenced to the local vacuum level, and core level peak positions will change with changes in the sample work function, as shown in the figure. Anomalous shifts to lower binding energies in certain overlayer systems where charge flow is insufficient to equilibrate Fermi levels, may therefore be explained by an increase in the system work function. Several systems with overlayers of low work function elements, have shown overlayer core level shifts to lower binding energies, accompanied by similar changes in the work function. These shifts have been discussed in terms of non-equilibrium processes.[2] The question of coupling to the substrate of metallic clusters which have been separated by condensed rare gas layers of varying thicknesses, has been addressed previously,[3] and is important for the present interpretation of systems of very thin oxide overlayers. Several time scales are of relevance to this problem of interpreting core level shifts: The time scale of the photoemission process, the time scale of the neutralization of the core hole, and the time scale of charge flow to equilibrate Fermi levels. If the time scale for neutralization of the photo hole is too slow, macroscopic charges will build up, and core level shifts to higher binding energies will occur. If that is not the case, and if charge are unable to flow to equilibrate Fermi levels on the time scale of the photoemission process, core level shifts that track changes in the work function will be observed.

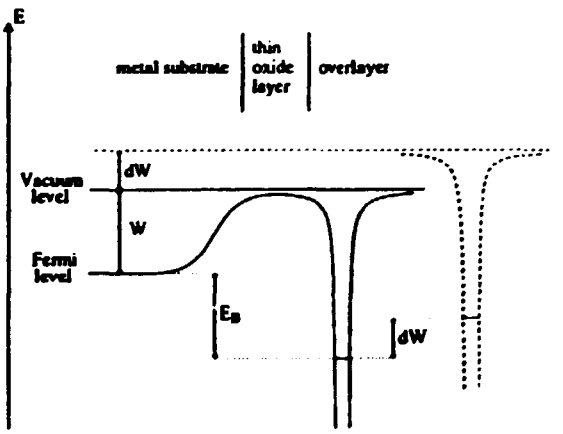

[1] Work supported by the Norwegian Research Council (NAVF)
[2] S. Raaen and N.A. Brasten, Phys. Rev. B 42, 9151 (1990)
[3] S.L. Qiu, X. Pan, M. Strongin, and P.H. Citrin, Phys. Rev. B 36, 9154 (1987)

AISa7

HIGH-RESOLUTION PHOTOEMISSION STUDIES OF HIGH-T_c SUPERCONDUCTORS

R. Manzke

Inst.f. Experimentalphysik, Universität Kiel, D-2300 Kiel, FRG

Angle-resolved photoemission spectroscopy (ARPES) applied with high energy and angle resolution on single-crystalline high-T_c superconductor surfaces has provided valuable experimental informations on the electronic structure in both the normal and superconducting state. Most of the work concerning the origin of the electronic states at the Fermi level E_F, their binding energies and dispersions, the Fermi surface in the normal state, and the opening and $\underline{k}$-dependence of the superconducting gap for $T<T_c$ has been performed on the cuprate $Bi_2Sr_2CaCu_2O_{8+\delta}$. In the meantime, after high-quality large single crystals are available similar investigations have started on twinned and untwinned $YBa_2Cu_3O_{7-\delta}$.However, since ARPES is a very surface sensitive technique with a probing depth of about 5-30Å the question has to be posed, how far the derived electronic structure is representative for the bulk material and therefore for high-T_c superconductivity.

For $Bi_2Sr_2CaCu_2O_{8+\delta}$ this problem seems to be solved because of its quasi two-dimensional character. Chemically stable surfaces can be prepared by cleavage between adjacent Bi-O layers, which are only weakly bonded by van-der-Waals-like forces with almost no valence charge between them. On the other hand, for the more three-dimensional $YBa_2Cu_3O_{7-\delta}$ the formation of a surface inevitably requires the breaking of strong ionic or covalent bonds and represents much more disturbance to the bulk electronic structure. Such surface effects leading to a rearrangement of the surface electronic charge have been first proposed from band structure calculations and possibly explain the puzzeling question why ARPES, so far, has been unable to detect the superconducting gap in $YBa_2Cu_3O_{7-\delta}$.
My present contribution summarizes latest photoemission results on $Bi_2Sr_2CaCu_2O_{8+\delta}$ and reviews critically the experimental evidence for surface effects on $YBa_2Cu_3O_{7-\delta}$. It will be shown that mapping of bulk-derived bands by ARPES remains to be a meaningful experiment, also for $YBa_2Cu_3O_{7-\delta}$.

ACSa8

ANGLE-RESOLVED PHOTOEMISSION INTENSITY CALCULATIONS IN $YBa_2Cu_3O_7$ *

M. Lindroos[1,2], A. Bansil[1] and J. C. Campuzano[3,4]

[1] Physics Department, Northeastern University, Boston, Massachusetts 02115 , U.S.A., fax:617-4372943,
[2] Physics Department, Tampere University of Technology, Tampere, Finland, fax 31-162600, E-mail: IN%"lindroos@cc.tut.fi"
[3] Materials Science Division, Argonne National Laboratory,Illinois 60439, U.S.A.
[4] Dept. of Physics, University of Illinois at Chicago,Illinois 60860, U.S.A.

We discuss first-principles computation of angle-resolved photoemission intensities (ARPES) in the high-T_c superconductors within the band theory framework. Definitive LDA-band-theory-based predictions would help interpret ARPES spectra in the high-T_c's, and also help isolate spectral features where such a description is not adequate. With this motivation, we have generalized and implemented the 'one-step' photoemission approach to treat systems with many atoms per unit cell; our codes can handle an arbitrary number of atoms in the layer unit cell, including effects of 'buckling' of the layers. We illustrate the methodology with results for the Γ-S symmetry direction for the (001)-surface of orthorhombic $YBa_2Cu_3O_7$ including all six possible surface terminations.

In the limited k-E range considered, a comparison of the theoretical predictions with the corresponding experimental spectra indicates a reasonable overall accord between the measured and computed intensities for three possible different crystal terminations; further experimental and theoretical work exploring larger k-E region is however needed to develop a consistent picture of the electronic spectrum in $YBa_2Cu_3O_7$.

Our computations also give insight into dependence of polarization of incident light on photoemission intensities and to some extent to the origin of spectral features.

Lindroos and A. Bansil, J. Chem. Phys. 52(1991)1447.
Lindroos, A. Bansil and J.C. Campuzano, in MRS Fall meeting 1991.

* This project is supported by Academy of Finland, and the US Department of Energy contract W-31-109-ENG-38, including a subcontract to Northeastern University, by the National Science Foundation, and benefited from the allocation of supercomputer time on the ER-Cray at NERSC, and the San Diego Supercomputer Center.

ACSa9

High-resolution Photoelectron Spectroscopy of C_{60} and K_xC_{60}

P.A. Brühwiler,* A.J. Maxwell,* A. Nilsson,*
N. Mårtensson,* R.L. Whetten†

*Department of Physics, Uppsala University, Box 530, S-751 21 Uppsala, SWEDEN, [Fax 46 18 183524] [email: paul@fysik.uu.se]

†Department of Chemistry and Biochemistry, UCLA, 405 Hilgard Ave., Los Angeles, CA 90024-156905, U.S.A.

We present high-resolution x-ray and soft-x-ray photoelectron and absorption spectra of C_{60}, K_6C_{60}, and K_xC_{60} (x=3) films, formed on Mo(110) substrates. In the C 1s and K 2p XPS spectra (hv=1487 eV) of these films, we find agreement with many of the features in published C 1s shakeup spectra, but with some notable differences as well. Reflection inelastic electron scattering studies at incident energies comparable to the kinetic energy of a C 1s electron show for pure C_{60} that the first two shakeup features cannot be explained as extrinsic losses; however, the rest of the shakeup spectrum shows a close correspondence to the inelastic loss data. The shakeup spectrum in the region of the plasmon-like feature (30 eV below the main line) develops a doublet structure for K-doped films, with a spacing in the doublet very near the spacing between the C 1s and K 2p lines. These data indicate that significant work remains to unravel the origin of most of the C_{60} C 1s shakeup spectrum.

The C 1s Auger spectra of these films is quite similar to that of other carbon compounds, but fine structure is visible in the form of small peaks on the near-threshold sloping shoulder of the spectrum for all films, indicating that strong intramolecular deexcitation processes remain even in the condensed form of buckyball; however, these features are less distinct for metallic K-doped films, as expected.

Photoemission and photoabsorption spectra of submonolayer films of C_{60} indicate a significant rearrangement of the molecular orbitals, particularly in the region of the lower π and upper σ bonding bands. Also observed is a general shift to lower binding energy of all features.

ACSa10

Theory of Alloy Sputtering

A. Oliva[1] and P. Sigmund
Physics Department, Odense University
DK-5230 Odense M, Denmark

Understanding alloy sputtering turned up to be a major challenge for theoreticians and experimentalists alike[2] . The systematics is unquestionably determined by several competing processes. At room temperature and below, the following are believed to be most prominent:

- Sputtering is a priori preferential, i.e., nonstoichiometric. Different species are ejected not only at different rates but also from different depths.
- Ion bombardment causes compositional changes over the whole penetration depth of the beam, via recoil mixing and related processes.
- The beam-induced disruption of lattice order activates Gibbsian segregation.

Preferential sputtering has been treated theoretically[3] on the basis of concepts that successfully explained elemental sputtering. The predictions of that theory are difficult to test experimentally since such experiments require extremely small bombardment fluences.

A general equation describing the effect of preferential sputtering and recoil mixing was derived some time ago[4] . The impact of this equation has been limited, not the least because one pertinent process was not included. Moreover, it was found to be a nontrivial task to find valid solutions analytically and numerically.

In the present contribution, we wish to demonstrate that the nonlinear integro-differential equation derived previously is comprehensive and readily allows incorporation of Gibbsian segregation and any other competing processes. Moreover, a scheme has been found to predict composition profiles in the target at high fluences without going over the transients at low fluences. The numerical effort that remains necessary reduces from hours on a large computer to seconds on a PC, and a potential for general scaling relations shows up.

The three effects mentioned above have each been analyzed individually, as has their mutual interplay, and various pitfalls not recognized in earlier work in the field have been identified.

---

[1] Present (permanent) address: Physics Department, University of Calabria, I-87036 Rende, Italy
[2] H.H.Andersen, in Advances in Ion Implantation, J.M.Poate et al. eds. Academic Press, N.Y. (1982)
[3] N.Andersen and P.Sigmund, Mat. Fys. Medd. Dan. Vid. Selsk. 39, no. 3 (1974)
[4] P.Sigmund, A.Oliva, and G.Falcone, Nucl. Instrum. Methods 194, 541-548 (1982)

ACSa11

NEXAFS study of the molecular orientation for physisorbed Oxygen on Graphite and Ag(110)

B. Hernnäs[1], R. J. Guest[2], A. Nilsson[1], O. Björneholm[1], P. Bennich[1], A. Sandell[1], R. E. Palmer[2] and N. Mårtensson[1]

[1]Department of Physics, Uppsala University, Box 530, S-75121 Uppsala, Sweden

[2]Cavendish Laboratory, University of Cambridge, Madingley Road, Cambridge CB3 0HE, United Kingdom

Near Edge X-ray Adsorption Fine Structure (NEXAFS) is an extensively used technique for determining the orientation of chemisorbed molecules. Only recently it has been used in studies of physisorbed molecules. Two systems were studied, O_2 on Highly Oriented Pyrolytic Graphite and O_2 on Ag(110). The first system exhibits an orientational phase transition in the submonolayer regime, and it is also known to have a complicated phase diagram at low temperatures. Our studies were concentrated to the temperature region where the lying down phase (∂-phase) and the standing up phase (ζ-phase) exist. Also multilayers of oxygen were studied. Figure 1 shows the intensities from the $1s \rightarrow 1\pi_g$ and the $1s \rightarrow \sigma$-states absorption spectra at different coverages. The results clearly show the phase transition between the ∂-and the ζ-phase. The average molecular tilt angles for the ∂- and ζ-phase were determined to be 24° and 53° from the surface plane, respectively, from the σ/π intensity ratio. In the intermediate (∂+ζ) region the molecules tends to line up towards the surface normal when increasing the coverage. At multilayer coverages the molecules become progressively more aligned to the surface normal. The second system has not been studied before at physisorption temperatures with NEXAFS, and since the Ag(110) surface is a rather corrugated surface an alignement of the molecules towards it would be possible to detect. This system shows also a tendency for alignment towards the surface normal at multilayer coverages. By evaluating the intensity ratios of the π and σ states in figure 2, it is clearly seen that there is a change in growth geometry when going from monolayer to multilayer. The monolayer is lying down but the second layer is standing up. No intermediate region where the molecules gradually lines up to the surface normal with the molecular axis is seen. The molecules in the monolayer phase are seen to be oriented towards the [001] direction (perpendicular to the grooves), with a out-of-plane tilt of 29°±5°. Earlier NEXAFS studies of the chemisorbed phase indicate that the molecules align in the [1$\bar{1}$0] direction with the molecular axis (parallel to the grooves), but ESDIAD measurements suggest the opposite. Our NEXAFS measurments of the chemisorbed phase show that neither of the two orientations can be clearly distingushed.

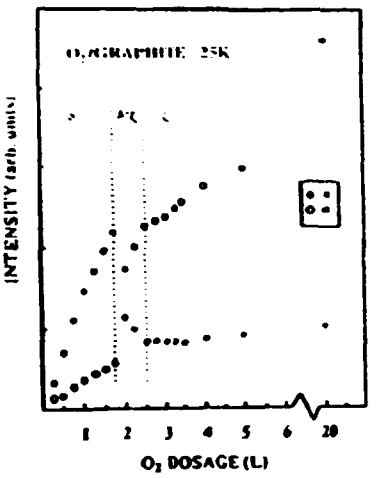

Figure 1.

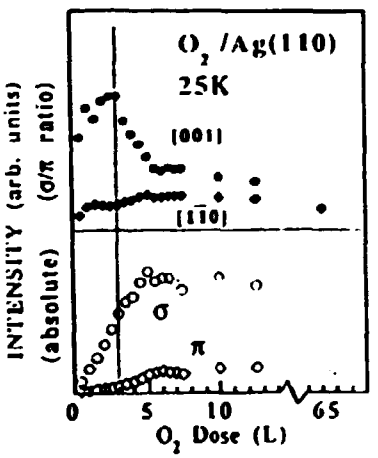

Figure 2.

ACSa12

The Structure of NiO, CoO and MnO studied by X-Ray Photoelectron Diffraction

C. Scharfschwerdt†, F. Schneider, J. Kutscher, T. Liedtke and M. Neumann

University of Osnabrück, Department of Physics, Postfach 4469, D-4500 Osnabrück, Germany, [FAX: ++49-541-9692670], [E-mail: mneumann@dosuni1.bitnet]

†Present address: University of Odense, Department of Physics, Campusvej 55, DK-5230 Odense M, Denmark, [FAX: ++45-66158760], [E-mail: chr@dou.dk]

The angular dependence of x-ray photoelectron spectra of in vacuo cleaved NiO (001), CoO (001) and MnO (001) single crystal surfaces has been investigated in detail. The intenities of the main peaks (O 1s and the metal 2p and 3p/3s lines) show characteristic modulations depending on the emission angle with respect to the surface. For CoO and MnO the detection angle was varied along two planes perpendicular to the crystal surface. By this, one can obtain a two-dimensional 'image' of the surface geometry.
The observed intensity variations are due to scattering of the outgoing photoelectrons on the neighbouring atoms and are commonly entitled as x-ray photoelectron diffraction (XPD). For the systems we investigated, a qualitative explanation of the observed maxima in intensity can be derived simply from crystal geometry, that means from the direction of atomic chains in the crystal. However, this does not explain the relative intensities and some subtle features. For a more complete description, calculations in a single scattering cluster (SSC) model have been performed, which in many cases already provide a rather good description of the experimental data. Further improvement is achieved by the inclusion of double and triple scattering events in the calculations, which have a significant influence on the relative intensities, especially along directions of close-packed atomic chains.
For NiO the influence of the surface preparation on the photoelectron diffraction effects above has been probed. To induce disorder the crystal was bombarded with argon ions, which led to a significant roughening of the surface, as could be seen from the LEED patterns. However, LEED probes the long range order, whereas XPD gives information on the short range order.

ACSa13

Investigations of the Electronic and Geometric Structures of Cu/ZnO(11$\bar{2}$0)[1]

Preben J. Møller and Jesper Nerlov

Laboratory of Physical Chemistry, H.C. Ørsted Institute,
University of Copenhagen, 5 Universitetsparken,
DK-2100 Copenhagen Ø, Denmark, [Fax: +45 31350609]

Upon surfaces of ZnO(11$\bar{2}$0) ultrathin films of copper have been deposited at room-temperature targets by e-beam evaporation.[2,3] The system of copper islands and films upon ZnO is of interest in heterogeneous catalysis in the synthesis of methanol.

The copper was deposited at average thickness steps that varied from 0.2 Å to 10 Å until coverages as high as 100 Å were reached. The Cu growth was analyzed by means of electron- and photon-induced Auger electron spectroscopy (AES). The mode of growth was found to be of the Volmer-Weber (VW) type (pure islanding), a mode that has been found to occur on some other oxide surfaces as well.[4,5] Epitaxy was investigated by low energy electron diffraction. So far, no clear epitaxial relationship has been established, however, over a surface annealing temperature range of 100 °C to 600 °C; this agrees with the observed growth mode.

The electronic structure for deposition of ultrathin layers of Cu upon ZnO(11$\bar{2}$0) was investigated by AES, electron energy-loss spectroscopy (EELS) and photoelectron spectroscopy. For the latter, both HeI ultraviolet and, at BESSY (Berlin), synchrotron-radiation-induced photon electron spectroscopy were used. The spectral changes, in terms of binding energy, kinetic energy and loss energy, as a function of copper coverage, are discussed with regard to changes in the initial and final state and valence band energies, respectively. A monotonous change of the binding-energy positions of the Cu2p and Cu3p peaks were observed. The copper bulk value Cu^0 was reached at an average deposit thickness d_{Cu} of 6 Å, both for the Cu2p and the Cu3p energies. A similar behaviour was found for the EELS and AES spectral features over the same coverage range.

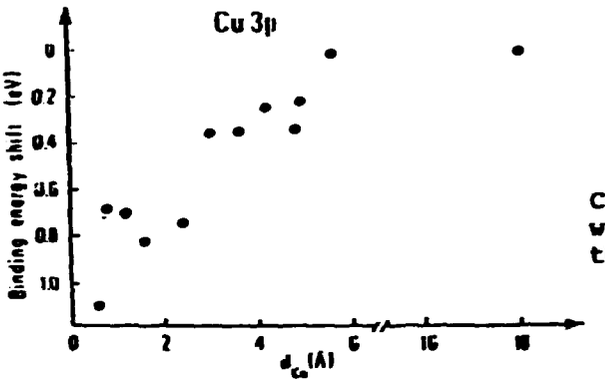

Cu3p binding energy shift with copper-deposit average thickness d_{Cu}.

[1]Work supported by the Danish Natural Science Research Councils and Center for Surface Reactions.

[2]P.J. Møller and J.W. He, J. Vac. Sci. Technol. A5, 996 (1987).
[3]P.J. Møller and M.C.Wu, Surface Sci. 224, 265 (1989).
[4]C. Argile and G.E. Rhead, Surface Sci. Reports 10, 277 (1989).
[5]J.E.T. Andersen and P.J. Møller, Thin Solid Films 186, 137 (1990).

ACSa14

The Nature of the Molecular Precursor and Final Atomic State for Oxygen Adsorption on Silicon (111) Surfaces [1]

Per Morgen
Fysisk Institut, Odense University, Campusvej 55, DK-5230 Odense M, Denmark
Fax: +45 66 15 87 60 , E--mail: per@dou.dk

Some of the fundamental, long standing controversies over the initial stages of the adsorption of oxygen on silicon surfaces *at room temperature* have been settled very recently through extensive - and mostly traditional - surface-spectroscopical investigations of the reaction of O_2 with Si (111) surfaces. [2,3,4]

High quality XPS, and XAES data, together with data from polarized UPS, NEXAFS and determinations of work-function changes were correlated, with very closely controlled and repeatable surface preparation and oxygen exposure methods. Initial studies underlined the differences in the reaction probability and -paths associated with different surface preparations, leaving the (111) surface in 1x1, 7x7, disordered or impurity stabilised structures. The well known oxygen take-up curve at room temperature is indeed found for all these surfaces. It breaks from high- to a low sticking probability at 1/2 monolayer coverage, but does not separate different adsorption mechanisms other than steric hindrance, contrary to several previous assumptions or models. In the initial stages of the adsorption reaction, a *metastable molecular precursor* is here unambiguously observed, together with atomic oxygen, which is *inserted in the surface layer*. The features of this precursor were studied at room temperature and at lower temperatures, increasing its lifetime. It is found to attach to two suitably oriented dangling bonds, before dissociation, which is mediated by a negative charge of the order of e, extracted from the substrate in this phase. The bond length is found to be 1.28 Å in a separate NEXAFS study by Höfer *et al.* [5], against 1.21 Å for O_2 gas. In later stages of the adsorption the ratio of the atomically inserted stable configuration to the molecular component strongly increases. However, the atomic component is observed *right from the beginning of the reaction*, and the precursor *never ceases completely*, unless perturbed by radiation, temperature or impurities. Throughout the exposure towards saturation, which occurs at around a monolayer of oxygen, LEED continues to show weak patches of the 7x7 structure, when that is the initial order. However, the strong 7x7 contrast vanishes during the build-up of the first 1/2 monolayer of adsorbate.

In the presentation, examples of spectroscopic data and the signatures differentiating the molecular and atomic states will be presented, with the available theoretical models. Reference to earlier work by other groups, supporting with data - but maybe not in conclusions - the current findings, will also be given. The most recent results obtained with STM methods will be briefly discussed, in which it is claimed that there may exist more than the single molecular configuration that we have found with the more traditional spectroscopies.

Finally the question will be posed, if - or how - these findings will help explaining or understanding three dimensional oxidation of silicon , or give clues to possible paths for this oxidation.

---

[1] Results of a project performed at The Technical University of Munich, by all the authors of refs. 2-4

[2] U. Höfer, P. Morgen, W. Wurth, E. Umbach, Phys. Rev. Lett. 55, 2979 (1985)

[3] P. Morgen, U. Höfer, W. Wurth, E. Umbach, Phys. Rev. B. 39, 3720 (1989)

[4] U. Höfer, P. Morgen, W. Wurth, E. Umbach, Phys. Rev. B. 40, 1130 (1989)

[5] U. Höfer, A. Puschmann, D. Coulman, E. Umbach, Surf. Sci. 211/212, 948 (1989)

ACSa15

OXIDATION OF GaAs(001) WITH THIN CE OVERLAYERS

A. Borg
SINTEF Applied Physics, 7034 Trondheim, NORWAY
[Fax:+47-7-593420], [E-mail: anne.borg@sintef.no]

J. K. Grepstad
Division of Physical Electronics, University of Trondheim - NTH
N-7034 Trondheim, NORWAY, [Fax:+47-7-591441]

Thin Ce overlayers have been found to enhance greatly the oxidation of selected metal surfaces[1,2] and the Si(100) surface[3]. In this work, we have investigated the effects of cerium on oxidation of GaAs(001) surfaces using x-ray photoelectron spectroscopy. Ce reacts with the semiconductor substrate to form a Ce-Ga intermetallic phase, as seen from a strong, shifted peak in the Ga $2p_{3/2}$ core level spectra. The respective As $2p_{3/2}$ spectra exhibit noticeable broadening and a minor shift to lower binding energy, which indicate formation of a Ce-As compound. Upon initial oxidation (~10L oxygen exposure) of this reacted surface layer the low binding energy Ga core level emission disappears, and the recorded spectra suggest that "reacted" Ga in the Ce-Ga intermetallic phase oxidizes immediately upon oxygen exposure. The As core levels sharpen up and the first traces of As-oxide appear concurrently with formation of a predominantly trivalent Ce-oxide. With further exposure to oxygen, the Ga spectra exhibit no change, while strong oxidation of As is observed. Thus, this oxidation appears to proceed by disruption of the Ce/GaAs(001) reaction layer. The shifted peaks of oxidized As atoms predominate the surface sensitive 2p core level spectra for exposures above 10^3L, at which no oxide emission could be discerned in data from oxidation of a pure GaAs(001) surface (see fig. 1). Such oxidation was observed after exposing the clean semiconductor to 10^7L oxygen. With increasing oxygen exposure, we also note a gradual conversion from trivalent Ce_2O_3 to tetravalent CeO_2, in agreement with previous data for catalytic oxidation of Nb and Ta by cerium[1,2]. From the present measurements, we conclude that the deposited Ce acts to promote oxidation of a clean GaAs(001) surface. The oxidation enhancement was found to depend on the effective thickness of the deposited Ce overlayer. The observations showed no evidence for sustained oxidation of the underlying, unreacted GaAs(001) substrate.

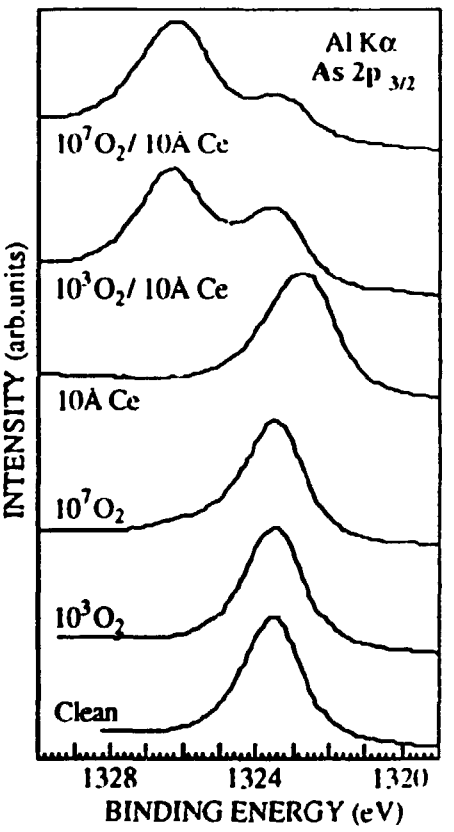

Fig. 1. XPS As $2p_{3/2}$ core level spectra of clean and oxidized GaAs(001) with and without a Ce overlayer.

[1]E.-E. Latta and M. Ronay, Phys. Rev. Lett. 53, 948 (1984); Phys. Rev. B 32, 5375 (1985).
[2]N. A. Braaten, J. K. Grepstad and S. Raaen, Surf. Sci. 222, 499 (1989).
[3]F. U. Hillebrecht , Maria Ronay, D. Rieger and F. J. Himpsel, Phys. Rev. B 34, 5377 (1986).

ACSa16

Towards a understanding of the core hole spectra of adsorbates

M. Ohno* and P. Decleva

*Department of Physics, Uppsala University, Box 530, S 751 21 Uppsala, Sweden
[Fax:46-18-183524]. [E-mail:Masahide@Fysik.UU.SE]

Dipartimento di Scienze Chimiche, Universita di Trieste, Via Valerio 38
I 34127 Trieste, Italy. [Fax:39-40-676-3946]. [E-mail:Vi1tsdc2@ICINECA2.bitnet]

We performed the ab initio 2h2p/3h2p CI calculations of XPS core hole spectra of NiCO, NiN_2, PdCO, PdN_2 and $NiNH_3$, using an extended basis set [1,2]. We could give a fairly good reproduction of the new spectral features of the recent high resolution spectra of adsorbates, such as newly resolved satellite lines and a large shakeup/off satellite intensity (for a description of which previous theoretical approaches turn out to be inadequate). The present many-body approach shows the potential for a systematic understanding of the chemically significant changes induced in the spectra by variation of the adsorbate/substrate system which are not easily understood in terms of simple arguments based on band structure of the substrate and coupling strength with the ligand. The strong spectral feature changes with the variations of the adsorbate/substrate system are explained by the present many-body approach in terms of the s-dσ hybrids and the s-dσ promotion which depend strongly on the changes in the local metal configuration anticipated on the basis of different ground state configurations in the isolated atom. The σ local metal excitation which reduces the σ repulsion between the core ionized ligand and metal, the magnitude of which is directly related to the amount of the valence s(sp)σ character on the adsorption site metal atom, is larger for the system with smaller d and larger s occupation (e.g. NiN_2) in comparison to the system with larger d and smaller s occupation (e.g. PdCO and PdN_2). The σ local metal excitation results in a drastic change in the metal σ orbitals (enhancement of the 5 eV giant satellite) in contrast to the π charge transfer (CT) relaxation which leads only to a modest variation of the π orbitals. The π CT, although significant, appears to be rather similar for both main line and satellite line states. Although the binding energy is notably reduced in PdCO in comparison to NiCO, the satellite structure is generally decreased (in particular the σ to σ^* satellite) and main line intensity is larger, despite the widely held assumption that weak coupling leads to increased many-body effects. In both Ni and Pd-ligands the binding of N_2 is much weaker. This gives rise to a dramatic spectral change for NiN_2, where the single hole state looses most of its intensity, as expected for a weakly coupled system, but the strongest excitation is given to the 5 eV σ to σ^* satellite associated with a local metal configurational change. On the contrary in the Pd-ligand case the weaker binding shows only a modest effect, with the satellite intensity even more suppressed, and the main line intensity closer to free ligand value. So the decrease of the binding strength has an opposite influence in the couple NiCO,NiN_2, and PdCO, PdN_2. This is tied to the different electronic structure of the substrate, so that weaker binding gives lower d population in Ni but higher in Pd, and consequently lowers main line and increases satellite intensity in the former, while it does the opposite for the latter. Preliminary results on $NiNH_3$ suggest, however, a more complex picture, indicating that the presence of valence π^* orbitals (absent in NH_3) leads to a cooperative effect.

[1] M. Ohno and P. Decleva, Surface Sci. 258, (1991), 91, Chem. Phys. 156, (1991), 309.

[2] P. Decleva and M. Ohno, Chem. Phys. 161, (1992) in press, in press. J. Chem. Phys. in press.

AISu1

Subpicosecond Laser Photoemission: Electron Dynamics in One-, Two-, and Three- Dimensions

Richard Haight*
IBM T.J. Watson Research Laboratory
P.O. Box 218 Yorktown Heights, N.Y. 10598
Fax: 914-945-2141, E--mail:rhaight at yktvmz

The semiconductor surface presents a fertile area for the exploration of the fundamental properties of systems with reduced dimension. When an atomically clean surface is created thermally or by cleavage, the resulting reconstruction can produce a variety of atomic rearrangements which must coexist with the underlying bulk system. As a consequence, the three-dimensional electronic system of the bulk can strongly couple to new states of lower dimension, which derive from the altered surface atomic structure. Such is the case for two semiconductor surface systems which will be discussed in my talk; the 2-D GaAs (110) 1x1 surface (1) and the 1-D Ge (111) 2x1 π – bonded chain system, both formed by cleavage (2).

While it is particularly interesting to study the dynamic behavior of electrons excited into states at semiconductor surfaces and interfaces, one is faced with the experimental challenge of obtaining surface sensitivity, and the necessary energy and time resolution required to observe such ultrafast phenomena. Our approach has been to use an intense, subpicosecond laser source which produces temporally synchronized pulses of both visible and extreme ultraviolet radiation. Visible 1.8 eV photons are used to photoexcite electrons into empty states above the Fermi level, while a separate pulse of 11 eV photons, derived from the same laser source, photoemits electrons from the occupied and transiently excited states of the semiconductor. Employing lasers to perform angle resolved photoemission capitalizes on many of the advantages inherent in the photoemission technique, such as surface sensitivity and wavevector resolution and additionally provides the capability of studying surfaces and interfaces in the excited state. Our investigations have revealed the manner in which electrons couple between bulk and surface bands, and interact with phonons which figures importantly in energy relaxation and electron-hole recombination.

In our study of the 2-D cleaved GaAs (110) surface, photoexcitation with 1.8 eV light results in population of the unoccupied bulk and surface states in the central valley region near the Brillouin zone center. The

---

*Work carried out in collaboration with J.A. Silberman at IBM and M. Baeumler, whose present address is: Fraunhofer Institut fur Angewandte Festkorperphysik, Tullastr. 72, D7800, Freiburg, Germany.

ACSu2

Surface Magnetism and Optical Second Harmonic Generation*

J. Reif, J.C. Zink, C.-M. Schneider, and J. Kirschner

Institut für Experimentalphysik, Freie Universität Berlin, Arnimallee 14, W-1000 Berlin 33, Germany, Fax: +(49)(30) 838 60 59

Optical Second Harmonic Generation (SHG) in reflection from centrosymmetric media has proven to be a highly surface sensitive optical spectroscopic technique[1]. On the other hand, the magneto-optical KERR effect (MOKE) has been well established as a rapid optical probe for the identification of magnetic domains at the boudary of magnetic materials[2], lacking, however, from surface selectivity.

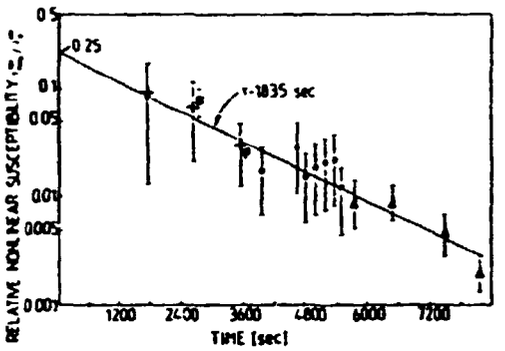

Figure 1. Relative "magnetic" nonlinear susceptiblity $\chi^{(2)}_{xxy}/\chi^{(2)}_{0}$ as a function of time elapsed since surface preparation.

In this contribution, we report on the first experimental realization of a combination of both techniques[3], in order to provide a sensitive probe for the magnetic properties of surfaces and interfaces. In a similar way as in MOKE, the internal (spin-orbit) magnetic field causes a rotation in the motion of the materials' electrons, forced to oscillate in the electric field of the incident light. This results, also for SHG, in a rotation of the polarization of the reflected light with respect to the incident one. Due to the exchange interaction in a ferromagnet, the spin-orbit fields parallel and antiparallel to the macroscopic magnetization are not equal, thus resulting in a net, readily observable effect.

With an appropriate experimental arrangement, this can be transformed in an increase resp. decrease of detected SHG signal, dependent on the direction of the macroscopic magnetization. In our experiments, we took a properly prepared Fe(110) crystal in ultra-high vacuum ($p \leq 10^{-9}$ torr), which was prepared before each experiment by sputtering and annealing. The magnetization was perpendicular, and the polarization of the fundamental and the second harmonic were parallel to the plane of incidence for the light. From the variation of the SHG yield upon reversing the direction of magnetization, we could deduce the "magnetic" contribution to the hyperpolarizability. As shown in Fig. 1, this nonlinear polarizbility decays rapidly with time after surface preparation, due to contamination from the residual gas in the vacuum chamber, predominantly CO. This clearly demonstrates the surface sensitivity of our technique, since *no* effect could be seen on conventional MOKE. The extrapolated contribution for the clean surface agrees surprisingly well with a theoretical estimate[3,4].

*Work supported by the Deutsche Forschungsgemeinschaft, Sfb 6

[1] Y.R. Shen; Ann. Rev. Mater. Sci. 86, 69 (1986)

[2] S.D. Bader; Proc. IEEE 78, 909 (1990)

[3] J. Reif, J.C. Zink, C.-M. Schneider, and J. Kirschner; Phys. Rev. Lett. 67, 2878 (1991)

[4] W. Hubner; Phys. Rev. B 42, 11 553 (1990)

ACSu3

Thermal Effects in ARUPS: Separation of Direct and Indirect Contributions

H.I. Starnberg and P.O. Nilsson

Department of Physics, Chalmers University of Technology
S-412 96 Göteborg, Sweden, Fax: +46 31 16 51 76, Bitnet: F1XHS@SECTHF51

It is well known that the presence of thermal vibrations affect ARUPS measurements by reducing the intensity of direct transitions by Debye-Waller-type factors.[1] The intensity of indirect transitions will increase with temperature, but the details of this contribution is very unclear. It was earlier thought of as rather featureless and without angular dependence, but White *et al.*[2] suggested that it may resemble the direct contribution, which makes separation of the two components extremely difficult.

We have performed ARUPS measurements on the layered compound VSe_2 at different temperatures, using He I radiation (hv = 21.22 eV). By making some simplifying assumptions we have been able to achieve a reasonable decomposition of spectra into direct and indirect components. The figure shows the decomposition of a room temperature spectrum measured at emission angle θ = 40° in the $\overline{\Gamma M}$ azimuthal direction. The results indicate that the indirect contributions already at room temperature are comparable in size to the direct components, and that they are characterized by strong angular dependence. In general the indirect component is quite similar to the direct one, but with broad diffuse peaks instead of the sharp peaks typical for the direct transitions.

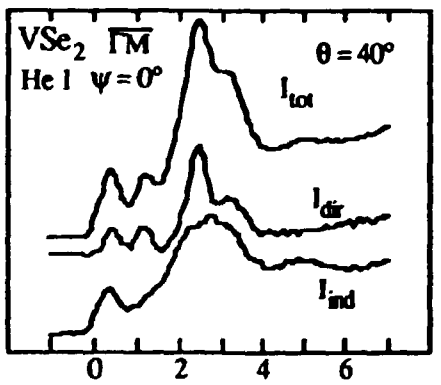

The progress made in separating direct and indirect transitions can lead to improvements in the interpretation of ARUPS spectra. The theory of indirect transitions may also benefit from the comparison with decomposed experimental data

---

[1] P O Nilsson, L Ilver, H I Starnberg and D S-L Law, J. Phys.: Condens. Matter 1, 6159 (1989).

[2] R C White, C S Fadley, M Sagurton and Z Hussain, Phys. Rev. B 34, 5226 (1986).

AlSu4

Melting and Roughening Transitions of the Copper (110) Surface

Hannu Häkkinen

Department of Physics, University of Jyväskylä,
SF-40351 Jyväskylä, Finland,
Fax: +358-41-602351, E-mail: hakkinen@jyfl.jyu.fi

A lot of recent theoretical and experimental work has been devoted to the understanding of the surface *premelting* property of crystalline materials, *i.e.*, the situation where *in equilibrium* the surface of the crystal is covered by a thin liquid like film below the thermodynamical melting point T_m. While the original idea of surface-initiated crystal melting can be traced back to the middle of the 19th century, direct measurements of clean single-crystal surfaces have been possible only during the last decade[1].

Another type of disorder, called *roughening*, is also proposed to occur on several loose-packed crystal surfaces[2]. Contrary to premelting, which includes the loss of crystallinity, atoms of the rough surface still occupy the crystalline positions, but the interface between the crystal and the vapour becomes diffuse. Quantitatively, the best measure of the rough surface is the logarithmic behaviour of the height-height correlation function between two surface elements separated by r: $G(r) \sim ln(r)$ at large r. On the atomically smooth surface $G(r)$ remains finite. Roughening is an infinite-order phase transition, hence, extremely hard to observe experimentally.

Computer simulations can, regardless of their finite-size and finite-time limitations, produce valuable information about the atomic-scale melting and roughening mechanisms. Here we report our recent investigations of thermal disordering of the copper (110) surface[3]. We employed the molecular dynamics method and a realistic many-atom potential[4] to study systematically the behaviour of Cu(110) at elevated temperatures up to the estimated bulk melting point of 1240 ± 25 K. We found that Cu(110) disorders first via anharmonic effects (up to 700 K), then by vacancy-adatom formation, and finally the surface melts around 1200 K, *i.e.*, about 40 K below the estimated bulk melting point. The melting seems to proceed via formation of atomic-scale (111) facets in the solid-melt interface, as seen in Figure 1, which shows atomic trajectories projected to a plane perpendicular to the surface.

Employing the same potential as in our surface melting study, recent lattice-gas Monte Carlo simulations[5], done in our group, have revealed that the growth mechanism of Cu(110) has a transition from a low-T layer-by-layer growth to continuous growth at high T. This is a sign of the roughening transition. The transition temperature seems to be below the surface melting temperature. A typical example of a rough surface generated by Monte Carlo at 1000 K is shown in Figure 2. At present, we are studying these initially rough configurations by molecular dynamics to confirm their stability against lattice relaxation and vibrations. We also aim to study the dynamics of the rough surface as well as the links between roughening and premelting.

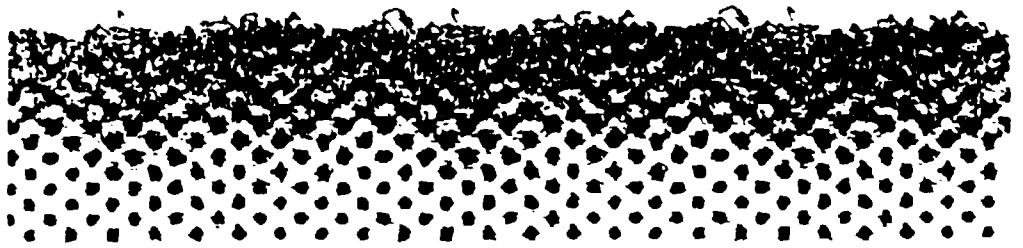

Fig.1. *Atomic trajectories of the Cu(110) (surface melt) - (bulk solid) interface projected to the plane perpendicular to the (110) face.* $T \approx T_m$.

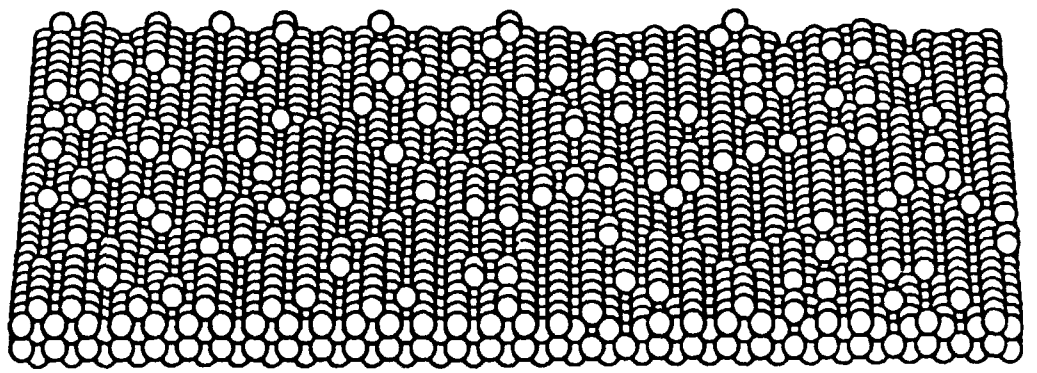

Fig.2. *A typical rough configuration of the Cu(110) surface generated by the lattice-gas Monte Carlo at 1000 K.*

---

[1]For review, see J. F. van der Veen, B. Pluis, and A. W. Denier van der Gon, in *Chemistry and Physics of Solid Surfaces* VIII (R. Vanselow and R. F. Howe, eds.) Springer, Berlin (1988).

[2]For review, see H. van Beijeren and I. Nolden, in *Structure and Dynamics of Surfaces* II (W. Schommers and P. von Blanckenhagen, eds.) Springer, Berlin (1987).

[3]H. Häkkinen and M. Manninen, Phys. Rev. B (accepted).

[4]K. W. Jacobsen, J. K. Nørskov and M. J. Puska, Phys. Rev. B 35, 7423 (1987).

[5]J. Merikoski, K. Kaski and J. Timonen, unpublished.

ACSu5

The premelting region of Pb(110) studied by low energy ion scattering

M. Schleberger, S. Speller and W. Heiland
Fb Physik, Universität Osnabrück, D-4500 Osnabrück, FRG
FAX: 49 541 969 2670

February 11, 1992

On the Pb(110) we observe point defects and an anomalous expansion of the $[1\bar{1}0]$ surface lattice constant in the premelting region (Table). Surface channeling experiments indicate that the surface roughening saturates at temperatures of about 480 K. i. e. 100 K below the surface melting temperature[1]. The channeling effects can be shown in real time (videotape).

Table: The root mean square thermal amplitude perpendicular to the surface $\sqrt{\overline{(\Delta z)^2}}$, the critical impact angle Ψ_c, the surface lattice constant a, the relative number of vacancies n in the two toplayer $[1\bar{1}0]$ chains and the mean square displacement q between the experimental and the calculated intensity vs impact angle distributions for three temperatures.

T	(K)	160	276	395
$\sqrt{\overline{(\Delta z)^2}}$	Å	0.207	0.271	0.324
$\Psi_c[1\bar{1}0]$	°	22.70	22.06	21.18
$\Psi_c[1\bar{1}2]$	°	14.66	14.66	14.66
$a_{1\bar{1}2}$	Å	6.06	6.06	6.06
$a_{1\bar{1}0}$	Å	3.50±0.01	3.63±0.01	3.82±0.01
$n_{1\bar{1}0}$	(%)	10.4±2	8.8±2	9.2±2
$n_{1\bar{1}2}$	(%)	10.3±2	9.2±3	13.6±4
$q_{1\bar{1}0}$	(10^{-5})	6.1	3.2	3.8
$q_{1\bar{1}2}$	(10^{-4})	6.2	3.2	2.5

[1] J. F. van der Veen and J. W. M. Frenken, Surf. Sci. 251/252 (1991) 1.

ACSu6

Interaction of Sulphur with Cu and Ni Surfaces studied by Scanning Tunneling Microscopy

I. Stensgaard, L. Ruan, F. Besenbacher and E. Lægsgaard
Institute of Physics, Aarhus University, DK-8000 Aarhus C
Denmark [Fax:+45 86 12 07 40] [E-mail:fysis@dfi.aau.dk]

Structural and dynamical aspects of the interaction of S (dosed from gas-phase H_2S) with several low-index Cu and Ni surfaces has been investigated with Scanning Tunneling Microscopy (STM) in conjunction with Low Energy Electron Diffraction (LEED). On Cu(111) two different phases, $\begin{vmatrix} 4 & 1 \\ -1 & 4 \end{vmatrix}$ and $(\sqrt{7}x\sqrt{7})R19°$ were observed. The mass transport involved in the formation of these phases, revealed by "filming" a large area of the surface with the STM during exposure, indicate that both phases are sulphide-like structures.

In contrast to this, both the p(5x2) and c(2x8) phases observed on Cu(110) appear consistent with pure overlayer structures formed by compression of a c(2x2)-like structure along the $[1\bar{1}0]$ direction and resulting in a height modulation of the S atoms. Prior to the formation of the p(5x2) phase an unusual mass transport was observed.

On Ni(110) the same sequence of structures appeared but a final (3x2) phase could be formed at saturation. This phase could be transformed into a p(4x1) reconstruction structure by running the STM under special tunneling conditions.

The Ni(111)-S system is presently being investigated.

Some of the results have been published in the following references:

1) I. Stensgaard, F. Besenbacher, F. Jensen, E. Lægsgaard and L. Ruan, Phys. Scripta T39 (1991) 314.

2) L. Ruan, I. Stensgaard, F. Besenbacher and E. Lægsgaard, J. Ultramicroscopy, accepted (Proceedings STM91).

3) I. Stensgaard, L. Ruan, F. Besenbacher, F. Jensen and E. Lægsgaard, Surface Sci., accepted (Proceedings ECOSS-12).

AP1

High resolution core level studies of $VC_{0.80}$ surfaces.

Leif. I. Johansson, Lennart Håkansson, Mattias Hammar* and Mats Göthelid*

Department of Physics and Measurement Technology, Linköping University, 58183 Linköping, Sweden

*Department of Material Science, KTH, 10044 Stockholm, Sweden

A calculation for TiC(100), using the full linearized augmented plane wave method (FLAPW), predicted [1] no surface core level shift in the C1s level and a surface induced shift of about 50 meV towards larger binding energy for the Ti s levels. Based on these findings it was argued that an interpretation made about the origin of surface states observed on nitride surfaces [2], as Tamm surface states, could not be correct. The absence of a surface induced shift in the C1s level was taken as evidence for that no overall electrostatic shift did exist in the surface layer potential of TiC. It was proposed that the extended valence states sample a less attractive potential in the surface vacuum region, due to charge rearrangement on the vacuum side of the surface layer, while the more localized core levels are very little affected and that this should be true also for nitrides having a similar ionicity. This thus raises the question if surface shifted C1s and N1s levels do exist on carbide and nitride surfaces. High resolution C1s photoemission spectra recorded from $VC_{0.80}$(111) (1x1) on beam line 22 at MAX-lab. are shown in the figure below and a surface shifted level is clearly observed! Results collected from the (100) surface and from the unreconstructed and reconstructed (111) surface will be presented and discussed.

1. E. Wimmer, A. Neckel and A.J. Freeman, Phys. Rev. B. 31, 2370 (1985).
2. J.E. Inglesfield, A. Callenås and L.I. Johansson, Solid State Commun. 44, 1321 (1982).

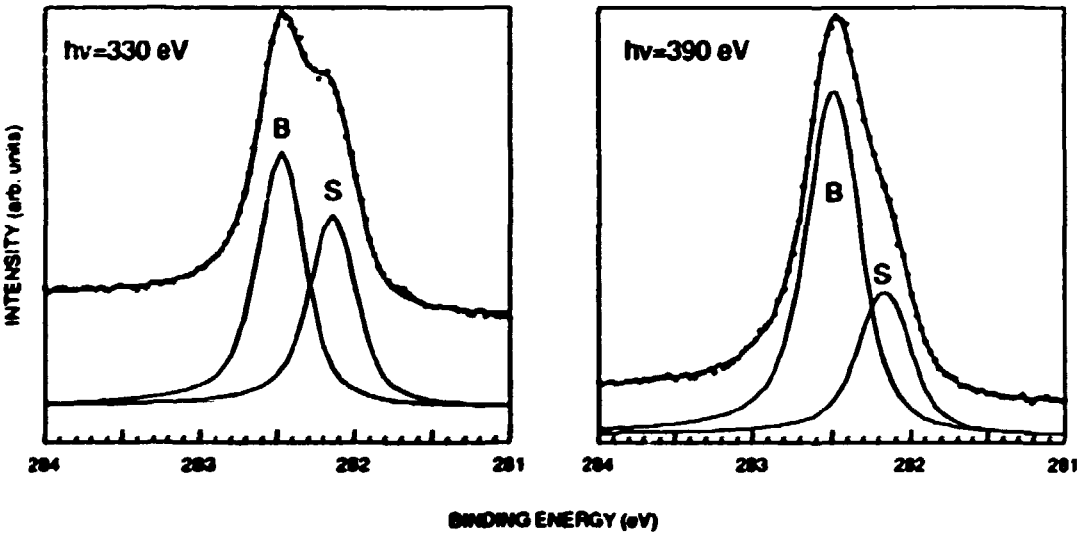

AP2

Display of LEED threshold in the Total Current Spectrum of ZnO(10$\bar{1}$0)[1]

P.J. Møller and S.A. Komolov[2]

Laboratory of Physical Chemistry, H.C. Ørsted Institute,
University of Copenhagen, 5 Universitetsparken,
DK-2100 Copenhagen Ø, Denmark, [Fax: +45 31350609]

Emergence of a LEED beam should be accompanied by a threshold decrease of the electron current transmitted through the sample. On the other hand, a decrease of transmitted current causes an appearance of the trough in the total (or target) current spectra[3,4] at this threshold energy.

In the upper part of the figure some TCS-curves are presented. The first one (1) was measured before the annealing process that is required to obtain a LEED pattern of the 1x1 ZnO(10$\bar{1}$0) surface. Curve (2) shows the spectra after annealing of the sample surface, i.e. after LEED pattern have arised in the primary energy interval 15-20 eV. Curve (3) was measured at the same surface but at an electron incidence angle of 10° with respect to the normal.

In the lower part of the figure difference spectra are displayed (curves measured at different angles are here subtracted from curve 1). The corresponding angle values are shown in the figure. It is seen that at the energy threshold at which the LEED beam emerges a pronounced trough appears in the TCS curve. This trough moves along the energy scale in accordance with the visible LEED threshold. Visible threshold and conditions of best LEED observation are marked in the figure by arrows for normal and inclined incidence.

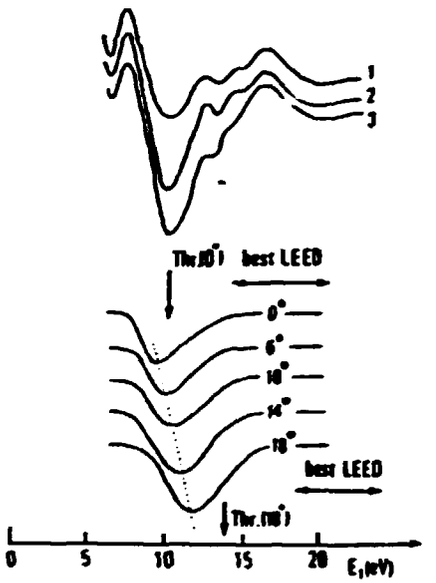

TCS spectra: $dJ(E_1)/dE_1$ against incident energy E_1 from a ZnO (10$\bar{1}$0) surface. Spectra were obtained from a room-temperature target and at the shown different angles of incidence.

[1]Work supported by the Danish Natural Science Research Council.
[2]Permanent address: Research Institute of Physics, St. Petersburg University, Russia.
[3]P.J. Møller and J.W. He, Surface Sci. 162, 209 (1985).
[4]P.J. Møller and M.H. Mohammed, Vacuum 35, 29 (1985).

AP3

SURFACE MORPHOLOGY OF CARBON FIBRES EXPOSED TO DEUTERIUM PLASMA

M. Rubel, H. Bergsåker, B. Emmoth and V. Dunaev*

Manne Siegbahn Institute of Physics, Frescativägen 24, S-104 05 Stockholm, Sweden, Fax: + 46 8 15 86 74, E-mail: "rubel@msivax.sunet.se"

*Department of Physics, St. Petersburg University, St. Petersburg, Russia

Plasma facing surfaces in controlled fusion devices undergo distinct modification caused by heat loads and interaction of particles escaping the plasma. Experimental simulation of such effects under laboratory conditions, outside the fusion machine, is difficult but necessary for preliminary tests of candidate materials for a future reactor. Carbon fibre composites (CFC) are considered as first wall components and for that reason studies of deuterium deposition and retention in such subtrates have been undertaken.

This contribution brings a report on CFC substrates exposed to the deuterium plasma in a hollow cathode device. The exposure conditions were following: total fluence up to 3 x 10^{25} m^{-2}, temperature 350 K, ion energy 100 eV. The irradiated surfaces were characterized by a number of complementary analytical techniques including nuclear reaction analysis, Rutherford backscattering spectroscopy, thermal desorption and scanning electron microscopy. The exposures of the substrates to the plasma resulted in formation of thick, up to 4 μm, deuterium containing deposits on the surfaces. The deuterium concentration in such deposits was 6.8 x 10^{22} m^{-2}. Moreover, pronounced content of deuterium, 10 - 15 times higher than the background level, was found a few millimiters beneath the exposed surface indicating deep penetration of D atoms through the leyered structure of CFC. Thermal desorption of deuterium was studied up to 1100 ° C showing the release of more than 99 % of D at that temperature. The disappearance of deuterium was accompanied by topographical changes of the surface layer as observed by scanning electron microscopy.

AP4

Surface Magnetism in Ultrafine alpha-Fe Particles[1]

F. Bødker[a], S. Mørup[a], C.A. Oxborrow[a], M.B. Madsen[b] and J.W. Niemantsverdriet[c]

[a] Laboratory of Applied Physics, Technical University of Denmark, DK-2800 Lyngby, Denmark. Fax:- (45)45 93 23 99.

[b] H.C. Orsted Institute, Universitetsparken 5, DK-2100 Copenhagen O, Denmark.

[c] Laboratory of Inorganic Chemistry and Catalysis, Eindhoven University of Technoiogy, 5600 MB Eindhoven, The Netherlands.

Ultrathin magnetic films are the usual systems used to study surface magnetism. However, ultrafine alpha-Fe particles, for which a large fraction of the atoms are in the surface layer, can also be used for these studies. Such particles are of great interest because of their many applications in catalysis, recording media, ferrofluids, etc. Using Mössbauer spectroscopy we have studied alpha-iron particles with an average diameter of 4 nm on carbon supports. Particles of this size have 25-30% of their atoms in the surface layer. Since such small particles also exhibit superparamagnetic relaxation, it is necessary to apply a field of 4 T so that the hyperfine field distributions can be studied over a range of temperatures (5–300 K).[2]

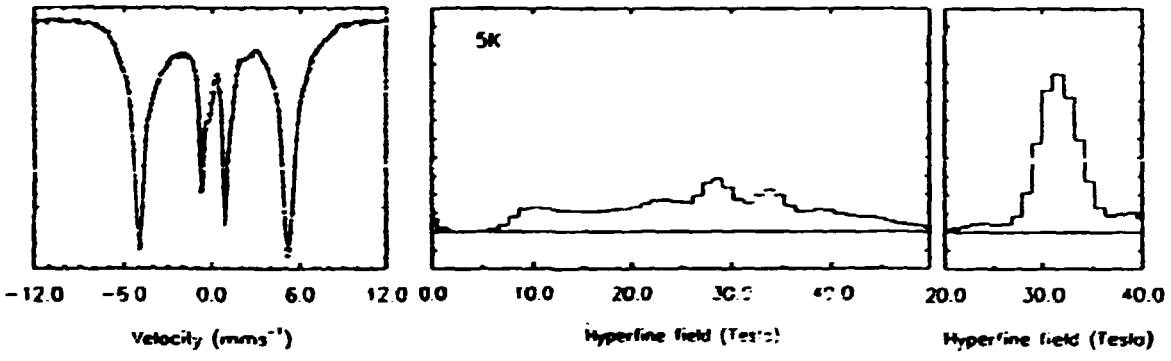

Using a computer fitting program[3] we have found that the Mössbauer spectra each contain two distributions of hyperfine fields, distinguised by their different isomer shifts. The bulk alpha-iron component has a narrow field distribution around 30 T with an isomer shift of about 0.13 mm/s at 5 K. The other component has a much broader distribution of fields with an isomer shift of about 0.54 mm/s at 5 K and accounts for 55–60% of the total absorption area of each spectrum (see figure above). Measurements on similar particles of amorphous iron-carbon alloys show that the lower part of the broad distribution is due to iron alloying with the carbon support.[4] The upper part of the distribution is due to surface iron atoms found in a variety of environments: edges, corners, planes etc. It was found that the surface hyperfine field decreases more rapidly with temperature than does the bulk iron field. Our results agree qualitatively with both other observations of surface magnetism and theoretical calculations.[5]

[1] Work supported by the Danish Council for Technical Research and the EEC Science Programme.

[2] F. Bodker, S. Morup, C.A. Oxborrow, M.B. Madsen and J.W. Niemantsverdriet, to be published in J. Magn. Magn. Mater.

[3] C. Wivel and S. Morup, J. Phys. E 14(1981)605.

[4] S. Morup, F. Bodker, J. van Wonterghem, M.B Madsen and M.D. Bentzon, Hyperfine Interactions 51(1989) 1071.

[5] P.V. Hendriksen, S. Linderoth and P.-A. Lindgård, to be published in J. Magn. Magn. Mater.

AP5

Hydrogen induced reconstruction of the Cu(100) surface studied by Transmission Channeling and Surface Peak measurements.

Morten Foss
Risø National Laboratory, 4000 Roskilde, Denmark
Fax: +45 42 37 01 15

Flemming Besenbacher and Ivan Stensgaard
Institute of Physics and Astronomy, 8000 Århus, Denmark
Fax: +45 86 12 07 40

One of the important subfields in surface science is hydrogen adsorption on metal surfaces. These systems have both technological (heterogeneous catalysis) and theoretical (hydrogen is the most simpel atom existing and is therefore a good test example) interest.
Normally, a surface is nearly "bulk terminated". However, in some cases more violent things happen: The substrate surface atoms move and a new surface structure occurs. This is in fact the case for H/Cu(100) where an exotic LEED-pattern, p4g(2×2), triggered our examination of this system.

Hydrogen is difficult or impossible to detect with most of the surface sensitive techniques like LEED, AES, XPS and XRD, but Transmission Channeling (TC) can in a rather direct and easy way detect the position(s) of hydrogen on a surface. By combining TC with a previously measured D(He,D)He scattering cross section it was possible as a function of coverage to determine the hydrogen positions relative to the bulk lattice. Furthermore the lateral displacement of the topmost layer of Cu-atoms was found by measuring the Surface Peak (SP) change when the surface reconstructed.

The idea of TC is very simple. When ions hit a single crystal near a highsymmetry axis the motion is governed by a correlated series of small angle scatterings by strings of atoms. These strings modify the initial uniform flux to a flux, which is strongly peaked in the center of the "channels" made by the strings and nearly zero near the crystalatoms. The crystal has produced an ion-probe with atomic resolution.
By measuring in several highsymmetry directions some kind of close encounter (eg RBS,FRD or NRA) events between the outgoing, modified, beam and the adsorbatatoms sitting at the exit side of the crystal, it is possible to determine the adsorbat position(s). The precise positions are found by comparing the experimental data to computersimulations. In this way it is possible to decide the vibrational amplitude, the height over the surface and the projekted position(s) of the adsorbat atoms.

SP measurements use the channeling phenomena, too, to suppress the RBS-background from the bulk of the crystal. In this way it is possible to detect the amount of RBS-scattering from the first 3-5 layers in the crystal, which is very sensitive to atomic displacements in the surface.

AP6

Surface Fractality Analysis of Porous Catalyst Support

Qingfeng Ge* and Shaofen Li

Department of Chemical Engineering, Tianjin University,
Tianjin 300072, P.R. CHINA

In heterogeneous catalytic reaction, the reaction between reactants takes place on the surface of catalyst particles. Particularly, the catalytic activity of supported catalyst is not only dependent on the form of active components, but also on the geometrical nature of support. The founding of fractal geometry provides an alternative selection to study the complex objects such as porous catalyst[1]. The surface pore structure of porous $\gamma - Al_2O_3$ was investigated with SEM and adsorption methods. The SEM photos with different magnifications show that the surface of $\gamma - Al_2O_3$ particle is of self-similarity qualitively. The monolayer values of different adsorbates was determined with the frontal gas chromatography and the results are given in Table 1.

Analyzing the experimental results we will find that the specific surface area measured with one method(eg. N_2-BET) can not be considered as the absolute value of the surface area for the solid with porous structure, because it depends on the method itself strongly. A very obvious example is the surface area from adsorption is a function of molecule size of adsorbate. Different size molecules can "probe" different part of surface. The surface pore structure was analyzed based on fractal geometry and the fractal dimension, 2.78, was calculated from the experimental data.

Table 1: Monolayer Value of Different Adsorbates on $\gamma - Al_2O_3$(317.5K)

Adsorbates	density (g/cm^3)	σ_m ($\AA^2$)	Ad.Val.(mmol/g)		Sur.Area(m^2/g)	
			size 1*	size 2	size 1	size 2
n-Butane	0.5380	34.70	0.825	0.822	172.4	171.8
Benzene	0.4825	31.34	0.954	0.963	180.1	181.8
n-Hexane	0.6250	40.83	0.663	0.675	163.0	166.0
n-Heptane	0.6545	43.78	0.615	0.623	162.2	164.3
n-Octane	0.6745	46.83	0.558	0.562	157.4	158.5
n-Nonane	0.6930	49.68	0.490	0.487	146.6	145.7

* size 1 and size 2 in table represent -80+100 and -250+280mesh respectively.

*Present address: Chem. Lab. III, H.C. Ørsted Institute, University of Copenhagen, DK-2100 Copenhagen, Denmark

[1] Avnir D. ed. "The Fractal Approach to Heterogeneous Chemistry", Wiley, Chichester(1989)

AP7

Ordered Water Adsorption on Ionic Crystals*

J. Reif, J.C. Zink, and E. Matthias

Institut für Experimentalphysik, Freie Universität Berlin, Arnimallee 14, W-1000 Berlin 33, Germany, Fax: +(49)(30) 838 60 59

We report on the investigation of controlled water adsorption on alkaline earth halide surface at room temperature, using surface sensitive optical Second Harmonic Generation[1] (SHG) to probe the symmetry of the surface/interface. In particular, we studied polished (111) cleavage planes of BaF_2 and CaF_2, mounted in an ultra-high vacuum environment and being, after cleaning by baking, exposed to well determined water doses. We measured the influence of the resulting water coverage on the azimuthally anisotropic polarization dependence of the SHG yield[2].

The principal result[3] is shown in Fig. 1: Despite identical C_{3v} symmetry for both crystals, after exposure to laboratory air only the SHG signal from the BaF_2 surface exhibits the expected azimuthal anisotropy, while that from CaF_2 is isotropic. In contrast, the clean surface behaves regularly for both substrates, with significantly higher nonlinear polarizability normal to the surface for BaF_2. For intermediate water exposure, the effect of the azimuthal structure appears to be even enhanced.

A more detailed investigation, as in Fig. 2, reveals that the total signal decreases for both crystals with water coverage, but that there is a distinct difference in the effect on the anisotropy. While for low coverage the surface symmetry is conserved and the corresponding hyperpolarizability is even increased, at high coverage both substrates show different responses: On BaF_2, the symmetry at the interface still is conserved, on CaF_2 it is obviously destroyed. This may be explained by pseudomorphus ice-I epitaxy on BaF_2, while on CaF_2 a rearrangement at the interface has to take place, once the water molecules get so close to one another that intermolecular hydrogen bonds start to be formed.

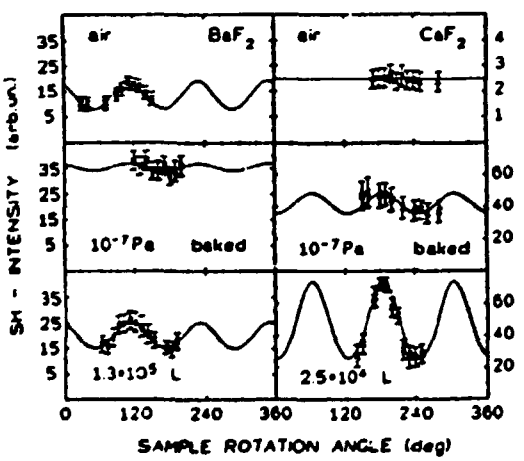

Figure 1. Azimuthal dependence of SHG yield from BaF_2(111) (left) and CaF_2(111) (right) in laboratory air (upper), for a clean surface (middle), and with intermediate water coverage (lower).

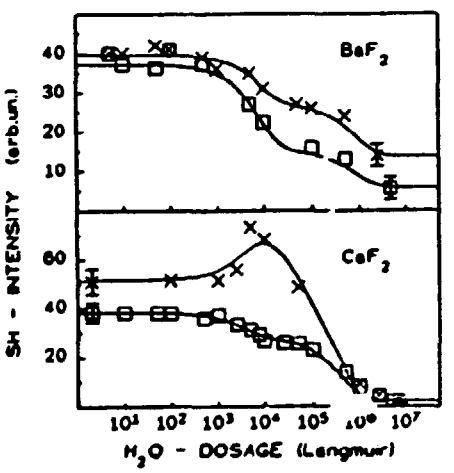

Figure 2. Dependence of SHG yield on water exposure. Shown is the effect on the maximum (×) and minimum (□) of the azimuthal dependence in Fig. 1. The solid lines are fits to Langmuir kinetics.

*Work supported by the Deutsche Forschungsgemeinschaft, Sfb 337

[1] Y.R. Shen; Ann.Rev.Mater.Sci. 86, 69 (1986)

[2] J. Reif, P. Tepper, E. Matthias, E. Westin, and A. Rosén; Appl.Phys. B 46, 131 (1988)

[3] J.C. Zink, J. Reif, and E. Matthias; submitted to Phys.Rev.Lett.

AP8

High Pressure Synthesis and Hydrogenation of Formate on Cu(100)

P. A. Taylor, P. B. Rasmussen, and I. Chorkendorff
Laboratory of Applied Physics, The Technical University of Denmark
2800 Lyngby, Denmark [FAX: (45)-45-93-23-99 E-mail: taylor@ltf.dth.dk]

On the commercial methanol catalyst, copper particles are highly dispersed on ZnO where the copper surface is believed to be the active catalyst component. To study the role of copper, the fundamental steps of methanol synthesis have been investigated on a well defined Cu(100) crystal. The studies were carried out in a UHV chamber containing a high-pressure-cell and traditional surface analysis tools.

The adsorption and desorption of H_2, CO_2, and HCOO (formate) have been studied individually and in various mixtures. It has been proved that formate, which is believed to be an important intemediate in the methanol synthesis, can be synthesized on the Cu(100) surface from a high pressure exposure to a CO_2/H_2 gas-mixture [1]. The kinetics of this reaction step have been studied in detail as a function of gas-mixture, pressure, and temperature. In a 70:30 CO_2/H_2 gas-mixture at 2.3 bar, the overall activation energy for the synthesis of formate was found to be 55.6 kJ mol^{-1}.

The formate surface species was also found to undergo further hydrogenation at high pressures of H_2 [2]. The rate of hydrogenation of formate has been studies as a function of both H_2 pressure and temperature. At 5.8 bar of H_2, the activation energy for hydrogenation was found to be 82 kJ mol^{-1}.

---

[1] P. A. Taylor, P. B. Rasmussen, C. V. Ovesen, P. Stolze and I. Chorkendorff., Surf. Sci. 261 (1992) 191.

[2] I. Chorkendorff, P. A. Taylor, and P. B. Rasmussen, J. Vac. Sci. Technol., in press

AP9

Stabilization of Carbon Dioxide on Cu(100) by co-adsorption of Formate

P. B. Rasmussen H. Christoffersen P. A. Taylor and I. Chorkendorff
Laboratory of Applied Physics, The Technical University of Denmark
2800 Lyngby, Denmark [FAX:(45)-45-93-23-99 E-mail: bilde@ltf.dth.dk]

The adsorption of CO_2 on Cu is an important step in industrial synthesis of methanol from $CO_2/CO/H_2$ gas mixtures on Cu based catalysts. Recently it has been conclusively shown that formate can be synthesized on Cu(100) from gas mixtures of CO_2 and H_2 [1]. The interactions of CO_2 with clean [2] and formate covered [3] Cu(100) have been investigated in the temperature range 80 to 130 K by high resolution electron energy loss spectroscopy (HREELS) and temperature programmed desorption (TPD).

On the clean surface, the HREEL spectrum of CO_2 exhibits only one energy loss of 82 meV due to the symmetric bending of the CO_2. This suggests that the molecule is lying flat, with the molecular axis parallel to the surface. The TPD spectra show that only one binding state with a peak temperature of 86 to 90 K exist on the clean surface. From the TPD spectra, it is found, that the binding energy of adsorbed CO_2 increases with increasing CO_2 coverage.

On the formate covered surface, the TPD spectra show, that the formate induces a new binding state with peak temperature increasing from 95 to 104 K with increasing formate coverage. The maximum obtainable population in the new state increases with increasing coverage of formate. In the HREEL spectrum, two new losses of 79 meV and 288 meV are observed besides those of formate. The new losses are identified as the CO_2 symmetric stretch and the CO_2 symmetric bending. The observation of the symmetic stretch suggests that the presence of formate has induced a geometrical change in the adsorbed CO_2.

---

[1] P. A. Taylor, P. B. Rasmussen, C. V. Ovesen, P. Stolze and I. Chorkendorff., Surf. Sci. 261(1992)191

[2] P. B. Rasmussen, P. A. Taylor and I. Chorkendorff., Surf. Sci. in press

[3] P. A. Taylor, P. B. Rasmussen and I. Chorkendorff., Accepted for publication in J. Vac. Sci. Technol. A

AP10

Growth of ultrathin films of Cu on CaO(001)[1]

Hanne M. Meergaard and P.J. Møller

Laboratory of Physical Chemistry, H.C. Ørsted Institute,
University of Copenhagen, 5 Universitetsparken,
DK-2100 Copenhagen Ø, Denmark, [Fax: +45 31350609]

Ultrathin films of copper have been deposited on room-temperature CaO(001) surfaces by atomic layer metal-beam epitaxy techniques.[2]

The metal was deposited at a rate of 1 Å/min varying from 0.1 Å at submonolayer coverages to 10 Å at higher coverages, in some cases until total coverages as high as 100 Å were reached.

The growth of copper was analyzed by means of Auger electron spectroscopy, low energy electron diffraction and quarz crystal microgravimetry. Upon a 1x1 CaO(001) surface the mode of growth was found to be of the Stranski-Krastanov type (layer-plus-islands), a growth mode that has been observed on several other metal oxide surfaces as well.[3-5] Epitaxial growth structures were observed upon annealing near-monolayer-covered surfaces until approximately 250 °C.

Electronic structures for the deposition of Cu upon 1x1 CaO (001) were investigated in situ at submonolayer coverages by AES and electron energy-loss spectroscopy (EELS) at primary energies of 190 eV and the low-energy feat[illegible] to the growth of Cu were clearly identified.

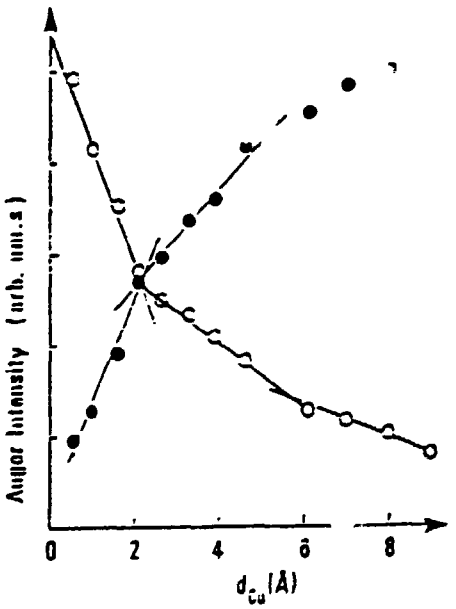

Auger dN(E)/dE intensity of copper (•) and of Ca to CaO ratio (○) versus averages deposition thickness d_{Cu} of Cu deposited at 293 K on 1x1 CaO (001). The first breakpoint corresponds to Cu monolayer coverage.

[1]Work supported by the Danish Science Research Councils and Center for Surface Reactions.

[2]P.J. Møller and J.W. He, J. Vac. Sci. Technol. A5, 996 (1987).
[3]J.W. He and P.J. Møller, Surface Sci. 178, 934 (1986).
[4]P.J. Møller and M.C.Wu, Surface Sci. 224, 265 (1989).
[5]C. Argile and G.E. Rhead, Surface Sci. Reports 10, 277 (1989).

AP11

Wear Resistant Sulphur Films on Stainless Steel Studied by Auger Electron Spectroscopy and Sputter Profiling, including Factor Analysis [1]

C. Jansson, Fysisk Institut, Odense University, Campusvej 55, DK-5230, Odense M, Denmark, G. T. Nielsen, and J. Jakobsen, AME, Building 403, The Danish Technical University, DK-2800, Lyngby, Denmark, and P. Morgen, Fysisk Institut, Odense University, DK-5230, Odense M, Denmark
(Fax: +45 66 15 87 60)

Tribological processing of 52100 steel elements with hardnesses of 850 Vickers or above has been monitored with Auger spectroscopy and sputter profiling. In particular, tribological procedures leading to highly scoring wear resistant surfaces were followed to understand the roles of *S* and *O*.

It was found that a characteristic *S* concentration profile ("film"), with 85 % *FeS*, established at surfaces after a specific running-in procedure with a saturated solution of clean, yellow *S* in paraffinic oil, delineated cases where scoring wear resistance is obtained (attainment of a static coefficient of friction of 0.74-0.76 in dry running situations) from other cases. The highest scoring wear resistance occurs at saturation of the surface layers with *S*. Additionally, a supply mechanism must be available, with a reservoir of bulk - or subsurface - dissolved *S*, to provide the surface with *S* through diffusion, during extended periods of dry running.

Oxides are always found in Auger analysis of the samples, but their presence in tribological contact situations is shown to be insignificant. Wear of hard steel surfaces, on the other hand, is found to occur through loss of oxide debris. Oxidation experiments show the scoring wear resistant surfaces to be the most difficult to oxidise. During oxidation the sulphur is displaced, or covered with oxide.

The present results are in qualitative agreement with earlier studies on *Fe-S* interactions, oxidation of *Fe-S* systems and findings for - or assumptions about - the mechanisms of *S* as an EP (extreme pressure) additive in lubricants through its binding to the surfaces. However, for the first time, we here clearly correlate mechanical surface properties with details of the surface chemical and physical compositions.

---

[1] Work supported by the Danish Technical-Scientific Research Council, grant no.5.17.1.6.04.

AP12

Influence of Defects on the Ni2p and O1s XPS-Spectra of Nickel-Oxide

St. Uhlenbrock, Chr. Scharfschwerdt, M. Neumann

Universität Osnabrück Fachbereich Physik, Postfach 4469, D - 4500 Osnabrück, FRG

FAX: 0541-969-2670, E-Mail: UHLENBRO@DOSUNI1 BitNet

G. Illing, H.-J. Freund

Lehrstuhl für Physikalische Chemie I, Ruhr-Universität Bochum

Universitätsstrasse 150, D-4630 Bochum, FRG

NiO was the subject of many experiments and discussions in the last decade. By now especially the Ni2p and O1s spectra are of great interest. It is well accepted that the Ni2p photoelectron spectrum of NiO exhibits a very strong satellite structure. In particular the satellite 2 eV above the main line has been interpreted by several authors. The O1s spectrum, where a peak at the high binding energy side appears is discussed controversially. Recent attempts tried to attribute the 2 eV Ni2p satellite to Ni^{3+} species, existing on the surface. A correlation to the additional feature in the O1s spectrum was found. We will show by comparisons of Ni2p, O1s spectra of different prepared surfaces that the situation is slightly more complicated.

All experiments were performed in Ultra-High Vacuum with monochromatized Al K_α radiation. Under these conditions the O1s spectrum of a freshly cleaved NiO single crystal shows no extra features and can be fitted with a single symmetric Gaussian line profile. On this perfect surface the Ni2p spectrum exhibits a satellite which cannot originate from Ni^{3+}-states. A sputter series shows the developing of a new feature at the low binding energy side and the growth of the satellite, whereas the O1s spectrum remains unchanged. The new Ni2p peak can be attributed to metallic Ni. Angle dependent measurements indicate that the satellite feature originates from a superposition of a bulk effect and Ni^{3+}-species localized close to the surface. Further measurements allow us to relate the O1s satellite to the adsorption of oxygen containing species on the surface of the NiO single crystal.

AP13

Free energy and entropy barrier for adatom selfdiffusion on Cu(100)

L. B. Hansen, P. Stoltze, K. W. Jacobsen and J. K. Nørskov
Laboratory of Applied Physics, Technical University of Denmark, DK 2800, Lyngby, Denmark
e-mail lhansen@ltf.dth.dk, FAX (+45) 45 93 23 99

For selfdiffusion of metal atoms adsorbed on a Cu(100) surface a more complex diffusion path compared to the ordinary bridge diffusion has been found both theoretical and experimentally [1].

Field emmision experiments on Ir(100) and Pt(100) suggest that the diffusion between two adjacent hollow sites occurs by exchange with one of the atoms in the surface, rather than the simpler diffusion path over the two-fold coordinated bridge cite. Local density calculations for Al adatoms on Al(100) has supported this picture and attributed it to a covalent bonding between the two moving atoms.

Recently we found the same mechanism on Cu(100) using the effective medium theory to calculate the energetic [2]. The activation barrier for the exchange diffusion was found to be 0.2 eV compared to 0.4 eV for the bridge diffusion [3].

The situation with two competing diffusion paths has led to interest in the finite temperature effects on the diffusion rates.

We have calculated the free energy differences for the adatom in the transition states and in the hollow site, using the monte-carlo Acceptance Ration Method by Bennett.[4]. This method uses canonical ensemble expressions for the partition functions to obtain the ratio of these for systems with different potential functions acting on the same configuration space. The method can however, by the use of configuration space transformations , also be used for one potential functions acting on different parts of the configuration space[4].

The entropi for both diffusion paths is found to be higher for the adatom in the transition state, compared to the adatom in the stable hollow site at room temperature. The entropi differences is compared to results in the quasi-harmonic approximation.

Financial support from the Danish Research Councils through the Center for Surface reactivity is gratefully acknowledged.

[1] G. Kellogg and P.J.Feibelman, Phys.Rev.Lett. 64, 3143, (1990)
[2] K.W. Jacobsen, J.K. Nørskov and M.J. Puska, Phys. Rev. B35 (14), 7423 (1987)
[3] L.B.Hansen, P. Stoltze, K.W. Jacobsen and J.K. Nørskov, Phys. Rev. B 44, 6523 (1991)
[4] Bennett C. Bennett, Jour. of Comp. Physics, 22,1976,245

AP14

Adsorption of K and CO on Cu(111) Studied by Photoemission and Thermally Stimulated Desorption

M.Christiansen, J.Onsgaard, E.V.Thomsen, B.Jørgensen, J.Storm, D.Batchelor* and D.Adams*

Fysisk Institut, Odense University, DK-5230 Odense M

*Det fysiske Institut, Aarhus Universitet, DK-8000 Aarhus C

Coadsorption studies of an alkali metal and low molecular gases like CO, CO_2 and H_2 on low-index surfaces of copper are of importance for an understanding of the basic mechanisms in the methanol synthesis. Here we report on the adsorption and coadsorption of K and CO on Cu(111) studied by the methods of synchrotron-radiation spectroscopy (SRS), thermally stimulated desorption (TSD), and work function measurements. A SX-700 monochromator and a concentric hemispherical analyzer were used in the photoemission experiments carried out at BESSY. The TSD measurements were carried out at [illegible] University. Work function measurements were used to establish the link between the two different set of measurements.

K adsorption on Cu(111) and CO adsorption on Cu(111)

The maximum reduction in the work function is 3.7 eV at half a monolayer coverage and the difference between clean Cu(111) and the K-saturated surface was 2.7 eV. Electron energy distribution curves of C(1s) from 2 L CO adsorbed on Cu(111) at 123 K are shown in the figure, curve (a). A three-peak structure with two distinct lines below the main line is observed.

Coadsorption of K and CO on Cu(111)

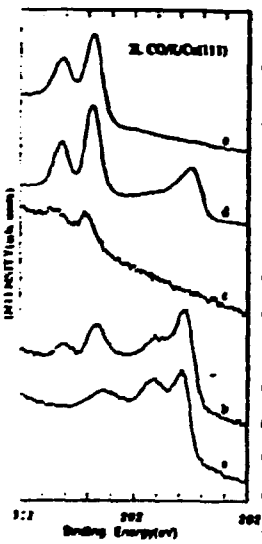

CO adsorption on a Cu(111) surface with different preadsorption coverages of K was studied with SRS and TSD. Graph (b), CO(2L)/K(0.1ML)/Cu(111), shows the 1s core lines of C and K. The effect of heating this interface to 300 K is very clear. Both C, graph (c), and O disappear. Deposition of 0.5 ML K on Cu(111), followed by a 2 L CO exposure, strongly changes the spectrum, graph (d). Heating this interface to 300 K results, (e), in disappearance of C whereas O is still present with a substantial chemical shift. CO dissociates during heating and C disappears from the surface. The present study shows the influence of the K-coverage on the binding state of CO on Cu(111), particularly the dissociation of CO on the surface when the crystal is heated from 120 K to 300 K. Chemical shifts and line shape variations of the C(1s) and O(1s) core electrons reflect both the local changes in the binding due to K and the final state effect in the photoemission process[1]. Another finding is that the adsorption of CO and K on Cu(111) differs from CO/K on Cu(110), where both new CO states and simultaneous desorption of CO and K were found[2], reflecting the difference in corrugation between the two surfaces.

[1]N.Mårtensson and A.Nilsson, Journal of Electron Spectroscopy and Related Phenomena, 52 (1990)1.

[2]M.Christiansen, E.V.Thomsen and J.Onsgaard, Surface Science 261 (1992) 179.

AP15

Microstructure on Al/Al_2O_3 interfaces investigated by optical second harmonic generation

C.Jakobsen* , D.Podenas‡ and K.Pedersen*
* : Institute of Physics, University of Aalborg, DK-9220 Aalborg
Denmark, Fax:+045 98 156502, E-mail:113chrj@vax87.aud.auc.dk
‡ : Physics Faculty, Vilnius University, Vilnius, Lithuania, Fax: (0122) 77 56 23

Mechanically polished Al(100) crystals cut with a small off-set angle in the [100] direction have been investigated by optical second harmonic generation (SHG) while they were kept in free air. The dominating part of the SH signal is generated at the interface between the metal and the oxide layer. With a pump wavelength of 1064 nm, a strong variation in the SHG yield is observed as the crystals are rotated about the surface normal (fig.1). This rotational anisotropy is found to increase quadratically with the off-set angle α, for small off-set angles (fig.2). When the pump wavelength is changed to 532 nm, the rotational variation in the SH signal largely disappear. The rotational anisotropy is also found to gradually disappear as the samples are electropolished. The behavior of the SH signal from the mechanically polished samples has a strong resemblance to the large polarizability of steps on vicinal clean Al and oxide covered Si surfaces witch has recently been observed.[1,2] Thus, for comparison a sample with $\alpha = 5^0$ has been cleaned in ultra-high vacuum and a double-spot LEED-pattern indicating monoatomic steps was observed. An order of magnitude enhancement of the SH signal occurred when the infrared pump beam was polarized perpendicular to the step edges relative to the signal from a beam polarized parallel to the steps. This anisotropy decreased significantly with temperature up to 350^0C as the steps got more and more disordered . For a green pump beam the steps had little effect on the SH signal.

The similarity in the frequency dependence found for the oxide covered samples and the clean sample with steps show that the same mechanism could be responsible for the rotational anisotropy. Furthermore, the quadratic dependence on the miscut angle points at regularly spaced SH sources. Thus, the SHG experiments on miscut Al(100) samples indicates that the mechanical polishing process probably through strains creates an interface between the metal and the oxide layer with steps with a high degree of order.

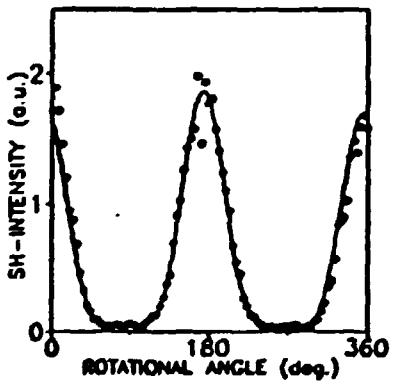

fig.1.

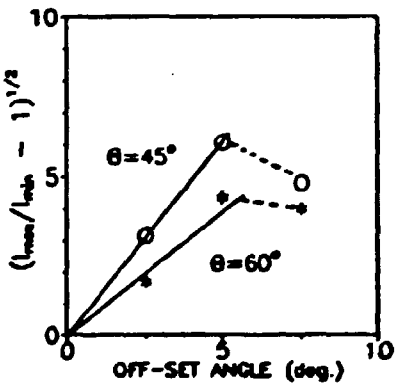

fig.2.

[1]S. Janz, D. J. Bottomley and H. M. van Driel, Phys. Rev. Lett. 66, 1201(1991).
[2]C. W. van Haggelt, M. A. Verheijen and Th. Rasing, Phys. Rev. B 42, 9263(1990).

AP16

Thermal Desorption Rates For Cs And Cs^+ On Ir Surfaces With Graphite Structures Present

Tony Hansson, Jan B.C. Pettersson, and Leif Holmlid

Department of Physical Chemistry, Chalmers University of Technology, S-41296 Göteborg, SWEDEN, [Fax: +46-31167194]

Rates for thermal desorption of caesium atoms as well as positive ions from a hot, polycrystalline iridium surface are studied. In particular, the influence of low and high coverages of graphite present on the surface is investigated. The measurements are performed in two temperature intervals 670-910 K[1] and 1130-1850 K[2]. In the upper temperature interval, the field-reversal method[3] is utilized. In these experiments, a surface coverage of 0.5 % graphite is present. At lower temperatures, and both with a full monolayer and 0.5 % of graphite on the surface, laser-induced thermal desorption is used as a probing tool. In both temperature intervals, the desorption rates obtained follow first-order kinetics, and the rate constants range from 10^{-5} s^{-1} to 10^{6} s^{-1}. The ionic desorption rate is alway greater than the neutral.

A comparison of the desorption barriers to the values measured on clean Ir and graphite surfaces shows that the neutral desorption is only taking place from graphite surface states. Further, two parallel desorption processes are detected at the highest temperatures, i.e. above 1540 K. The fastest has a frequency factor typical for direct desorption from the graphite surface. The slower process exhibits the same barrier to desorption, but a lower frequency factor. This means that the "slower" neutrals desorb from the same state, but first have to migrate from some other place, probably from below the graphite islands. In the low temperature experiments, the neutral desorption rate is unmeasurably slow, both with low and high graphite coverage.

At low graphite coverage, the ionic desorption is originating from iridium at temperatures below 1320 K. Above 1320 K, also the ionic desorption proceeds via states on the graphite surface. At even higher temperatures, above 1640 K, the desorption rate becomes diffusion (to the graphite islands) limited. In the low temperature and high graphite coverage experiments, three parallel desorption processes are obtained. They all have identical activation barriers to desorption, but different frequency factors. This is interpreted as being due to desorption of Cs adsorbed on the graphite layer, migrating from graphite grain boundaries, and migrating from below the graphite layer.

---

[1] T. Hansson, J.B.C. Pettersson, and L. Holmlid, Surf. Sci. 253 (1991) 345.

[2] T. Hansson and J.B.C. Pettersson, Surf. Sci. in press.

[3] L. Holmlid and J.O. Olsson, Rev. Sci. Instr. 47 (1976) 1167.

AP17

MATRIX CORRECTIONS AND THEIR ROLE IN QUANTITATIVE AUGER ANALYSIS.

S. Mróz

Institute of Experimental Physics, University of Wrocław, ul. Cybulskiego 36, PL 50-205 Wrocław, Poland. Fax: (4871)201467.

Methods of experimental determination of an inelastic mean free path λ of electron in solids[1] and a backscattering factor R in Auger electron spectroscopy[2] were elaborated. λ and R obtained for noble metals with the use of those metods are presented[2,3] and compared with results of theoretical calculations known from literature.

The role of matrix corrections, including corrections for λ and R, in the quantitative Auger analysis (QAA) of metallic alloys is discussed on the basis of the experimental data known from literature. It was found that correction for atomic densities n of of the sample - and pure standards of its components[4] (n - correction) is much more important than corrections for λ and R. The average error of QAA for 6 independent analyses of numerous metallic alloys performed without any corrections, with only n - correction and with the full correction is equal to 4.61, 2.04 and 1.77 %, respectively.

Thus, the attention in further QAA development should be focused on the improvement of the sample surface preparation and Auger signal measurement including the correct background subtraction.

---

[1] W. Dolíński, H. Nowicki and S. Mróz, Surf. Interf. Analysis 11, 229 (1988).

[2] J. Palczyński, W. Dolíński and S. Mróz, Surface Sci. 247, 395 (1991).

[3] W. Dolíński, S. Mróz, J. Palczyński, B. Gruzza, P. Bondot and A. Porte, Acta Physica Polonica, in press.

[4] S. Mróz and A. Mróz, phys. status solidi (a) 95, 407 (1986).

AP18

A high resolution core level study of the low index surfaces of Cr_3Si

K.L. Håkansson*, L.I. Johansson* and A.N. Christensen**

*Dep. of Physics and Meas. Technol., Linköping University,
S-581 83 Linköping, Sweden, [Fax: +46 13 13 75 68]
**Dep. of Chemistry, Aarhus University, DK-8000 Aarhus C, Denmark

High resolution angle-resolved photoemission investigations of core levels of the (100), (110) and (111) surfaces of Cr_3Si have been performed using synchrotron radiation from beam line 41 at MAX-lab. The crystals were cleaned in situ by a short Ar+ ion bombardment followed by repeated short annealings to temperatures in the range 800-1100° C. The cleaning procedure were checked using Auger electron spectroscopy (AES) and low energy electron diffraction (LEED) to produce clean and well ordered surfaces. Distinct 1x1 LEED-patterns were observed from the (110) and (111) surfaces. The (100) surface exhibited weaker superstructure spots that we suggest to originate from a two domain c($\sqrt{2}$x2$\sqrt{2}$)R45° overlayer structure. Surface shifted Si 2p levels were observed on all three surfaces but no shifted Cr 3p levels could be identified. The core level shifts were extracted using a curve fitting procedure and it was found necessary to use two surface shifted components for each surface.

The reaction rate for these surfaces upon oxygen exposure was investigated and significant differences were observed. Initial Si oxidation was observed on all three surfaces while Cr oxidation could be revealed only after higher oxygen doses. Clear diffraction effects were observed in the Si 2p surface to bulk intensity ratio both as a function of electron emission angle and photoelectron kinetic energy.

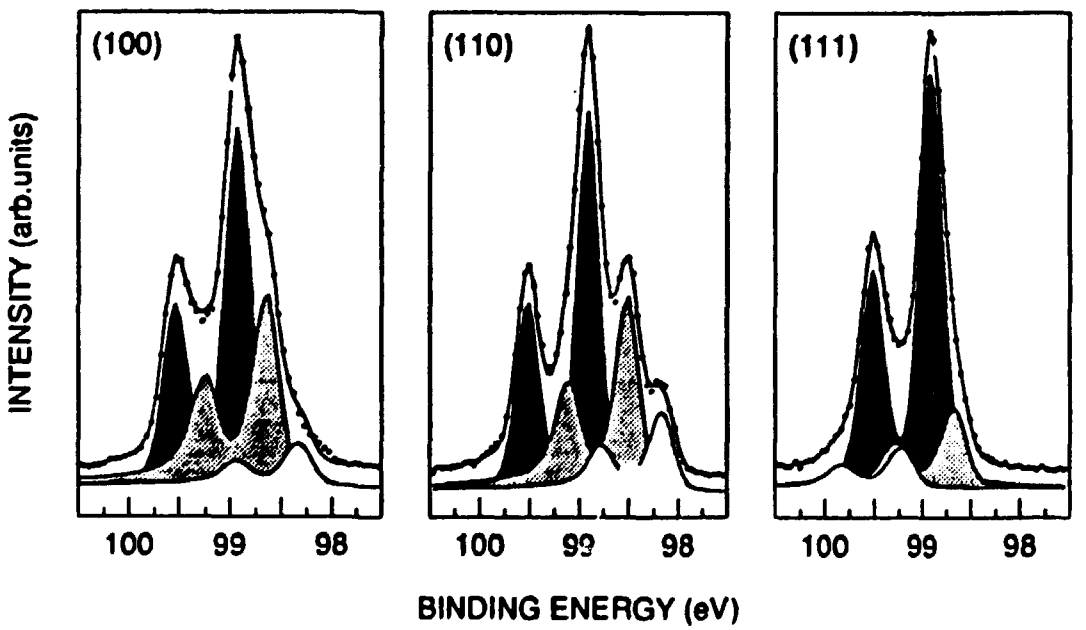

Si 2p core level spectra recorded at normal emission from the three different surfaces using a photon energy of 130 eV. The shaded curves show the extracted bulk (dark) and surface shifted (lighter) components.

AP19

Sputtering of thick nitrogen and oxygen films by keV hydrogen ions

O. Ellegaard[*], J. Schou[*], B. Stenum[*], H. Sørensen[*], R. Pedrys[$], D.J. Oostra[£], A. Haring[£] and A.E. deVries[£].

[*]Risø National Laboratory, DK-4000 Roskilde, Denmark,
[$]Institute of Physics, Jagellonian University, PL-30059 Krakow, Poland, and
[£]FOM-Institute for Atomic and Molecular Physics, NL-1098 SJ Amsterdam, The Netherlands.

The sputtering yield of frozen nitrogen and oxygen has been determined for primary hydrogen ions with energies from 5 to 10 keV. The films of the frozen gases (3-4 $.10^{17}$ molecules/cm^2) were deposited at an oscillating quartz microbalance kept at liquid-helium temperature. The sputtering yield was determined directly from the weight loss of the film during ion irradiation[1)].

None of the frozen gases shows any yield dependence apart from a minor contribution from backscattered ions for very thin films (< 1.10^{17} molecules/cm^2). The sputtering yield ranges from 5 N_2/H_n^+ to 20 N_2/H_n^+ for solid nitrogen, whereas the yield for solid oxygen varies from 10 O_2/H_n^+ to 100 O_2/H_n^+ with increasing energy. The data indicate largely that the sputtering yield is proportiona. to the stopping power squared. This behaviour demonstrates that the erosion process is electronic sputtering rather than ordinary (knockon) sputtering[1,2)]. The surprising difference between the yield from solid nitrogen and oxygen is primarily caused by effective dissociation processes, which take place in oxygen during the electronic deexcitation.

---

1) B. Stenum, J. Schou, O. Ellegaard, H. Sørensen and R. Pedrys, Nucl. Instr. Meth. B 58, 399 (1991).
2) K.M. Gibbs, W.L. Brown and R.E. Johnson, Phys. Rev. B 38, 11001 (1988).

AP20

Weighted density functional theories of drying at solid-fluid interfaces: clarification of recent controversies

J.R. Henderson[§], P. Tarazona[†], F. van Swol[‡] and E. Velasco[¶†]

[§]School of Chemistry, University of Leeds, Leeds LS2 9JT, UK
[†]Departamento de Física de la Materia Condensada,
Universidad Autónoma de Madrid, E-28049 Madrid, España
[‡]Department of Chemical Engineering,
University of Illinois, Urbana, Illinois 61801, USA
[¶]Kemisk Laboratorium III, H.C.Ørsted Institutet,
Universitetsparken 5, DK-2100 København Ø, Danmark

Abstract

The statistical mechanics of contact angle phenomena and wetting/drying transitions at wall-fluid interfaces has benefitted from a series of recent computer simulation studies and density functional treatments. Various groups have contributed to this effort and none of the results published to date appear to be in agreement. In particular, seemingly conflicting reports on the nature of the drying transition at model wall-liquid interfaces have generated significant confusion. We have clarified[1] the situation by (i) demonstrating full consistency between two weighted density-functional studies of wall-fluid interfaces, previously thought to be in conflict, and by (ii) reporting on a new density-functional analysis of an earlier controversy surrounding the measurements of contact angle by computer simulation procedures involving 'live' walls.

[1] J. Chem. Phys. (in press)

AP21

A STM STUDY OF Sn INDUCED RECONSTRUCTIONS ON Ge(111)

M. Göthelid, M. Hammar, C. Törnevik, U.O. Karlsson, N.G. Nilsson and S.A. Flodström
Department of Physics, Royal Institute of Technology,
S-10044 Stockholm, Fax +46 8 249131

Ultra high vacuum (UHV) scanning tunneling microscopy (STM) has been applied to some of the Sn induced surface reconstructions on the Ge(111) surface, to reveal the surface atomic geometry and to study the atomic species of the adatoms on some of the reconstructions.

After deposition of 0.4 monolayers (ML) of Sn and subsequent annealing at 400°C three surface superstructures were found, (7x7), (5x5) and ($\sqrt{3}$x$\sqrt{3}$)R30°, hereafter denoted $\sqrt{3}$. Increasing of the annealing temperature to 500°C made the $\sqrt{3}$ structure disappear. At 0.1 ML Sn coverage the $\sqrt{3}$ structure could be seen in the STM image, although no LEED pattern corresponding to the surface geometry was detectable. The STM image showed the top layer to be a mixture of Ge and Sn atoms in a random order, this mixture of different atomic species could be the reason for the absence of LEED spots.

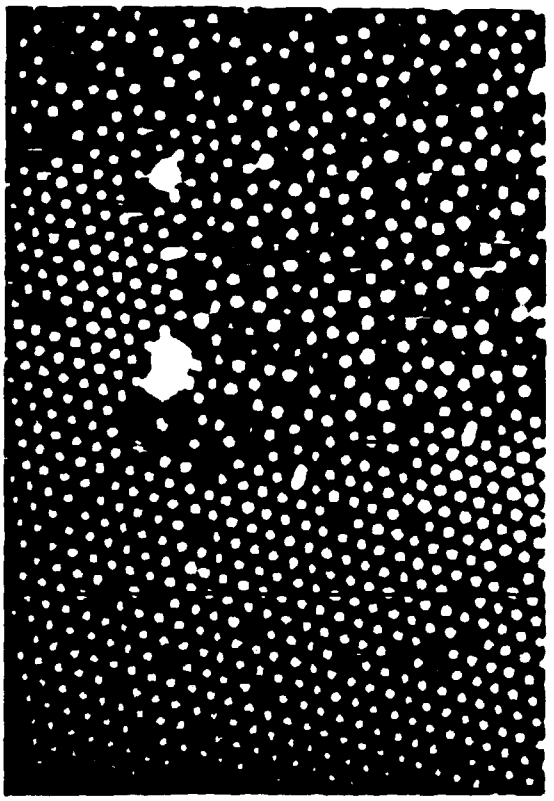

From earlier experiments using this and other techniques, the (7x7) superstructure is known to be of DAS type[1,2]. Through careful examination of phase boundaries in the STM images, between (7x7) and (5x5) reconstructed areas and between (5x5) and $\sqrt{3}$ areas, we conclude that the (5x5) structure is of DAS type, and the adatom position in the $\sqrt{3}$ structure are threefold sites directly over second layer atoms (T_4), at 0.4 ML Sn coverage. We have also found that the adatoms are Sn in the (7x7) structure as well as in the (5x5) phase.

In the figure to the left a scanning tunneling image of the Ge(111) surface after deposition of 0.4 ML of Sn is shown. Two phases are present, the $\sqrt{3}$ and the (5x5) surface structures.

References
1. J.S. Pedersen, R. Feidenhans'l, M. Nielsen, F. Grey, and R.L. Johnson, Phys. Rev.B38, 13210 (1988)
2. R.S. Becker, B.S. Swartzentruber, and J.S. Vickers, J. Vac. Sci. Technol. A6, 472 (1988)

AP22

Thermal cleaning of air-exposed $YBa_2Cu_3O_{7-\delta}$ thin film surfaces

F. Vassenden, Z.H. Gong, R. Fagerberg and J.K. Grepstad.

Institute of Physical Electronics, University of Trondheim - NTH,
N-7034 Trondheim, Norway. Fax: +7 591441

Surface cleaning of air-exposed thin films of high temperature superconductors is important e.g. to the fabrication of multilayer electronic devices. Available cleaning techniques are wet chemical etching, ion bombardment, thermal cleaning (annealing) in a controlled atmosphere, and combinations of these. In this study we examine the effects of thermal cleaning of $YBa_2Cu_3O_{7-\delta}$ (YBCO) thin film surfaces, using XPS and LEED.

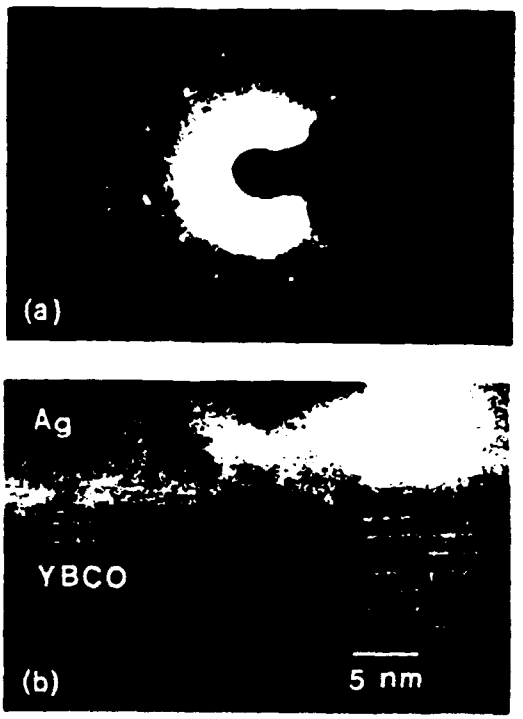

Figure 1: (a) LEED pattern of oxygen annealed c-axis oriented thin film of YBCO, (b) TEM image of Ag interface to this film.

Sputter deposited, c-axis oriented thin films of YBCO were exposed to air and subsequently annealed at 450°C in a $1 \cdot 10^{-6}$ mbar O_2 ambient. The oxygen pressure was chosen so as to ensure structural stability of the superconductor. Equally important to surface cleaning, gaseous impurities must be kept below certain partial pressures in order to assure decomposition of surface contaminant phases, e.g. $BaCO_3$ will not decompose at 450°C in a CO_2 partial pressure which exceeds $1 \cdot 10^{-8}$ mbar. This low level of CO_2 cannot be achieved at atmospheric pressure, even in highly purified oxygen.

Distinct (1x1) LEED patterns were obtained reproducibly from the YBCO film surfaces after oxygen annealing. This demonstrates the efficacy of the adopted cleaning technique. The in-plane lattice parameter was estimated at 3.84 ± 0.06 Å, close to the bulk value, which shows that the bulk structure of YBCO persists to the film surface. XPS measurements showed reduced amounts of carbonaceous and oxide impurity phases and unveiled a different chemical environment of surface Ba (as compared to bulk), even for surfaces proven by LEED to be structurally ordered. Thermal cleaning at this low O_2 pressure was found to cause the films to be non-superconducting at 77 K, however, which renders practical applications questionable.

Cross-section TEM images of Ag/YBCO contacts prepared on air-exposed, thermally cleaned thin films displayed a clean, crystalline interface. This observation contrasts that reported for Ag/YBCO contacts prepared on films exposed to 100 mbar of commercial grade O_2 prior to Ag deposition, for which a disordered interface layer was found[1].

[1] Z.H. Gong et al. Appl.Phys.Lett., January 27, 1992.

AP23

Core and valence spectroscopy of chemisorbed CO/Ag(110)

P. Bennich, O. Björneholm, B. Hernnäs, R.J. Guest[#], A. Nilsson and N. Mårtensson

Department of Physics, University of Uppsala, Box 530, S-751 21 Uppsala, Sweden

[#]Cavendish Laboratory, Madingley Road, Cambridge, CB3 0HE, U.K.

A study of CO adsorbed on Ag(110) with a coverage of 1 ML at 50 K is presented. The system has been studied by means of synchroton radiation, thereby allowing photoelectron, Auger, autoionization and NEXAFS (Near Edge X-ray Adsorption Fine Structure) spectra to be recorded. High resolution XPS has also been used in order to study the core level regions.

CO is concluded to be chemisorbed since the Auger and autoionization spectra are similar, which implies that the spectator electron is delocalized due to hybridization between the adsorbate and substrate. Furthermore, the strong satellites observed both in the core and valence photoelectron spectra indicate that the chemisorption is weak. A comparison to other similar systems such as CO chemisorbed on Ni, Cu and Pd is made, thereby showing that the chemisorption in CO on Ag is the weakest among these systems.

A small enhancement of the intensity in the Ag sp-band close to the Fermi level indicates a weak ground state population of the $2\pi^*$ orbital, which means that the orbital participate in the bonding of the molecule to the surface.

Finally, the orientation of the molecule on the surface at this coverage has been studied by means of NEXAFS. A preliminary analysis of these results indicates that the molecule does not lie flat to the surface, in contradiction to previously suggested interpretations of orientational studies.

AP24

The growth of Zn and ZnO_x on Cu(111)

E.V.Thomsen, M.Christiansen and J.Onsgaard

Fysisk Institut, Odense University, Campusvej 55, DK-5230 Odense M, Denmark

The copper-zinc oxide system, a catalyst for methanol synthesis, water-gas shift, and methanol steam reforming, is an interesting and challenging example on a binary catalyst in which the chemical interaction gives rise to chemisorption properties that are absent in the individual components[1].

Here we report on the growth of Zn on two low-index surfaces of Cu, namely Cu(110) and Cu(111). Further, the formation of ZnO on Cu(111) is followed. The measurements, based on thermally stimulated desorption (TSD) and X-ray photoelectron spectroscopy, were performed at room temperature and at 140 K. There is a clear difference between the growth processes at the two surfaces. The zinc deposition on the Cu(110) surface is followed by a mixing of the two components. Contrary, the growth of Zn on Cu(111) is characterized by a sharp interface with formation of one monolayer. Further Zn deposition results in island formation. From TSD-measurements it is concluded that the sticking coefficient of Zn on Cu is one and the Zn desorption is characterized as a first order process. A 50% reduction in the activation energy of Zn, with coverage varying from zero to one monolayer, reflects the increased Zn-Zn interaction and the build up of islands when the one monolayer coverage is reached.

The present study shows that oxidation of the Zn/Cu(111) interface at room temperature creates ZnO, for Zn depositions below one monolayer, since all the liberated Zn in TSD desorps at a temperature 270 ^{0}C higher than that determined for the non-oxidized case. It is also a finding that the ZnO formation only takes place in the first layer as further Zn deposition gives rise to TSD peak positions analogue to those characteristic of the Zn/Cu interface.

[1]K.Klier, Applications of Surface Sci. 19 (1984) 267.

AP25

V/MgO : Metal-Insulator thin films and superlattices.

R. Feidenhans'l and E.Findeisen

Department of Solid State Physics, Risø National Laboratory, Denmark [Fax:+45 42370115]

Magnesium Oxide (MgO) is an insulator with a NaCl structure. MgO can be evaporated from an electron beam evaporator[1] and grows epitaxially on MgO(001) in the temperature range 20° to 600°C. We have investitated the growth of MgO in our metal MBE-apparatus. With Reflecting High Energy Electron Diffraction (RHEED) we can investigate the growth *in-situ*. Evaporating MgO on MgO(001) does not change the diffraction pattern, however, the background is lowered. This means that the surface quality improves. No oscillation as a function of time are observed meaning that the growth proceeds via step flow. The MgO films have been investigated by x-ray diffraction and no differences between virgin MgO(001) substrates and MgO substrates with deposited MgO could be found. This means that the films are not only epitaxial but also stoichiometric.

As evidenced by RHEED and x-ray diffraction V(001) grows epitaxial on MgO(001) with $[001]_V \parallel [001]_{MgO}$ and $[100]_V \parallel [110]_{MgO}$. However, MgO also grows epitaxial on V(001) with the same orientation as above. This is already evident from the RHEED diffraction pattern. An X-ray diffraction scan of a 30 Å V(001) layer capped by 100 Å MgO is shown in Figure. The scan is performed along the specular rod of the surface and is measured at the BW2 beamline in HASYLAB. The broad peak at momentum transfers q=3.9 Å^{-1} arises from the (002) reflection of the V layers. The bulk position is at q=4.16 Å^{-1} and the shift must either be due to strain induced from the MgO substrate or from a chemical mixing between V and MgO. The position of the MgO(002) bulk Bragg peak is at q=2.984 Å^{-1}. The oscillation between 3.0 Å^{-1} and 3.5 Å^{-1} are finite size oscillation from the 100 Å MgO cap layer. The oscillations show that the MgO cap layer is epitaxial. Scans along the off-specular Crystal Truncation Rods show that the V film is also in-plane oriented with respect to the substrate.

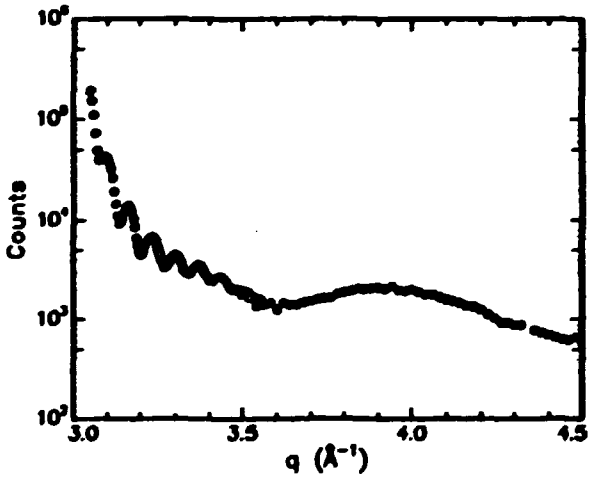

The observation decribed above suggest that it should be possible to make a metal/insulator superlattice. We have made a structure consisting of 7 × (30 Å V/50 Å MgO) grown on MgO(001). The growth was performed sequentially while the substrate was held at 650°C. The RHEED pattern showed that the crystallinity was maintained during growth. X-ray diffraction measurements have been made both at the rotating anode source in the department and at BW2 in HASYLAB.

[1] S. Yadavalli, M.H. Yang and C.P. Flynn, (1990). Phys. Rev. B41, 7961.

AP26

Control of Tip-Surface Distance in Near Field Optical Microscopy

Sergey Bozhevolnyi, Ole Keller and Mufei Xiao

Institute of Physics, Aalborg University, DK-9220 Aalborg Denmark, Fax: 98156502, E-mail: I13SER@VAX87.AUD.AUC.DK

The usage of the fiber tip to detect the evanescent field of the light being totally internally reflected by the sample surface has appeared to be a very fruitful technique for near field optical microscopy. Different near field microscope configurations have been experimentally studied and a number of theoretical methods to describe the tip-surface interaction have been developed. However, the interpretation of the experimental data is still too uncertain to reveal finer details expected from the theoretical point of view. It seems that the crucial problem is connected with the evaluation of the tip-surface distance because of the exponential behaviour of the evanescent field.

We have developed an experimental technique to control the tip-surface distance by measuring the intensity of the interference pattern from the light directly emitted by the fiber tip and reflected by the surface under an oblique angle of incidence. Using another fiber with a polished edge placed at the surface near the fiber tip we were able to determine the tip-surface separation with less than 5% error in the range $0.2 - 20\mu m$ and with about $10nm$ error at smaller distances. We have found it important that one distinguishes clearly between the positions of the end of the tip and of the imaginary point inside the tip, where the light is accumulated by or irradiated from the fiber. The distance between these points should be regarded as a radius of the sphere in the sphere-like representation of the fiber tip widely used in theoretical models. By using our technique we have measured this distance for a single-mode fiber tip to be about $300nm$. We have found our technique to be very helpful for the detailed study of the light emitted by the fiber tip in order to characterize other properties of the tip which are relevant to the detection of the evanescent waves.

AP27

Near-Field Optical Microscopy: A Rigorous Point-Dipole Approach

Ole Keller, Mufei Xiao and Sergey Bozhevolnyi

Institute of Physics, Aalborg University, DK-9220 Aalborg Denmark, Fax: 98156502, E-mail: I13MUFEL@VAX87.AUD.AUC.DK

The technique of Near-field Optical Microscopy (NFOM) [1] can be used to obtain microscopic resolutions well below the wavelength of light. In this paper, a theoretical analysis based on a microscopic description of the interaction between the dielectric probe and the tested surface is presented. The probe tip is assumed to be a point-like sphere and the surface is represented by a two- dimensional discrete lattice with subwavelength structure. Using a Green's function technique we established a set of selfconsistent integral equations to describe the local field at the site of the probe tip and the selvedge. All contributions including bulk reflection and many-body interactions have been taken into account. Using point-dipole approach we have solved the selfconsistent equations exactly.

The results have been compared with various approximate solutions. We have found that the approximate solutions are very different from the exact solution in the case of strong interaction . The approximate solutions tend to infinity only when the tip-surface distance decreases to zero, and the results depend strongly on the number of Born iterations performed. However, for the exact solution it is shown that there is a region close to the surface where an enhanced field can be induced by the probe, and when the tip-surface distance decreases to zero the induced field tends to zero. Thus, we have found the resonance interaction between the probe tip and the surface. The qualitative comparision of our results with the experimental data from single-particle plasmon studies [2] revealed the similar features of the system behaviour near the resonance. It is shown that in the absence of damping the resolution of the system can be as close to infinite as the tip-surface distance is close to the resonance value, which is essentially nonzero. The induced field at site of the probe as a function of scan coordinate is calculated for different tip-surface distance and other system parameters.

[1] R. Reddich, R. Warmack, T. Ferrell Phys. Rev. B39 767 1989

[2] U. Ch. Fischer and D. W. Pohl Phys. Rev. Lett. 62 458 1989

AP28

Resonant Optical Excitations in Semiconductor Quantum Wells

Ansheng Liu and Ole Keller
Institute of Physics, University of Aalborg, DK-9220 Aalborg
Denmark, Fax: 98156502, E-mail: I13ANL@VAX87.AUD.AUC.DK

Quantum wells are artificial semiconductor heterostructures whose microscopic spatial configuration is especially designed so as to modify significantly some of the properties of the parent semiconductors. In particular, the spatial confinement of carriers quantizes their motion and gives rise to the interesting optical properties in the electronic excitation spectrum. Based on the random-phase-approximation (RPA) approach, the nonlocal linear optical conductivity response function of the quantum well has been analysed. By combining the expression for the field-induced current density and the Maxwell wave equation for the field, the self-consistent electric field inside the single quantum well can be obtained by use of the well known Green's function techniques[1,2]. In order to focus our attention on the physics that we want to address, we model the semiconductor quantum well by an infinite square-well potential with a finite width, and incorporate only the two lowest sub-bands (two-level approximation) in our calculations. We note that these approximations do not affect our results in any essential way. For a GaAs-AlGaAs quantum well, numerical computations of the local electric field distributions inside the quantum well have been performed. For s-polarized light, our numerical results show that the locai field correction to the external field is small. The first Born approximation thus can give excellent results. For the p-polarization, it is demonstrated that the electric field component perpendicular to the well deviates so much from the external field that the Born iteration approach does not converge. When the photon energy is somewhat above the energy separation between the two levels, resonant electronic excitations of the quantum well by the electromagnetic radiation occur.

[1]O. Keller, in Proceedings from the International Seminar on "Problems in Quantum Optics", Dubna, Russia, 1991 (World Scientific, 1992).
[2]D. A. Dahl and L. J. Sham, Phys. Rev. B 16, 651(1977).

AP29

Layer dependent core level shifts measured by photo electron spectroscopy: Na, K and Cs on Al(111).

E. Lundgren, J.N. Andersen, M. Qvarford and R. Nyholm

Department of Synchrotron Radiation Research, Institute of Physics, University of Lund, Sölvegatan 14, S - 223 62 Lund, Sweden
and
Max - lab, University of Lund, Box 118, S - 221 00 Lund, Sweden.

Layer dependent core level shifts are presented for Na, K and Cs overlayers on Al(111). The development of the core level spectra above one monolayer (ML) with increasing amount of alkali deposited on the substrate will be shown. From this development we will demonstrate how surface, bulk and interface shifted spectral features can be identified. We will also compare the Na, K and Cs core level spectra in the 3 ML situation to illustrate the different shifts for different Z.

In figure 1 are shown the Na 2p, K 3p and Cs $4d_{5/2}$ core levels from approximately 3 ML depositions of the respective alkali metal on Al(111). The spectra can in all cases be decomposed into three contributions, each of which may be assigned to a different layer of the alkali film.

The experimentally obtained values of the different alkali layer dependent binding energy shifts will be compared with calculations based on a thermodynamic model /1/. It is found experimentally (see figure 1) that the shifts are increasing with increasing Z, as one would expect from comparisons with semi-empirical estimations. Furthermore, the binding energy shifts provide information on the adhesion and interfacial segregation energies /2/ in the alkali/Al system.

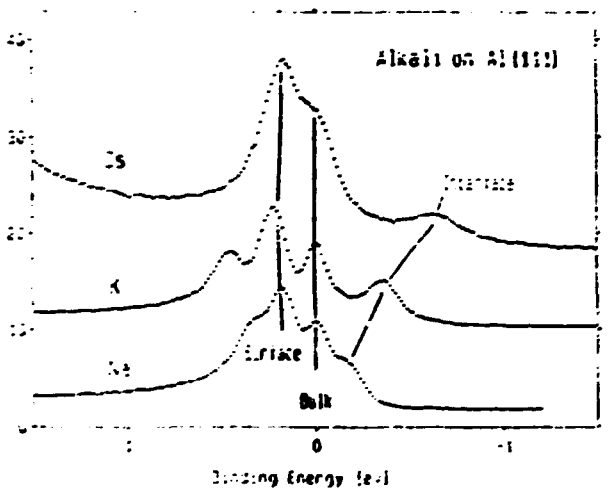

Figure 1. Alkali core level spectra from 3 ML depositions of Cs, K and Na on Al(111).

1. J. Gerkema and A.R. Miedema, Surf. Sci. 124, 351, 1983.

2. N. Mårtensson, A. Stenborg, O. Bjorneholm, A. Nilsson and J.N. Andersen, Phys. Rev. Lett. 60, 1731, 1988.

AP30

Dimer Formation and Electronic Structure on the Ge(100)(2x1):Sb Surface

M. C. Håkansson, U. O. Karlsson, J. Kanski*, P-O. Nilsson*, Y. Khazmi*.

Department of Synchrotron Radiation Research, Institute of Physics, Lund University, Sölvegatan 14, S-223 62 Lund, Sweden.
* Department of Physics, Chalmers University of Technology, S-412 96 Göteborg.

Deposition of antimony on clean Ge(100) and annealing to 450° C results in a well-ordered, highly passivated, and stable surface showing a (2x1) reconstruction, as seen in Low Energy Electron Diffraction (LEED). The electronic structure of the Ge(100)(2x1):Sb surface has been studied by angle-resolved photoelectron spectroscopy of the valence band and the shallow core-levels. As displayed in Fig 1, the Sb 4d core-level photoelectron spectra consists of only one component, which indicates occupation of a single type of binding site. The Ge 3d core-level is narrow and appears bulklike, but a detailed analysis of the spectra reveals two components, one attributable to the bulk Ge and the other to Ge interacting with the Sb overlayer. Angle Resolved Energy Distribution Curves (AREDC's) were measured at three different photon energies along the two high symmetry azimuths [001] and [011]. A surface state band was identified corresponding to the lone-pair state of the Sb atoms and in the [001] direction a back-bond state to the Ge substrate was found. From these results and from comparison with similar studies of As terminated Si(100) and Ge(100) surfaces we conclude that the observed 2x1 reconstruction is caused by the formation of symmetric Sb-Sb dimers on the ideal Ge surface.

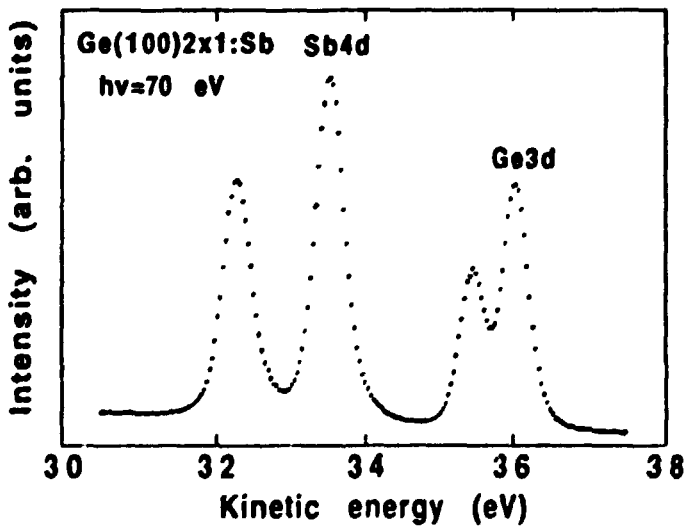

Fig1. Ge3d and the Sb4d core-level spectra at hv=70eV

AP31

Macroscopic Analysis of Sample - Tip Interaction in Near Field Microscopy.

S.Berntsen [$], E Bozhevolnaya and S. Bozhevolnyi.[†]

$ Institute of Electronic systems, Aalborg University.E-mail: sb@iesd.auc.dk

† Institute of Physics, Aalborg University.

The recent development of near field optical microscopy, where the extremity of an etched optical fiber is used to detect the nonradiative (evanescent) field with high spacial frequencies, has already shown the possibility of increasing the optical resolution far beyond the Rayleight criterion. It has also put a rather complicated theoretical problem connected with the correct interpretation of the images provided by this technique. In order to reach the subwavelength resolution the fiber tip should be scanned over the illuminated surface at the appropriate distance which leads to the strong tip-surface interaction. To describe this interaction properly the selfconsistent optical field has to be determined. Microscopic analysis of the problem is widely exploited, where the fiber tip is assumed to be a small sphere and the conversion of the induced field at the site of the tip to the propagating one in the fiber is leaving aside.

We have attempting to implement the selfconsistent macroscopic approach by using the Maxwell equations in a two- dimensional geometry and considering TE waves. Using well known formulations of the partial differential equations as coupled integral equations give a very complicated structure of equations. Thus we have been looking for a much simpler approach. The basic idea is the formulation of the problem as a single integral equation involving the Fourier Transform of the field at a plane. This equation represent the exact Maxwell equations. The field on the tip surface may be found in terms of the field on the used plane, and finally the propagating field in the fiber can be calculated in the usual way from the field on the tip surface. The power of the propagating toward the detector field was calculated as a function of the fiber tip position under various configurations of the tip and the surface.

AP32

The interaction of CH_4 at high temperatures with clean and oxygen precovered Ni(100) and Cu(100) surfaces

I. Alstrup[1], I. Chorkendorff[2] and S. Ullmann[1]

[1]Haldor Topsøe Research Laboratories, Nymøllevej 55
DK-2800 Lyngby, Denmark

[2]Laboratory of Applied Physics, Technical University of Denmark
DK-2800 Lyngby, Denmark

A strong interest in developing better processes for transforming natural gas into other useful chemicals has recently motivated a number of studies of the interaction of methane with metal surfaces. The principal process used industrially is steam reforming in which synthesis gas ($CO + H_2$) is produced from CH_4 and H_2O on a nickel catalyst. In the present work the dissociative chemisorption of CH_4 on Ni(100) and Cu(100) without and with preadsorbed oxygen has been studied as function of temperature and exposure by using XPS for monitoring the concentration of surface species. Oxygen precovered surfaces are included in the study because they correspond to steam reforming conditions and because a dramatic enhancement by adsorbed oxygen of the reactivity of nickel surfaces towards CH_4 has been reported recently.

The carbon coverage on the nickel surface was measured as a function of exposure to extremely clean CH_4 at 1 Torr in the temperature range 425-550 K. The experimental curves can be accurately accounted for by assuming that the dissociative chemisorption is a direct process which can only take place if the methane molecule hits a free site with free neighbour sites. The activation energy of the initial sticking coefficient is found to be 52±1 kJ/mol. The present results for the oxygen covered surface show, contrary to recent reports, that preadsorbed oxygen atoms block ensembles of sites for CH_4 chemisorption on Ni(100) in the same way as carbon atoms.

The dissociative chemisorption of CH_4 on clean Cu(100) was studied at 10 Torr CH_4 pressure in the temperature range 900-1000 K. The initial sticking probability is at 1000 K three orders of magnitude smaller for Cu(100) than for Ni(100) and the activation energy is about 4 times larger (201±4 kJ/mol). The carbon growth curves and the XPS C 1s binding energy correspond to the growth of graphite islands on the Cu(100) surface, while carbidic carbon was formed on Ni(100). The studies of the interaction of CH_4 with Cu(100) with preadsorbed oxygen show that CH_4 reacts with the surface oxygen already at temperatures below 700 K, i.e. far below the temperature necessary for observing dissociative chemisorption of CH_4 on the clean Cu(100) surface. An Arrhenius plot of the initial reaction probability of CH_4 with oxygen on Cu(100) shows that the activation energy is about 120 kJ/mol.

AP33

Sulfur Adsorption on an Oxygen Preadsorbed Ni(110) Surface Studied with STM[1]

L.Ruan, F.Besenbacher, I.Stensgaard and E.Lægsgaard
Institute of Physics, University of Aarhus
DK-8000, Aarhus C, Denmark [Fax:45-86120740]

Sulfur chemisorption on the oxygen preadsorbed Ni(110) surface has been studied for the first time by scanning tunneling microscopy at room temperature. The adsorbed oxygen is replaced by the sulfur, both the oxygen and the sulfur covered structures were observed at the atomic scale, and a mechanism for the surface reaction is proposed in this paper.

The oxygen adsorption induces a reconstruction on the Ni(110) surface, producing a perfect p(2x1)-O structure in which rows form along [100] direction. By bonding the nickel, the oxygen plays an important role in stabilizing the added-row structure (0.5 ML of Ni and 0.5 ML of O).

The sulfur adsorption was carried out by exposing the oxygen covered crystal to H_2S gas at a pressure of $\sim 10^{-8}$ mbar. In the AES, XPS and HREELS measurements, D.R.Huntley[2] has found that the adsorbed oxygen was removed by reacting with H_2S to form water which desorbs from the surface at room temperature. Saturated sulfur adsorption produced a p(4x1)-S structure which is supposed to be a reconstructed structure.

Individual images and the STM movies clearly show the dynamics of the surface reaction. The initial sulfur adsorption produces many small islands and patches which exhibit the c(2x2)-S structure. For the island, the Ni atoms which are from the primary -Ni-O- chains of the p(2x1)-O structure form the Ni(1x1) substrate on which the sulfur atom adsorbs in the two-fold hollow position. The island formation shows that the replacement occurs locally, and the stability of the island structure under the condition of no further sulfur dosing implies that surface diffusion is unlikely to occur, since the nickel atoms are bonded by the sulfur atoms. When the Ni atoms from the p(2x1)-O structure (0.5 ML) form the Ni(1x1) structure, a lateral contraction of the topmost layer to form the islands results in the formation of the patches.

The islands disappear after the continuous sulfur adsorption and the p(4x1) structure forms. Comparing with sulfur adsorption on the clean Ni(110) surface for which the final structure is a simple S overlayer, p(3x2)-S structure, we believe that the island structure in the Ni(110)-O-S system is crucial for the p(4x1)-S formation. In the former case, the sulfur adsorption does not induce surface reconstruction because the energy to break the Ni-Ni bonds of the flat Ni top layer is rather high, unless the crystal is heated to 250 °C. In the latter case, the islands offer the Ni atoms for forming the p(4x1) structure which is a adsorbate-metal phase.

---

[1]This work has been supported by the Danish Research Council through the Center for Surface Reactivity.

[2]D.R.Huntley, Surf. Science 240, 24 (1990).

AP34

Multidimensional properties of the dynamics of sticking of molecules on metal surfaces.

C. Engdahl* and U. Nielsen†

*Institute of Theoretical Physics, Chalmers University of Technology, S-412 96 Göteborg, Sweden.

†Institute of Physics, University of Aarhus, DK-8000 Aarhus C, Denmark.

The sticking of molecules on metal surfaces is studied using classical trajectory simulations to investigate the role of the molecular and surface degrees of freedom.

For the dissociative sticking of hydrogen on Cu and Ni[1] an effective medium potential is used which takes the molecular orientation as well as the lateral impact point on the surface into account. For H_2/Cu(110) a large variation of the sticking with azimuthal angle is found. Molecules oriented along the troughs dissociate much more readily than those oriented across the troughs. For H_2/Cu(111) we find that paths not restricted to a plane yield the lowest dissociation barrier. The six-dimensional effects will tend to eliminate the large difference in translational onset between the two crystal faces that would be anticipated from the lowest barriers to dissociation corresponding to paths where only the molecule-surface distance and the intramolecular distance are varied. Such a difference would be in conflict with experimental observations. For H_2/Ni such a two-dimensional analysis works better. This is due to the earlier barrier on this metal making the variation with molecular orientation and impact point much smaller. Thus we find that the experimental trends in the dissociative sticking probability of H_2 on different crystal faces of Cu and Ni can be understood only if all six molecular degrees of freedom are considered. The order of magnitude of the sticking also comes in better accord with experiments.

The role of surface atom motion in molecular physisorption trapping is investigated using a pair potential where the orientational anisotropy can be varied. The trapping is found to depend on the surface temperature in a way characteristic of the anisotropy strength.

[1] C. Engdahl, B. I. Lundqvist, U. Nielsen and J. K. Nørskov, Phys. Rev. B, to be published.

AP35

THE HIGH-ENERGY RESONANCE ELECTRONIC STATES AT THE W-Pd(111) TUNNEL JUNCTION[1]

Leszek Jurczyszyn[$], Maria Stęślicka[$] and Leonard Dobrzynski[@]

[$]Institute of Experimental Physics, University of Wroclaw, ul.Cybulskiego 36, 50-205 Wroclaw, Poland, [Fax: 201-467]

[@]Equipe Internationale de Dynamique des Interfaces, Laboratoire de Dynamique des Cristaux Molecularies, Unite de Formation et de Recherche en Physique, Universite de Lille I, 59655 Villeneuve d'Ascq CEDEX, France

The oscillations observed in scanning tunneling microscopy of the tunneling conductance with applied bias voltage are implied by the resonance electronic states inside the potential barrier.[2]

Using the Green function formalism we have calculated the complete spectrum of high-energy resonance electronic states of the W-Pd(111) tunnel junction as well as the density-of-states distributions. The free-electron-like model was used to represent tungsten electrode while palladium was described via the two band model within the nearly-free-electron approximation.

We have shown that the inclusion of the lattice potential:
a) changes distincly the energy positions (towards lower values) and sharpens the corresponding maxima of the density of states.
b) influences much more significantly the density-of-states distributions than the transition to more abrupt interface does.
It seems therefore that the discrepancy between theoretical and experimental results for W-Au tunnel junction, discussed in [2], may be caused mainly by neglecting the lattice potential of Au (in [2] both metals were treated within the free-electron approximation).

---

[1] Work partially supported by the State Committee for Science Research - grant No 2 0123 91 01

[2] J.M.Pitarke, F.Flores and P.M.Echenique, Surface Sci. 234 (1990) 1, and references therein

AP36

Quantum Mechanical Calculations of Electron Stimulated Desorption of Positive Ions

Carl Johan Setterlind
Institute of Theoretical Physics, Chalmers University of Technology,
S-412 96 Göteborg, Sweden.
Fax: (+46) 31 416984 E-mail: tfycjs@fy.chalmers.se

The present work is a continuation of an earlier article[1] where kinetic energy distributions (KED) of H^+ ions, desorbing from a metal surface during a MGR (Menzel-Gomer-Redhead) process, were calculated. This was done by solving the time-dependent Schrödinger equation, with the help of the split time operator FFT method. The reneutralization was included, but the H^+/metal surface interaction potential consisted of a crude, exponentially repulsive, model. Since it is expected that the ion-surface interaction plays an important role in DIET (Desorption Induced by Electronic Transitions), there is an interest in using as good diabatic potential curves as posssible.

The purpose of the present paper is to extend the calculations in [1], to include a diabatic potential-energy (PE) curve based on the local density functional (LDF) approach. The PE curve is taken from a work by Walkup et al.[2] and describes H^+ interacting with a metal surface characterized by $r_s = 3$ bohr. A screened classical image potential is used for distances greater than 8 a.u. from the surface. Our calculation should be compared with others, where the ionic PE curve has been assumed to be of a repulsive, exponentially decaying form or has been constructed by adding a classical image potential to a short-range repulsion.

We claim that a diabatic LDF curve gives, in the present case, a different impact on the quantum mechanically calculated KED (MGR process), compared with applications of the above mentioned, more crude, models of ionic PE curves. The computed results are compared with experiment. A similar type of conclusion has been made by Walkup et al., but for another DIET process: the Antoniewicz process. Our contribution is that we don't exclude that the conclusion is also valied for MGR processes.

[1] C.J. Setterlind. Surf. Sci. (in press)

[2] R.E. Walkup, Ph.Avouris and N.D. Lang, in: *Desorption Induced by Electronic Transitions IV.* (Springer. Berlin. 1990), p.24.

AP37

Nucleation and growth of a H-induced reconstruction of Ni(110)

L. P. Nielsen, F. Besenbacher, E. Lægsgaard, and I. Stensgaard

Institute of Physics and Astronomy, University of Aarhus, Dk-8000 Aarhus C, Denmark.
[Fax: 86 12 07 40], [Email: lapn@dfi.aau.dk]

We have used Scanning Tunneling Microscopy (STM) to study in real space and time the dynamics, ie. the nucleation and growth of the *'streaky'* (1x2) hydrogen phase on Ni(110) at room temperature [1]. This phase is characterized by elongated half-order LEED spots, indicating a long/short coherence length along the [1$\bar{1}$0] direction and the [001] direction respectively.

The nucleation and growth of the *'streaky'* phase depends on whether it is occurring on large, flat terraces or close to monatomic steps. On terraces far from steps, we observe that the reconstruction develops through the removal of Ni atoms, as missing rows, in the [1$\bar{1}$0] direction and nucleation of these Ni atoms into added rows directed in the same direction on the terrace. These missing Ni rows and the added -Ni-H- rows are initially more or less randomly distributed in the [001] direction. In contrast to this, the growth mode close to a step edge is observed to develop by creating missing rows, directed along the [1$\bar{1}$0] direction, into the upper terrace from the step edge. These removed Ni atoms diffuse out on the terrace where they react with the impinging hydrogen and nucleate into perfect (1x2) chains/islands closed to the step edge.

The reconstruction proceeds by a combined added/missing-row growth mode with a substantial mass transport, which explains why the restructuring is an activated process.

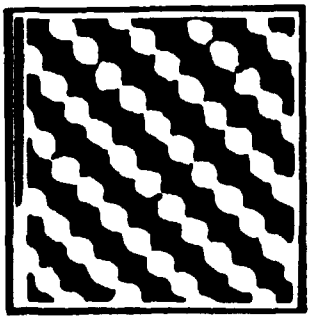

Atomically resolved STM topograph of bare Ni(110) (21x21 Å^2).

Perfect (1x2) reconstruction (102x107 Å^2).

[1] L. P. Nielsen, F. Besenbacher, E. Lægsgaard, and I. Stensgaard, Phys. Rev. B 44, 13156 (1991).

AP38

Temperature-programmed desorption of H_2 as a tool to determine metal surface areas of Cu catalysts[1]

Martin Muhler[2], Lars P. Nielsen[3], Eric Törnqvist,
Bjerne S. Clausen and Henrik Topsøe
Haldor Topsøe Research Laboratories, DK-2800 Lyngby, Denmark
Fax: 45 27 29 99, E-mail: TOPEOT@NEUVM1

Temperature-programmed desorption of H_2 (H_2 TPD) has been developed into a new tool for the determination of Cu metal surface areas (1). The technique was used for on-line characterization of binary Cu/Al_2O_3 and ternary $Cu/ZnO/Al_2O_3$ catalysts in a combined TPD-microreactor setup and the catalysts were studied both after reduction and after water gas shift activity tests. A main H_2 TPD peak is observed around 300 K which can be assigned to desorption from Cu metal surface sites. The H_2 TPD method is compared with the N_2O frontal chromatography method which has been extensively used in previous studies (see, e.g., (2)) for the determination of Cu surface areas. Figure 1 shows the amount of copper as measured by the N_2O frontal chromatography method versus the amount obtained from the H_2 TPD method, in μmol copper per gram catalyst. The amount of N_2 formed from the dissociative adsorption of N_2O is plotted against the area of the peak at 300 K for the H_2 TPD, including the following adjustment for the stoichiometry. Since the H_2 molecule probes two copper sites, the value from the H_2 TPD must be multiplied by two, and since the saturation coverage for oxygen and hydrogen is 0.5, the values from both methods have to be multiplied by two in order to obtain the amount of copper. The filled and open squares are for $Cu/ZnO/Al_2O_3$ and Cu/Al_2O_3 catalysts, respectively. It is found that the dissociative adsorption of N_2O may induce significant changes in the catalyst structure leading to errors in the surface area determination. With the H_2 TPD procedure, such irreversible changes can be avoided. A further advantage of the H_2 TPD method is the possibility of providing insight into the nature of the exposed Cu metal surfaces.

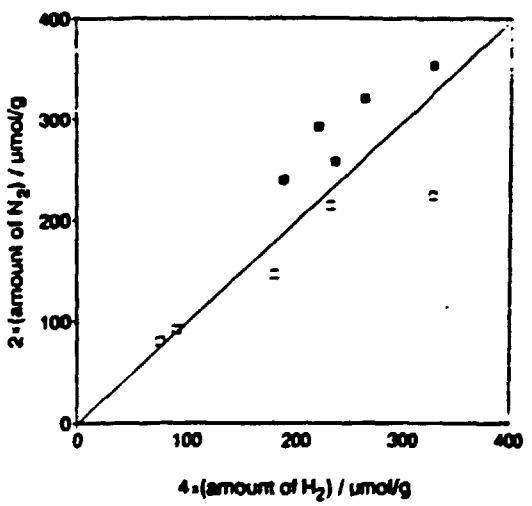

Figure 1

1) M. Muhler, L.P. Nielsen, E. Törnqvist, B.S. Clausen, and H Topsøe. Submitted for publication.
2) G.C. Chinchen, C.M. Hay, H.D. Vandervell, and K.C. Waugh, J. Catal. 103 (1987) 79.

[1]Work supported by the Danish Research Councils through "Center for Surface Reactivity".

[2]Present address: Fritz-Haber-Institut der Max-Planck-Gesellschaft, W-1000 Berlin 33, Germany.

[3]On leave from Institute of Physics, University of Aarhus, DK-8000 Aarhus C, Denmark.

AP39

Carbidic Carbon on Ni(100) and Ni(110) Investigated with STM.[1]

C.Klink, F.Besenbacher, I.Stensgaard and E.Lægsgaard

Institute of Physics and Astronomy, University of Aarhus,
DK-8000 Aarhus C, Denmark, [Fax:45-86120740].

Carbidic carbon has been adsorbed on Ni(100) and Ni(110) surfaces by exposure to 0.5-60 L ethylene (C_2H_4) at temperatures between 450 and 550 K. At this temperature the ethylene fully decomposes and only carbon is left on the surface. Exposure to 60 L saturates the surface as measured with Auger Electron Spectroscopy.

On the Ni(100) surface the adsorption of C yields a p4g LEED pattern, that is a p(2x2) mesh with 2 orthogonal glide planes observed as an extinction of the $(n+\frac{1}{2},0)$ and $(0,n+\frac{1}{2})$ spots. Atomically resolved STM pictures show the real space structure as being the rotation model proposed by Onuferko et al[2]. Furthermore the STM pictures show that every Ni-atom is displaced laterally 0.6 ± 0.1 Å.

On the Ni(110) surface we observed a good quality (4x5) LEED pattern when saturating the surface at high temperature. The absence of some of the spots indicates a glide line along the $[1\bar{1}0]$-direction (the close-packed direction) which is clearly confirmed by the STM images. The images show troughs along the $[1\bar{1}0]$-direction 5 lattice spacings apart. Atomically resolved pictures show 8 "hills" in each unit cell making up 2 squares with a side length close to the lattice parameter of Ni and the centers lying on the diagonal of the unit cell. Pictures of large areas of an only partially covered surface show that there is a considerable Ni mass transport involved in the reconstruction. This is deduced from the fact that on large flat terraces the reconstruction is seen at 2 levels, above and beneath the clean unreconstructed area. That is, in order to form the reconstruction it is necessary to remove Ni atoms from one place to build up the reconstruction at another place. At the same time the reconstruction is formed at the place where Ni atoms have been removed. The reconstruction grows much faster along the close-packed direction, the reconstructed islands are an order of magnitude longer in this direction than the other.

Further investigations with high energy ion scattering have been initiated and hopefully it will be possible to present at least preliminary results from these measurements.

At adsorption temperatures lower than 490K the $(n+\frac{1}{2},m)$ spots were rather intense but there were always reminiscences of the (4x5) pattern and a high background. The STM images show a reconstructed surface with the same square "building block" as the (4x5) structure but with very many defects both in the $[1\bar{1}0]$- and [001]-directions, consistent with the large background and rather diffuse spots observed in the LEED pattern.

---

[1]This work has been supported by the Danish Natural Science Research Council through the "Centre for Surface Reactivity".

[2]J.H.Onuferko, D.P.Woodruff and B.W.Holland, *Surf.Sci.* 87 (1979) 357

AP40

Adsorption of Brownian particles on a solid liquid interface

Jan-Olov Brånander
Institute of Theoretical Physics, Chalmers University of Technology,
412 96 Göteborg, Sweden
Fax: 031/41/6984, E-mail: tfyjobafy.chalmers.se

Using a classical Brownian description for protein molecules in solution we study the adsorption dynamics in time.
We solve the Langevin equations for a simple linear surface potential, introducing a feedback dependence in the effective potential(force).
The calculation produce an initial exponential behavior in time, recently verified experimentally (figure 1).
We also discuss the existence of adsorption fluctuations, and concentration effects in the theory.
Comparison between standard theories is also done.

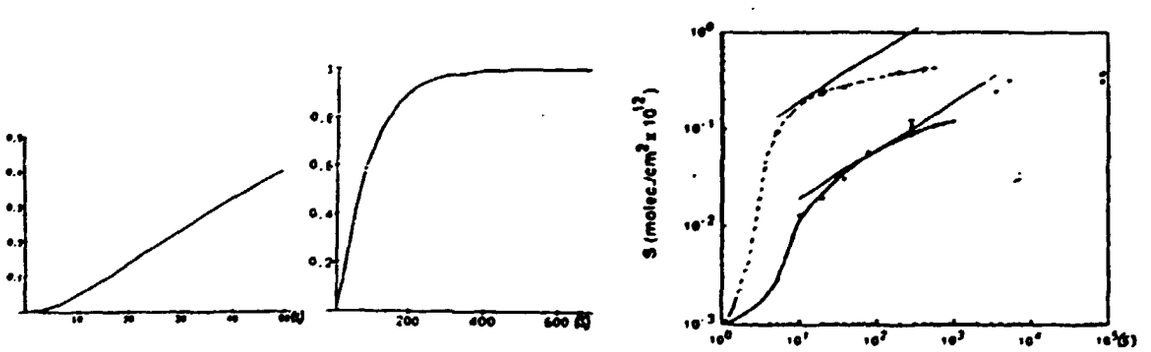

Figure 1: Theoretical adsorption curves-A(t) (left), corresponding measurements(right) at conc=10,100 µg/ml.

AP41

Structures at Solution Surfaces Studied by Electron Spectroscopy

H.O.G. Siegbahn, F. Bökman*, O. Bohman*
Department of Physics, University of Uppsala, Box 530, S751 21 Uppsala, Sweden
(Fax:46-18-183524)
*Department of Organic Chemistry, University of Uppsala, Box 531,
S751 21 Uppsala, Sweden

The concept of double layer formation at liquid interfaces is well established in a variety of fields in physical chemistry .[1] Colloidal stability, electrode processes, biological membranes and detergency are a few of the areas where double layers play a fundamental role. In organic synthesis, electric double layer systems formed by so-called phase transfer catalysts (PTCs), e.g. tetraalkyl-ammonium and -phosphonium salts, act as transfer agents of ions from aqueous to organic phase and facilitate reactions in the latter phase.

The structure of the double layer is a function of several parameters which may be broadly divided into nonspecific electrostatic interactions (i.e. those that do not depend on the internal structure of the ions and may be treated within a classical Poisson-Boltzmann type of double layer description or development thereof) and those interactions that depend specifically on the chemical character of the ions involved. The latter give rise to short-range ion-pairing effects in the topmost surface layers of the solution. In this poster we present recent experimental results using angular resolved electron spectroscopy[2] on two classes of double layer systems (fatty acid salts and phase transfer catalysts) which show distinctly different characteristica in terms of such short-range interactions. Results are obtained primarily from the solvent formamide which may be considered akin to an aqueous medium.

Fig. 1 shows the C1s binding energy region of a 0.5 m solution of potassium octanoate in formamide. The spectra, recorded at different take-off angles, shows the well-resolved lines from the three relevant species in the solution; cation (K2p,left lines), solvent (C1s in $HCONH_2$, middle line) and anion (C1s in hydrocarbon moiety of octanoate, right line; the carboxyl carbon signal is hidden under the solvent line). Comparison between bulk concentration and relative line intensity shows that the potassium octanoate is strongly surface segregated within the effective sampling depth of the photoelectrons (<25 Å). At the lower take-off angles the intensities of both the cation and the solvent lines are substantially reduced with respect to the anion line compared to the relation between the lines at 40°. This relative intensity reduction is also observed to be larger for the solvent line than for the cation line. This shows unambigously the relative ion distribution to be that characteristic of an electric double layer with the hydrophobic anions in the topmost layer of the solution and the chargecompensating counterions distributed between this layer and the bulk of the solution. The anion coverage is estimated from the spectra to be of the order of half a monolayer at this concentration.

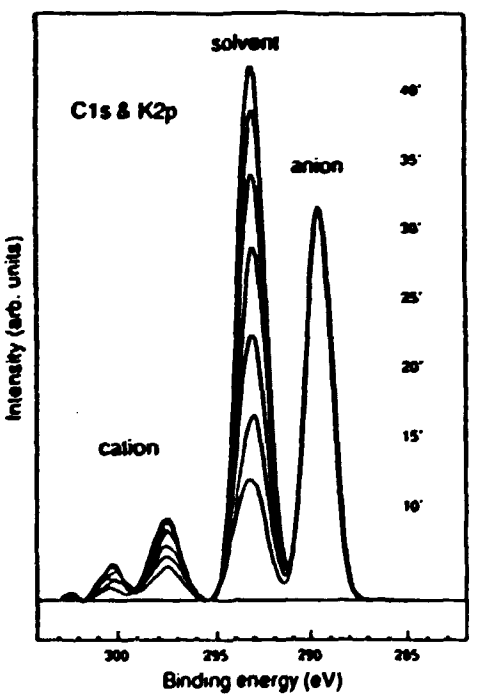

[1] R.Parsons, Chem.Rev.90, 813 (1990)
[2] R.Moberg, F.Bokman, O.Bohman and H.O.G.Siegbahn, J.Chem.Phys.94, 5226 (1991) and J.Am.Chem.Soc.113, 3663 (1991)

AP42

New method to determine the dielectric function of solids from REELS spectra.

F.Yubero[1] and S.Tougaard[2]

[1]Departamento Fisica Aplicada C-XII. Universidad Autónoma de Madrid. Cantoblanco. 28049 Madrid. Spain.

[2]Fysisk Institut. Odense Universitet. 5230 Odense M. Denmark.

A new method for experimental determination of the dielectric function of solids is proposed. The method relies on a quantitative model for the description of the physical processes in a reflection electron energy loss experiment (REELS)[1].

The model takes into account the effect of the surface, the momentum transfer in the inelastic processes as well as the effect of the field set up by the incoming electron on the outgoing electron. From this a formula for the inelastic scattering cross section was derived[1]. The cross section is a function of the complex dielectric function and the primary electron energy.

In the method the dielectric function is adjusted until a reasonable quantitative agreement is found between a set of experimental and theoretical cross sections. Thus by choosing a suitable dielectric function we reproduce simultaneously the inelastic scattering cross sections for a wide range of primary electron energies (300-10000 eV). This was done for several materials.

The thus determined dielectric functions are compared to the dielectric functions obtained by alternative methods.

The advantages of using REELS rather than electron energy loss spectroscopy in the transmission mode (TEELS) or optical methods is that in the TEELS experimens large experimental difficulties arise because of the need of extremely thin and self supporting films while in the optical method a synchrotron radiation light source is needed to cover a wide range of energy loss. In contrast to this, the REELS experiment is simple and the technique is available in practically all standard surface science instruments.

[1] F.Yubero and S.Tougaard. Phys. Rev. B (1992) (in press).

AP43

Interface formation between Bi and ceramic ZnO : a model varistor grainboundary.

K.O. Magnusson[H] and S. Wiklund[S]

[H]ABB HV Switchgear AB, S-771 80 Ludvika, Sweden
[S]Dept. of synchrotron radiation research, University of Lund, Sölvegatan 14, S-223 62 Lund, Sweden

Varistor compounds are ceramic semiconductors with electronically active grainboundaries[1]. In the case of ZnO-based compounds the introduction of various metal oxides, in particular Bi, creates back-to-back (double) Schottky barriers at the ZnO-ZnO grainboundaries. These barriers act as reverse-biased diodes with a very low leakage current below a certain voltage where the barriers suddenly break down and allow a high current to flow. This effect where the resistivity changes by 12 orders of magnitude is known as the varistor effect, and is utilized in electronics and power transmission to protect equipment from voltage surges (from switching or discharges, e.g. lightning).

We have studied a prototype varistor grainboundary by forming an interface between a sintered n-doped(Al) ZnO polycrystal and metallic Bi. The ceramic was fractured in ultra-high vacuum and the metal was evaporated from a tungsten filament *in situ* in a spectrometer for angle-resolved photoelectron spectroscopy at MAX-lab, the synchrotron radiation laboratory in Lund, Sweden. Using photoelectron spectroscopy, changes in workfunction, core-level energy shifts and intensities, and valence band shapes have been studied as a function of Bi evaporation time (i.e. metal coverage). We find that at room temperature multilayers of Bi can be grown, and present result for the initial stages with coverages below 10 Å (approximately 3 monolayers). In this range the workfunction changes by 0.5 eV, as evident from the shift of the cut-off of secondary electron emission. The shape of the cut-off indicates some inhomogeneous growth, which is expected on this polycrystalline surface. The Zn 3d and Bi 5d core-level intensities, however, show developments very similar to linear growth, from which we can conclude that the dominant adsorption mechanism is linear without e.g. island growth. Shifts of the apparent binding-energy of Bi 5d show that band-bending is induced by Bi adsorption. The shift after 10 Å of Bi is equivalent to an upward band-bending of 0.43 eV (the ZnO bandgap is 3.2 eV). Studies of valence band and bandgap emission have identified the states responsible for the band-bending : Bi induces states in the ZnO bandgap 1.4 eV above the valence band maximum, i.e. roughly midgap states. The surface stays semiconducting. This is the first direct observation of varistor-forming bandgap states and proves the importance of Bi in this compound.

---

1 See e.g. M. Matsouka, Jpn.J.Appl.Phys., 10, 736 (1971) ; L.M. Levinson and H.R. Philipp, J.Appl.Phys., 46, 1332 (1975)

AP44

Surface Induced Effects in Narrow Channels[1]

P. Norberg, L.-G. Peterson and I. Lundström

Department of Physics and Measurement Technology, Linköping University
S - 581 83 Linköping, Sweden, [Fax: +46 13 13 75 68]

The development of microfabrication techniques gives new possibilities in studying molecular flows, since long and very narrow channels can be fabricated in a reproducible way. Gas transport in a channel structure etched in silicon, consisting of 33 parallel, 100 nm deep and 20 μm wide channels covered with a glass lid, has been characterized with the use of a masspectrometric system.[2] The channel structure is used as a leak between a masspectrometer and a gas mixing chamber. The experiments are performed mainly with helium and argon in pressure regions where the channel depth is significantly smaller than the mean free path of the gas molecules. Some unexpected findings are here suggested to be due to surface induced effects. One observation made is that the diffusion delay time *increases* with decreasing absolute pressure in the gas mixing chamber. The diffusion constant for molecular flows under the conditions above, D_K, first considered by Knudsen does not account for this behaviour. The explanation we suggest for the phenomenon is based upon a few assumptions. Firstly, we assume that a clean surface gives a diffuse reflection, while a surface covered with adsorbed molecules gives a more specular reflection. Secondly, we assume that the diffuse reflection corresponds to the Knudsen diffusion constant D_K, while the specular reflection corresponds to another, larger diffusion constant D_s. With these assumptions as a point of departure we arrive at an effective diffusion constant D:

$$D = (D_K n_c + D_s n_c)/(n_c + n_c).$$

n_c is the volume concentration of molecules in the gas mixing chamber and n_c^{-1} is the equilibrium constant controlling the adsorbtion at the channel walls.

Since the diffusion delay time for helium is always smaller than for argon, and helium shows smaller pressure dependence we assume that helium adsorbs stronger and/or gives a more specular surface than argon. The latter assumption is further confirmed in experiments with a mixture of helium and argon, where an increasing amount of helium decreases the diffusion delay time of argon and vice versa. A preliminary observation of ethane formation from a mixture of ethene and hydrogen in one of the channel structures further illustrates the importance of the gas-wall interaction. This observation specifically points out a catalytic effect, due to the large number of collisions made by molecules with the walls.

1. Work supported by a grant from the Swedish National Board for Technical and industrial Development (NUTEK) with their programme on "Micronics"

2. P. Norberg, L.-G. Peterson, I. Lundström, submitted for publication in Vacuum

AP45

On the Effect of a Surface Oxide Layer on the Diffusion of Implanted Lead in Aluminium

L. Yu, S. Steenstrup, A. Johansen, E. Johnson,
L. Sarholt-Kristensen and K. K. Bourdelle
Physics Laboratory, H. C. Ørsted Institute, University of Copenhagen,
Universitetsparken 5, DK-2100 Copenhagen Ø, Denmark [Fax: +45 31350628]

A surface oxide layer on Al crystals has been shown to have an effect on the diffusion behaviour of implanted Pb[1]. The experimental evidence is provided by an RBS analysis. Al single crystals (< 110 > perpendicular to the surface) were implanted with 150 keV Pb ions to fluences of 1, 5 and $18 \times 10^{15} cm^{-2}$ in a random direction at room temperature, and subsequently annealed and analyzed by RBS measurements. Two different experimental conditions were used: *in-situ* (sample kept in vacuum for the period of all the measurements) and *ex-situ* (sample exposed to air in between the measurements). The large difference between the two sets is certainly due to the formation of an oxide layer at the surfaces of the *ex-situ* samples. Diffusion and evaporation for the two types of samples were analyzed by fitting the general solution to the simple diffusion equation (with the boundary condition at the surface that evaporation is proportional to the the concentration there) to the directly measured Pb concentration profiles. The diffusion coefficients and evaporation rates obtained are enhanced in the presence of a surface oxide layer (see Fig.1). Analysis by an RBS/channeling measurement reveals the following: Radiation damage recovery is reduced in the presence of an oxide surface layer and surface segregation is increased. A quantitative analysis by a simulation based on a model of vacancy dependent diffusion of inclusions (the volume diffusion mechanism)[2] was carried out. One outcome was that the vacancy annihilation rate is smaller for the *ex-situ* samples by one order of magnitude than for the *in-situ* samples. A possible interpretation of this reduction in damage relaxation is that Al interstitials are attracted by oxygen atoms at the surface and hence has a reduced possibility to recombine with vacancies.

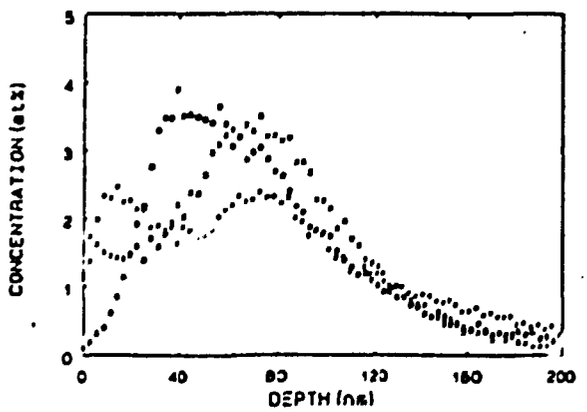

Fig. 1. An example of evolutions of measured Pb concentration profiles; o: as implanted profile; *: *ex-situ*; × - *in-situ*. Both samples were implanted to a fluence of $18 \cdot 10^{15}$ cm^{-2} and annealed at 480°C for 4 hours.

[1] L. Yu, S. Steenstrup, A. Johansen, E. Johnson, L. Sarholt-Kristensen and K.K. Bourdelle, in *proceedings of the 10th International Conference on Ion Beam Analysis*, Eindhoven,1991, to be published in Nucl. Instr. and Meth. B.

[2] L. Yu, S. Steenstrup, A. Johansen, E. Johnson, L. Sarholt-Kristensen and K.K. Bourdelle, submitted to Phil. Mag. A, 1992.

AP46

Cu and Ni Upper Bands Mapped by Very Low Energy Electron Diffraction (LEED)

Vladimir N. Strocov

St. Petersburg International Institute of Interphase Interactions, P.O.Box 1146, St. Petersburg 194291. Russia, FAX: (812) 292-51-93

Independent information on upper states is highly desirable for PES and IPES. Within one step photoemission theory, these states are essentially time reversed LEED states. So they may be effectively probed with (LEED) technique. Indeed, matching approach of LEED states that every feature of elastic reflection R relates to definite feature of band structure (BS) along $k_{\parallel} = \kappa_{\parallel} + g$ direction of BZ [1] But direct mapping of upper bands turned possible only under the guide of preliminary rough calculations of reference BS with associated R(E) curves [2], [3].

EXPERIMENT. R(E) curves were measured on Cu(111) and Ni(111) at 0-35 eV range in target current regime using a conventional LEED setup with 1.300V applied to the grids [4]. Retarding fields keeps constant $\kappa_{\parallel}$ along any experimental R(E) curve taken for constant rotation of sample [3]. So any curve was associated with its own constant direction in BZ. Incidence angle was varied in $\overline{\Gamma}\overline{K}$ and $\overline{\Gamma}\overline{M}$ azimuths. Angular dispersion of all R(E) features demonstrated their purely elastic origin.

CALCULATIONS. Fast pseudepotential scheme was adopted to calculate both reference BS and R(E). This scheme generates plane wave expansion of Bloch functions as a by-product. This expansion is used for very fast evaluation of R(E) curves when the new approximation was applied through a simple function. It relates directly R(E) to that plane-wave component ("conducting component") which associates right with primary plane wave. This component is fixed by $k_{\parallel}+G_{\parallel} = \kappa_{\parallel}$ condition, and R(E) relates to its amplitude through a simple function F : $R = F(C_{k_{\parallel}+G_{\parallel}=\kappa_{\parallel}})$.

MAPPING OF BANDS CRITICAL POINTS. Every Extremum of dR/dE plot corresponds to rapid change of reflection and therefore to rapid change of wave functions that takes place right near some critical point (CP) of E(k). So every dR/dE extremum represents definite CP. Having calculated reference BS, it turns possible to pick up the very CPs that manifesting in R(E)|| near those point just the conducting plane component changes.

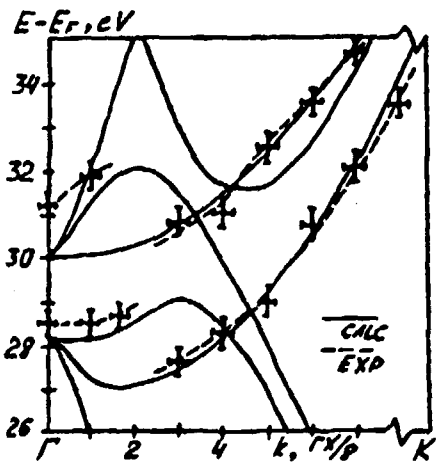

Energy shift ΔE of any experimental dR/dE extremun relative its calculated counterpart reveals that associated experimental CP is shifted by the same ΔE relative its calculated position. So this shift exactly fixes the energy of CP and allow its mapping. Changing incidence angle, we mapped this way CP of bands in variety of BZ (non-symmetry) directions.

MAPPING OF WHOLE BANDS. With incidence $\kappa_{\parallel}$ in $\overline{\Gamma}\overline{K}$ azimuth, $k_{\parallel} = \kappa_{\parallel} + g$ lines are perpendicular to ΓK symmetry axis of BZ. So bands have their CPs strictly at ΓK line. When the incidence angle is scanning, these CPs are drawing bands along ΓK. Some of these CPs manifested them selves in R(E). Having mapped them for the set of $\kappa_{\parallel}$, we obtained bands along ΓK as a whole. An example is presented on figure (Ni).

[1] R.C. Jaklevich, L.C. Davis, Phys. Rev. B26, 5391 (1982)
[2] V.N. Strocov, Solid State Commun. 78, 545 (1991)
[3] V.N. Strocov, S.A. Komolov, Phys. Stat. Sol(b)167, 605 (1991)
[4] S.A. Komolov, L.T. Chadderton, Surf. Sci. 90, 359 (1979)

B : 6TH NORDIC SYMPOSIUM ON COMPUTER SIMULATION

BFr1

Molecular Dynamics of Fluid-Solid Systems*

Jayanth R. Banavar[1], P. Keblinski[1], J. Koplik[2], W.J. Ma[1], A. Maritan[3], and J.X. Yang[2]

[1]Department of Physics and Materials Research Laboratory, Pennsylvania State University, University Park, PA 16802, USA

[2]Levich Institute and Department of Physics, City College of New York, New York, NY, USA

[3]Dipartimento di Fisica, Universita di Padova, Italy

We have used molecular dynamics simulations to investigate a number of problems which lie between the few-molecule and continuum levels. Our focus is on understanding special situations where either the spatial averaging implicit in a continuum description is not applicable or the microscopic structure is of interest itself, or even when the entire system is large, crucial microscopic sub-regions dominate the resulting dynamics. A discussion of specific examples including the dynamics of interface rupture, the dynamics of the spreading of a drop on a solid surface, and wall-directed spinodal decomposition will be presented.

*Supported by the National Science Foundation Fluid, Particulate and Hydraulic Systems Program and the NASA Microgravity Program.

BFr2

NUMERICAL LANGEVIN EQUATION SOLUTION FOR DROPLET SPREADING

A. Lukkarinen, J. Heiniö, K. Kaski

Department of Electrical Engineering, Tampere University of Technology
P.O.BOX 527 SF-33101 TAMPERE FINLAND

Recently there has been renewed interest and progress in the study of wetting and spreading of liquids on solid surfaces. This is understandable when we think of the many applications of technological importance which involve wetting and spreading of liquids, e.g. lubrication, adhesion, painting or oil recovery from porous rocks. Experimentally, over the past ten years, ellipsometric studies of nonvolatile liquids have given a lot of information about morphology of the spreading drop. However, the details of the spreading mechanisms are still not fully understood, especially at the microscopic level.

Here we investigate the problem of fluid spreading on a solid surface using Horizontal Solid-On-Solid model, with Langevin approach for the two-dimensional and three-dimensional cases. The substrate interaction with the droplet has first been described with one monolayer range chemical potential and second with long range van der Waals type potential. Partial and complete wetting regimes have been studied by investigating dynamic droplet profiles, spreading speed, contact angle and their charasteristic time behaviours. The change from partial to complete wetting happens when the total interaction of the substrate with the droplet exceeds the interatomic interaction between fluid particles. The thickness and speed of the precursor film depend on the value and the range of the substrate potential.

In case of complete wetting a rapidly proceeding precursor film is observed far ahead of the rest of the spreading drop. The time behaviour of this layer is linear, which is in agreement with the analytical results of the Langevin theory [1]. If the long range substrate potential is used, precursor film is consisted of separate precursor layers, which are moving with different velocities. This is called *layering* effect. If the range of the substrate potential is suitable, the precursor film can also be formed of separate layers proceeding with same velocity. This is called *glueing* effect.

Analytical results have only been calculated for the two-dimensional systems with some simplifying approximations. In our numerical models no approximations have been made an in addition the three-dimensional case has been studied. As expected our results are in good agreement with the analytical results.

[1] D. P. Abraham, P. Collet, J. Coninck and F. Dunlop, Phys. Rev. Lett. 65, 195 (1990)
J. Heiniö, K. Kaski, D. P. Abraham, Phys. Rev. B. Feb. 15, (1992)

BFr3

Molecular Dynamics Simulations of Wetting, Lubrication and Friction

J. A. Nieminen

Department of Physics, Tampere University of Technology,
P.O.Box 692, SF-33101 Tampere, Finland
Fax: +358-31-162600, Email: jniemine@ee.tut.fi

Two Molecular dynamics studies using interatomic pair potentials are shown in this presentation.

First, the spreading of a non-volatile liquid drop[1] on a solid substrate is studied[2]. The lattice constant of Silicon substrates is very small compared to the size of the oil molecules. Thus, we treat the substrate as a continuum. In accord with experimental results, we observe an atomic precursor film spreading on the substrate. Two régimes for the speed of the spreading can be distinguished: linear and diffusive between which a sudden cross-over occurs. Our study suggests that the Langevin and Monte Carlo studies of solid-on-solid like models predicting linear growth of the precursor have a certain domain of validity. On the other hand, the asymptotically diffusive growth is in agreement with hydrodynamical theories and the recent experiments with very tiny droplets.

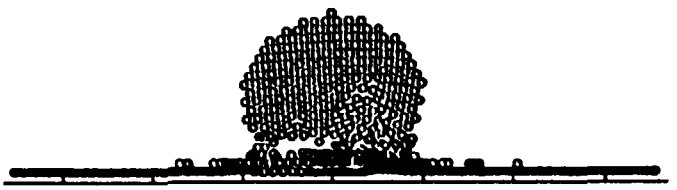

A liquid droplet spreading along a solid substrate.

Secondly, nanometre-scale friction and lubrication between an Atomic Force Microscope (AFM) tip and a solid substrate is studied[3]. The tip and the substrate are chosen to be of the same material. Under compressive loading junction growth occurs in connection with merging of atomic layers of the tip during sliding across the surface. The lowest parts of the tip remain in epitaxial contact with the substrate, and the sliding takes place inside the tip. Stick-and-slip phenomenon according to Mate et. al.[4] is observed in the frictional force, but the sharp decreases of the force follow the periodicity of the surface only on average.

In the presence of a monolayer film of soft material on the surface, the nature of sliding changes entirely. The tip does not leave material behind, neither does it penetrate the film. Hence, no wear is present, but the tip becomes blunter in the course of sliding. Stick-and-slip phenomenon is clearly seen in the frictional force. The results indicate the capability of a monolayer film to act as a lubricant between two surfaces.

/1/ P.G. de Gennes, Rev. Mod. Phys. 57,827(1985); F. Heslot, N.Fraysse and A.M. Cazabat, Nature 338, 640(1989).

/2/ J.A. Nieminen, D.B. Abraham, M. Karttunen and K. Kaski, submitted to Phys. Rev. Letters.

/3/ J.A. Nieminen, A.P. Sutton and J.B. Pethica, Submitted to Acta Metallurgica.

/4/ C.M. Mate, G.M. McClelland, R. Erlandsson and S. Chiang, Phys. Rev. Lett. 50, 1942(1987).

BFr4

Thermodynamic and Kinetic Studies of Homogeneous Vapor Condensation

Günther H. Peters[¶] and John Eggebrecht[§]

[¶] Department of Chemistry, H.C. Ørsted Institutet,
Universitetsparken 5, DK-2100 Copenhagen Ø, Denmark
[§] Department of Chemical Engineering, Iowa State University,
Ames IA 50011, U.S.A.

Abstract

The results of vapor/liquid phase transition studies of Lennard-Jones and ionic model fluids are presented which challenge the conventional interpretation of the mechanism of the condensation process. We have lifted the usual approximations (incompressible phases, constant surface tension, and non-depleting vapor phase) applied in classical nucleation theory to investigate the nature of the barrier to condensation. Based on the 1st Yvon-Born-Green integro-differential equation we have developed a thermodynamically consistent molecular theory which accurately predicts the radially dependent surface tension and the location of the surface of tension of microscopically small droplets. The droplet size dependence of the interfacial free energy is sufficiently strong that the free energy barrier to the nucleation is absent[1].

Computer simulations of ionic and neutral fluids have been performed to study the dynamical behavior of the fluid during the phase separation. We find that phase transitions in the metastable region for both systems are characterized by the instantaneous formation of concentration fluctuations. The shape of the clusters formed during the phase separation depends strongly on the nature of the intermolecular forces [2]. In the vapor phase of the Lennard-Jones fluid nearly spherical, disjoint, high density regions are formed, whereas in the ionic vapor a network of charged chains is observed. The connectivity between the clusters and their linearity diminishes with charge asymmetry. The short induction time where small clusters are spontaneously formed is followed by two rate determining regimes. First, the clusters absorb surrounding atoms and smaller clusters. During this regime, the evolution of the number of atoms in the cluster is linear in time and can be described by a modified Lifshitz-Slyozov theory. Second, the clusters undergo Brownian motion and further growth is mainly driven by coalescence. The Brownian character of this motion is due to unsymmetric internal motion near the surface. This is in contrast to the usual interpretation of the origin of Brownian motion as environmental noise.

These results support our earlier conclusions that the free energy of formation of a spherical droplet is irrelevant to a description of vapor condensation, but require an alternative mechanism for the persistence of metastability. We have constructed a new model for the vapor/liquid phase transition, which regards the phase separation as a cascade of Brownian walkers whose mass grows linearly in time. The nucleation rate is then simply determined by the sum over the first passage times required for the binary coalescence event. These intervals scale like time to the 11/6 and supersaturation to the -2/3 providing an explanation of the sensitivity of nucleation rate to supersaturation. The results are compared with experimentally determined nucleation rates for water and ammonia. It is found that both, theory and experiments, are in good agreement [3].

[1] Günther H. Peters and John Eggebrecht, J. Chem. Phys., 95, 909, 1991.
[2] Günther H. Peters, Ph.D. Thesis, 1991, Iowa State University, Ames, Iowa, U.S.A.
[3] Günther H. Peters and John Eggebrecht, J. Chem. Phys., to be submitted.

BFr5

Rheological properties of n-alkane models

Paz Padilla and Søren Toxværd
Department of Chemistry. H. C. Ørsted Institute
DK-2100 Copenhagen Ø, Denmark

Abstract

The knowledge of the rheological properties of complex molecules is essential in the development of important technologies such as lubrication or chemical processing. Nonequilibrium molecular dynamics (NEMD) has shown to be a powerful tool for studying fluids away from equilibrium[1]. In this work we present some results of NEMD simulations of n-butane modeled as the anisotropic version (AUA) of the United-atom (UA) model. In previous works[2 3 4 5]has been shown that the AUA model for n-alkanes provides results for the equation of state, as well as the diffusion, in good agreement with experimental data. The goal of the present work is to test the ability of the AUA model to reproduce experimental data of viscosity, as well as to test the sensitivity of properties such as viscosity, birefrigence and normal stress to some of the details of the model. The simulations were performed for samples of 64 n-butane chains modeled as described in ref. 2-4. The interatomic distances were kept constant by applying holonomic constraints. The homogeneous isothermal shear algorithm, also known as the SLLOD algorithm, together with the usual sliding bricks periodic boundary conditions was used. The temperature was controlled by a Gaussian isokinetic thermostat and the equations of motion were integrated by the leap-frog algorithm.

[1] Edberg R., Morriss, G. P. and Evans D.J.,J. Chem. Phys., 86,4555,1987 and references therein.
[2] Toxværd S.,J. Chem. Phys.,93, 4290,1990
[3] Padilla P. and Toxværd S., J. Chem. Phys.,94,5650, 1991
[4] Padilla P. and Toxværd S., J. Chem. Phys.,95, 509, 1991
[5] Padilla P. and Toxværd S. Molec. Phys. (in press)

BFr6

SCALING BEHAVIOUR AND THE EXTREMA STATISTICS OF A PARTICLE TRAJECTORY IN THE LENNARD-JONES LIQUID

M. Dzugutov

Department of Neutron and Reactor Physics
Royal Institute of Technology, S-100 44 Stockholm, Sweden

Geometry of an irregular curve can be characterized by its length $L(\varepsilon)$ as a function of the yardstick ε with which the curve was measured. A behaviour when $L(\varepsilon)$ varies as $\varepsilon^{-\alpha}$, where α is a positive real number, is referred to as fractal; it is characteristic of the curves constructed in self-similar manner [1]. The Brownian trajectory is known to be fractal with $\alpha=1$; also, its mean squared maximum displacement $Z_2(t)$ and its mean squared displacement $X_2(t)$, both scale linearly with time so that $Z_2(t)/X_2(t)=1.4024$ [2]. In this study, a molecular dynamics (MD) model of 16384 particles was employed to test the above predictions for a particle trajectory in the Lennard-Jones (LJ) liquid. In contrast to the previous results on a system of 108 particles [3], in this simulation we were able to reach the indicated Brownian values for both $L(\varepsilon)$ (Fig. 1) and for $Z_2(t)/X_2(t)$ (Fig. 2). It was also found that the long-time behaviour of $L(\varepsilon)$ is related to $Z_2(t)$ rather than $X_2(t)$ as has been suggested [4].

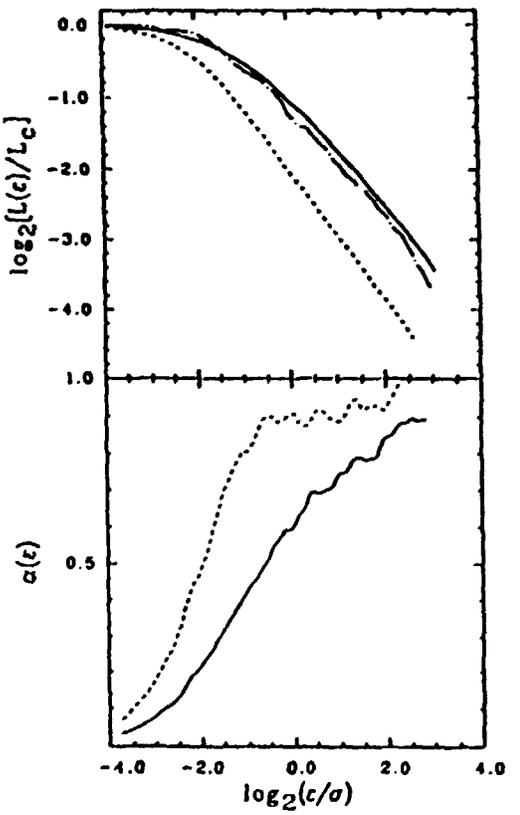

Fig. 1. Fractal analysis of a particle trajectory in the simulated LJ liquid. Solid line: $T^*=0.93$, $\rho^*=0.65$; dashed line: $T^*=0.76$, $\rho^*=0.85$; chain-dotted line: a system of 108 particles at $T^*=0.93$ and $\rho^*=0.65$.

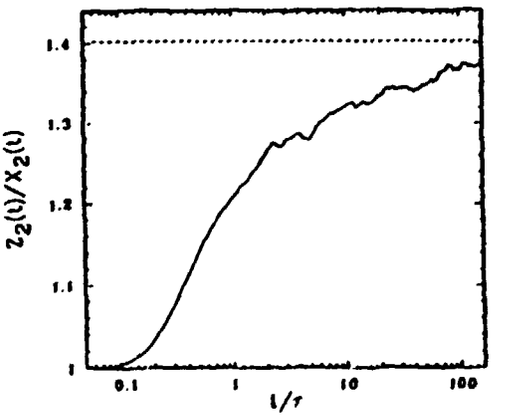

Fig. 2. The time variation of $Z_2(t)/X_2(t)$ for the LJ liquid at $T^*=0.76$ and $\rho^*=0.85$; dashed line indicates the Brownian limit [2].

REFERENCES

1. B. Mandelbrot *The Fractal Geometry of Nature*, W. H. Freeman and Co, NY, 1982
2. V. Seshadry and K. Lindenberg, *Journ. Stat. Phys.* 22, 69 (1980)
3. J. G. Powles *Phys. Lett.* 107A, 403 (1985)
4. S. Toxvaerd, Phys. Lett. 114A

BFr7

THERMODYNAMIC MASTER EQUATIONS FOR VISCOUS LIQUIDS

Jeppe C. Dyre

IMFUFA, Roskilde Universitetscenter, POBox 260, DK-4000 Roskilde, DENMARK [DYRE@JANE.RUC.DK].

The problem of understanding viscous liquids and the glass transition is still an active field of research [1]. On the one hand, a number of completely phenomenological models are avalable for describing, e. g., the influence of thermal history on glass properties. On the other hand, the mode-coupling theories approach the problem by means of standard liquid theory, supplemented with a number of well-defined simplifying assumptions. The first type of models may be critisized as an advanced curve-fitting exercise, while the latter type of models seem to fit experiment only in the relatively non-viscous regime. The present work studies a phenomenological master equation, whereby consistency with statistical mechanics is ensured all along. The master equation is a generalization of an earlier proposed equation [2,3]. The idea is to regard the liquid as divided into regions, assuming they reorient via a unique transition state. This introduces cooperativity into the model if the regions are relatively large.

The master equation illuminates the following experimental observations: The non-Arrhenius average relaxation time (e. g. viscosity), the Kauzmann "paradox", the correlation between fragility and with of relaxation time distribution. All well-known thermal history phenomena are reproduced by the model, including the prepeak phenomenon. New predictions are: It is only possible to quantitatively reconcile (alpha) dielectric relaxation loss peaks with the non-Arrhenius average relaxation time by assuming additional faster configurational degress of freedom; thus it seems that beta relaxation must exist! A further surprising prediction is a decopuling of thermal relaxation times from dielectric relaxation times, in agreement with experiment.

1. "Proceedings of Conference on Relaxation in Complex Systems", J. Non-Cryst. Solids 131-133 (1991).
2. S A Brawer, J. Chem. Phys. 81 (1984) 954.
3. J C Dyre, Phys. Rev. Lett. 58 (1987) 792.

BFr8

Crossover Between Equilibrium and Non-Equilibrium Dynamics In Ising Spin Glasses : A Monte Carlo Study[1]

J. - O. Andersson , J. Mattsson and P. Svedlindh

Solid State Physics , Institute of Technology , Uppsala University , Box 534 , S-751 21 Uppsala , Sweden , Fax: +46-18 55 50 95 , Email: joa@dab.teknikum.uu.se

Simulations have been a valuable tool in understanding the complex problem of spin glasses. However , the majority of the simulations have been aimed at studying the static and the equilibrium properties of spin glasses. Still it is evident that the equilibration process itself is almost as interesting as the equilibrium properties and this part of the problem has mostly been neglected.

Our work considers the crossover between equilibrium and nonequilibrium dynamics and the phenomenon of spin glass aging[2]. This crossover has been studied in Monte Carlo simulations of two- and three-dimensional short-range Ising spin glass systems. The spin system was quenched in zero field to a low temperature T. After equilibrating for a time t_w , a weak magnetic field was applied and the time dependence of the magnetization M(t) and the spin autocorrelation function $q(t) = \langle S_i(t)S_i(0)\rangle_{T,J}$ was studied. As can be seen in fig.1 the relaxation rate , $S(t) = \partial M(t) / \partial \log(t)$, exhibits a maximum at $t = t_w$. If the temperature is lowered or raised, immediately prior to the field application , the apparent age (t_a) of the system , as defined by the maximum in relaxation rate , is shifted to longer or shorter time scales, respectively. No significant differences between the aging behaviour in 2 and 3 dimensions are found.

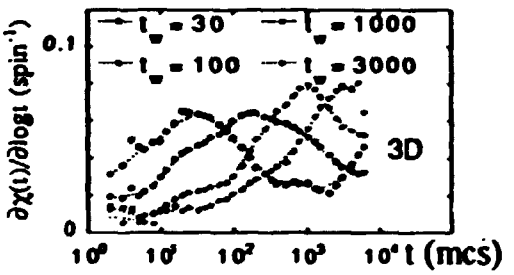

Fig.1 $S(t;t_w) = \partial M(t) / \partial \log(t)$. $T = 0.30J$.

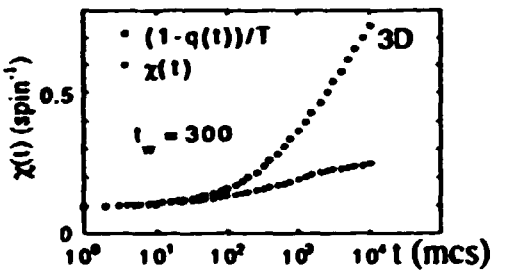

Fig.2 $\chi(t)$ and $(1-q(t))/T$. $T = 0.10J$. $t_w = 300$ mcs

As can be seen in fig. 2 , the relation $\chi(t) = (1-q(t))/T$ holds only for short time scales ($t << t_w$), while clear deviations are found at longer time scales ($t > t_w$) . Since this relation according to the fluctuation-dissipation theorem should hold for a system in equilibrium, this result is an indication of a crossover between equilibrium and non-equilibrium dynamics.

Our results are qualitatively in agreement with experiments as well as with theoretical models for the nonequilibrium spin glass dynamics.

---

[1]Work supported by the Swedish Natural Science Research Council

[2]L. Lundgren, P. Svedlindh, P. Nordblad and O. Beckman, Phys. Rev. Lett. 51, 911 (1983)

BFr9

Computer Simulation of Biomolecular Systems: possibilities and limitations

Wilfred F. van Gunsteren

Laboratory of Physical Chemistry, Swiss Federal Institute of Technology Zürich, ETH Zentrum, CH-8092 Zürich, Switzerland [Fax: +41-1-252-3402], [E-mail: wfvgn@igc.ethz.ch]

Computer simulation is a powerful tool to study the properties of fluid-like systems at the atomic level. The method of molecular dynamics involves solving Newton's equations of motion for 10^2-10^5 atoms. Its limitations are threefold:

1. quantum mechanical effects cannot be treated properly,
2. the time scale is limited to the nanosecond region, unless time-saving techniques are used,
3. the accuracy of the simulation depends on the quality of the atomic interaction function that is used.

The usefulness of a computer simulation largely depends on its quality. The most important factors that limit the accuracy of simulated results will be discussed. The accuracy of different simulation studies can differ by orders of magnitude. The accuracy will depend on the type of biomolecular system and process studied. It will also depend on the choice of force field, the simulation set-up and the protocol that is used.

Possibilities and limitations of computer simulation methods will be discussed using biomolecules as examples. It will be shown that computer simulation is a tool complementary to experimental methods, which can be used to access atomic details inaccessible to experimental probes. Examples will be given in which computer simulation augments the experimental information by providing an atomic picture of high resolution with respect to space, energy or time.

Reviews:

W.F. van Gunsteren, *Computer Simulation of Biomolecular Systems: Overview of time-saving techniques*, in:"Advances in Biomolecular Simulations", R. Lavery, J.-L. Rivail and J. Smith, eds., 1991, American Inst. of Physics (A.I.P.), Conference Proceedings, Vol. 239, pp. 131-146.

W.F. van Gunsteren and A.E. Mark, *On the interpretation of biochemical data by molecular dynamics computer simulation*, Eur. J. Biochem. (1992) in press.

BFr10

Computer Simulation of Lipid Enrichment and Selectivity by Integral Membrane Proteins[1]

Maria M. Sperotto and Ole G. Mouritsen

Department of Physical Chemistry, The Technical University of Denmark, Building 206
DK-2800 Lyngby, Denmark
[Fax: 45--42--880977], [E--mail: FYMEARMONEUVM1]

One of the unresolved problems of modern membrane biology is the question whether the activity of membrane–bound proteins and enzymes is specific with respect to certain types of lipids and whether or not such specificity is controlled by chemical or physical factors. A microscopic model is considered with a view to determining to which extent bare physical effects may be relevant for lipid selectivity and specificity of membrane proteins. The basic idea behind the model is that, via a hydrophobic matching condition,[2] the lipid chains of varying hydrophobic length experience the perturbation of the protein hydrophobic surface to different extents and that the lipid species which can most easily adapt to the matching condition will be closest to the lipid–protein interface. A model recently used to study lipid–protein interactions in membranes[3] has been extended in order to include two different lipid species characterized by different acyl-chain lengths. The model, which is a statistical mechanical lattice model, assumes that hydrophobic matching between lipid-bilayer hydrophobic thickness and hydrophobic length of the integral protein is an important aspect of the interactions. By means of Monte Carlo simulation techniques the lateral distribution and density profiles of the two lipid species near the protein-lipid interface has been determined in the fluid phase of the lipid membrane. In equilibrium, the results indicate that there is a very structured and heterogeneous distribution of the two lipid species near the protein. Out of equilibrium, the results show that the density profiles of the two species evolve oscillatory characteristics corresponding to successive layers of enrichment and depletion. The oscillations are controlled by the competition between slow lateral diffusion (slaved by the conservation law) and fast selection of species at the lipid–protein interface. The observed phenomena, statically as well as dynamically,[4] is an example of interface enrichment. Such enrichment and depletion phenomena could contribute to a medium-mediated long-range protein–protein attractive force which may influence protein organization in the membrane and hence control the functional specialization of membrane regions. The enrichment of a region around the protein in one of the lipid components may provide a mechanism for modulating the enzymatic activity of proteins.

[1]Work supported by the Danish National Science Research Council (11-7785) and by the Danish Technical Research Council (16-4890-1).

[2]O. G. Mouritsen and M. M. Sperotto, in *Thermodynamics of Cell Surface Receptors*, (M. Jackson, ed.) CRC Press, Inc., Boca Raton, Florida (in press, 1992).

[3]M. M. Sperotto and O. G. Mouritsen, *Biophys. J.* 59, 261-270 (1991); *Eur. Biophys. J.* 19, 157-168 (1991).

[4]K. Binder and H. L. Frisch, Dynamics of Surface Enrichment (preprint, 1991)

BFr11

Simulated Folding - A Method for Calculating the Three-Dimensional Structure of Proteins from Nuclear Magnetic Resonance Data[1]

Magnus Ullner[§] and Olle Teleman[†]

[§]Physical Chemistry 2, Lund University, POB 124, S-221 00 Lund, Sweden
Fax: +46-46-104543, E-mail: fk2mul@dix.fkem2.lth.se

[†]VTT, Biotechnical Laboratory, POB 202, SF-02151 Espoo, Finland
Fax: +358-0-4552028, E-mail: Teleman@geeni.bio.vtt.fi

The determination of protein threee-dimensional structure in solution relies on interproton distances measured by nuclear magnetic resonance spectroscopy. Some dihedral angles can also be obtained. This information together with the knowledge of the covalent structure has to be transformed into coordinates of the individual atoms.

The experimental data can be treated as constraints in a simulation as extra force field contributions. Starting from a more or less extended conformation the constraints will force the protein to fold. In restrained molecular dynamics simulation a full force field is used. This is time consuming and much can be gained by simplifying the description of nonbonded interactions, which are normally the bottleneck. This strategy is used in simulated folding. Another advantage with the soft repulsion used for nonbonded interactions in simulated folding is that the energy needed to superimpose two atoms is large, about 30 kT, but not infinite, which makes it possible for atoms to pass through each other. This reduces the risk of obtaining trapped conformations during folding. Contrary to a related method, simulated annealing, the calculation is performed at constant temperature since annealing, i.e. heating and cooling to overcome energy barriers, does not improve performance.

Simulated folding has been used to calculate the three-dimensional structure of a 42-residue fragment containing the N-terminal EGF-homologous module of blood coagulation factor X. This module binds calcium and both the calcium free form[2] and the calcium loaded form[3] have been determined.

In the calcium free case using 370 distance constraints and 27 dihedral constraints, 13 out of 60 random initial conformations converged to conformations with low values of nonbonded energies, constraint energies and sums of constraint violations. The average pairwise root mean square deviation (rmsd) for the backbone atoms (N, C_α, C) of these conformations is 0.95±0.18 Å and 1.77±0.21 Å for all atoms.

In the calcium loaded case 60 runs were made with 420 distance constraints and 29 dihedral constraints. This led to 15 accepted conformations with average rmsd of 0.78±0.17 Å for the backbone atoms and 1.54±0.20 Å for all at ms. The calcium binding site, which is of a new kind and presumed to play an important role in a large number of proteins of varying function, could readily be discerned by visual inspection.

---

[1]Work supported by the Swedish Board of Technical Development (NUTEK) under grant 90-02478P.

[2]M. Ullner, M. Selander, O. Teleman, T. Drakenberg, E. Persson and J. Stenflo, in press.

[3]M. Selander, M. Ullner, E. Persson, O. Teleman, J. Stenflo and T. Drakenberg, submitted.

BFr12

Load Balancing Issues in Molecular Dynamics Simulation on MIMD Architectures

John W. Perram
Henrik G. Petersen
Center for Mathematical Modelling and Numerical Simulation
Department of Mathematics and Computer Science
Odense University
DK-5230 Odense
Denmark

April 7, 1992

email: jperram@imada.ou.dk, hgp@imada.ou.dk

The domain decomposition paradigm will usually work for both SIMD and MIMD simulation of atoms and small molecules interacting via short ranged forces. This is because the compressibility theorem ensures good balancing of the computing load for each subdomain and the short ranged forces ensure that local communications patterns are regular and that global communication does not become an issue.

If the small molecules contain charges or distributions of charges, it is usual to evaluate the forces in truly periodic boundary conditions using the Ewald method. This splits the force computation into a shortranged part and a global Fourier part. In this case, the load balancing is still good and the global communication remains under control.

For large molecules with charge distributions, this may no longer be the case. Firstly, the distribution of charges between the sub-domains will generally not be uniform. Secondly, the coordinates of all the sites in a given molecule are required to implement the constraint dynamics, which imposes irregular and possibly long-ranged communications needs. We will discuss various hybrid addressing schemes which may overcome this problem.

We will discuss preliminary work on using migration of objects as a possible load-balancing tool within the runtime support system currently being developed at KU Leuven.

BFr13

An Efficient Massively Parallel Molecular Dynamics Program for Liquids with Million+ Particles

Fredrik Hedman[¶] and Aatto Laaksonen[§]

[¶]Parallel Computer Center (PDC), Royal Institute of Technology,
S–100 44 Stockholm, Sweden

[§]Division of Physical Chemistry,
Arrhenius Laboratory, Stockholm University,
S–106 91 Stockholm, Sweden

An efficient massively parallel molecular dynamics algorithm, suitable for a very large number of particles in a liquid or solid state, is developed for computing systems built on data parallel (SIMD) architectures.

The computationally heavy force calculations are based on a Linked-cell (LC) scheme by dividing the simulation cell to small cells with dimensions comparable to the used cut-off radius. With an increasing number of particles in the entire simulation cell, the computational effort using the LC scheme becomes proportional to the number of particles N, rather than N^2 as in the conventional scheme.

Massively parallel (SIMD) computing systems have been successfully used to simulate solid matter during the last ten years. In the simulations of liquids, an efficient programming of the periodic update of the moving neighbors to each particle is quite tricky because of high communication costs between the computing nodes in data parallel systems with local memories. In our method the communication costs are drastically minimized and the pure computing maximized:
i) by implementing *coarse-grained* cells in the massively parallel scheme.
ii) after observing that a large part of the inter-cell interactions are negligible. The particles in various zones of the cells are "coloured" according to their relative distances to the particles in the center-cell and the computation is reorganized thereafter.

The implementations are done on a *Connection Machine* CM200 with 8K processors at the PDC in Stockholm using the *Slicewise* protocol. The MD source code is written both in CM Fortran (extension of Fortran 90) and C*.

The apparent differences between the two languages turn out to have a substantial effect on exactly how the algorithm can be implemented. These differences tell about the expressive power between these two languages which a major part of the scientific codes are written in today.

BFr14

Early experiences on the Danish Parallel Supercomputers

Jørgen Moth

The Danish Computing Centre for Research and Education (UNI•C)

Technical University of Denmark, Bldg. 305, DK-2800 Lyngby, Denmark

Abstract

Scientific Supercomputing in Denmark advanced in 1987 when we installed an Amdahl VP1100 as a national facility. Today's top end workstations are approaching the VP1100 in performance, and it is rather obvious that only parallel machines are able to deliver the much talked-about TFlops systems of tomorrow. At UNI•C we are looking at two candidates to replace our VP1100. The KSR1 from Kendall Square Research, a MIMD machine with a shared memory programming model, and the CM-5 from Thinking Machines Corporation, which is more like a SIMD, data parallel programmed system. Last summer UNI•C purchased Europe's first CM-200 to give Danish scientists a first hand impression of working with parallel supercomputers. The talk concentrates on my experience with this machine for the last six months in collaboration with a Molecular Dynamics group of scientists. The intrinsics of the CM-200 are studied in some detail. Key architectural design characteristics with a bearing on system performance have been found and explained. These include computation and inter processor communication issues. They reflect the Fortran run time implementation as much as the underlying machine architecture. The simple magic number rules prescribed by Thinking Machines Corporation in the CM-200 documentation are investigated and their performance implications are measured. We demonstrate our results by predicting the performance of a 2D implementation of Boris's monotonic logical grid method for a Lennard-Jones potential molecular dynamics simulation.

BFr15

Solving the 3-D ASYNNNI Model on the Connection Machine

Thomas Fiig[1], H. F. Poulsen[1], N. H. Andersen[1], P. A. Lindgård[1] and O. G. Mouritsen[2]

[1] Physics department,Risoe National Laboratory, Denmark, [fiig@risoe.dk]

[2] Department of Physical Chemistry, The Technical University of Denmark

The oxygen ordering in the high T_c superconductor $YBa_2Cu_3O_{6+x}$, has previously been studied using the simple 2-D anisotropic lattice gas model, the ASYNNNI model. This model has been able to describe a vast majority of experimental data on the structural phases and termodynamics of the material[1]. However, the structural phase transformation between the tetragonal and the orthorombic phase is associated with the formation of 3-D ordered domains. The spatial extension of these domains was recently studied experimentally using neutron diffraction[2].

We have proposed to model the structural phase transformation in 3-D, by adding an attractive term to the ASYNNNI model Hamiltonian. This model has been termed the 3-D ASYNNNI model.

In the present study we have performed Monte Carlo simulations of the equilibrium behaviour and the dynamics of the 3-D ASYNNNI model. The simulations are done on a massively parallel computer, the Connection Machine (CM), capable of performing 1 GFlop pr. sec. The simulations constitute the first work done on the 3-D ASYNNNI model.

Our preliminary results indicate that a pseudo phase transition separating the disordered tetragonal phase from 2-D ordered orthorhombic phases exists at higher temperature than predicted by the 2-D ASYNNNI model. In this pseudo phase the correlation length along the c-axis is negligible, as witnessed by fig. 1. At a lower temperature we obtain a second phase transition, which is associated with the divergence of the correlation length along the c-axis. We have attributed the word pseudo to the upper phase transition and the 2-D ordered phase because the split between the two transition temperatures would disappear in the thermodynamic limit. However, the effect which is due to the large difference between the interaction strength in the plane and perpendicular to the plane, is a genuine effect in a finite system corresponding to the size of a twin domain in the experimental sample. Below this temperature we obtain a truly 3-D ordered system.

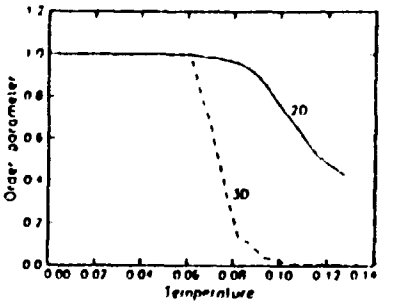

Figure 1: The graph show two order parameters as function of temperature. The solid curve is in plane order (2D), while the dashed curve represents 3D order.

[1] N. H. Andersen et al., Physica C, 172 (1990)

[2] T. Zeiske et al., Nature, 353 (1991)

BFr16

Superconductivity and the XY model in two and three dimensions

Peter Olsson

Department of Theoretical Physics, University of Umeå, S-901 87 Umeå, Sweden,
[Fax: +46 90 166673], [E-mail: olsson@tp.umu.se]

The linearly screened vortex interaction $V_l(r)$ in the two-dimensional XY model is shown to be equal to a particular link correlation function. It is shown that $V_l(r)$ at zero temperature is proportional to the lattice Greens function. At finite temperatures the function $V_l(r)$ calculated by means of Monte Carlo simulations is shown to be entirely consistent with the two-dimensional Coulomb gas analogy. At $T_c \approx 0.9J$ the results are consistent with the universal value of the helicity modulus and at even higher temperature the screening of the logarithmic interaction due to free vortices is clearly visible.

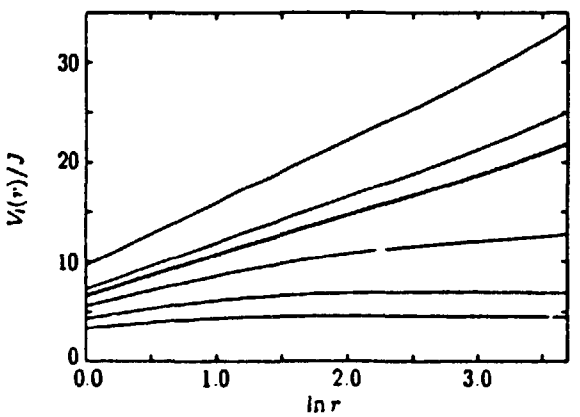

The linearly screened interaction at the five temperatures, from top to bottom, T/J = 0.0, 0.8, 0.9, 1.0, 1.1 and 1.2. For temperatures up to $T_c \approx 0.9J$ (thick line) $V_l(r)$ is to a good approximation logarithmic in r. The saturation at certain finite values in the large-r limit at higher temperatures is a demonstration of vortex unbinding.

The linearly screened interaction is also shown for the vortex loops in the anisotropic three-dimensional XY model - a model of relevance in the context of High-T_c superconductors. In this case it is shown that the vortex-loop interaction is linear in r for temperatures below T_c. The phase transition is again visible as a saturation of the linearly screened interaction at large distances [1].

Vortex loop in the 3D XY model. This particular loop is the shortest one connecting the + and the − squares.

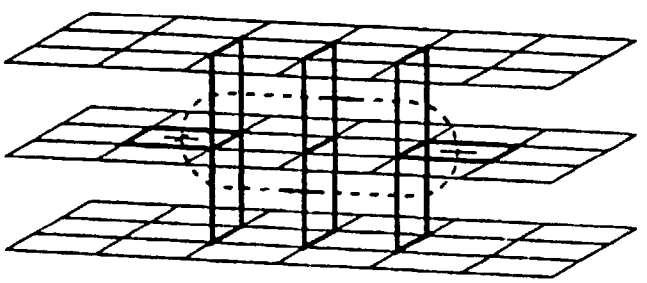

[1] P. Minnhagen and P. Olsson, Phys. Rev. B 44 4505 (1991).

BSa1

Electric Double Layer Forces

Bo Jönsson and Torbjörn Åkesson
Physical Chemistry 2, Chemical Centre POB 124, S-22100 Lund, Sweden

When approaching the electric double layer within a statistical mechanical framework two basic approximations are usually introduced. The first and maybe the most drastic is when the molecular solvent is replaced by a structureless dielectric continuum characterized simply by its dielectric permittivity. The second is when the mean field is used as an approximation to the exact field generated by the charged species in the system.

The first part of this lecture will deal with the mean field approximation and in particular its consequences for the force between two charged aggregates. The way to investigate the Poisson-Boltzmann or mean field approximation will be by means of Monte Carlo (MC) simulations. The mean field theory turns out to be qualitatively correct as long as only monovalent species are present, however, in the presence of divalent or multivalent ions it is qualitatively wrong. The most spectacular manifestation is the appearance of attractive interactions due to ion-ion correlations between equally charged aggregates. Recent experimental force measurements of systems containing divalent ions and also the well-known limited swelling of clays support these results. More refined theories like the hypernetted chain equation confirm these findings, but also simpler approaches based on density functional theory can incorporate a significant part of the ion-ion correlations.

Flexible polyelectrolytes are often used as additives in order to stabilize/destabilize colloidal suspensions. Experimental double layer forces in these systems show a rich behaviour, which to some extent can be modelled within a simple continuum model using MC simulations. The connectivity of ions and their grafting to colloids give rise to additional forces between charged and neutral particles. For example, a new type of attractive interaction is seen between equally charged aggregates, which is due to bridging of polyelectrolytes stretching from one aggregate to another. The attraction is strong and more long ranged than the correlation attraction mentioned above. The bridging mechanism in these polyelectrolyte double layers leads to an unexpected salt behaviour.

BSa2

Monte-Carlo Studies of the Temperature Dependent Size of Polyelectrolyte Chains[1]

Mattias Severin

Department of Physics and Measurement Technology,University of Linköping, S81 83 Linköping, Sweden, Fax:+46 13 137568, E-mail:

We have performed off-lattice Monte-Carlo simulations of isolated short (N=40), fully ionized polyelectrolytes[2] in the presence of a low molecular mass, monovalent salt in the concentration range $0.0 \leq C \leq 1.0$ mol dm^{-1}. The polyelectrolyte is modelled as a freely jointed chain of N hard spherical beads of radius a=2.0 Å. Each bead carries a charge e and interacts repulsively with every other bead on the chain via a screened Coulomb interaction given by the Debye-Hückel potential $V(r)=e^2/\varepsilon_0\varepsilon_r r \exp(-\kappa(r-a))$ where the salt is taken into account through the inverse screening length $\kappa^2=8\pi e^2 C/\varepsilon_0\varepsilon_r kT$. The solvent is represented by a dielectric continuum with dielectric constant ε_r.

The mean square end-to-end distance and the radius of gyration has been calculated as functions of the Bjerrum length Λ, where $\Lambda=e^2/\varepsilon_0\varepsilon_r kT$. $1/\Lambda$ is thus proportional to the temperature. As is shown in the figure, we have found an interesting temperature dependence; at high temperatures the polyion size decreases with increasing temperature, which is tc be expected from simple considerations of the energy/entropy balance. On lowering the temperature, however, we have found that the polyion reaches a maximum size at a certain temperature, which depends on the salt concentration. Further cooling then results in a contraction of the chain. For low salt concentrations, the maximum size represents a rod like configuration, and the polymer shows a coil-to-rod-to-coil transition as the temperature is increased. We suggest that this behavior is due to the increased screening at low temperatures. The Debye-Hückel approximation does not take into account the fact that for $\Lambda/2a>1$ Manning condensation will reduce the effective charge of the chain. We have also incorporated this phenomenon into the model in an *ad hoc* fashion by reducing the charge of each bead according to the Manning fraction.

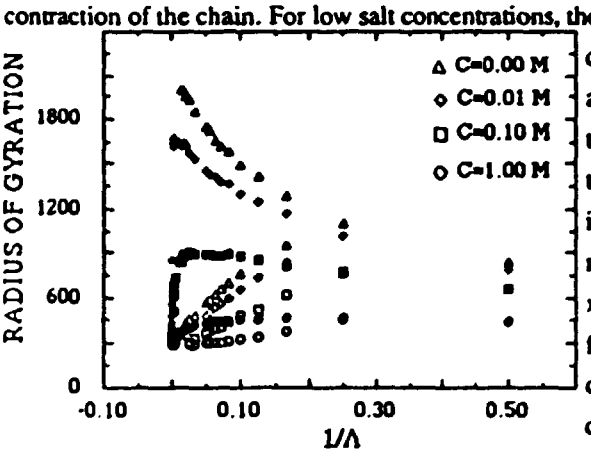

R_G as a function of $1/\Lambda$ for various salt concentrations without (filled symbols) and with (unfilled symbols) Manning condensation explicitly taken into account.

[1]Work supported by STUF under grant 90-00283p and the National Supercomputer Centre in Linköping

[2]M. Mandel, in *Encyclopedia of Polymer Science and Engineering 11(J. Kroschwitz ed.) Wiley, New York (1988), p.739.*

BSa3

Molecular Dynamics Simulation of the Solvation of Benzene Anion. Structural and Dynamical Aspects.

by

K. V. Mikkelsen[1], P. Linse[2], P.-O. Åstrand[3] and G.Karlström[3]

[1]Department of Chemistry, H. C. Ørsted Institute, Copenhagen University
Universitetsparken 5, 2100 Copenhagen Ø, Denmark
[2]Physical Chemistry 1, Chemical Center, Lund University
P. O. Box 124, S-221 00 Lund, Sweden
[3]Theoretical Chemistry 1, Chemical Center, Lund University
P. O. Box 124, S-221 00 Lund, Sweden

As an ongoing research project on improving the understanding of electron transfer reactions in solution we present investigations concerning the solvation of benzene anion radical ($C_6H_6^-$) in water. We present a new intermolecular potential for the interactions between benzene anion radical and water. This potential is determined from ab-initio calculations and is employed in the molecular dynamics simulations. The molecular dynamics simulations provide both structural and dynamical information about the solvation of benzene anion.

Previously we have utilized a somewhat ad-hoc potential for investigating the solvation of $C_6H_6^-$ with either a localized or delocalized charge distribution[1] and we have found approximate similarities with the work by Geiger[2] on solvation of anionic systems. We will discuss the similarities and differences between our recent results and the results in ref.1,2,3.

The intermolecular potential for $C_6H_6^-$ and H_2O is constructed by the NEMO approach[4] and we illustrate some of the properties of this potential.

The structural aspects are given in terms of radial and angular distribution functions. We illustrate the dynamics of solvating $C_6H_6^-$ by presenting time correlation functions, self-diffusion and exchange rates of water molecules between the first solvation shell and the bulk.

BSa4

Computational Statistical Physics of Surfaces and 2-D Systems: Accomplishments and Limitations

Theodore L. Einstein[1]

Department of Physics, University of Maryland
College Park, MD 20742-4111 USA
[Fax: 301-314-9465], [e-mail: TEDEINST@UMDD.UMD.EDU]

Atoms on surfaces interact with each other in complex ways. Comparing theories of these interactions—and of the striking phase transitions which they cause—poses difficult problems in many-body physics. Over the last decade or so, computational techniques have expanded insights into both universal properties (such as critical exponents of the phase transitions) and non-universal properties (such as the energies of the interactions), not just for adsorbed atoms on surfaces, but also for steps on tilted surfaces and for pure two-dimensional systems. Particularly when interactions are short-range, computations are facilitated by confining particles to a lattice. This approximation is generally reasonable, though there are some noteworthy exceptions: 2-d melting (e.g. of a Leonard-Jones system) and high-coverage, weakly adsorbed particles. For general lattice-gas systems, Monte Carlo simulation is typically the method of choice. For systems in which critical slowing down or frustration lead to slow dynamics, the advances in acceleration algorithms in recent years have provided dramatic improvements. When interactions between particles are very short range, transfer-matrix finite-size scaling is often the most rapid and accurate way to map out phase boundaries and investigate critical properties and avoids the drudgery of repeated Monte Carlo calculations. (In this method, one computes correlation lengths from the eigenvalues of infinitely long strips and uses finite-size scaling theory to extrapolate to the limit of infinitely wide strips.) For investigation of global critical properties, one gains considerable insight from analysis of position-space renormalization group flows. Difficulties include the inability to improve the numerics systematically and the rather ill-defined nature of the initial prefacing transformation needed to begin the process. The same reduced dimensionality that makes these techniques so efficient (compared to 3-d) also enhances the role of fluctuations, so that mean field approximations (which neglect these fluctuations) usually lead to quantitative and even qualitative errors. Cluster variation methods do somewhat better, but generally seem to involve at least as much effort as the more reliable methods mentioned above. Computations can serve a variety of roles in advancing understanding, as will be illustrated. On the other hand, some cases will be discussed in which computation is unable to resolve conflicts.

From the standpoint of surface science, arguably the major contribution of computational statistical mechanics has been the ability to find the thermodynamic consequences of interactions either conjectured or computed from electronic properties. By comparing phase diagrams of model systems with experimentally determined ones, one can reject some models and refine others.[2] Non-uniqueness problems plague this process: often the phase diagram contains too little detail to give much information about all but the largest interactions. Another pursuit has been the assessment by simulation of whether

[1]Most of my work on these areas has been in collaboration with Dr. N. C. Bartelt. My research is supported in part by NSF Grants DMR 91-03031, 2 89-18829, and NATO Grant 86/073.

[2]X.-S. Wang, J. L. Goldberg, N. C. Bartelt, T. L. Einstein, and E. D. Williams, Phys. Rev. Lett. 65, 2430 (1990); T. L. Einstein, Langmuir 7, 2527 (1991).

surface-science experiments are capable of probing the long-length-scale behavior of interest to theorists studying 2-d critical phenomena (or, from another viewpoint, whether these theories have any relevance for experiments). Diffraction experiments in particular give considerable information about long-range order.[3] By simulating the structure factor of lattices having the size of defect-free regions and using plausible interactions, we have gauged what sort of accuracy might be expected in estimating critical exponents and amplitude ratios.[4] A key underlying issue is where crossover occurs between critical and mean field behavior. Often the analytically tractable models are different from the models appropriate for experiments or used in simulations. The history of attempts to understand the size of the critical region in the wetting problem is unusually rich. When looking for some subtle effect, such as logarithmic behavior or corrections to scaling, simulations share many of the difficulties of experiments. Recent progress in applications of conformal invariance to 2-d transitions has led to predictions of the form of the critical structure factor. This continuum approach, however, cannot assess over what neighborhood of T_c the predicted form should be measurable. Monte Carlo simulations being performed may provide some indication. [5]

In another class of 2-d problems, computer simulations provide the definitive "experiment" to test theoretical concepts, since there are few if any physical realizations. For the random-field Ising model [6] and for a random surface model,[7] there were some conflicting predictions of critical behavior based on analytic analyses. The cited computer experiments settled which viewpoints were correct. For the latter problem, recent analytic work suggests that when the random surfaces can have arbitrary genus, the critical behavior might change.[8] With high-performance computation[9] it is now possible not only to test these predictions numerically but also to gain further insight by displaying and manipulating the configurations. On the other hand, in numerical studies of the de Fontaine-Wille model of oxygen ordering in $YBa_2Cu_3O_z$, Rikvold *et al.*[10] and we[11] obtained similar information from transfer-matrix finite-size scaling calculations but came to opposite conclusions about the existence of a low-temperature, low-density phase because of differing perspectives. Since the matrices for this subtle problem quickly became large with increasing strip width, numerical methods were unable to resolve the dilemma definitively.

---

[3] Y.-N. Yang, E. D. Williams, R. L. Park, N. C. Bartelt, and T. L. Einstein, Phys. Rev. Lett. 64, 2410 (1990); N. C. Bartelt, T. L. Einstein, and E. D. Williams, Surface Sci. 244 149 (1991).

[4] N. C. Bartelt, T. L. Einstein, and L. D. Roelofs, Phys. Rev. B 32, 2993 (1985); 35, 1776, 4812, 6786 (1987).

[5] N. C. Bartelt and T. L. Einstein, J. Phys. A 19, 1429 (1986); Peter Kleban, in *Applications of Statistical and Field Theory Methods to Condensed Matter*, ed. by D. Baeriswyl *et al.* (Plenum, New York, 1990), 83.

[6] J.-S. Wang, W. Selke, Vl. S. Dotsenko, and V. B. Andreichenko, Europhys. Lett. 11, 301 (1990).

[7] U. Glaus and T. L. Einstein, J. Phys. A 20, L105 (1987); J. O'Connell, F. Sullivan, D. Libes, E. Orlandini, M. C. Tesi, A. L. Stella, and T. L. Einstein, *ibid.* 24, 4619 (1991).

[8] J. R. Banavar, A. Maritan, and A. Stella, Science 252, 825 (1991).

[9] E. Orlandini, M. C. Tesi, F. Sullivan, I. Beichl, A. L. Stella, and T. L. Einstein, unpublished.

[10] T. Aukrust, M. A. Novotny, P. A. Rikvold, and D. P. Landau, Phys. Rev. B 41, 8772 (1990).

[11] N. C. Bartelt, T. L. Einstein, and L. T. Wille, Phys. Rev. B 40, 10759 (1989).

BSa5

Computer Modeling of Oxygen Ordering in $YBa_2Cu_3O_{6+x}$ [1]

Per Arne Rikvold[†§‡ 2] and Mark A. Novotny[§‡ 3]

[†] Department of Physics B-159, and
[§] Center for Materials Research and Technology B-159, and
[‡] Supercomputer Computations Research Institute B-186,
Florida State University, Tallahassee, FL 32306, U.S.A.

The superconducting critical temperature of the high-temperature superconductor $YBa_2Cu_3O_{6+x}$ depends crucially on the concentration and ordering of oxygen ions in the CuO_x basal planes[1]. If $x<\approx\frac{1}{2}$, the material is in a nonsuperconducting tetragonal phase (T). Orthorhombic phases with $x\approx\frac{1}{2}$ (OII) and $x\approx1$ (OI) become superconducting at approximately 60 K and 90 K, respectively. The existence as equilibrium ordered phases of OI and OII has been confirmed by a number of experimental methods[2]. The corresponding ground-state configurations are shown as inserts in Fig. 1. The OI phase consists of densely packed parallel chains of O atoms connected by Cu atoms, whereas in the OII phase every other such chain is empty. Other phases, including $2\sqrt{2}\times2\sqrt{2}$ [3], have also been observed, but their thermodynamic stability is still unclear[4].

Here we report results of nonperturbative transfer-matrix (TM) and Monte Carlo (MC) finite-size-scaling (FSS) studies of a simple lattice-gas model[5] with Hamiltonian

$$\mathcal{H}-u\frac{x}{2}N = -\Phi_{NN}\sum_{(NN)}c_ic_j-\Phi_{Cu}\sum_{(NNN_{Cu})}c_ic_j-\Phi_V\sum_{(NNN_V)}c_ic_j-u\sum_i c_i ,$$

where $c_i\in\{0,1\}$ are the O site-occupation variables, and $x=2N^{-1}\sum_i c_i$. The effective O–O nearest-neighbor (NN) interaction is Φ_{NN}, and Φ_{Cu} and Φ_V are locally anisotropic next-nearest-neighbor (NNN) interactions, with and without a Cu atom between the O sites, respectively. The oxygen chemical potential is u. The lattice and the NNN interactions are shown in the inserts in Fig. 1. With $\Phi_{NN}<0$ (repulsive), $\Phi_{Cu}>0$ (attractive), and $-1<\Phi_V/|\Phi_{NN}|<0$ (repulsive), this model reproduces the phases T, OI, and OII.

Early studies[6-9] used interaction constants $\Phi_{Cu}/|\Phi_{NN}|=+0.5$ and $\Phi_V/|\Phi_{NN}|=-0.5$. Phase diagrams in reasonable agreement with early experimental results were obtained[6,7], and the transitions were shown to be continuous for all T (in contrast to some cluster-variation results), belonging to the universality class of the two-dimensional Ising model for the T/OI and OI/OII transitions, and that of the XY model with cubic anisotropy for the T/OII transition. Maxima in the response function dx/du, which had been experimentally observed in the disordered T phase at high temperatures[10], were explained in terms of essentially one-dimensional local fluctuations associated with the formation of short fragments of oxygen chains[9]. It was also shown how a slight modification of the Hamiltonian, involving weakly attractive O–O interactions of longer range, may bring about first-order T/OII and OI/OII transitions at low T [8].

[1] Supported in part by FSU through supercomputer time and through its Supercomputer Computations Research Institute (U.S DOE Contract DE-FC05-85ER25000) and Center for Materials Research and Technology, and by the U.S. NSF Grants DMR-9013107 and DMR-9146922, The Petroleum Research Fund, and the Florida Graduate Scholars' Fund.

[2] Fax: (904) 644-0098, E-mail: rikvold@scri.fsu.edu or rikvold@fsu.bitnet

[3] Fax: (904) 644-0098, E-mail: novotny@scri.fsu.edu or novotny@fsu.bitnet

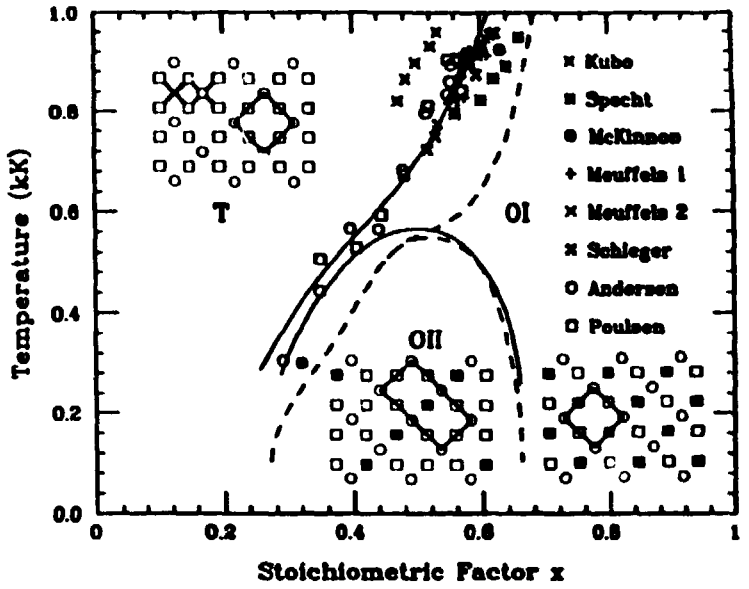

Figure 1: The x,T phase diagram, showing second-order phase boundaries (solid lines) calculated by TM FSS with Φ_{NN}= (−2.8±0.4)kK, Φ_{Cu}=(+2.38±0.06)kK, and Φ_V=(−0.27±0.04)kK, obtained by a nonlinear least-squares fit to the experimental data shown[2,11]. The dashed lines are phase boundaries obtained with interaction constants from LMTO calculations[4,12]. The inserts show the configurations in the CuO_x planes, corresponding to the phases T, OII, and OI. Cu atoms are open circles, O atoms filled squares, and vacant O sites open squares. In the insert for the phase T are also shown the NNN interactions Φ_{Cu} (zig-zag lines) and Φ_V (straight lines).

Recently we have estimated the interactions by a nonlinear least-squares fit to experimental data[2] of the TM FSS phase diagram with strip widths 8 and 12 [12]. The resulting phase diagram is shown in Fig. 1, and the interaction constants are given in the caption.

The results reported here support the view that this lattice-gas model gives an essentially correct description of the mechanism causing the orthorhombic–tetragonal structural phase transitions in $YBa_2Cu_3O_{6+x}$, at least in certain regions of the phase diagram.

[1]R. J. Cava, B. Batlogg, C. H. Chen, E. A. Rietman, S. M. Zahurak, and D. Werder, Phys. Rev. B 36, 5719 (1987); H. Claus, S. Yang, A. P. Paulikas, and B. W. Veal, Physica C 171 (1990).

[2]See references cited in Ref. 11.

[3]R. Sonntag, D. Hohlwein, T. Brückel, and G. Collin, Phys. Rev. Lett. 66, 1497 (1991).

[4]A. A. Aligia, J. Garcés, and H. Bonadeo, Physica C, in press, and references cited therein.

[5]D. de Fontaine, L. T. Wille, and S. C. Moss, Phys. Rev. B 36, 5709 (1987); L. T. Wille, A. Berera, and D. de Fontaine, Phys. Rev. Lett. 60, 1065 (1988).

[6]N. C. Bartelt, T. L. Einstein, and L. T. Wille, Phys. Rev. B 40, 10759 (1989).

T. Aukrust, M. A. Novotny, P. A. Rikvold, and D. P. Landau, Phys. Rev. B 41, 8772 (1990).

[8]C. C. A Günther, P. A. Rikvold, and M. A. Novotny, Phys. Rev. B 42, 10738 (1990).

[9]P. A. Rikvold, M. A. Novotny, and T. Aukrust, Phys. Rev. B 43, 202 (1991).

[10]W R. McKinnon, M. L. Post, L. S. Selwyn, G. Pleizier, J. M. Tarascon, P. Barboux, L. H. Greene, and G. W. Hull, Phys. Rev B 38, 6543 (1988); P. Schleger, W. N. Hardy, and B. X. Yang, Physica C 176, 261 (1991).

[11]D. K. Hilton, B. M. Gorman, P. A. Rikvold, and M. A. Novotny, submitted to Phys. Rev. B.

[12]P. A. Sterne and L. T. Wille, Physica C 162–164, 223 (1989).

BSa6

THEORY OF ADSORBATE INDUCED SURFACE RECONSTRUCTION ON W(100)

Kari Kankaala [*,†], Tapio Ala - Nissila[‡,†,], and See-Chen Ying[‡]**

[‡] Physics Department, Box 1843, Brown University, Providence, RI 02912, USA

[*]Center for Scientific Computing, P.O. Box 40, SF-02101 Espoo, Finland

[†] Department of Electrical Engineering, Tampere University of Technology, P.O. Box 692, SF-33101 Tampere, Finland

[**]Research Institute for Theoretical Physics, University of Helsinki, Siltavuorenpenger 20 C, SF-00170 Helsinki, Finland

E-mails:kankaala@csc.fi, ala@phcu.helsinki.fi, ying@brownvm.brown.edu

Structural phase transitions have been observed on a number of surfaces. One of the most extensively studied systems undergoing a surface reconstruction is the clean W(100) surface. It has a very rich phase diagram with a reconstructive phase transition from a disordered (1×1) phase into an ordered $c(2 \times 2)$ phase.

Hydrogen adsorption on a W(100) surface is known to cause a switching transition in the symmetry of the displacements of the W atoms within the ordered c(2x2) phase. Experimental results on this transition show behavior consistent with both first and second order phase transition.

We report results of a theoretical study of this transition combined with extensive Monte Carlo renormalisation group calculations. Our model is essentially an anisotropic XY model. We found that the character of the switching transition at low temperatures depends strongly on the interplay of the four fold and eight fold anisotropy fields. It changes from a first order transition for enhancing fields to two sequential second order transitions for competing fields. Detailed numerical work as well as mean field arguments will be presented.

BSa7

Monte Carlo simulation of two-dimensional corrugated systems

Eduard Vives[†] **and P.-A.Lindgård**

Risø National Laboratory, Roskilde, DK-4000, Denmark, PAL@RISOE.DK

Structural phase transitions in systems of adsorbed particles on a corrugated surface are studied. The general interest of such systems is the competition phenomena between the particle-particle and the single site particle-substrate interaction, leading to frustration. In such systems defects play a very important role in the stabilization of the different phases. We have focused on the case of D_2 adsorbed on graphite. Using realistic interactions we have performed Monte Carlo[1] simulations changing both coverage and temperature. The phase diagram and structure factors have been calculated yielding quantitative agreement with existing experimental results[2]. At low coverages a commensurate $\sqrt{3} \times \sqrt{3}$ phase is found, while at high coverages a rotated incommensurate phase (RIC) is the most stable. At intermediate coverages a γ-phase (γ) appears, in agreement with experiments. The structure factor in q-space has been obtained up to very high q values which has furnished an understanding of the γ-phase as a two-q modulated structure. The phase transition between the RIC and γ phases can be understood as a transition between a phase with non-soluble defects to a phase with soluble defects. The unexpected epitaxial rotation angle observed experimentally for the γ phase can also be explained with this defect driven mechanism.

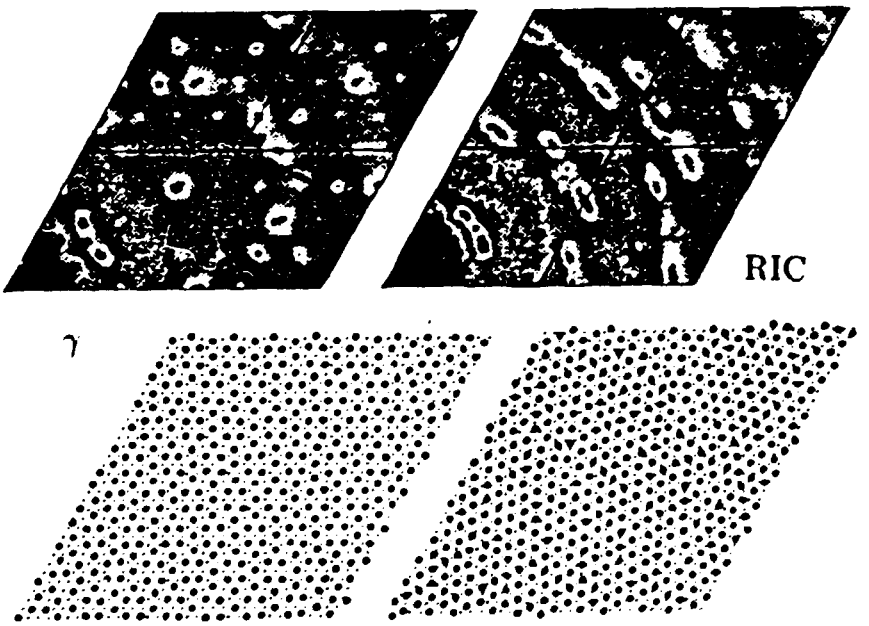

[†] On leave from: Barcelona University, ECM-department, Diagonal 617, E-08028 Barcelona, Catalonia Spain. (Supported by Ministerio de Educación y Ciencia).

[1] E.Vives and P.-A.Lindgard, Phys. Rev. **B44**, 1318 (1991); E.Vives and P. A. Lindgard, Submitted to Phys. Rev. Let.(1992)

[2] J. Cui and S.C. Fain Jr, Phys. Rev. **B39**, 8628 (1989); H. Freimuth, H. Wiechert, H.P. Schildberg and H.J. Lauter, Phys. Rev. **B42**, 587 (1990).

BSa8

Materials Simulations: Defects in Semiconductors and Diamond Growth

Risto Nieminen

Laboratory of Physics, Helsinki University of Technology, 02150 Espoo, Finland,
(RNIEMINE@FINHUT)

A summary is given of the recent work in the ·terials simulation group at HUT. We discuss the large-scale application of Car-Parrinell· 'niques to the structural and electronic properties of point defects (vacancies, antisites and impurities) in semiconductors Si, GaAs and InP. The importance of the close coupling between the charge state and the local atomic relaxations is emphasized. The computational aspects of first-principles simulation are also discussed.

In a second topic, the application of classical molecular dynamics techniques to high-energy surface processes such as sputtering and ion-beam-induced film growth is discussed. The interplay of the collision cascade dynamics and the interatomic potential is elucidated.

BSa9

Molecular Dynamic Simulations of Defect Generation in Strained Metallic Heterostructures.

E. Peter Münger

Department of Physics and Measurement Technology, Linköping University, S-581 83 Linköping, Sweden, [Fax: +46 13 137568], [E-mail: pemun@ifm.liu.se]

Simulations of epitaxial growth of strained heterostructures are becoming increasingly important for prediction and interpretation of experimental results. It is experimentally known[1] that (001) oriented epitaxial Mo/V superlattices grown by magnetron sputtering changes from strained layers without misfit dislocations to unstrained layers with misfit dislocations when the layer thicknesses increase above 1.2 nm. We report on molecular dynamic simulations of defect generation in two-dimensional strained metallic heterostructures. The simulations were carried out using Lennard-Jones potentials, open boundary conditions perpendicular to the layers and periodic conditions parallel to the layers. The size of the simulation box parallel to the layers were chosen to match both of the two lattice mismatched materials, with a difference of one unit cell, at the simulation temperature. Simulations started with a layer of one material on top of a layer of the other material, both in perfect lattice positions for the bottom material. Hence, one strained layer on top of an unstrained layer.

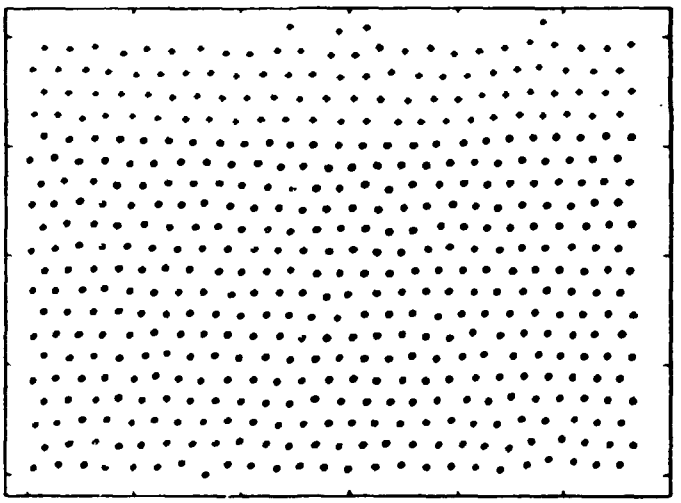

We have used a lattice mismatch of 4% in our simulations compared to the experimental lattice mismatch of 3.6% for Mo/V bcc superlattices. Our simulations show that a compressively strained layer is transformed, by moving atoms to the surface, into a structure with misfit dislocations between the layers and atoms on the otherwise flat surface (See fig.). This occurs for simulations in a narrow temperature range. For higher temperatures first interdiffusion and then melting take place and for lower temperatures no transformations are observed. Our simulations show that in the temperature range where the transformation occur even a thin compressed layer consisting of a single monolayer do transform. We have not found any temperature range where a tensilely strained layer is transformed. In conclusion, our two-dimensional simulations using Lennard-Jones potentials show that there exist a temperature range where compressively strained layers are transformed into unstrained layers. However, we have not found any temperature range where a thin strained layer is stable but a thick strained layer is unstable.

[1] J. Birch, Y. Yamamoto, L. Hultman, G. Radnoczi, J-E. Sundgren and L. R. Wallenberg, Vacuum 41, 1231 (1990)

BSa10

Molecular Dynamics of Hydrogen Diffusion in Pd—Nonadiabatic Effects

Yinggang Li and Göran Wahnström

Institute of Theoretical Physics, Chalmers University of Technology, S-412 96 Göteborg, Sweden, [Fax: 46 31 416984], [E-mail: tfsyl@fy.chalmers.se]

During the last decade, several approaches have been developed for describing the interatomic interactions in solids. All are based on the Born-Oppenheimer (B-O) separation of the electronic and nuclear degrees of freedom. The aim is to be able to make quantitative statements and predictions about real materials. However, the application of B-O approximation to metals may pose additional problems due to the presence of conduction electrons. Electron-hole pairs may be excited with infinitesimal energy and this may become an important mechanism for energy dissipation for hydrogen in metals.

A molecular dynamics simulation has been carried out for hydrogen diffusion in Pd at hydrogen concentration $x = 3\%$ and temperature $T = 623$ K. Under these conditions detailed quasi-elastic neutron scattering (QNS) experiments have been performed. A potential based on the embedded-atom method (EAM) is used, which incorporates some essential many-atom interactions in metals. We find that the EAM-potential alone cannot reproduce the details of the H diffusion: a large discrepancy with the QNS data is observed in the width curve, i.e., the width of the QNS peak as a function of wave-vector (see the figure). By incorporating couplings to low-lying electron-hole pair excitations among the conduction electrons, close agreement with the experimental results is achieved (see figure). We therefore conclude that the discrepancy is most likely due to the use of a single adiabatic potential energy surface, and not due to the particular form of the EAM-potentials. This is a strong indication that in some cases one has to go beyond the B-O approximation in order to characterize correctly the diffusive motion of hydrogen in metals.

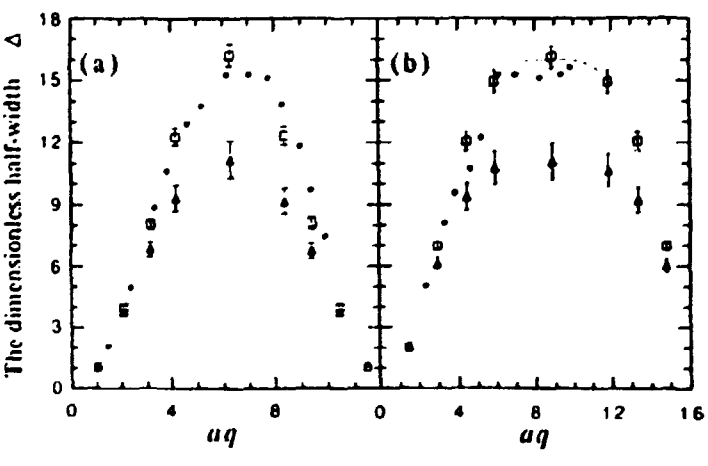

The QNS half-width *vs* aq for wave-vector q (a) along [100] and (b) along [110] directions. ●: experimental results (Phys. Rev. Lett. 29, 1250 (1972)); △: adiabatic potential (EAM) alone; □: with coupling to e-h pair excitations; and dotted lines: the Chudley-Elliott model (Proc. Phys. Soc. London 77, 353 (1961)). The error bars represent a 95% confidence interval.

BSa11

GROWTH OF DIAMOND-LIKE FILMS BY ENERGETIC CARBON ATOM BEAMS

H.-P. Kaukonen and R.M. Nieminen

Laboratory of Physics, Helsinki University of Technology, 02150 Espoo, Finland

Considerable effort has been devoted to the development of methods to synthesize diamond and diamond-like films motivated by the unique characteristics of diamond.

The physical properties of ion-beam deposited (i-C) diamond-like films, such as density, hardness, wear resistance, electrical resistivity and optical transparency are strongly interrelated. Using atomic beam techniques, the optimal values are invariably obtained within an energy interval of incident particles which is practically the same for all parameters typical of diamond-like qualities.

In this work the growth of diamond-like films and overlayers by the deposition of energetic carbon atoms has been investigated using classical molecular dynamics simulations [1]. The interatomic many-atom potential for carbon suggested by Tersoff [2] is used. Structural analysis of the grown films shows that there is an energy window between 40 and 70 eV for the deposited atoms, where the growth most closely results in a dense diamond-like structure. This observation supports earlier experimental suggestions for optimal deposition conditions [3], and indicates that a description neglecting inelastic (electronic) effects is sufficient to understanding the experimental observations of an energy window for optimal growth.

[1] H.-P. Kaukonen and R.M. Nieminen, Phys. Rev. Lett. 68, 620 (1992).

[2] J. Tersoff, Phys. Rev. Lett. 61, 2879 (1988).

[3] D.R. McKenzie, D. Muller, and B.A. Pailthorpe, Phys. Rev. Lett. 67, 773 (1991).

BSa12

Constant-NVT Molecular Dynamics Simulation of Self-Pipe-Diffusion in Gold

J. von Boehm and R.M. Nieminen
Helsinki University of Technology, 02150 Espoo, Finland

Self-pipe-diffusion of vacancies (v) and interstitials (i) in the stacking fault region of a [112] Shockley partial dislocation pair in gold is studied with constant-NVT molecular dynamics (MD) using the many-atom forces of the ATVF[1] and glue[2] models. We find the following formation energies at the edge of a partial dislocation for the ATVF (glue) model: $E_f(v) = 1.4$ (0.8) eV and $E_f(i) = 2.7$ (1.5) eV. The vacancy is found to migrate in the whole stacking fault region at the temperatures 1000, 1150 (Fig. 1(a)) and 1300 K (the melting temperature $T_m = 1336$ K). The corresponding migration energy $E_m(v) \approx 0.2$ (0.3) eV is estimated from the jump frequency relation $f \sim \exp(-E_m/k_BT)$. The interstitial remains – after a transient of about 20-50 ps – vibrating around an equilibrium position at all temperatures above (Fig. 1(b) shows the pattern at 1150 K). Interstitial migration is thus negligible. The activation energy for vacancy self-pipe-diffusion, $E_f(v) + E_m(v)$, equals 1.6 (1.1) eV that is significantly less than $E_f(i)$ alone. Our result agrees accordingly with the traditional view favouring vacancy mechanism[3] and differs from the recent MD study for Cu[4] where vacancies and interstitials were found to contribute comparably. Our results indicate, in agreement with Refs. 4 and 5, that the spread of the diffusion into the whole stacking fault region and not the decrease of the Burgers vector[3] is responsible for the wellknown slowing down of self-pipe-diffusion in Shockley partial dislocation pairs compared to self-pipe-diffusion in perfect dislocations.

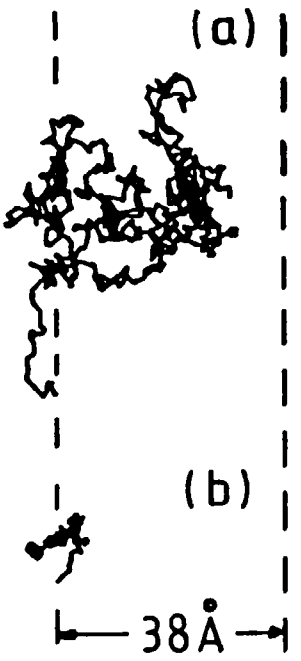

Figure 1. Side view of vacancy (a) and interstitial (b) migration at 1150 K. The simulation time is in (a) 103 ps and in (b) 74 ps including the transient time of 25 ps. Dashed vertical lines denote the edges of the partial dislocations.

[1] G.J. Ackland, G. Tichy, V. Vitek and M.W. Finnis, Phil. Mag. A56, 735 (1987).
[2] F. Ercolessi, M. Parrinello and E. Tosatti, Phil. Mag. A58, 213 (1988).
[3] R.W. Balluffi, Phys. Stat. Solidi 42, 11 (1970).
[4] J. Huang, M. Meyer and V. Pontikis, Phys. Rev. Lett. 63, 628 (1989).
[5] M. Wuttig and K.H. Birnbaum, Phys. Rev. 147, 495 (1966).

BSa13

The Relation between Energy Barriers and the Activation Energy for Na^+ Diffusion in Na-β"-alumina – A Molecular Dynamics Study

Xiaoyun Li and Bjørn Hafskjold

Division of Physical Chemistry,
University of Trondheim - Norwegian Institute of Technology,
N-7034 Trondheim, Norway

A non-stoichiometric NA-β"-alumina system ($Na_{1+x}MG_xAl_{11-x}O_{17}$ with $x = 2/3$) has been studied in detail by molecular dynamics simulations. Special attention was paid to the activation energy and energy barriers for sodium ions in the two-dimensional conduction planes of the solid. We find that the fluctuations of the potential energy for a single sodium ion are much bigger than the experimentally derived activation energy (E_a=0.03-0.09 eV at 250 K<T<400 K and E_a=0.22-0.36 eV at 600 K<T<850 K; Briant and Farrington, 1980; Engstrom et al. 1981).

As an example, curves 1, 2, 3, and 4 in Figure 1 show the displacement of a Na^+ ion from its initial position, the distance between the ion and the nearest ideal Na^+ site, the ion's kinetic energy, and its potential energy, respectively, as function of time at T=400 K. The ion's potential energy fluctuations are so big (2-3 eV) that they completely overshadow the possible energy barrier between two lattice sites. The kinetic energy of the Na^+ ion is small compared to the ion's potential energy fluctuations. The amount of potential energy exchanged with its surrounding ions is much larger than the energy exchange between its potential and kinetic energy. This implies that the activation energy determined from an Arrhenius plot of the diffusion coefficient versus temperature cannot be identified as the energy barrier to the single particle move from one lattice site to another, and if the energy barrier is there, it is a quantity that changes dynamically with the ionic motions in the lattice. The same phenomena are also observed in a Y_2O_3-ZrO_2 system, which is currently the subject of a similar study.

References: Briant, J.L. and Farrington, G.C., 1980, *J. Solid State Chem.*, 33, 385.
Engstrom, H., Bates. J.B., Brundage, W.E. and Wang, J.C., 1981, *J. Solid State Ionics*, 2, 265.

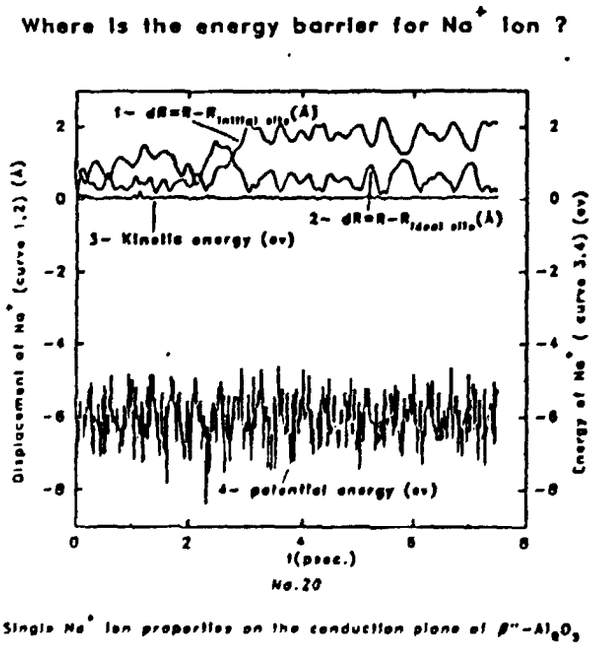

BSa14

Brownian Dynamic Simulation of Restricted Diffusion on Surfaces[1].

I.I Fedchenia and P.-O. Westlund.
Department of Physical Chemistry, University of Umeå,
S-901 87 UMEÅ, [Igor@seumdc51,Fax 090-136310]

INTRODUCTION

Nuclear spin relaxation and Electron spin lineshapes are often governed by orientational fluctuations of a second-rank tensorial property of the molecular system. The copuling between the spin system(S) and the thermal bath (T) may be written in a form where the different motional degrees of freedom can be identified. We introduce three coordinate systems denoted L(Laboratory), M(Molecular), and P(Principal). The stochastic fluctuating spin-thermal bath hamiltonian then takes the form

$$H_{SL}(t) = \sum_n (-1)^n S^2_n \sum_{m'} \sum_m F^{2(P)}_{m'} D^2_{m'm}(\Omega_{PM}(t)) D^2_{m-n}(\Omega_{ML}(t)) \qquad (1)$$

where $D_{mm'}{}^2(\Omega_{ML})$ is a element of the second-rank Wigner rotation matrix. The Euler angles Ω_{ML} specifying the orientation of the M and L frames. In NMR and ESR relaxation studies the relevant correlation function $< H_{ST}(t)H_{ST}(0)>$ studied is formed from Eq.(1). In our study of this correlation function we focus on the fluctuation in $\Omega_{ML}(t)$ brought about by diffusion of the spin-bearing molecule over dividing surfaces separating polar and apolar regions of different liquid crystalline phases. The orientation, $\Omega_{ML}(t)$ of the long axis of the spin-bearing molecule may be described as a restricted random walk on part of the surface of a sphere. This "cone" may then be associated to the dividing surfaces by a Gauss map. The correlation function studied then reflect the geometry of the dividing surface or the surface diffusion dynamics.

COMPUTATIONAL APPROACH

Traditional method of solving the diffusion equation[2], ($\nabla^2_{\xi\eta}$ is the Laplacian and ξ,η are some parameterization of the dividing surface

$$\frac{\partial}{\partial t} P(\xi,\eta,t|\xi_o,\eta_o) = \frac{1}{2} D(\xi,\eta) \nabla^2_{\xi\eta} P(\xi,\eta,t|\xi_o,\eta_o) \qquad (3)$$

with reflecting boundary conditions, by expanding $P(\xi,\eta\ t|\xi_O,\eta_O)$ into series of eigenfunctions of the surface Laplacian becomes untractable for most surfaces of interest. That is, bicontinues liquid crystalline phases[3] where the local parameterization do not determine the global property of the surface.

In the Langevin approach the probability density of a Markoff process, $P(\xi,\eta\ t)$ satisfies the stochastic differetial equation

$$d\{\xi,\eta\} = D(\xi,\eta)\ dW\{\xi,\eta\} \qquad (4)$$

which allow us to simulate the process correctly.

We report a series of numerical realizations of this approach for simulating the relevant correlation function refering to various dividing surfaces.

In one approach we treat $\nabla^2_{\xi\eta}$ as a projected part of the complete Laplacian defined in Cartesian coordinates which simplifies the simulations of the Langevin equation considerably. In a second approach we keep the spin-berairg particle on the surface at every step. Intrinsic locality of eq.(4) allowes for numerical realizations that switches to a new Riemann sheet in a proper way. The boundary condition for a restricted surface is simulated by reflecting tracjectories of (4) into the diffusion domain. The possibility of reducing the computational error is discussed.

1 Supported by the Swedish Natural Research Council and Computer Center of Umeå University.

2. H.Risken, The Focker-Planck Equation, Springer Verlag, 1989.
3 G. Lindblom and L. Rilfors, Biochimica et Biophysica Acta, 988, 221, 1989.

BSa15

LATTICE MODEL OF ELASTICITY AND FRACTURE FOR DISORDERED FIBROUS MATERIALS

M. Karttunen, K. J. Niskanen[§] and K. Kaski

Tampere University of Technology, Microelectronics Laboratory
P.O Box 527, 33101 Tampere, Finland
Fax:+358-(9)31-162 620
[§]Paper Science Centre, The Finnish Pulp and Paper Research Institute
P.O. Box 70, 02151 Espoo, Finland
Fax:+358-(9)0-464 305

In our study we are investigating elastic properties and fracture of disordered fibrous materials, such as paper, by using lattice models. In general, fracturing process is sensitive to all kinds of inhomogenities in the material (fracture also enhances the effects of them). Experimentally it is very difficult to resolve the most important characteristics of these inhomogenities. Such knowledge would give new possibilities to optimize the quality and properties of fibrous materials.

We are approaching this problem by using Monte Carlo simulation method at a mesoscopic length scale. In our model both the breaking of individual cells and of borders between neighboring cells are allowed. The breaking itself is determined by the local stress field. The model is a generalization of the random fuse network[1] in which the burning of an individual fuse due to external voltage corresponds to the breaking of a bond in the elastic network because of increasing stress.

The use of lattice model gives the advantage of larger samples in comparison with a microscopic network model[2]. Nevertheless, this can be used to determine the coupling constants for the lattice model offering a possibility to study the effects of different fiber properties. Disorder in the system is introduced as "quenched" local density, i.e. the local density is initialized as randomly distributed and remains fixed thereafter.

In addition to the above, other points of interest are viscoelastic behavior, i.e. time-dependence of elastic properties upon loading, correlation between fracture path and density distribution, and the effects of crack formation and propagation on stress distribution in the lattice.

---

1. L. de Arcangelis, S. Redner, H.J. Herrmann, J. Physique Lett. 46 (1985) L-585
2. J. Åström, K. Niskanen, submitted to Phys. Rev. Lett.

BSa16

SYMMETRY-BREAKING FRACTURE IN FIBER NETWORKS

K.J. Niskanen and J.A. Åström

Paper Science Centre, KCL, Box 70,
SF-02151 Espoo, FINLAND, Fax +358 0 464305

The fracture process of a two-dimensional high-density fiber network of random topology (Fig a) is studied using computer simulations and effective medium approximation[1]. The fiber segments fail if the axial strain exceeds a breaking treshold (thick lines in Fig a). In the computer simulations the segments strains are obtained from a beam model using the finite element method. In the effective medium approximation the fiber segments are embedded in a homogeneous medium and thus segment strain is a function of the in-plane angle only. The stress-strain curve is obtained by summing up all the unbroken segments.

At small network strain, the failure events spread out over the entire network whereas at large strain most failures occur in a one-dimensional failure zone. The symmetry-breaking transition between the two modes is characterized by a discontinuous size-dependent drop in the network stress. Fig b shows two stress-strain curves obtained in typical simulation runs together with the effective medium result (thick line). The initial fracture phase is a two-dimensional random process characterized by universal scaling laws[2] whereas the final phase is a non-universal one-dimensional random process governed by the probability distribution of breaking strains. The symmetry-breaking mechanism gives a possible explanation to the lack of universality of the final fracture phase observed in certain analogous lattice models[2]. The model is also consistent with experimental results on real paper.

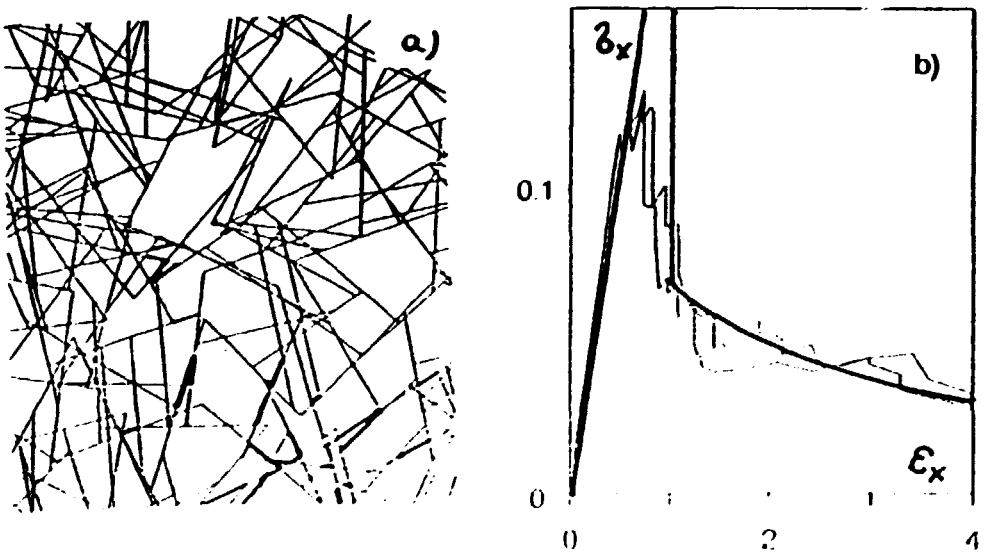

1. J. Åstrom and K. Niskanen, in Proc. of 1991 Int'l Paper Physics Conf. (TAPPI, 1991); PSC Comm. 21. (ISSN 0786-9924, Paper Science Centre, Espoo, Finland, 1991).
2. L. de Arcangelis, in "Statistical models for the fracture of disordered media", H.J. Herrmann and S. Roux, eds., (North-Holland, Amsterdam, 1990), p. 243.

BSa17

Strategy and Early Work in a Theoretical Study of Cellulose and its Degradation;

Lauri Kuutti and Olle Teleman

Biotechnology Lab., VTT, SF-02151 Espoo, FINLAND
Fax: int+358 - 0 - 455 20 28, E-mail: teleman@geeni.bio.vtt.fi

Cellulose is the most abundant organic compound in the biosphere. In nature, its crystalline forms are hydrolysed by cellulases. Understanding these enzymatic processes will aid development of energy saving and non-polluting methods for cellulose degradation and modification as well as of improved methods for wood conservation.

In crystalline cellulose the cellulose chains hydrogen bond to each other. In natural cellulose, cellulose I, these hydrogen bonds connect the chains to sheets, but there are no inter-sheet hydrogen bonds. The structure of cellulose I as published by Gardner and Blackwell [1] was studied by molecular dynamics simulation, using the computer program Discover [2]. Short simulations, 15-20 ps, were made of two systems. One represents a flat surface, 4 sheets with 8 chains each, each chain contained 14 sugar monomers, a total of 8128 atoms forming a slab of approximately 60*60*15 Å. The bottom sheet was kept fixed as well as the chain ends. The other system contains a cellulose ridge, consisting of 14 chains in a triangular arrangement covered by 3700 water molecules.

Short simulations were also made of the cellulose binding tail domain of Cellobiohydrolase I from *Trichoderma reesei* outside the cellulose surface. The structure of this domain has been determined by NMR [3], it is wedge-like with two relatively flat faces, one of which contains three tyrosines. The domain was placed outside the cellulose surface with the tyrosines towards the cellulose. Two short runs were made, 15-20 ps, one for each of the above cellulose arrangements. The runs are too short for identification of detailed binding interactions.

We expect that the precise nature of the hydrogen bonding is important for cellulose properties. We have begun an *ab inito* study of cellulose together with Helsinki University to improve the force field model. We plan to extend the simulations of the perfect cellulose surface, as well as with different surface defects. More recent crystal data will be incorporated. On putting the pure cellulose model on a firmer footing, studies on the binding of the Cellobiohydrolase I tail will be resumed.

[1]Gardner, K. and Blackwell, J., Biopolymers 13, 1975 (1974).

[2]Discover, BIOSYM Technologies Inc., San Diego, USA.

[3]Kraulis, P., Clore, G., Nilges, M., Jones, T., Petterson, G., Knowles, J. and Gronenborn, A., Biochemistry 28, 7241 (1989).

BSu1

Vortex Turbulence

Tomas Bohr

The Niels Bohr Institute
Blegdamsvej 17
2100 Ø

In this talk we shall discuss turbulence in extended (i.e. *large*) dynamical systems. Turbulence, defined as temporally chaos combined with spatially disorder, occurs widely - not only in hydrodynamics. Examples are the motion of flame fronts or the concentration fields of certain inhomogenuos autocatalytic (oscillatory) chemical reactions.

In the Belousov-Zhabotinsky (BZ) reaction the concentrations can oscillate. If the system is large the different parts become dephased and *vortices* or *spiral waves* can occur. Close to the onset of oscillatory behaviour, the system can be described by a complex Ginzburg-Landau equation. We have simulated a discrete version of that equation and found an interesting transition to turbulence, quantified by the largest *Lyapunov exponent*. [1] In particular we found that the system has bound vortex-antivortex states and that transient turbulent states typically end up in such "entangled" states. Further we found that turbulent states can occur in a regime which was thought stable. Recently simulations have been performed on a connection machine [2] confirming this picture and giving the critical behaviour of the transient time near the onset of turbulence in terms of the nucleation of large entangled vortices.

The complex Ginzburg-Landau equation describes a slowly varying disturbance in a time-periodic state. The order parameter is *complex* and on the figures below it is shown as a small vector on each site of a 2-d lattice. Figure 1 shows a single vortex (spiral wave). Equiphase lines are spirals and the wavelength of the spiral is selected by the equation as function of the parameters. Figure 2 shows a turbulent state with several vortices (dots) and where creation and annihilation of vortex-antivortex pairs is continually taking place.

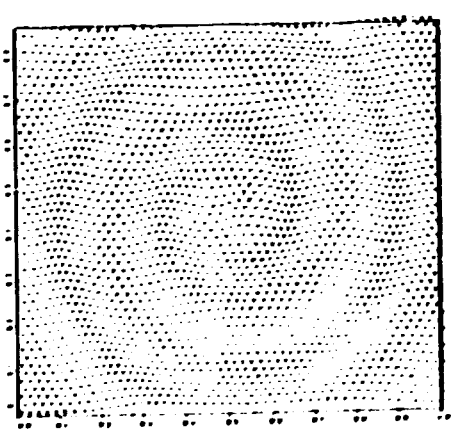

1

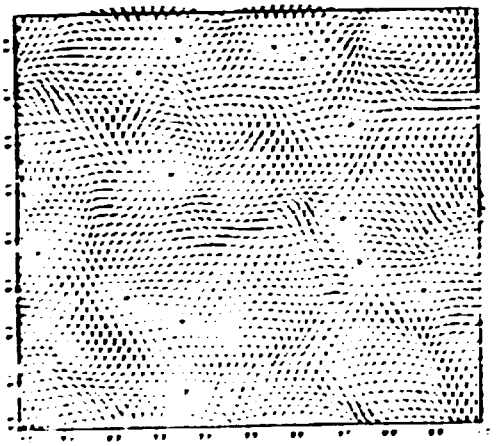

2

[1] T. Bohr, M. H. Jensen and A. W. Pedersen, Phys. Rev. A 42, 3622 1990
[2] G. Huber, P. Alstrøm and T. Bohr, preprint 1992

BSu2

Evolution and Co-evolution in Rugged Fitness Landscapes

Per Bak[§], Henrik Flyvbjerg[‡] and Benny Lautrup[‡]

[§] Department of Physics, Brookhaven National Laboratory, Upton NY 11973, USA,
email: bak@bnlux1.bnl.gov fax: +1 516 282 2918

[‡] CONNECT, The Niels Bohr Institute, Blegdamsvej 17, DK-2100 Copenhagen Ø
email: flyvbj@nbivax.nbi.dk, lautrup@connect.nbi.dk fax: +45 3142 1016

Some time ago Stuart Kauffman suggested a simple model for biological evolution, the so-called *NKC-model*[1]. In an abstract, mathematical way it describes genetic evolution and mutual adaption of interacting species in an ecology. Evolution is Darwinian, driven by random mutations, the fitter of which are selected. As a higher fitness of one species may reduce the fitness of another, the *fitness landscape* in which evolution takes place, is itself, to some extent, a dynamically changing entity. So is the complexity of the evolving life-forms and their interactions.

From a physicist's point of view, the NKC-model is a quenched disordered system with stochastic dynamics, but with the extra twist relatively to the usual spin-glass-like problems that interaction strengths and the size of phase space are parts of the dynamics — and the latter may grow unlimited.

It has been suggested that this kind of dynamical system has a frozen and a chaotic phase, and that evolution drives it to the critical point separating the two phases, i.e. "life" is self-organized critical. This suggestion is based on the idea that co-evolving species drive each other through evolution and to higher fitness faster than individual species can evolve. The latter tend to get stuck at local fitness maxima, while the former may pull each other out of such low-lying maxima. This scenario selects against the behaviour characterizing a frozen phase. On the other hand, if the fitness of individual species depends very much on the state of other species, they may never reach a significant degree of collective adaption, but instead constitute an ever-changing environment to each other. This scenario selects against the behaviour characterizing a chaotic phase. At the phase boundary, the best characteristics of both phases are attained: an evolution of extended duration with the ability to retain acquired fitness.

If the NKC-model in all its abstract generality is self-organized critical for these reasons, this result lends some rigour to speculations about the dynamics of evolution, and its characterization in qualitative terms. It is difficult, however, to investigate the NKC-model in the obvious way its complexity invites: by Monte Carlo simulation. The reason for this is its very complexity. So to have some guide-lines regarding where and what to look for, we have solved a version of the NKC-model analytically[2]. In the talk we present results, and discuss possible simulations.

---

[1] S. A. Kauffman, *Origins of Order: Self-Organization and Selection in Evolution* (Oxford Univ. Press, Oxford, 1990)

[2] P. Bak, H. Flyvbjerg and B. Lautrup, *Evolution in a Rugged Fitness Landscape*, preprint, NBI-CS-92-??, and *Co-Evolution in a Rugged Fitness Landscape*, preprint, NBI-CS-92-??

BSu3

Diffusive description of lattice gas models

Thomas Fiig[1] and Henrik J. Jensen[2]

[1] Physics department,Risoe National Laboratory, Denmark, [fiig@risoe.dk]

[2] Niels Bohr Institute, Denmark, [jensen@nbivax.nbi.dk]

We have investigated numerically a deterministic lattice gas model, driven by a white noise boundary condition, by calculation different ensemble properties of the system, including the power spectrum of the number of particles on the lattice, the lifetime distribution, and the spatial correlation function [1]. These average properties are in turn discussed on the basis of the simplest possible diffusive description, the two dimensional linear diffusion equation [2]. The description prove to be valid for a moderate boundary drive, while it fails altogether when the drive goes to zero. Finally we introduce a deterministic lattice gas model, where the stochastic element is substituted by periodic boundary conditions. This model still exhibits a $1/f$ power spectrum for the number of particles inside an imaginary box on the lattice.

The linear diffusion equation, for a finite system, has been solved in one and two dimensions, using Greens functions, resulting in a power spectrum of the following form

$$S(f) \propto \left(1 + AN^4 f^2\right)^{-1/2},$$

where A is a constant, depending of the diffusion constant and N the linear extend of the system. This expression can be used to check the validity of the diffusive description of the deterministic lattice gas model.

Below on fig. 1 is shown computer simulations of the power spectrum for the lattice gas model for different sizes of the lattice. We see that for high frequencies $S(f)$ behaves as $1/f$-noise, while for f less than some critical frequency we obtain white noise.

This observation is in accordance with the analytic formula, which reproduces both limits of the power spectrum and further predicts that the critical frequency should scale with the reciprocal of the volume. A plot of f_c versus N, show that this is in fact the case.

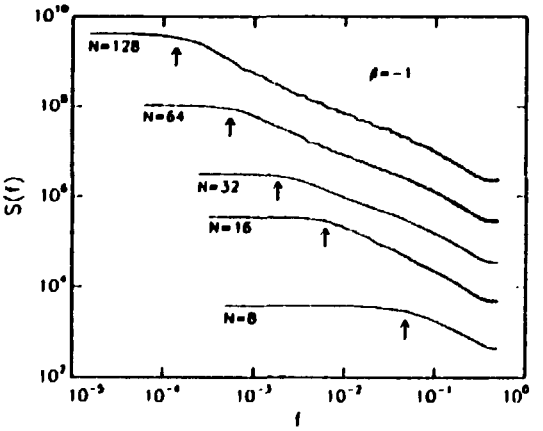

Figure 1: Power spectra for the deterministic lattice gas model for different latticesizes. The arrows indicate the cross-over frequency f_c from $1/f^1$ to $1/f^0$.

[1] H. J. Jensen, Mod. Phys. Lett. B, 5 (1991)

[2] H. J. Jensen, Physica Scripta 43, (1991)

BSu4

Critical Spin-Exchange Dynamics in Spatially-Modulated Ising Chains using Minimal-process Algorithm

Stephen J. Cornell

Département de Physique Théorique, Université de Genève,
24 quai Ernest Ansermet, CH 1211 Genève 4, Switzerland.
Email: cornell@sc2a.unige.ch, Fax: (+41.22)781.21.92

The non-universal dynamic critical behaviour of spatially-modulated 1-dimensional Ising systems has aroused considerable interest in recent years. Whilst the non-universality for the case of single-spin-flip dynamics can be explained simply in terms of the presence of an energy barrier[1], the case of spin-exchange dynamics has provoked considerable controversy. The Renormalization Group and all other analytical approaches [2] find the same value for the dynamic critical exponent, but this value is inconsistent with the dynamic scaling theory that is expected to hold in such activated systems[1] and is also smaller than the supposed lower bound afforded by physical 'domain-wall' arguments (DWA).

The pathological divergence of relaxation times at low temperatures renders traditional (Metropolis or similar) Monte-Carlo simulations unable to settle the controversy. Unlike other, simpler cases of activated dynamics[3], it is not possible simply to factorize out the Arrhenius factor. However, the so-called '*Gillespie*' or '*mimimal-process*' algorithm is ideally suited to this kind of problem, where there are anomolously long waiting times between processes. This type of algorithm has found widespread use in chemical physics (e.g. reaction-diffusion problems), but appears inexplicably to have been neglected in the field of Ising model simulations. Although the algorithm is not suited to vector or parallel machine architecture, the simulation time becomes essentially independent of the energy barrier and so very low temperatures may be simulated at no extra cost. The simulations, which took some 100 hours or so on a Sun IP-X workstation, would have required several years (!) of Cray time using a conventional algorithm.

We use the same technique as previously used for the 1-d BEG model[4]. By using a scaling theory to relate the growth of domains to the dynamical critical exponent, we reproduce the results of the DWA to very good accuracy. We interpret this by showing that the analytic approximations are only valid in the short-time regime. Finally, we study the case of randomly distributed +ve and −ve bond values, and comment on the usefulness of this algorithm for spin glasses and other frustrated systems.

---

[1] S. Cornell, M. Droz, and N. Menyhárd, *J. Phys. A: Math. Gen.* 24, L201 (1991)

[2] J. Luscombe, *Phys. Rev* B 36, 501 (1987); J. M. Nunes da Silva and E. J. S. Lage, *Phys. Rev.* A 40, 4682 (1989)

[3] S. Cornell, K. Kaski and R. B. Stinchcombe, *Phys. Rev.* B 45, in press (1992)

[4] J. F. F. Mendes, S. Cornell, M. Droz, E. J. S. Lage, *J. Phys. A: Math. Gen.* 25, 73 (1992)

BSu5

Computer Simulation of Self-Organization in Domain-Boundary Dynamics[1]

Jørgen Vitting Andersen[§] and Ole G. Mouritsen[‡]

[§]Laboratoire de Thermodynamique Physico-Chimie Metallurgiques, Institut National Polytechnique de Grenoble, ENSEEG Domaine Universitaire B. P. 75, F-38402 Saint-Martin-d'Heres CEDEX, France.
[Fax: 33--76826630], [E--mail: FYMJV@NEUVM1]

[‡]Department of Physical Chemistry, The Technical University of Denmark, Building 206, DK-2800 Lyngby, Denmark.
[Fax: 45--42--880977], [E--mail: FYMEARN@NEUVM1]

Self-organizing dynamics of two-dimensional magnetic domain patterns has recently been studied in a experimental setup[1] as well as in a theoretical study of a random-neighbor model.[2] In the experiment it was observed that the magnetic domain pattern self-organizes into a state of barely stable configurations. In this state, small field increments trigger avalanches of cell destruction that span more than two orders of magnitude in size and lifetime. The experimental distributions of avalanche sizes and lifetimes appeared to follow power laws, and it was suggested that the system might have arranged itself into a self-organized critical state.[3] Later theoretical work[2] has described the dynamical properties of these domain patterns within a mean-field-type random-neighbor model, where it is found that the domain pattern self-organizes in a *sub*critical state.

In this paper[4] we go beyond the mean-field description and allow fully for thermal fluctuations by presenting a computer-simulation calculation of the dynamical self-organization of domain patterns in a two-dimensional ferromagnetic impure Ising spin model which thermally has been quenched into its unstable regime. By driving the system very slowly using a uniform magnetic field we produce a dynamical situation which is analogous to that in conventional self-organized critical systems, which are slowly driven steady-state systems.[3] We have analyzed the lifetime- and size-distribution functions for the avalanches in the model. The avalanche-like rearrangements of domain patterns are found to have the signature of a self-organized state which is subcritical. The avalanche-size distribution function displays, however, an effective power-law behavior and the power spectrum is $1/f$-noise-like. Our results are in accordance with the findings from the random-neighbor mean-field model study[2] and the experiment[1] on the dynamics of domain patterns in magnetic garnet films.

1. K. L. Babcock and R. M. Westervelt, Phys. Rev. Lett. **64**, 2168 (1990).
2. P. Bak and H. Flyvbjerg, Phys. Rev. A **45**, Feb. 15 (1992).
3. P. Bak, C. Tang and K. Wiesenfeld, Phys. Rev. Lett. **59**, 381 (1987); Phys. Rev. A **38**, 364 (1988).
4. J. V. Andersen and O. G. Mouritsen, Phys. Rev. A (in press, 1992).

[1]Work supported by the Danish Natural Science Council (11-7785 and 11-9319-1), by the Danish Technical Research Council (16-4296 K), and by the Maxwell Foundation

BSu6

The Effect of Impurities in a Driven Diffusive System[1]

Kent Bækgaard Lauritsen[a] and Hans C. Fogedby[b]

Institute of Physics and Astronomy, Aarhus University
DK-8000 Aarhus C, Denmark
E-mail: [a]kent@dfi.aau.dk and [b]fogedby@dfi.aau.dk

The driven diffusive system (DDS) is a simple model which has been extensively used in the study of stationary nonequilibrium states. An external electric field drives the particles through the system and because of periodic boundary conditions a stationary nonequilibrium steady state is reached.[2]

Locally the particles interact by a nearest-neighbour force which can be either attractive or repulsive. If the interaction is repulsive it is found that the system belongs to the Ising universality class with the critical temperature being a decreasing function as the external field is increased. With a ferromagnetic interaction the DDS system settles down into a stationary state consisting of a "strip" of particles parallel to the external field. As the temperature reaches a certain critical value this strip breaks up and dynamic renormalization group arguments together with an anisotropic finite-size scaling analysis show that this kinetic phase transition is described by new critical exponents different from the Ising values.

We study the effect of quenched impurities in the ferromagnetic driven diffusive lattice gas model by carrying out Monte Carlo simulations. The system still undergoes a second order kinetic phase transition as the temperature is varied. The critical temperature is determined from an anisotropic finite-size scaling analysis and it is found to decrease linearly as the impurity concentration is raised. Critical properties are estimated to be equal to those of the driven system without impurities. Furthermore, the power spectrum of the current correlations at the determined critical temperature has been calculated and agreement with the result for the DDS system is obtained.

For the antiferromagnetic DDS system diluted with small amounts of fixed impurities a standard finite-size scaling analysis shows that this system is described by the Ising exponents.

---

[1]This work has been supported by the Danish Natural Science Research Council under Grant No. J. Nr. 11-9001-2. KBL gratefully acknowledge support from the Aarhus University Research Foundation and the Carlsberg Foundation.

[2]For a review see B. Schmittmann, *Int. J. Mod. Phys.* B4, 2269 (1990)

BP1

Molecular Dynamics Studies on Regulatory Peptides[1]

Berith Bjørnholm,[§] Thue W. Schwartz,[‡] and Flemming S. Jørgensen[§]

[§]Department of Organic Chemistry, Royal Danish School of Pharmacy, Universitetsparken 2, DK-2100 Copenhagen Ø, Denmark, Fax: 45 35 37 57 44, E-mail: berith@dfhvax.nbi.dk

[‡]MRC-Laboratory for Molecular Endocrinology, University Department of Clinical Chemistry, Rigshospitalet 6321, DK-2100, Copenhagen Ø, Denmark, Fax: 45 31 35 29 95

We report molecular modelling and molecular dynamics studies on turkey Pancreatic Polypeptide (PP), human Neuropeptide Y (NPY) and lamprey Peptide MY (PMY).[2] This work has been done in order to obtain solution structures of the peptides and thereby be able to reveal the important factors governing their unique structural stability.

The pancreatic polypeptide (PP)-fold family of regulatory peptides share sequence similarity among their 36 amino acids and have a common, very stable, tertiary structure, the so-called PP-fold. In mammals, the PP-fold peptides are represented by neuropeptide Y, a neurotransmitter in the central and pheripheral nervous system, peptide YY (PYY), a hormone from the lower intestine, and pancreatic polypeptide, a pancreatic hormone. Only the structure of pancreatic polypeptide from turkey has been determined experimentally by X-ray crystallography. This peptide has a compact globular structure with a hydrophobic core comprising two anti-parallel helices, an N-terminal polyproline-like helix (residues 2-8) and an amphipathic α-helix (residues 14-32), connected by a β-turn[3] (see figure).

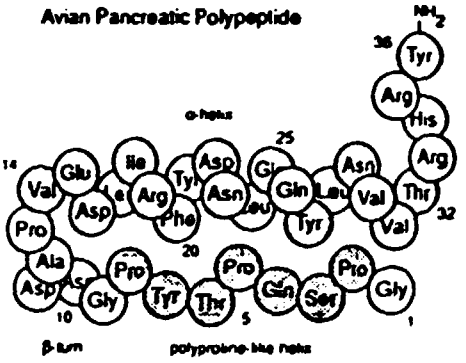

In this work the computer programs Discover and Insight (Biosym Technologies Inc. San Diego, USA) were used to make free dynamics simulations on the peptides in a water box using periodic boundary conditions. Different strategies were applied on turkey PP and a structurally unstable analog of turkey PP by changing the temperature, the length of time used for the dynamics simulation, as well as the amount of solvent water included in the simulation. This was done in order to evaluate the influence of these parameters on the results.

The dynamics simulations compare well with experimental results since in our studies turkey PP, experimentally shown to be stable in aquas solution,[3] undergoes no significant changes in the overall folding during a 100 psec simulation. On the other hand the unstable analog of turkey PP[4], PP_{1-32}, where residues 33-36 of turkey PP is cut off, looses its tertiary structure during the same period of simulation. Solvent structures of human NPY will be presented, and the relative stability of avian PP and human NPY will be discussed.

---

1. Work supported by the Danish Technical Research Council and the PharmaBiotec Research Center.

2. Conlon, J.M., Bjørnholm, B., Jørgensen, F.S., Youson, J.H. and Schwartz, T.W. *Eur. J. Biochem.*, 199, 293 (1991).

3. Clover I.D., Barlow, D.J., Pitts, J.E., Wood, S.P., Tickle, I.J., Blundell, T.L., Tatemoto K., Kimmel, J.R., Wollmer A., Straßburger, W., and Zhang, Y.S. *Eur. J. Biochem.*, 142, 379 (1984).

4. Tonan, K., Kawata, Y. and Hamaguchi, K. *Biochemistry*, 29, 4424 (1990).

BP2

Molecular modelling of chymotrypsin-substrate interactions: Calculation of enantioselectivity[1].

Martin Norin[1], Anders Mattson[2], Torbjörn Norin*[2] and Karl Hult*[1]

[1]Department of Biochemistry and Biotechnology, [Fax: +46-8-7231890], [E-mail: martin@physchem.kth.se]

[2]Department of Organic Chemistry, The Royal Institute of Technology, S-100 44 Stockholm, Sweden, [Fax: +46-8-791 23 33], [E-mail: andersm@physchem.kth.se]

ABSTRACT

In the search of fast and robust methods to calculate interaction energies of protein/ligand binding and enzyme catalysis we have developed a molecular mechanics and molecular dynamics protocol to calculate the enantioselectivity of chymotrypsin catalysed hydrolytic reactions. Nine different ester substrates, which are hydrolysed by the enzyme over a wide range of reaction rates have been studied. Models of the transition state of the ester hydrolysis were built using computer aided molecular modelling. The energies of the transition state models were calculated by molecular mechanics and molecular dynamics methods[2]. The point charges of the substrates were modelled from known force field parameters and by semiempirical methods. The difference in free energy of activation between the enantiomers of each substrate were compared with experimental values. The calculations approximated the experimental results. The calculated structure of the transition state model of the chymotrypsin catalysed hydrolysis of acetyl-phenylalanine ester was virtually the same as the published crystal structure of a chymotrypsin-trifluoromethyl ketone inhibitor complex (Brady et al., Biochemistry 29:7600-7607, 1990).

[1]This work was supported by the National Swedish Board for Technical Development, Swedish Research Council for Engineering Sciences and Carl Tryggers Stiftelse. Knut och Alice Wallenbergs Stiftelse is acknowledged for financial support of equipment.

[2]van Gunsteren, W. F. and Berendsen, H. J. C. (1990) Computer simulations of molecular dynamics: Methodology, applications, and perspectives in chemistry. Angew. Chem. Int. Engl., 29, 992-1023

BP3

Molecular dynamics simulation of 22 amino acid peptide hormone motilin in aqueous solution

J.Zdunek and A.Gräslund Email:medbio@biovax.umdc.umu.se
Department of Medical Biochemistry and Biophysics
University of Umeå, 901 87 Umeå, Sweden Fax: +46 90/136310

It is not fully obvious that a small polypeptide (like 22 amino acid hormone motilin with the sequence PHE VAL PRO ILE PHE THR TYR GLY GLU LEU GLN ARG MET GLN GLU LYS GLU ARG ASN LYS GLY GLN) has any stable secondary structure in aqueous solution. In order to increase our knowledge with regard to this problem (which is of great importance not only structurally but also functionally for the living processes), molecular dynamics simulations of motilin in water have been performed. The starting structure of motilin was obtained from 2D NMR measurements (in water with 30% hexafluoro-2propanol) followed by Distance Geometry calculations, Restrained Molecular Dynamics (in vacuum) and refined by an Iterative Full Relaxation Matrix method[1]. This starting conformation consists of an alpha-helical part (residue 9 to 20) and a wide turn (not well defined by NMR data) near the hydrophilic N-terminal part of motilin.
The motilin molecule was placed in a rectangular box with 1296 molecules of water previously equilibrated by MD. The system consisting of 3787 atoms in the box with periodic boundary conditions was subjected to a molecular dynamics simulation by using the programm CHARMM with its standard force field (except for the hydrogen-bond term) and the TIP3P model of water molecules.
The whole system was initially energy minimized (Powell algorithm), heated to the desired 298 K and equilibrated during 11 ps with the reassignment of velocities from Maxwellian distribution (1ps) and rescaling of velocities (following 10 ps) for all atoms. The all hydrogen model was used and in order to allow for a timestep of 1 fs, the SHAKE algorithm was applied for constraining of all covalent bonds of hydrogen atoms. Subsequent analysis runs were performed without any external perturbations and the trajectories (coordinates) and velocities were recorded every 50 fs.
Our preliminary results after 100 ps simulation show that there is an ongoing transition between the starting structure and the final conformation (if any) for motilin in water. For the RMSD (Root Mean Square Deviation) value between the starting structure and the current structure we have observed a very rapid increase to 1.5 Å after the first few picoseconds followed by a period of slowly increasing RMSD which then stabilized at a value of about 2.7 Å during the subsequent simulation. The helical part of motilin becomes more regular with a tendency to extend also over the residue 7 and 6. At the same time the behaviour of the hydrophilic C-terminal part of the molecule tends to start unwinding the alpha helix.
After (up to now) only 100 ps of simulation it is not possible to predict if the present conformation will be stable or not. The detailed structural and dynamical analysis will be done and presented after accomplishing of the whole simulation.

[1]S.Edmondson, N.Khan, J.Shriver, J.Zdunek and A.Graslund
The solution structure of motilin from distance constraints, distance geometry, molecular dynamics, and an iterative full relaxation matrix refinement. Biochemistry 1991, 30, 11271-11279.

BP4

Computer Simulation of Membrane Behaviour and Ordering Processes in Two-component Lipid Membranes[1]

Kent Jørgensen,[*] Maria M. Sperotto,[*] Ole G. Mouritsen,[*]
John Hjort Ipsen,[*] and Martin J. Zuckermann[&]
[*]The Technical University of Denmark and [&]McGill University, Canada.
[Fax: 45 42880977], [E-mail: jorgense@virus.fki.dth.dk]

Mixtures of lipids can undergo phase separation phenomena resulting in stable coexisting domains due to the non-ideal mixing properties of the lipids. The coexistence of different phases in the lateral membrane plane can be induced by a change in temperature, pressure, ionic strength or pH. The question of whether such phase separated regions also exist in biological membranes and moreover whether the coexistence of different phases and the associated differentiated regions in the membrane play any functional role in relation to the many biological processes e.g. enzymes and proteins associated with a biological membrane is a question of considerable importance in modern membranology.

An extensive Monte Carlo computer-simulation study is performed on a simple but general molecular model developed to describe the non-ideal phase behavior of two-component mixtures of phospholipid bilayers. The model is an extension of an earlier model successfully used to describe the gel-to-fluid chain melting transition of fully hydrated one-component saturated phospholipid bilayers. The calculations reveal that the non-ideal phase behavior of two-component phospholipid bilayers can effectively be modelled as a function of the difference in chain length between unlike lipids. The non-ideality is manifested in immiscibility in the gel phase of mixtures of phospholipids (DLPC-DSPC) having six carbon atoms or more in difference and miscibility in the gel phase of lipid mixtures (DMPC-DSPC) having only four carbon atoms in difference. Interesting non-equilibrium effects have been observed in the phase-separated regions including a slowing down of the growth of the non-equilibrium phases caused by an enrichment of the phase boundaries by the low-melting lipid. This leads to a membrane with long-living non-equilibrium differentiated lateral regions. Such phenomena might be important in a biological membrane composed of many different lipids by giving rise to a heterogeneous membrane state with highly differentiated regions.

[1]Work supported by the Danish Natural Science Research Council (11-7785 and 11-7498) by Lovens Kemiske Fabriks Fond, by FCAR du Quebec, and by NSERC of Canada

BP5

Computer Simulation of Local Structure in Lipid Bilayers Containing Cholesterol[1]

T. E. R. Hønger, K. Jørgensen, J. H. Ipsen, and Ole G. Mouritsen

Department of Physical Chemistry, The Technical University of Denmark, Building 206
DK-2800 Lyngby, Denmark
[Fax: 45--42--880977], [E--mail: FYMEARH@NEUVM1]

The fluid lipid–bilayer component of biological membranes is a piece of liquid-crystalline matter with exceptional thermodynamic and mechanic properties. Being no more than 50Å thick, the lipid bilayer is a highly anisotropic system with a thermotropic phase behavior which involves pseudo–two–dimensional solid as well as liquid phases. The lateral structure of these phases, in particular the local structure, is of interest in relation to membrane lateral organization and function. Specifically, it is of interest to unravel how additional molecular compor ·:s dissolved in the membrane may change the local structure on the scale 5-100Å.

The present paper presents a computer–simulation study of the effect of cholesterol on the fluctuations and the local structure of a phospholipid membrane. The simulation study is based on a statistical mechanical model of a pseudo–two–dimensional system of molecules with translational (crystalline) as well as internal (conformational) degrees of freedom. The model is formally a lattice–gas Potts model[2] in which cholesterol's different modes of interaction with the different membrane phases are taken into account.[3] The phase diagram derived from the model is in close agreement with recent experimental measurements.[4] The simulation results reveal an intricate interplay between ordering processes governed by the two different degrees of freedom. Results are presented for the thermodynamic and microscopic properties in the phase containing high levels of cholesterol, above 20–30 mol%. This phase is a fluid with a high degree of lipid–chain order. By analysis of the microscopic structure of the membrane as a function of temperature, it is revealed how cholesterol acts so as to break the crystallinity but conserve the membrane structure locally. The structure of the membrane is compared to that of a structured fluid (microemulsion).

[1]Work supported by the Danish National Science Research Council (11-7785 and 11-7498) and by Lovens Kemiske Fabriks Fond.

[2]J. H. Ipsen, G. Karlström, O. G. Mouritsen, H. Wennerström, and M. J. Zuckermann, *Biochim. Biophys. Acta* 905, 162 (1987).

[3]M. J. Zuckermann, J. H. Ipsen, and O. G. Mouritsen, in *Cholesterol and Membrane Models*, (L. X. Finegold, ed.) CRC Press, Inc., Boca Raton, Florida (in press, 1992).

[4]M. R. Vist and J. H. Davis, *Biochemistry* 29, 451 (1990).

BP6

Computer Simulation of fluid Interfaces[1].

Claus Jeppesen, John H. Ipsen
Department of Physical Chemistry.
The Technical University of Denmark
[Fax: 45 42880977], [E-mail: ipsen@virus.fki.dth.dk]

The properties of flexible, fluid interfaces plays a significant role in our understanding of phenomena like wetting of solid surfaces, the stability of complex fluids and the nature of lipid membranes. In the recent years the properties of solid-like membranes have been explored in detail by use of RG-analysis of continuum models and computer simulation of tethered membranes. Notably the so called crumpling transition of self-intersecting solid membranes, taking the membrane from rough and spiky to smooth configurations at some finite transition temperature, has been subject to interest. Fluid membranes are expected to crumple unless self-avoidance, volume constaints, or osmotic swelling prevent it. However discretized models of fluid membranes with extrinsic curvature seems to display crumpling transitions. In the present study the effect of self-avoidance on the crumpling of fluid membranes is investigated by Monte Carlo simulation of a model, where the fluid properties is represented by dynamical triangulizations of the surface.

[1]Supported by the Danish National Research Council (11-7498)

BP7

Increasing the Time Step in Molecular Dynamics Simulations with the Langevin/Implicit-Euler Scheme

Anna M. Nyberg[a,b] *and Tamar Schlick*[a]

(a)Courant Institute of Mathematical Sciences
251 Mercer Street
New York, New York 10012

(b)Department of Theoretical Physics
Royal Institute of Technology
S-100 44 Stockholm, Sweden

In typical molecular dynamics simulations the Newtonian equations of motion are solved numerically using explicit schemes such as Verlet. Such schemes are simple to formulate and fast to solve but they impose a severe restriction on the integration time step: Δt must be at leat as small as the most rapid vibrational mode. The Langevin/implicit-Euler scheme is a combination of an implicit numerical scheme applied to the Langevin equation. The scheme has two properties that differ from the standard explicit scheme; stability over large time-steps and effective damping of high-frequency vibrations. The implicit scheme has been applied to a simple bead-model of liquid butane. For time steps smaller than or equal to 25 fs (and the quantum-mechanical cut-off frequency), the kinetic energy is larger than 85% of its value at time steps of 1 fs. The time step has been increased to 40 fs with a low cut-off frequency. At time steps larger than 40 fs the translational motion is affected by the numerical damping, and difficulties in finding a solution to the equations of motion were experienced.

We have studied the energy-loss in collisions and dihedral distributions at different time steps. For large time steps the random force will dominate the motion (if chosen such that the numerical damping is compensated for) and a large part of the phase space may be probed but the detailed motion is far from the solution to the Newtonian equations of motion. A possibility is to use the method with an adaptive or adjustable time step.

---

[1]A transition-rate investigation by molecular dynamics with the Langevin/implicit-Euler method. A. Nyberg & T. Schlick, J. Chem. Phys. 95 4986 (1991)

[2]Increasing the Time Step in Molecular Dynamics Simulations with the Langevin/Implicit-Euler Scheme. A. Nyberg & T. Schlick, preprint

[2]*Numerical Methods*, G. Dahlquist and Å. Björk (Prentice-Hall, New Jersey, 1974)

BP8

Prediction with Recurrent Neural Networks

Niels Holger Wulff and John A. Hertz
CONNECT, Niels Bohr Institute and NORDITA,
Blegdamsvej 17, 2100 Copenhagen Ø, Denmark
fax: (+45) 31 38 91 57
Email: wulff@nordita.dk, hertz@nordita.dk

We study extrapolation of time series using recurrent neural networks. We use the Real-Time Recurrent Learning (RTRL) algorithm introduced by Williams and Zipser[1], both in the original form for first order nets ($V_i(t) = g(\sum_j w_{ij} V_j(t-1))$) and in a form for second order nets ($V_i(t) = g(\sum_{jk} w_{ijk} V_j(t-1) V_k(t-1))$. We show that both first order and the second order nets are able to learn to simulate the Mackey-Glass series. The prediction quality of the results is comparable to that from feed-forward nets.

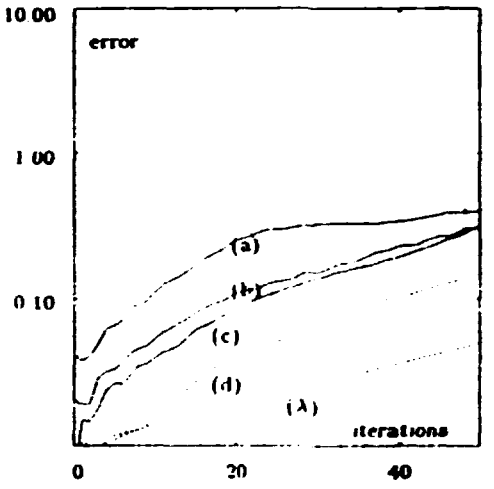

The Figure shows the increase of the error when doing iterated prediction of the Mackey Glass series defined with parameters as in [3].
Line (a) is a feed forward net like in [2]. Line (b) is from a first order recurrent net and line (c) is from a second order recurrent net. The dotted line (d) is from [3]. The line with (λ) indicates the Liapunov exponent.

[1] Williams, R J and D Zipser (1989) *A Learning Algorithm for Continually Running Fully Recurrent Neural Networks* Neural Computation 1, 270-280

[2] Lapedes, A and R Farber (1987) *Nonlinear Signal Processing Using Neural Networks Prediction and System Modelling* Technical Report LA-UR-87-2662, Los Alamos National Laboratory, Los Alamos, NM

[3] Stokbro, K , D K Umberger and John A Hertz (1990) *Exploiting Neurons with Localized Receptive Fields to Learn Chaos*, Complex Systems 4 603-622

BP9

Generalization in two–layer Neural Networks

H. Schwarze,* J. Hertz
Nordita/NBI, Blegdamsvej 17, DK–2100 Copenhagen

M. Opper, W. Kinzel
Inst. für Theoretische Physik, Universität Würzburg, F.R.G.

An interesting aspect of feedforward neural networks is their ability to learn classification tasks from a set of training examples and to generalize their knowledge to new examples.[1] The quality of network performance on novel data is measured by the generalization error as a function of the number of training examples.

Single layer networks (*perceptrons*) with one layer of input units and a single output unit have recently been studied in great detail. However, they can only implement linearly separable problems, and additional layers of *hidden* units have to be added to solve more complicated tasks. We present both analytical and numerical results for the generalization ability of two–layer networks with fixed hidden to output couplings.

As an example of a two–layer network we study the committee–machine, which implements a majority decision of the hidden units. For a stochastic learning algorithm statistical mechanics can be applied to calculate the average generalization error.[2]

When a fully connected committee–machine with discrete couplings is trained to implement a simple task given by a single layer *teacher* network it exhibits a sequence of phase transitions. With an increasing number of training examples we find a successive condensation of the committee–members into the teacher yielding discontinuous transitions to better generalization.[3]

A large committee–machine with nonoverlapping receptive fields trained to implement a task of equal complexity is studied yielding a replica–symmetric phase diagram. A similar sequence of a discontinuous phase transition followed by a region of metastability as in single–layer perceptron learning is found.

Monte–Carlo simulations have been performed for both models to verify the analytic results.

---

*E–mail: holm@nordita.dk

[1] as an introduction see e.g.: J. Hertz, A. Krogh, R.G. Palmer, *Introduction to the Theory of Neural Computation*, Addison Wesley, 1991

[2] G. Györgyi and N. Tishby in *Neural Networks and Spin Glasses*, ed. by K. Thuemann and R. Köberle (World Scientific, Singapore, 1990

[3] H. Schwarze, M. Opper, W. Kinzel, preprint 1991

BP10

Computer Simulations of Optical Properties of Random Fractal Clusters

Vadim A. Markel

Institute of Automation and Electrometry, Siberian Branch of the Russian Academy of Sciences, Universitetski Pr. 1, 630090 Novosibirsk, Russia.
FAX:(383-2)354851, Telex: 133183 KWANT SU

A fractal cluster is considered as a set of N identical grains obeying scalar dipole susceptibility χ and interacting via dipole fields. The transitional dipole momenta $\vec{d}_i$ (i=1,N), induced by the incident light, are coupled by the equation

$$\vec{d}_i = \chi\vec{E}_i + \chi\sum_{j\neq i}\hat{W}(i,j)\vec{d}_j \qquad (1)$$

where $\vec{E}_i$ is the field of the incident wave at the site $\vec{r}_i$ where i-th grain is placed and $\hat{W}$ is the symmetrical matrix of dipole interaction. This equation is solved numerally for different types of fractal clusters.

The solution of the equation (1) allows to calculate cross-sections of scattering and absorption. Analysis and numeral simulations show that the absorption and scattering spectra are inhomogeneously broadened, band width being determined by the spectral radius of the matrix $\hat{W}$.

The results of computer simulations are compared with experimental spectra of fractal clusters built from small silver grains (size of the grains being of the order of 100Å) It is shown that (i) Interaction of grains is essentially collective (one cannot describe experimental spectra using only pair interaction[2] of grains) (ii) Only interaction in the far-zone can give rise strong broadening of the absorption band that is seen in the experiment and (iii) The coupled-dipole approximation adequately describes interaction of light with complex disordered systems.

[1] V. A. Markel, L. S. Muratov, M. I. Stockman and T. F. George, Phys. Rev. B 43, 8183 (1991).

[2] V. A. Markel, J. Mod. Opt. (1992), in press.

BP11

First principles molecular dynamics calculations for defects in semiconductors

M. Alatalo A. P. Seitsonen R. Virkkunen
K. Laasonen M. J. Puska and R. M. Nieminen

Helsinki University of Technology, 02150 Espoo, FINLAND,
Fax: +358-0-465077

We present a review of the recent results of the *ab initio* molecular dynamics calculations for defects in semiconductors. In these calculations we have used the unified scheme of density functional theory and molecular dynamics, developed by Car and Parrinello[1] (CP) and recently rewieved by Pastore et al.[2] and Kremler and Madden[3]. The materials studied include GaAs, InP and pure and phosphorous doped Si.

Calculations have been done for the vacancies in GaAs[4,5], Si and InP in different charge states. As results we obtain the atomic relaxations, electron energy levels, vacancy formation energies and relaxation energies. In some cases the relaxations are found to be very large and large changes may occur between adjacent charge states. We have calculated for the different vacancies the corresponding positron lifetimes, which are very sensitive to the atomic relaxations. The theoretical predictions agree with experimental results, giving credence to the theoretical relaxation patterns and experimental charge state experiments.

Moreover, we have done calculations for He in Si, obtaining the relaxations and relaxation energies associated with the He impurity and the heat of solution of He in Si. The results indicate that the He impurity always goes to the tetrahedral interstitial site and the most probable migration path goes through the open interstitial channels.

[1] R. Car and M. Parrinello, Phys. Rev. Lett. 55, 2471 (1985)
[2] G. Pastore, E. Smargiassi, and F. Buda, Phys. Rev. B 44, 6334 (1991)
[3] D. K. Remler and P. A. Madden, Mol. Phys 70, 921 (1990)
[4] K. Laasonen, M. Alatalo, M. J. Puska, and R. M. Nieminen, J. Phys. C: Cond. Matt. 3, 7217 (1991)
[5] K. Laasonen, M. J. Puska, and R. M. Nieminen, Phys. Rev. B, in print

BP12

First principles study of silicon

R. Virkkunen M. J. Puska and R. M. Nieminen

Helsinki University of Technology, 02150 Espoo, FINLAND,
Fax: +358-0-465077

The structural and electronic properties of bulk Si and monovacancies in different charged states in Si are studied using *ab initio* molecular dynamics. Other defects of interest are divacancies and the phosphorus-vacancy-pair in Si.

The electronic states and the ionic positions are solved simultaneously within the Car-Parrinello method [1]. We consider 64 atoms in a simulation cell with periodic boundary conditions in all three dimensions. The electronic orbitals are expanded in plane-waves and a norm-conserving pseudopotential with s- and p-nonlocality is introduced for the Si atoms. Only the Γ point is used to sample the Brillouin zone of the supercell.

The calculations of Si bulk show that a high energy cut-off (14-16 Ry) is needed for the plane-wave expansion. This is much higher than the previously adopted cut-off of 6-10 Ry in Car-Parrinello simulations of Si [2]. Our simulations are performed with the cut-off of 14.6 Ry which corresponds to about 4000 plane-waves per eigenstate.

For perfect Si bulk we derive an equilibrium lattice constant of 5.36 Å which is close to the experimental lattice constant of 5.43 Å. We find large relaxations of the atoms around the vacancies in Si. For example, in the negative vacancy the relaxations are about 20 % of the nearest neighbour distance (two of the nearest neighbours relax inwards and two outwards). These relaxations are quite different from those obtained using the Car-Parrinello scheme with a lower cut-off energy and only s-nonlocality. We make contact also with experiments by calculating for the vacancies the corresponding positron lifetimes, which according to experiment show a remarkable charge state dependence.

---

[1] R. Car and M. Parrinello, Phys. Rev. Lett. 55, 2471 (1985)

[2] F.Buda, Ph.D. thesis, unpublished (1989), E.Smargiassi, Ph.D. thesis, unpublished (1990)

BP13

Thermodynamics of Josephson-junction arrays using path integral methods

Jens M. Houlrik

Department of Theoretical Physics, University of Umeå, S-901 87 Umeå, Sweden,
[Fax: +46 90 166673], [E--mail: houlrik@tp.umu.se]

The effect of quantum fluctuations in arrays of small Josephson-junctions[1] is studied numerically using a path integral representation of the partition function. If the Josephson E_J coupling dominates, the Ginzburg-Landau phase angle associated with each superconducting island can be treated as a classical XY-spin variable. The array will be superconducting at low temperatures due to phase coherence while the high-temperature phase will be resistive due to the presence of free vortices. The charge on a site, which can change in units of $2e$ when Cooper pairs tunnel between neighboring islands, is represented by an operator canonical conjugate to the phase angle. If the capacitance of the islands becomes small, the charging energy of order $E_C = (2e)^2/C$ can be comparable to the Josephson energy and the behavior of the array is strongly modified by quantum fluctuations. For sufficiently large values of E_C/E_J, phase coherence is destroyed at all temperatures.

In the present study, the role of a finite imaginary-time discretization $\Delta\tau$ in the path integral representation is investigated. The dependence of thermodynamic functions on grid size is studied in detail for a single junction. The specific heat has a nonphysical maximum at intermediate values of $\Delta\tau$.

For a square array of junctions, the boundary of the superconducting phase is located as a function of charging energy. It is argued that the first-order quantum induced phase transition (QUIT) observed in a previous Monte Carlo study[2] is an artifact of the employed path integral method. Also, no indications of a reentrant normal phase is seen.[3]

---

[1] G. Schön and A. D. Zaikin, Phys. Rep. **198**, 237 (1990)

[2] L. Jacobs, J. V. José, M. A. Novotny, and A. M. Goldman, Phys. Rev. B**38**, 4562 (1988).

[3] D. Ariosa and H. Beck, *Quantum fluctuations in the two-dimensional XY model: Variational approach*, preprint

BP14

Computer Simulation of the Nematic–Isotropic Phase Transition in the 3–d Lebwohl–Lasher Model[1]

Zhengping Zhang,[§] M. J. Zuckermann,[§] and Ole G. Mouritsen[‡]

[§]Centre for the Physics of Materials, Department of Physics, McGill University, Montreal, PQ H3A 2T8, Canada
[Fax: 514--398--6524], [E--mail: ZHANG@PHYSICS.MCGILL.CA]

[‡]Department of Physical Chemistry, The Technical University of Denmark, Building 206, DK-2800 Lyngby, Denmark.
[Fax: 45--42--880977], [E--mail: FYMEARN@NEUVM1]

The Lebwohl–Lasher model[1] is a simple lattice version of the Mayer–Saupe model of a nematic crystal. The Lebwohl–Lasher model is defined by the Hamiltonian

$$H = -J \sum_{\langle i,j \rangle} P_2(\cos\theta_{ij}),$$

where $P_2(\cos\theta_{ij})$ is the second Legendre polynomial and $J > 0$. The nature and the properties of the nematic–isotropic phase transition in the three–dimensional Lebwohl–Lasher model have been under active investigation for a long time[2]. We have exploited the modern numerical techniques of analyzing phase transitions to show that the transition in this model is a very weak first–order transition, which is possible even weaker than in the three–dimensional, three–state Potts model. By using a combination of the Ferrenberg–Swendsen histogram technique[3] and the Lee–Kosterlitz trick[4] we have analyzed the distribution functions for the internal energy, $\langle H \rangle$, and the nematic order parameter, $\langle P_2(\cos\theta_{ij}) \rangle$, and studied the derived free–energy function as a function of system size. The free–energy function has a barrier which scales with linear system size, L, as $\Delta F \sim aL^{d-1}$, where $d = 3$ is the spatial dimension. The hight of the barrier is related to an interfacial tension. The scaling behavior demonstrates that the phase transition is of first order. However, the finite–size scaling regime is obtained only for relatively large lattice sizes and the amplitude, a, in the scaling relation is very small, indicating that the first–order transition is very weak.

1. P. A. Lebwohl and G. Lasher, Phys. Rev. A 6, 426 (1972).
2. U. Fabri and C. Zannoni, Mol. Phys. 58, 763 (1986).
3. A. M. Ferrenberg and R. H. Swendsen, Phys. Rev. Lett. 61, 2635 (1988).
4. J. Lee and J. M. Kosterlitz, Phys. Rev. B 43, 3265 (1991).

[1]Work supported by the Danish Natural Science Council (11-7785), by the FCAR de Québec under a center and team grant, and by the NSERC of Canada.

BP15

Molecular Dynamics Simulation of Intermolecular Dipole-Dipole Nuclear Spin Relaxation.

Michael Odelius and Aatto Laaksonen

Division of Physical Chemistry. Arrhenius Laboratory.
Stockholm University. S-106 91 Stockholm

The dipole-dipole interaction is an important mechanism for nuclear spin relaxation in liquids. The contributions to the relaxation are divided into intramolecular, and intermolecular interactions. The intramolecular dipole-dipole relaxation is dominant, but contains only information about the individual motions of the molecules. The intermolecular relaxation depend on the relative motions of the molecule and contains information about the structure, and dynamics of the liquid. The intermolecular relaxation can be measured, either in specially designed experiments, or when examining systems without intramolecular interactions like ions and rare gases.

We have studied intermolecular dipole-dipole relaxation by MD simulations of pure liquids of monoatomic, polyatomic non-polar, and polyatomic highly polar model molecules containing spin = 1/2 nuclei. Comparison is made with results obtained from early analytical models. In the calculations of dipole-dipole time correlation functions, both the autocorrelation of the interactions and the cross correlation between different interactions are included (*cf* the treatment of quadrupolar relaxation). In earlier literature[1] the cross correlation effect are assumed to be negligible. The cross correlations (omitted in the previous models) are shown to give significant contributions to the total relaxation rate.

From a theoretical point of view it is not clear, whether, or not, the cross correlations can be treated in the same way as the autocorrelations. We are right now occupied by carefully deriving expressions for the dipole-dipole relaxation. Hopefully the question will be answered in time for the conference in Nyborg.

---

[1] H.G. Hertz, in *Progress in Nuclear Magnetic Resonance Spectroscopy*, Vol 3, Pergamon Press, 1967.

BP16

Molecular Dynamics Simulations of Lipase Activation

[1]M. Norin, [2], O.H. Olsen, [2,3]G. Peters and [2]A. Svendsen

[1]Dept. Biochem, KTH, Stockholm FAX: 46-8-72318901,
E-mail: martin@physchem.kth.se

[2]NOVO Research Institute, NOVO Alle 1, DK-2880 Bagsværd, Denmark.
FAX: 45-44-490555, E-mail: oho@novo.dk

[3]Dept. Chem., H.C. Ørsted Institute, DK-2100 Ø, Denmark

The action of lipases is investigated by molecular dynamics simulations. Recent published structures of Mucor miehei lipase show that the lipase activation is coupled to a conformational change. In the present study the importance of charged residues is explored by changing amino acid sidechain charges in the vicinity of the binding cleft. Further an adiabatic energy mapping method is used to estimate the magnitude of the activation energy.

BP17

Self-Organized Criticality and $1/f$ Noise in Nonconservative models.

Kim Christensen, Per Bak, and Zeev Olami

Department of Physics,

Brookhaven National Laboratory

Upton, New York 11973

USA

April 3, 1992

Abstract

We introduce a new nonconservative self-organized critical model. This model is equivalent to a quasistatic two-dimensional version of the Burridge-Knopoff spring-block model of earthquakes. Our model displays a robust power law behavior. The exponent is not universal, rather it depends on the level of conservation. A dynamical phase transition from localized to non-localized behavior is seen as the level of conservation is increased.

Moreover, this generic, nonconservative model is shown to exhibit $1/f$ noise. The exponent of the power spectrum depends on the level of conservation.

C : 3RD NORDIC SYMPOSIUM ON SUPERCONDUCTIVITY

CIFr1

Marginal Fermi-Liquids

C. M. Varma

AT&T Bell Laboratories, 600 Mountain Avenue,
Murray Hill, NJ 07974, USA

In an attempt to focus on the central issue in the diverse anomalous normal state properties of high temperature superconductors, a phenomenological hypothesis about the excitation spectrum in the normal state was suggested. The hypothesis of the "marginal Fermi liquid" (MFL) phenomenology is that over a wide range of momenta the charge (ρ) and spin (σ) polarizabilities have a low energy scale given by the temperature of measurement rather than any intrinsic scale in the Hamiltonian.

$$\mathrm{Im}\bar{P}_{\rho,\sigma}(q,\omega) - \begin{cases} -N(0)\omega/T, & \omega << T \\ -N(0), & \omega_c >> \omega > T. \end{cases}$$

Here ω_c is a cut-off energy. As a result the frequency dependence of the one-particle self-energy is given by

$$\Sigma(\omega) = \lambda(\omega \ln\frac{x}{\omega_c} + i\frac{\pi}{2}x\,\mathrm{sgn}\omega),$$

where $x = \max(|\omega|,T)$ and λ is a coupling constant. This leads to a quasiparticle spectral weight, z, which depends logarithmically on energy or temperature, namely

$$1/z = (1 + \lambda \ln(y/\omega_c)),$$

where $y = \max[(E_k - \mu),T]$ with E_k the real part of the quasiparticle energy. It is the weakest imaginable way in which the quasiparticle concept of the conventional Fermi liquid theory could be violated (suggesting the term "marginal" in MFL).

Recall that in Landau theory, for $\omega << qv_F$, $\mathrm{Im}\, P_{\rho,\sigma}(q,\omega) \sim N(0)(\omega/qv_F)$, multiplied by appropriate Landau parameters. Correspondingly $\mathrm{Im}\,\Sigma(\omega,k_F) \sim \omega^2\mathrm{sgn}\omega$.

The MFL hypothesis reconciles the experimental observation of a Fermi-surface similar to the band-structure calculations with the anomalous scattering observed in transport measurements. Angle resolved photoemission results have been found consistent with these predictions. The MFL spectrum in the charge channel provides a retarded attractive interaction in the Cooper channel and has been used to calculate several properties of the superconductive state. Recent neutron scattering results have been observed to be directly consistent the hypothesis in the spin-channel.

Of special interest is the prediction that below T_c, the quasi-particle scattering rate decreases exponentially. This leads to a two peaked spectral weight, a sharp peak near the superconducting gap Δ and a broad hump starting at 3Δ. This has been observed in both photoemission and tunneling measurements.

The MFL hypothesis implies a vertex in the particle-hole channel which is weakly singular over most of q-space. In recent work, done in collaboration with Andrei E. Ruckenstein of Rutgers University, a possible microscopic theory for such a breakdown of Landau Fermi-liquid theory is presented. The physical idea is that in certain strongly correlated models of Cu-O materials, with electron density not too far from 1/2 filling, a ghost of the incoherent upper band of the insulator exists. The residual interactions between such a band and excitations near the chemical potential pull a resonance down in energy. In its simples manifestation the resonance has a fermionic three-body character. For medium to strong coupling, the chemical potentials is self-consistently pinned to such a resonance. The excitation spectra in such a state has the MFL spectra.

A new prediction following from this microscopic theory is that the one particle spectra near the chemical potential has besides the quasi-coherent MFL part which disperses with momentum, a nondispersive incoherent part.

The requirements on the microscopic model to lead to MFL behavior are rather stringent. The coupling between the incoherent and the coherent one-particle excitations must be the same order as the energy splitting, of the order of the insulating gap, between them. This requirement is met in the models with copper-oxygen interactions. Numerical diagonalization for a small number of sites yield results consistent with the approximate theory.

CIFr2

Spectroscopy and Critical Temperature of the High T_C Oxides: correlation between Microstructure and Properties

Vladimir Z. Kresin[1] and Stuart A. Wolf[2]

[1]Lawrence Berkeley Laboratory, University of California, Berkeley

[2]Naval Research Laboratory, Washington, D.C.

The presence of different structural units (e.g., planes and chains in $Y-Ba-Cu-O$), along with the short coherence length, leads to peculiar charge transfer which can be described on the microscopic level. The spectroscopy appears to be very sensitive to the oxygen content; oxygen depletion leads to the appearance of a gapless state, whereas T_C changes relatively slowly.

Evaluation of the major parameters, including the coupling strength and the Coulomb pseudopotential for various high T_C systems (such as the cuprates and the doped fullerenes) will be described.

CIFr3

Organic Superconductors

K. Bechgaard

University of Copenhagen, Denmark
Telephone: 31425600

Organic or molecular superconductors can be divided into three distinct groups. The very anisotropic materials such as $TMTSF_2X$ exhibit competition between superconducting and SDW ground states and T_c's in the 1.2 K region. In socalled κ-phase BEDTTTF salts sheets of molecular dimers are seperated by polymeric anions. These materials exhibit closed FS and T_c can reach aoout 12 K. Finally, if we consider C_{60} as the "ultimate" spherical molecule , isotropic properties are expected and it has been demonstrated that T_c's may increase to the 30 K region.
We discuss how molecular properties influence the structure and properties of these molecular materials.Also we present some new results concerning SDW's and non-linearity in $TMTSF_2X$ salts.

CIFr4

STRUCTURAL DEFECTS IN HIGH Tc SUPERCONDUCTORS

G. Van Tendeloo, T. Krekels, S. Amelinckx
EMAT, University of Antwerp (RUCA)
Groenenborgerlaan 171, B2020 Antwerp, Belgium (Fax: +32-32180257)

Many of the new high Tc superconductors contain a large number of (complex) defects which can strongly influence superconducting properties such as critical temperature Tc and critical current Jc. High resolution electron microscopy has proven to be an excellent technique for the atomic scale analysis of these defective structures. The idea of these investigations is to relate physical and chemical properties to the structural and microstructural characteristics.

Y-Ba-Cu-O is by far the most widely studied superconducting system; its general formula can be written as $Y_2Ba_4Cu_{6+x}O_{14+x}$; known members of this series are $YBa_2Cu_3O_7$ with a critical temperature Tc of 93K; $Y_2Ba_4Cu_7O_{15}$ with a Tc value of 75K and $YBa_2Cu_4O_8$ with a Tc of 80K. The three superconductors are structurally very related; in the 1-2-3 compound there is a single CuO layer between two BaO layers, in the 1-2-4 compound all single CuO layers are replaced by double CuO layers, while for the 1-2-3.5 composition only one in two single layers is replaced by a double layer. These stable compounds (x=0, x=1 and x=2) are clearly three out of a systematic family. Other members of the series have never been produced as single crystals; however they have been observed by electron diffraction in samples with intermediate compositions. In the Tl-compounds extremely long period superstructures have been found. In these structures double as well as single TlO layers occur but at the same time the number of perovskite units in the perovskite blocks also varies between 3 and 4. Since many different periodicities (up to several hundred Å) have been found, their occurrence is most probably related to spiral growth of the crystals.

Oxygen-vacancy ordering in 123 YBCO superconductors will be discussed; the origen of the 60 K plateau has to be attributed to the Ortho II phase.

Fullerites (crystalline C_{60} and C_{70}) are the host lattice for superconducting materials such as K_xC_{60}, Rb_xC_{60} and others of which the critical temperatures are even above 40 K. They are therefore included in this overview. We will show that from a crystallographic point of view these molecular structures behave very much like "ordinary FCC based metals".

This work was performed with financial support of the Incentive Program on High Tc Superconductors of the Belgian State Science Policy Office under contract nr SU/03/17 and of the National Fund for Scientific Research (Belgium)

CCFr5

Study of charge distribution in $YBa_2Cu_3O_7$ by electron diffraction[1]

K. Gjønnes, N. Bøe, J. Gjønnes and J. Taftø

Department of Physics, University of Oslo
P.O. Box 1048, 0316 Oslo 3, Norway

Electron diffraction probes the electrostatic potential, $U(r)$, in the material, and thus incident electrons with large impact parameters, i.e. those scattered at low angles, are strongly influenced by the charge distribution and the ionicity of the atoms. For $YBa_2Cu_3O_{7-x}$ with the relatively large c-axis of 11.7Å, the (001) and (002) reflection are in this low angle regime, suggesting that the issue of hole distribution[2,3] may be addressed using electron diffraction.

We have studied a nearly fully oxygenized sample of $YBa_2Cu_3O_7$ with $T_c \approx 90K$. Many beam dynamical calculations of the diffraction intensities for different models of the charge distribution were compared with convergent beam electron diffraction observations obtained with a 200 keV transmission electron microscope. The calculated diffraction intensities showed a strong model dependence. A charge distribution model corresponding to the majority of the holes beeing on the CuO_2 planes, agrees well with the observed diffraction intensities.

---

1 Work supported by the Norwegian Council for Science and Humanities.

2 N. Nücker, H. Romberg, X.X.Xi, J. Fink, B. Gegenheimer and Z.X. Zhao, Phys.Rev. B39, 6619 (1989)

3 J.D. Jorgensen, B.W. Veal, A.P. Paulikas, N.J. Nowicki, G.W. Crabtree, H. Claus and W.K. Kwok. Phys.Rev. B41, 1863 (1990).

CCFr6

Relation Between Critical Current and In-Plane Ordering of $YBa_2Cu_3O_{6+x}$ on MgO(001) and $SrTiO_3$(001)

R. Kromann*, R. de Reus*, N.H. Andersen*, J.B. Bilde Sørensen†, P. Vase‡, and T. Freltoft‡

*Department of Solid State Physics, Risø National Laboratory
DK - 4000 Roskilde, Denmark
†Materials Department, Risø National Laboratory, Denmark
‡NKT Research Center, Sognevej 13, DK - 2605 Brøndby, Denmark

For many applications of thin-film high-T_c superconducting $YBa_2Cu_3O_{6+x}$ excellent transport critical currents are required. This may only be obtained by reliable processes for deposition of epitaxial layers without structural defects. Not only the deposition process, but also the substrate material plays a key role in obtaining superconducting films with the desired properties. In this work the crystalline quality of thin-film $YBa_2Cu_3O_{6+x}$ deposited onto MgO(001) and $SrTiO_3$(001) under almost identical conditions by a laser ablation process is investigated. The observed differences in critical current are therefore attributed to the difference in substrate type and quality. The structural analysis of the samples was carried out by x-ray diffraction and planar view high resolution transmission electron microscopy. This is the first time that a quantitative relationship between critical current and structural quality of $YBa_2Cu_3O_{6+x}$ has been established.

The $YBa_2Cu_3O_{6+x}$ films investigated all have the ideal 1:2:3 composition. No impurity phases were observed. Furthermore, the films were epitaxial with the *c*-axis perpendicular to the substrate, but minor traces of *a*-axis oriented material were observed. Films on MgO exhibited critical currents (measured at 77 K) ranging from 3.5×10^5 to 1.5×10^6 A/cm^2, whereas for films on $SrTiO_3$ a range from 2.9×10^6 to about 1.0×10^7 A/cm^2 was measured. The lower critical currents of films on MgO in comparison to films on $SrTiO_3$ are attributed to the larger in-plane mosaicity of the films on MgO. This difference in mocaicity is caused by the difference in lattice match between $YBa_2Cu_3O_{6+x}$ and the two substrate types MgO and $SrTiO_3$. The lattice match of the superconductor with the $SrTiO_3$ substrate material is close, resulting in higher quality $YBa_2Cu_3O_{6+x}$ films than in the case of MgO substrates. The differences in critical currents of the films deposited on the individual type of substrates can be explained as follows. For the films deposited onto MgO the lowering of the critical current by 75% can directly be related to the presence of smaller grains, microtwins, and an increased density of small- and high-angle grain boundaries, because approximately 5% of the $YBa_2Cu_3O_{6+x}$ film consisted of domains rotated 45° with respect to the substrate axes. For films deposited onto $SrTiO_3$ the lowering of the critical current by 70% is attributed to an increase of $YBa_2Cu_3O_{6+x}$ having the *a*-axis oriented perpendicular to the substrate from 0.6 to 8.3%.

CCFr7

Grain Boundaries in YBaCuO Thin Films - A Semiconductor?

Z. G. Ivanov, T. Claeson, R. I. Shekhter, D. Winkler
Department of Physics, Chalmers University of Technology, S-412 96
Gothenburg, Sweden, [Fax: +46 31 16 51 76, E-mail: F4ATC@SECTHF51]

E. A. Stepantsov and A. Ya. Tzalenchuk
Institute of Crystallography, Russian Academy of Sciences
[Fax: +7 095 1351011]

The [001] tilt grain boundary weak links were developed by pulsed laser deposition of 300 nm thick YBaCuO film on Y-ZrO_2 bicrystal substrates and a non-destructive patterning. Details of sample preparation, structure, and transport properties of low and high angle boundaries were described elsewhere.[1] It was shown that the grain boundaries were clean, spatially homogeneous and the weak links based on them showed Josephson effects.

Here, we report on the observation of a non-monotonic temperature dependence of the critical current and a field effect in asymmetric grain boundary weak links with misorientation angles higher than 40°.

The $j_c(T)$ dependence in this case has a maximum value at about 6 K, and the j_c is strongly suppressed at lower temperatures. The curve can be fitted to a theoretical dependence[2] of the S-SemiC-S Josephson junction, modified for a "dirty" semiconductor close to degeneracy (S and SemiC being superconductors and semiconductor correspondingly):

$$j_c \sim [\Delta^2/(\Delta^2+\pi^2T^2)]\ T^{5/2}\ \exp(-\gamma T^{1/4}),$$

where Δ – an order parameter
γ – a parameter dependent on the thickness of the Josephson barrier, the effective mass and mean free path of the carriers
T – a temperature

To investigate an electric field effect on the grain boundary transport properties, a gate was placed on the top of $SrTiO_3$ insulating layer covering the boundary. Having applied a voltage of a positive polarity to the gate we were able to increase the critical current of the weak link. No such effects have been observed for other misorientations including a 45° symmetric grain boundary. This strongly suggests that the observed effect is not due to varying properties of the superconducting electrodes. An increase in the carrier density in the boundary region might be responsible for the increase in j_c.

The two effects give a hint that an asymmetric grain boundary with high misorientation angles behaves as a semiconductor, however no direct structural evidence for this has yet been found.

---

[1] Z.G.Ivanov, P.Å.Nilsson, J.A.Alarco, D.Winkler, T.Claeson, E.A.Stepantsov, and A.Ya.Tzalenchuk, Appl. Phys. Lett., 59, 3030 (1991).

[2] I.F.Itskovich and R.I.Shekhter, Sov. J. Low Temp. Phys., 7, 418 (1981).

CCFr8

Ion Beam Stimulated Bi-epitaxial Josephson Junctions

Jaime Ramos, Zdravko G. Ivanov and Tord Claeson

Department of Physics, Chalmers University of Technology, S-412 96 Gothenburg, Sweden, [Fax: 031 16 51 76], [E-mail:F4ATC@SECTHF51]

The artificial grain boundary Josephson junctions grown on Y-ZrO_2 bi-crystal substrates have shown excellent performance at 77K.[1] The adoption of this type of junctions to integrated circuits led to the bi-epitaxial technology developed by the Conductus group.[2] A seed layer was used to create a 45° grain boundary in the junction area. Another possible technology is to modify the surface of the substrate in order to change the conditions for the in-plane epitaxy. It has recently been shown that chemical or mechanical treatment[3] or ion milling[4] of MgO substrates create conditions for 45° in-plane epitaxy on MgO.

We have investigated the possibility to control the in-plane epitaxy by ion beam etching of MgO substrate and to develop Josephson junctions and dc SQUIDs. One half of the substrate was ion beam milled to 5-15 nm depth and an YBaCuO film was deposited on top by using pulsed laser deposition. A 45° degree grain boundary was formed between the two halves of the substrate. Microbridges which include the grain boundary were patterned and studied.

Three substrates were processed to different stepheights, 5, 10 and 15 nm. In all cases ,the grain boundary weak links showed Josephson effects and most of them worked above 77K. The critical current density at the grain boundary was depressed about four orders of magnitude compared to the film. We observed a tendency in the critical current decreasing by increasing the step height. However, we are confident that the influence of the step itself on current transport is minimal. The critical current vs. temperature dependence, $I_c(T)$, showed a behavior typical for S-N-S Josephson junctions, some junctions ,however, showed a nonmonotonic $I_c(t)$ dependence with a well developed maximum at temperatures of 4-30 K, typical for an S-SemiC-S weak link, see for example the abstract: *Z.G.Ivanov et al.* at this conference (where S-superconductor, N-normal metal and SemiC-semiconductor). For the substrate with a 15 nm step several maxima were observed and we speculate that there are several weak links in parallel with different critical currents. For smaller steps there was mainly one maximum indicating a single junction with misorientaion of 45°. An S-N-S behavior might be explained by a low angle grain boundary. Further investigations are in progress to optimize the conditions for uniform in-plane epitaxy.

---

[1] Z.G.Ivanov, P.Å.Nilsson, J.A.Alarco, D.Winkler, T.Claeson, E.A.Stepantsov, and A.Ya.Tzalenchuk, Appl. Phys. Lett., 59, 3030 (1991).

[2] K.Char, M.S.Colclough, L.P.Lee, and G.Zaharchuk, Appl.Phys.Lett.,59,2177 (1991).

[3] B.H.Moeckly, S.E.Russek, D.K.Lathrop, R.A.Buhrman, Jian Li, and J.W.Mayer, Appl.Phys.Lett.,57,1687(1990).

[4] N.G.Chew, S.W.Goodyear, R.G.Humphreys, J.S.Satchell, J.A.Edwards, and M.N.Keene, submitted to Appl.Phys.Lett.

CCFr9

Preparation and Characterization of High-T_c Superconducting Cross-overs and Coils

Y. Q. Shen, P. Vase, and T. Freltoft
NKT Research Center A/S, Sognevej 11, DK-2605 Brøndby, Denmark

In production of electronic circuits of any complexity one has to develop techniques for depositing multilayer structures. A flux-transformer, which consists of a large area pick-up coil connected to a small area multi turn input coil, is an example of a component that needs multi-layers since the current has to be guided from the center to the edge of the coil without short circuiting the windings.

At NKT Research Center we have made such a coil based on the shadow mask technique, i.e. the formation of structures using masks placed at the substrate surface during film deposition. In this way, all layers may be deposited in situ without ex situ lithographic techniques among depositions which might cause contamination of the interfaces.

In practice a wheel with the necessary masks is placed in front of the substrate which enables the change of masks between the deposition of each layer in situ.

The current status for the coil development may be summarized in the table below.

	$T_{c.0}/T_{c.m}$ (K)	J_c(80K) (A/cm²)	I_c(80K) (mA)
Bottom strip	86.0/89.0	$1.7 \cdot 10^5$	100
Outer winding	89.5/90.5	$8.9 \cdot 10^5$	100
Complete coil	86.0/89.8		100

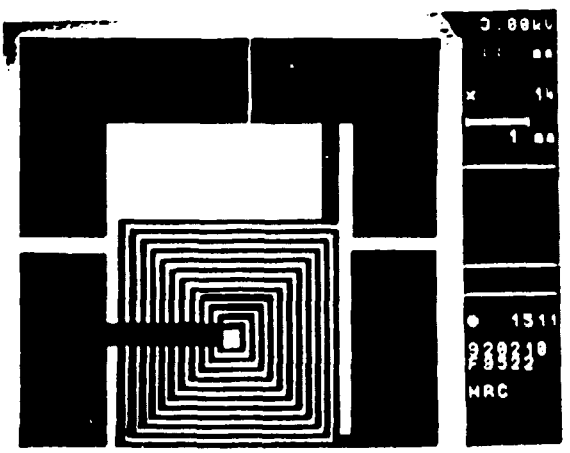

To ensure that the electrical current was actually following the turns and not shorting through the insulation layer, a Hall probe was mounted in the center of the coil and the magnetic field was monitored as a function of current and temperature. The measured magnetic fields correspond within error to expected values for a coil of the present geometry.

CCFr10
LINEWIDTH OF JOSEPHSON OSCILLATIONS IN $YBa_2Cu_3O_{7-\delta}$ GRAIN-BOUNDARY JUNCTIONS

Yu.Ya.Divin[*§], J.Mygind[§], N.F.Pedersen [§] & P.Chaudhari [■]

§ Physical Laboratory I, The Technical University of Denmark, Bldg. 309, DK-2800 Lyngby. [Fax: +45 45 93 16 69]

■ IBM Thomas J. Watson Research Center, Yorktown Heights, NY, USA [Fax: +1 914 945 2141]

We have studied the ac Josephson effect in $YBa_2Cu_3O_{7-\delta}$ grain-boundary junctions in the temperaturer tange from 4 K to 90 K. The temperature dependence of the linewidth of Josephson oscillations as derived from the shape of microwave/rf-induced steps was measured. The effective noise temperatures of high-T_c grain boundary Josephson junction were equal to their physical temperatures at low temperatures and at temperatures close to the transition temperature; but at intermediate temperatures the noise temperature might be higher than the physical temperature by a factor of 2. The latter is attributed to contributions from thermally activated vortices in the barrier of the grain boundary Josephson junction. It was also shown that the linewidth of the Josephson oscillations in the millimeter wave range might be as low as 380 MHz at liquid nitrogen temperatures.

* Permanent address: Institute of Radioengineering & Electronics, Russian Academy of Science, Moscow, SNG.

ClFr11

Exponent Relations for Spectator Fermion Superfluids

A. Kallio, V. Apaja and X. Xiong

Department of Theoretical Physics, University of Oulu, Linnanmaa
SF-90570 Oulu, Finland, [Fax: 358 81 561 278]

We propose a new exponent classification of superfluids[1], which is based on a generalization of the earlier EHL-model[2] to a spectator fermion situation (SFS). The theory is consistent with the existence of a quasigap for $T>T_c$. The BCSsuperconductors are obtained if the lowest sound mode is Landau damped. Also ^{4}He comes out as a special case from this formalism. For other superfluids of $^1S_0$-type we obtain a power law behaviour in their specific heats and derive an approximate expression for the coefficient of this power law. On the basis of the pressure dependence we have shown that the HFS and HTS can be placed into specific SFS categories, where their pressure dependence for T_c and c_p can be understood. The spectator component will give an additional linear term to the specific heat. The coefficient of the linear term is determined by the density and the effective mass of this component. In the BCS-case this component may also be localized. Our theory is in agreement with experiments for the main HFS: UPt_3, $CeCu_2Si_2$, and UBe_{13}, which all have power law specific heats, giving us the value of the exponent γ. Using the theoretical relation $\beta = 1 - 5\gamma/3$, derived here we obtain the exponent β. We then show, that the calculated exponents β give a good account of ultrasound attenuation experiments in UPt_3 and UBe_{13}[3].

Since in the HTS-case the electronic specific heat is only a fraction of the lattice contribution, the determination of the values of exponents cannot be done at present. We show that the Knight shift measurements can be used to obtain the pairbreaking function experimentally. Similar purpose is served by the Hall density R_H^{-1}. Based on the sign of the Hall coefficient, we place thehole doped HTS in the category (e^-, B^{++}) and the electron doped ones into (e^-, B^{--}), whereas of the HFS both UPt_3 and UBe_{13} would most likely be of the type (h^+, B^{++}). To calculate the quasiparticle contribution to quantities like c_p or the ultrasound attenuation for $T \approx T_c$ would require the knowledge of the dispersion law for quasiparticles i.e. an explicite boson model.

---

[1] A. Kallio, V. Apaja and X. Xiong, Physica C (1992) (in press)

[2] A. Kallio and X. Xiong, Phys. Rev. B 41 2530 (1990), Phys. Rev. B 43 5561 (1991)

[3] B. Golding, B. Batlogg, D.J. Bishop, W.H. Haemmerle, Z. Fisk, J.L. Smith and H.R. Ott, Proc. 2nd Intern. Conf. on Phonon Physics (World Scientific, Singapore), 406 (1985), V. Müller, D. Maurer, E.W. Scheidt, C.H. Roth, K. Lüders, E. Bucher and H.E. Bömmel, Solid State Commun. 57 319 (1986)

CIFr12

Schwinger-bosons and high-T_c superconductors

Per Hedegård

Physics Laboratory, H. C. Ørsted Institute, University of Copenhagen,
Universitetsparken 5, DK-2100 Copenhagen Ø, Denmark
Fax: 45 31 35 06 28, Email: hedegard@nbivax.nbi.dk

We review the development of the Schwinger-boson approach to the Hubbard-model. The method was designed to describe quantum anti-ferromagnets and has recently been extended to include holes moving in the background of the spins. A mean-field description is used to discuss experiments like neutron-scattering, magnetic susceptibility, photoemission, tunneling, NMR-relaxation. Most recently the model has been extended to include the coupling to lattice degrees of freedom. A mechanism that can explain the observed tetragonal to orthorombic transition has been identified. Several shortcomings of the mean-field description is discussed and corrections involving long-range forces between quasiparticles, mediated by certain gauge-fields who's existence is a consequence of the strong correlations in the system, is introduced.

CIFr13

Magnetic Dynamics of $La_{2-x}Sr_xCuO_4$

T.E. Mason, G. Aeppli,
Risø National Laboratory, Department of Physics, 4000 Roskilde
[Fax: 42 37 01 15], [E-mail: mason@risoe.dk] and AT&T Bell Laboratories,
Murray Hill, USA,
and H. Mook,
Oak Ridge National Laboratory, Oak Ridge, TN, USA

Studies of the magnetic dynamics of $La_{2-x}Sr_xCuO_4$ have been carried out with particular emphasis on a sample with $x=0.14$ which becomes superconducting at $T_c=33$ K. This material exhibits incommensurate peaks in the inelastic magnetic neutron scattering with the same geometry as found for a metallic (but not superconducting) sample with $x=0.075$[1]. In both cases the peak in $\chi''(Q,\omega)$is shifted from the commensurate position, (π,π) (in the notation of the square lattice of the CuO_2 planes), to $(\pi,\pi)\pm\delta(\pi,0)$ and $(\pi,\pi)\pm\delta(0,\pi)$ (see inset to Fig. 1). The magnitude of the incommensuration, δ, increases with doping, x, as $\delta=2x$.

Figure 1 shows a collection of constant $\hbar\omega$ scans along the trajectory shown in the inset for T=35 K ($>T_c=33$ K) obtained on TAS6. At the lowest energy probed, $\hbar\omega$ =3.5 meV, there are two sharp peaks at $(\pi,\pi)\pm\delta(\pi,0)$ and $(\pi,\pi)\pm\delta(0,\pi)$ where $\delta=0.245\pm0.004$. As the frequency is increased the peaks become somewhat broader, which implies shorter correlation lengths for higher energy fluctuations. The peak intensity is roughly independent of frequency, so that the q-integrated spectral weight must rise with $\hbar\omega$. The lines in Figure 1 correspond to a least squares fit to a form for $\chi''(Q,\omega)$ that describes the paramagnetic scattering from the intinerant antiferromagnet Cr[2] (appropriately modified to reflect the two dimensional Fermi surface of $La_{1.86}Sr_{0.14}CuO_4$).

Figure 1: Magnetic scattering at T=35 K ($>T_c=33$ K) obtained on TAS6. The inset shows reciprocal space with solid circles indicating locations near (π,π) with maximal magnetic response and open circles corresponding to (nuclear) Bragg points for a square lattice. The main figure consists of a series of background corrected constant energy scans, collected along the reciprocal space trajectory indicated by a dashed line in the inset.

The temperature dependence of the magnetic response is summarized in Figure 2. The top panel, a), shows the T dependence of the raw scattered intensity (closed circles) for $\hbar\omega = 4$ meV and $Q = Q_e = (\pi,\pi) - \delta(0,\pi)$. The gradual upward trend of the signal stops abruptly at T_c, below which there is a precipitous decline. That this decline corresponds to a substantial reduction of the magnetic response is obvious from our results for $\chi''(Q_e,\omega)$ (open circles) obtained via the fluctuation dissipation theorem from the raw data, corrected for the constant background indicated by the dashed line. Figure 2b) shows the temperature dependence of κ^2, a parameter extracted from the least squares fits mentioned above which is proportional to the zero frequency limit of the inverse correlation length squared. Figure 2c) shows the temperature dependence of the gap parameter, 2Δ, which characterizes the energy below which the decrease in scattering shown in panel a) becomes apparent. Although the actual scale for 2Δ is somewhat model dependent, the evolution below T_c is well described by the temperature evolution of a BCS order parameter. This means that the development of a gap in the quasi-particle excitation spectrum, which occurs in all superconductors, is accompanied by a corresponding gap in the spin fluctuations in $La_{1.86}Sr_{0.14}CuO_4$.

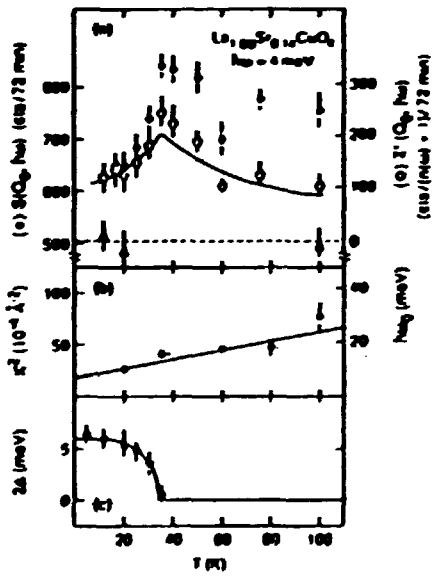

Figure 2: a) Temperature dependence of raw intensity for $\hbar\omega = 4$ meV, with $Q = Q_e = (\pi,\pi) - \delta(0,\pi)$ (solid circles) and $Q = (0.55\pi,1.15\pi)Q$ (open triangles). Open circles represent $\chi''(Q_e,\omega)$ obtained by application of the fluctuation dissipation theorem to the data indicated by the solid circles, where the background is identified with the dashed line through the open triangles. b) Value of κ^2 and the corresponding characteristic energy $\hbar\omega_e$ obtained from the fit described in the text. c) Value of 2Δ obtained from fits to the data.

1) S.W. Cheong, G. Aeppli, T.E. Mason, H. Mook, S.M. Hayden, P.C. Canfield, Z. Fisk, K.N. Clausen, and J.L. Martinez, (1991). Phys. Rev. Lett. 67, 1791.
2) D.R. Noakes, T.M. Holden, E. Fawcett, and P.C. de Camargo, (1990). Phys. Rev. Lett. 65, 369.

CISa1

Composition, Structure, and Superconductivity in the Copper Oxides*

J. D. Jorgensen[a], D. G. Hinks[a], B. A. Hunter[b], P. G. Radaelli[b], R. L. Hitterman[a], A. W. Mitchell[a], B. Dabrowski[a], and J. L. Wagner[b]

[a]Materials Science Division and [b]Science and Technology Center for Superconductivity, Argonne National Laboratory, Argonne, IL 60439 USA

We propose that three requirements for superconductivity in copper-oxide compounds are: (1) An appropriate carrier concentration; (2) The absence of defects in the CuO_2 conduction planes; and (3) Structural coherence of the CuO_2 conduction planes on a length scale that exceeds a critical length on the order of the superconducting coherence length.[1]

There is general agreement that the carrier concentration is determined by the chemical composition but the specific relationship is not established. Most of the copper-oxide superconductors require the incorporation of defects to create carriers in the CuO_2 conduction planes.[2] There are important exceptions among the Tl-based compounds. The La_2CuO_4 system offers an instructive example. La_2CuO_4 is an antiferromagnetic insulator, but it can be made metallic and superconducting by substitution of Sr^{2+}, Ba^{2+}, or Ca^{2+} for La^{3+} or by inserting interstitial oxygen defects into the La_2O_2 layer. The highest T_c is obtained for a doping level of about 0.15 holes per formula unit, as shown in the Figure for $La_{2-x}Sr_xCuO_4$. Such data have been the basis for concluding that T_c increases with increasing carrier concentration until the optimum value is reached and then decreases in the so-called "overdoped" region. However, this concept of T_c versus chemical composition is now being challenged. In $La_{2-x}Sr_xCuO_4$ the superconducting phase fraction does not reach its full value until T_c peaks at $x=0.15$. For $x<0.15$, the depression of T_c can be explained on the basis of competing antiferromagnetic fluctuations. For $x>0.15$, the compound is chemically metastable and will phase separate or decompose under conditions of thermodynamic equilibrium. Thus, an alternative explanation for the maximum T_c occurring at $x=0.15$ is that this optimum composition is sandwiched between two composition regions where other phenomena destroy superconductivity and is, therefore, the only composition for which bulk superconductivity with the maximum T_c is observed.

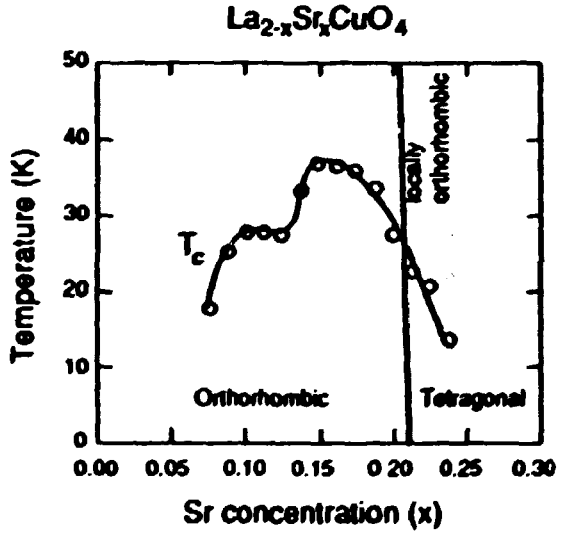

Although the incorporation of defects may be required to create carriers, it is clear that defects can also destroy superconductivity. Such effects are especially pronounced for defects that form in or near the CuO_2 layers. Substitution of metal atoms at this copper site or the creation of vacancies at this oxygen site are both known to destroy superconductivity for very small defect

concentrations.[2] In the two-layer compounds based on the $La_2SrCu_2O_6$ structure, the incorporation of excess-oxygen defects at a site bridging the copper atoms of the two CuO_2 layers, leading to compositions of $O_{6+\delta}$, is also thought to destroy superconductivity. We also propose that in the compound $Tl_2Ba_2CuO_{6+x}$ the deleterious effects of oxygen interstitial defects, rather than "overdoping", are responsible for the decrease of T_c with increasing oxygen content, even though the defects are in the Tl-O layer. A general conclusion that could be drawn is that, while defects may be required to create a carrier concentration adequate for superconductivity, the increasing defect concentration may eventually be responsible for destroying superconductivity, leading to metallic but nonsuperconducting behavior.

It has been observed experimentally that the superconducting properties can also be extremely sensitive to changes in the structure. However, only recently has it been appreciated that the structural length scale relevant to superconductivity is very short. For example, oxygen-atom ordering on the chain-layer sublattice of $YBa_2Cu_3O_{6+x}$ on a length scale that can be achieved by diffusion of oxygen at room temperature (perhaps a few unit cells) can result in changes in T_c as large as 20K.[3] In $La_{2-x}Sr_xCuO_4$, fluctuations of the low-temperature-tetragonal (LTT) phase for compositions near x=0.12 are sufficient to significantly depress T_c (see Figure) even though the transition to the LTT phase never occurs. When the importance of the local structure is considered, we conclude that in compounds based on the La_2CuO_4 and $YBa_2Cu_3O_{6+x}$ structures, superconductivity occurs only when the long-range or local structure is orthorhombic or some other ordered supercell of the basic tetragonal unit cell. No superconductivity is observed in the tetragonal phase except in regions where orthorhombic fluctuations or microdomains are present.[4] This may be explained by the fact that the tetragonal phases are actually incoherent structures due to random displacements of the oxygen atoms out of the plane of the copper atoms in addition to random atom displacements or site occupancies in other parts of the structure. These structures exhibit average tetragonal symmetry but are actually disordered on a short length scale. The proposal that structural coherence of the CuO_2 planes is a requirement for superconductivity is based on this experimental observation.[4] Incoherence (the lack of two-dimensional translational symmetry) of the CuO_2 planes destroys superconductivity in much the same way as do chemical defects.

---

* Work supported by the U. S. Department of Energy, Division of Basic Energy Sciences - Materials Sciences, contract No. W-31-109-ENG-38 (JDJ,DGH,RLH,AWM,BD) and the National Science Foundation Science and Technology Center for Superconductivity, grant No. DMR 88-09854 (BAH,PGR,JLW).

[1] J. D. Jorgensen, D. G. Hinks, P. G. Radaelli, S. Pei, P. Lightfoot, B. Dabrowski, C. U. Segre, B. A. Hunter, Physica C 185-189, 184 (1991).

[2] J. D. Jorgensen, Physics Today, June 1991, p. 34; J. D. Jorgesnen, P. Lightfoot, S. Pei, Supercond. Sci. Technol. 4, S1 (1991).

[3] J. D. Jorgensen, S. Pei, P. Lightfoot, H. Shi, A. P. Paulikas, B. W. Veal, Physica C 167, 571 (1990).

[4] J. D. Jorgensen, D. G. Hinks, B. A. Hunter, J. L. Wagner, P. G. Radaelli, E. C. Larson, B. Dabrowski, R. L. Hitterman, A. W. Mitchell, and H. Takahashi, Proc. Conf. on Lattice Effects in High-T_c Superconductors, Sante Fe, NM, 13-15 Jan 1992, Y. Bar-Yam, T. Egami, J. Mustre-de Leon, A. Bishop, eds., (World Scientific Publ., Singapore) in press.

CISa2

Flux Dynamics in Anisotropic and Layered Superconductors

Ernst Helmut Brandt

Max-Planck-Institut für Metallforschung, Institut für Physik,
W-7000 Stuttgart 80, FRG

High-T_c superconductors (HTSC), even as most alloy and compound superconductors, are superconductors of the extreme type-II. This means that magnetic flux penetrates in a very large range of applied fields $B_{c1}(T) \le B_a \le B_{c2}(T)$ in form of Abrikosov vortices each carrying a quantum of flux Φ_0. Under the action of an applied current these flux lines move and dissipate energy provided they are not pinned by material inhomogeneities. A really loss-free current (e.g. a persistent current in a ring or coil) can flow only if all flux lines are ideally pinned. In conventional superconductors this is the case for current densities $J < J_c$. However, in HTSC thermally activated depinning occurs in a wide range of temperatures below the superconducting transition temperature T_c. The reason for this is not only the larger T_c value but also the smaller activation energy U. In HTSC, U is small because of at least three reasons: (a) The coherence length ξ is small; this reduces the pinning energy of the vortex core (of radius $\approx \xi$). (b) The penetration depth λ is small and (c) the anisotropy is large; the latter two properties make the flux-line lattice (FLL) soft and the flux lines very flexible. This softening typically *increases* the critical current density but *decreses* the pinning energy by the following arguments.

A large λ causes a small shear stiffness of the FLL, $c_{66} = B\Phi_0/16\pi\mu_0\lambda_{ab}^2$ (B = induction, λ_{ab} = penetration depth of currents flowing in the crystalline ab-plane of a uniaxial HTSC, $B \| c$-axis, $B \ll B_{c2}$). This allows the FLL to adjust better to the randomly positioned pins. A soft FLL is better pinned in the sense that its average pinning force density $J_c B$ is large due to a more effective statistical summation of the elementary pinning forces. – The same argument applies to the stiffness (more precisely: line tension) of a flux line or of the FLL. This tension is described by the (dispersive) tilt modulus $c_{44}(\mathbf{k})$ of the FLL. While being large for uniform tilt, $c_{44}(0) = BB_a/\mu_0$, this tilt stiffness becomes very small for short-wavelength tilt,

$$c_{44}(\mathbf{k}) = (B^2/\mu_0)/(1 + k_\perp^2\lambda_c^2 + k_z^2\lambda_{ab}^2) + (B/\Phi_0)P(k_z)$$

where

$$P(k_z) = (\Phi_0^2/4\pi\mu_0\lambda_c^2)\ln\tilde{\kappa}$$

is the line tension of an isolated FL with $\tilde{\kappa}^2 = (\Gamma^2\kappa^2 + k_z^2\lambda_{ab}^2)/(1 + k_z^2\lambda_{ab}^2)$. Here $\kappa = \lambda_{ab}/\xi_{ab}$ is the Ginzburg-Landau parameter and $\Gamma = \lambda_c/\lambda_{ab} = \xi_{ab}/\xi_c$ the anisotropy ratio, $\Gamma \approx 5$ for YBCO and $\Gamma \approx 60$ for BSCCO. For sufficiently large k_z (short bending

wavelength $2\pi/k_z$) or large $k_\perp$ (e.g. if only one FL is deformed) the tilt energy is given mainly by the line tension $P(k_z)$ of an isolated FL, which is extremely small when λ_c is large. This means each FL can easily adjust to the pins. Note that the flux-line self-energy is $\propto 1/\lambda_{ab}^2$ and the line tension $\propto 1/\lambda_c^2$, which is much smaller. The physical reason for the small line tension of flux lines in anisotropic HTSC is that the flux lines want to lie in the ab-plane. Their tendency to tilt away from the c-orientation thus almost compensates the self-energy required to increase the flux-line length during tilting [1].

The same softening which *increases* the pinning *force* (or J_c) will *decrease* the pinning *energy* U, i.e. the barrier for thermal depinning. For example, a line pin $\|B\|c$, which can be implanted by high-energy heavy-ion bombardement, has a pinning energy per cm $U_p = \epsilon\Phi_0^2/4\pi\mu_0\lambda_{ab}^2$ with $\epsilon \approx 1$ or $\epsilon < 1$. If all flux lines are pinned this gives $J_c \approx U_p/\Phi_0 R$ where $R > \xi_{ab}$ is the radius of the pins. The nucleus for thermal depinning of the flux lines from these line pins is a trapezoid (or double kink) of height a (the distance to the next line pin) and width $2L = (2P/U_p)^{1/2}a$ [2]. The energy of this nucleus is $U = (8PU_p)^{1/2}a = 4LU_p$. This means that with increasing anisotropy (increasing λ_c) the decreasing line tension leads to a shrinkage of the depinning segment of a flux line and thus to a decrease of the barrier U.

In the very anisotropic BSCCO the nucleus length $2L$ formally becomes smaller than the distance d between the weakly coupled CuO layers. The above result of anisotropic London theory then does no longer apply. The depinning energy now becomes $U_p d$ since the contribution of the elastic line-tension energy of the FL is negligible. This means that the point vortices (pancake vortices) in the layers can depin individually [3]. As a consequence, flux creep is large in BSCCO down to rather low temperatures.

[1] E.H. Brandt and A. Sudbø, *Physica C* 180, 426 (1991).

[2] E.H. Brandt, *Europhys. Lett.*, in print.

[3] W. Gerhäuser et al., *Phys. Rev. Lett.* 68, 879 (1992).

CISa3

Flux dynamics and irreversibility in $YBa_2Cu_3O_7$ with Y_2BaCuO_5 inclusions and in single crystal $YBa_2Cu_3O_7$

K. Fossheim, M.G. Karkut, L.K. Heill, M. Slaski, and L.T. Sagdahl
Division of Physics, The Norwegian Institute of Technology and SINTEF Applied Physics, N-7034 Trondheim, Norway

V.M. Vinokur
Materials Science Division, Argonne National Laboratory, Argonne, Illinois, 60439 USA

M. Murakami, H. Fujimoto, N. Koshizuka, and S. Tanaka
ISTEC, SRL, 1-10-13, Shinonome, Koto-ku, Tokyo 135 Japan

F. Gencer, J.S. Abell, and C.E. Gough
School of Physics, University of Birmingham, Birmingham, B15 2TT UK

Abstract

We have measured the ac magnetic permeability response function $\mu = \mu' + i\mu''$ in melt-processed melt grown $YBa_2Cu_3O_7$ with Y_2BaCuO_5 inclusions (MPMG) and in single crystal $YBa_2Cu_3O_7$ (SC) in applied magnetic fields up to 8 Tesla oriented either parallel or perpendicular to the crystalline c-axis. The ac response of the two samples has been mapped out as a function of temperature, frequency, ac field amplitude, dc applied field, and field orientation. The peak in the lossy part of the susceptibility μ'' is used to probe the flux dynamics in the vicinity of the irreversibility line. The data are interpreted by comparison with expectations for an anisotropic vortex glass- to -liquid transition. The inferred melting lines as well as the frequency dependence and non-linear response are in overall agreement with the expected behavior. In the range of available parameters and variables we find the system to be in the solid vortex phase for H⊥c since there is a strong H_{ac} dependence and only a weak frequency dependence on the temperature position of the loss peak. For H∥c, the situation is reversed, and the loss peak depends only weakly on H_{ac} and strongly on the frequency.

CISa4

Quasi Two-dimensional Vortex fluctuations in High-T_c Superconductors[1]

Petter Minnhagen

Department of Theoretical Physics, University of Umeå, S-901 87 Umeå, Sweden,
[Fax: +46 90 166673], [E--mail: minnhagen@tp.umu.se]

The apparent 'quasi'-2D character of properties related to vortex fluctuations for high-T_c superconductors has recently attracted a lot of interest. The rationale is that the CuO_2-planes give rise to superconducting parallel planes which are relatively weakly coupled. In case of the superlattice structures, like YBCO/PBCO superlattices, the interplane coupling between the superconducting YBCO planes can be systematically varied. These superlattice structures appear to be very suitable for studying how 2D vortex-fluctuations get modified by the coupling between superconducting parallel planes. Much of the recent discussion in the literature has been focused on the critical region associated with a Kosterlitz-Thouless (KT) vortex unbinding transition. Under certain conditions such a KT critical region should *in principle* be observable for superconducting films.

In contrast the assertion is made here that the critical region associated with a KT-transition is *in practice* not observable in case of superconducting films. Fortunately there is an alternative way of describing 2D vortex fluctuations which is valid also outside the non-observable KT critical region. This description is based on the Ginzburg-Landau Coulomb gas model and the Coulomb gas scaling concept.[2] It is briefly recapitulated here. It is demonstrated that this description is in fact also applicable to coupled superconducting planes and high-T_c superconductors.[3] Furthermore, by analysing resistance data for YBCO/PBCO superlattices and high-T_c superconductors using the 2D Coulomb gas scaling concept, one obtains information about the coupling between superconducting planes. The applicability of the 2D Coulomb gas scaling concept for the resistance is due to an abrupt 3D to 2D decoupling of the vortex fluctuations just above the critical temperature.[4]

Also in the case of coupled superconducting planes the phase transition can be viewed as a vortex-unbinding transition. A vortex-antivortex pair in this case corresponds to a vortex loop where the loop only penetrates one plane. The interaction between the vortex and the antivortex associated grows linearly with distance. At the phase transition the linear interaction vanishes causing a vortex-unbinding transition. This vortex-unbinding transition is not of the KT-type. The phase transition belongs to the same class as the 3D XY model. The linear interaction is directly related to the interplane coupling and gives rise to a critical current.[5]

---

[1]The present material to large extent derives from collaborations with P. Olsson, H. J. Jensen, V. Cataudella, M. Nylén and O. Westman.

[2]P. Minnhagen, Rev. of Mod. Phys. 59, 1001 (1987).

[3]P. Minnhagen and P. Olsson, Phys. Rev. B in press (1992).

[4]P. Minnhagen and P. Olsson, Phys Rev. Lett. 67, 1039 (1991)

[5]H. J. Jensen and P. Minnhagen, Phys. Rev. Lett. 66, 1630 (1991).

CCSa5

Monte Carlo study of the mean-field theory of the three-dimensional anisotropic XY model.

Hans Weber and Henrik J. Jensen

Department of Physics, Technical University of Luleå, S-951 87 Luleå, Sweden,
[Fax: +46 920 91047], [E--mail: weber@mt.luth.se]

Experiments on single crystal high temperature superconductors [1] and on artificially constructed superlattices [2 3] of YBCO/PrBCO and V/Si [4] and their interpretation in terms of vortex fluctuations suggests that the two-dimensional (2D) vortex fluctuations [5] in the order parameter play an important role in the phase transition. A key problem in the study of these systems is the dependence of the critical temperature on the degree of anisotropy. The layered structure of these compounds is probably well described by the three-dimensional (3D) anisotropic XY-model. This model contains 2D planes with a strong intraplane coupling compared to the coupling between the planes. The strong coupling 2D XY planes correspond to the superconducting planes and the weak interplane coupling represents the Josephson coupling of the phase of the superconducting order parameter in different planes.

The 3D model has been studied in a mean field approach by Ito [6]. The weak coupling between the planes is here taken into account in the form of a mean field coupled to the phases in a 2D XY-model. A further study of the mean-field model was done by Cataudella and Minnhagen [7] There results where later confirmed by several authors [8 9] We use Monte Carlo simulations of a two dimensional XY-model in a magnetic field to study a self-consistent mean field theory for the 3D anisotropic XY-model. The relation between the critical temperature T_c and the interplane coupling $J_\perp$ is determined. We make a comparison of the mean-field solution and results for the 3D $XY-$model. [10 11]

---

[1] S. Martin, A. T. Fiory, R. M. Fleming, G .P. Espinosa, and A. S. Cooper, Phys. Rev. Lett. 62, 677 (1989).

[2] J.M. Triscone, Ø. Fisher, O. Brunner, L. Antognazza, A. D. Kent, and M. G. Karkut, Phys. Rev. Lett. 64, 804 (1990).

[3] D.H. Lowndes, D. P. Norton, and J. D. Budai, Phys. Rev. Lett. 65, 1160 (1990).

[4] K. Kanoda, H. Mazaki, T. Mizutani, N. Hoosoito, and T. Shinjo, Phys. Rev. B. 40, 4321 (1989).

[5] P. Minnhagen and P. Olsson, *Vortex-fluctuations and 2D Coulomb gas scaling for crystaline YBCO/PBCO superlattices.* Preprint (1991).

[6] M. Ito, Prog. Theor. Phys. 66, 1129 (1981).

[7] V. Cataudella and P. Minnhagen, Physica C 166, 442 (1990).

[8] H. Weber and H. J. Jensen, Phys. Rev. B 44, 454 (1991).

[9] P. Minnhagen and P. Olsson, Phys. Rev. Lett. 67, 1039 (1991).

[10] S.T. Chui and M.R. Giri, Phys. Lett. A 128, 49 (1988).

[11] P. Olsson, Monte Carlo result for 64^3 XY-model $\beta = 0.32$. Private communication (1991).

CCSa6

PROCESSING, AND CRITICAL CURRENT ENHANCEMENT IN BULK OXIDE SUPERCONDUCTORS.#

Kathleen Terryll, Lingna Wang, I. Zakharchenko, M. Muhammed* and K.V.Rao*

Dept of Condensed Matter Physics, and (*) Dept of Inorganic Chemistry,
Royal Institute of Technology, S-100 44 Stockholm, Sweden,

and

U. Balachandran
Argonne National Laboratories, Argonne, IL., USA .

Functional properties of the oxide superconductors strongly depend on the preparation techniques of the precursors and the microstructure of the final processed bulk material. We will present some of the highlights of our current ongoing efforts to produce and characterize *critical current enhanced materials* which can be summarized as follows:

1) Chemical techniques to produce emulsions with nano-size particle dispersion, as well as sub-micron size precursor materials,

2) Characaterization of the above precursors mainly by using ICP, SEM, X-ray as well as magnetic techniques,

3) Characterization and studies of the field and temperature dependence of the critical currents of the final material processed by techniques such as melt-growth processing MG, QMG etc..,

4) Extensive X-ray characterization by rocking curve and such techniques to *correlate* the possible role of orientational disorder with the functional properties of the MG, QMG processed materials.

We will also present data on our investigations of *defect structure enhanced materials* like Y-based 1-2-4 produced at ambient oxygen pressures and at low processing temperatures (600 to 700 K). These Y-based 1-2-4 materials have been successively heat treated to produce Y-based 1-2-3 superconductors with a fine dispersion of CuO particles which act as additional pinning centres and enhance considerably the critical currents through the bulk. From magnetic measurements, both the temperature and field dependence of the enhanced critical currents have been determined. Time permitting we hope to present some of our magnetic relaxation studies on processed materials in order to provide further insight into the nature and strength of the additional flux pinning centres introduced by controlled processing.

Research in Sweden supported by the STU.

CCSa7

MAGNETISATION OF RING-SHAPED SINGLE CRYSTALS OF YBCO AND BISCO

G.Yang, M.Slaski*, M.Z.Shoushtari, T.G.N.Babu, F.Gencer, J.S.Abell, and C.E.Gough, Superconductivity Research Group, University of Birmingham, Birmingham B15 2TT, UK, Fax: (21) 414 6709/4577

The role of sample geometry in flux line motion proccesses as well as the associated dynamics, flux pinning, creep and flow in high temperature superconductors is still an open question. Magnetic measurements enable us to study these properties and provide useful information and better understanding of the phenomena observed in high-T_c materials.

In this paper we present the detailed studies of magnetisation (VSM) of disk and ring-shaped specimens made from single crystals of $YBa_2Cu_3O_{7-x}$[1] and $Bi_2Sr_2CaCu_2O_y$. Hysteresis loops for different temperatures, sweep rates, and different magnetic field orientations with respect to the crystallographic c-axis have been obtained. Small fields measurements on ring-shaped samples (up to 1000 Oe) enable an unambiguous determination of the bulk transport current J_c^T. This is interpreted in terms of a model of weakly-coupled superconducting subdomains[2] within the "single - crystals". The bulk J_c^T is clearly distinct from the intergrain critical current J_c^D inferred from the high-field (up to 5 T) experiments, if the assumption of the critical state model is made. Such a model of Daeumling and Larbalestier[2] is applied to explain the dependencies of the interdomains shielding in discs and rings on an applied field.

Similarities and differencies between the magnetic behavior of $YBa_2Cu_3O_{7-x}$ and $Bi_2Sr_2CaCu_2O_y$ crystals are discussed.

1. C.E.Gough, G.Yang, M.Z.Shoushtari, T.G.N.Babu, F.Gencer, and J.S.Abell, Physica C 185-189 (1991) 2359
2. M.Daumling and D.C.Larbalestier, Phys. Rev. B 40 (1989) 9350
M.Daumling, J.M.Seuntjes, and D.C.Larbalestier, Nature 346 (1990) 332

*Permanent address: Institute of Physics, Technical University of Krakow, Krakow, ul. Podchorazych 1, Poland

CCSa8

Orbital Glass in HTSC- New State of Condensed Matter

Feodor V. Kusmartsev

Department of Theoretical Physics, University of Oulu, Linnanmaa
SF-90570 Oulu, Finland, [Fax: 358 81 561 278], [E-mail: feo@jussi.oulu.fi]

Landau Institute, Moscow, Russia

We show[1] that in granular High-Temperature Superconductors (HTSC) at small magnetic field the Meissner effect may disappear. We demonstrate that a possible explanation for this effect may be related to existence of special loops of Josephson junctions with positive and negative Josephson couplings. These loops have been observed in large number of experiments in granular HTSC. On the Josephson loop with the odd number of negative couplings a spontaneous orbital moment is created. The new state of the HTSC with orbital moments, which *indeed is a new state of Condensed Matter*, is characterized by *the coexistence of the orbital paramagnetic state with the superconducting state.*

The effects of Coulomb blockade have been also taken into account. Coulomb blockade does not qualitatively break the conclusions of our theory about existence of orbital glass. But under Coulomb Blockade the critical field H_{c0} of the transition into the new state of orbital glass increases. The new state exists only if magnetic field $H \leq H_{c0}$. We have estimated the value of orbital moments and also the influence of the charging energy on orbital magnetism.

We show that the critical field H_{c0} of the orbital paramagnetic glass transition is inversely proportional to the area S of the average loop of Josephson junctions in granular HTSC or the cross-area of an average grain S:

$$H_{c0} \sim \Phi_0 / S$$

where Φ_0 is the elementary flux quantum. Recent experiments by Wohlleben et.al. (Köln)[2] demonstrate that at small magnetic fields $(1-5.Oe)$ the Meissner effect in granular HTSC (2212-Bi-Compound) disappears. If we put in our formula the cross-section of average grain of granular HTSC we do obtain a value of the order $2.Oe$. This confirms the prediction of our theory for the discovered critical field H_{c0}, which we call as *orbital glass critical field.*

---

[1] F.V.Kusmartsev, Phys. Rev. Lett. to be published (1992). Europhys. Lett. 15, 863 (1991), and Int J. Mod. Phys. B5, 1809 (1991).

[2] D.Wohlleben et al., Phys. Rev. Lett. to be published (1992)

CCSa9

Calculations of the electronic Raman spectra for High-T_c superconductors

S. N. Rashkeev † and G. Wendin

Institute of Theoretical Physics, Chalmers University of Technology, S-412 96 Göteborg, Sweden
†Permanent address: *P.N.Lebedev Physical Institute, 117924 Moscow, Russia*

The problem of strong electronic Raman scattering over a wide frequency range in the high-T_c materials in the normal state is discussed. Due to the strong electron-phonon interaction in these materials the usual Fermi-liquid description with well-defined single-particle excitations of the electronic system is violated. In a wide range of temperatures and frequencies its behavior is similar to the *marginal* Fermi-liquid semi-empirical theory. The electronic Raman cross section in this case is proportional to the polarizability constructed with one-electron Green functions where the self-energy $\Sigma(\omega)$ is defined by the electron-phonon interaction. The coefficients of proportionality are defined by the generalized inverse effective mass tensor. We estimated numerically the spectrum of the electronic Raman scattering for the $YBa_2Cu_3O_7$ compound for different polarizations of the incident and scattered light using the Eliashberg function $\alpha^2 f(\omega)$ taken from tunneling experiments. The generalized inverse mass tensor is calculated from a first-principles band structure approach using one-electron band energies and optical matrix elements. We show that in order to describe the electronic Raman scattering in a wide energy region it is necessary also to take into account the interband scattering processes. They are especially significant at the frequencies $\omega \geq 2000\ cm^{-1}$. The results are in qualitative agreement with experiment. The possible role of the far infrared interband electronic transitions is also discussed.

CCSa10

An X-ray absorption and resonant photoemission study of Ca in the high temperature superconductor $Bi_2Sr_2CaCu_2O_8$.[1]

M. Qvarford, J.N. Andersen, S. Söderholm[2], H. Bernhoff[2], R. Nyholm, J.F. van Acker, E. Lundgren, U.O. Karlson[2], S.A. Flodström[2] and I. Lindau

MAX-lab, Lund University, Box 118, S-221 00 Lund, Sweden, [Fax: +46 46 104221]

The electronic structure of Ca in the high temperature superconductor $Bi_2Sr_2CaCu_2O_8$ has been studied by X-ray absorption spectroscopy (XAS) and resonant photoemission at the Ca $L_{2,3}$ absorption edge. In the XAS spectrum no absorption edge is seen at the energy corresponding to the Ca $2p_{3/2}$ binding energy, in agreement with the very low Ca density of states at the Fermi level predicted by band structure calculations. Furthermore, the crystal field splitting of the Ca 3d level, which is characteristic of compounds containing ionic Ca, is clearly seen in the XAS spectrum. The resonant photoemission spectra (cf. FIG.) display strong enhancements of the Ca 3s and 3p core levels as well as strong changes of the line shape of the Ca $L_{2,3}M_{2,3}M_{2,3}$ peak, showing the localized nature of the 3d states in core-ionized Ca. The 3d spectator shift of the Ca $L_{2,3}M_{2,3}M_{2,3}$ peak is fairly small compared to that reported for CaF_2[3], indicating that the screening of the normal Auger final state by the conduction electrons in the surrounding Cu-O_2 layers is quite efficient.

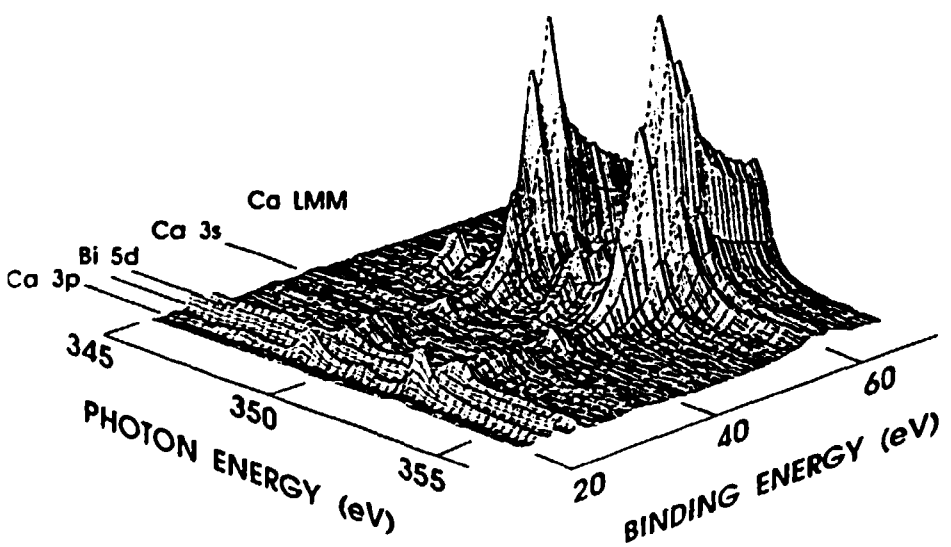

FIG. "Three-dimensional" plot of the resonant photoemission at the Ca $L_{2,3}$ edge. The plot is dominated by the high intensity of the Ca $L_{2,3}M_{2,3}M_{2,3}$ peak at photon energies corresponding to the main Ca $L_{2,3}$ peaks. The Ca 3p and 3s resonances are also clearly seen.

[1]Work supported by the Swedish Natural Science Research Council and the Swedish National Board for Technical Development.

[2]Materials Science, Department of Physics, Royal Institute of Technology, S-100 44 Stockholm, Sweden

[3]T. Tiedje et al., Phys. Rev. Lett. 65, 1243 (1990)

CISa11

MAGNETIC PROPERTIES OF DOPED SUPERCONDUCTING C-60 FULLERINES: *MANIFESTATIONS OF PHASE TRANSITIONS AND ORIENTATIONAL ORDERING.*#

J.L. Costa, and K.V.Rao

Dept. of Condensed Matter Physics
Royal Institute of Technology,
S-100 44 Stockholm, Sweden.

It is well known that in C-60 fullerines there exists a first order phase transition at around 260K which is followed by a continuous orientational ordering at lower temperatures. Moreover, there is also evidence that the C-60's at room temperature from an fcc lattice from which the sublattice changes to bcc at lower temperatures. The consequence of doping C-60 (with K, Cs, Rb and Ca etc..) on the distortion of these fcc/bcc lattices and the role of such distortions play in the superconducting properties are or considerable interest in order to gain further insight into the microstructure, mechanism and functional properties of these superconductors.

The highlights of our extensive SQUID-magnetometric measurements on various superconducting doped C-60 fullerines* with transition temperatures ranging from 25 to 42K may be summarized as follows:

a) We find an unusual field dependence for the Meissner fraction (the ratio of the flux expelled normalized to the flux shielding property) determined from the magnetic data for these new class of superconductors. Unlike the sharp decrease followed be a plateau in the field dependence of the Meissner fraction -a behaviour observed for the oxide superconductors - in the case of C-60 doped material the Meissner fraction is found to decrease strongly with a power law dependence on the field.

b) The structural transition at 260K in C-60 manifests itself as a well defined kink in the magnetic data as a function of temperature. The effect of the levels of K-doping on this structural transition has thus been investigated. In some cases we observe ferromagnetic-like hysteretic loops indicating the co-existence of possible precipitates at the grain boundaries in the K-doped superconducting material.

c) By rapidly freezing to helium temperatures the possible physical states existing at high temperatures we have studied the effects of various warming rates on the observed superconducting transition temperatures.

d) One manifestation of the expected orientational ordering is the observed non-logrithmic time dependence of magnetic relaxation which has been studied both as a function of temperature and magnitude of the field.

Supported by the NFR-NUTEK *Consortium on Clusters and Ultrafine particles.*

* *Some these studies are in collaboration with Drs. Iqbal and Ray Baughman at Allied Signals.*

CISa12

RAMAN SCATTERING IN HIGH-T_C SUPERCONDUCTORS

LARS BÖRJESSON

Department of Physics, Chalmers University of Technology, S-41296 Göteborg, Sweden, [FAX: 31-723177], [E-mail: f5xlb@secthf51]

Raman scattering is a powerful tool in investigations of high-T_C superconductors[1,2]. It has attracted considerable attention since it is a high resolution technique that conveys both energy and symmetry information about lattice, electronic, and spin excitations. Thus it can provide detailed information about normal state excitations. Moreover, it offfers an alternative to far-infrared absorption, photoemission and tunneling as a probe of the superconducting gap. The application of Raman scattering for studies of the various excitations will be discussed. Some of the most important observations reported so far can be summarized as follows:

Phonons are of interest for investigations of the phonon mediated pairing within the BCS theory for superconductivity. For certain phonons assymetric Fano-type lineshapes have been observed which are indicative of strong electron-phonon coupling. Indeed, some of the phonons are also profoundly influenced by the opening of the superconducting gap. critical temperature.

Two-magnon light scattering is observed in almost all of the semiconducting or insulating parent compounds of the high-T_C superconductors. The magnetic exchange parameter is found to have a value of 100-120 meV for most parent compounds. The magnon scattering and its possible extension to the superconducting compounds has attracted considerable attention for the superconducting mechanism.

Of principal interest for high T_C superconductors is the presence of a flat electronic continuum scattering extending to energy transfers as high as 1 eV. It has attracted considerable fundamental interest, for example in the marginal Fermi-liquid theory[3]. This low frequency electronic scattering, as well as the anomalous " mid-IR" optical absorption to which it likely relates, imposes an important constraint on realistic models of the cuprate superconductors.

Below T_C the continuum is redistributed to higher frequency shifts and exhibits a clear gap structure. Two gaps of different sizes has been found in $YBa_2Cu_3O_7$ in the ab-plane and in the c-axis direction, respectively. The c-axis gap is consistent with the BCS-value of $3.5k_B T_C$, while the gap in the ab-plane is about $5\text{-}7k_B T_C$.

In addition to a general review of the application of the Raman technique to high-T_C superconductors, the effect of isomorphous substitutions for Cu in $YBa_2Cu_3O_7$ on the phonon Raman scattering will be discussed and related to the structural properties.

1. M.V. Klein, Comments Cond. Mat. Phys., 15.99.(1990).
2. C.Thomsen and M. Cardona, in "The Physical Properties of High Temperature Superconductors, ed. D. Ginsberg, (World Scientific , Singapore, 1989) Chapter VIII
3. Varma et al, Phys. Rev. Lett. 63, 1996, (1989)

CISa13

Oxygen Order and Superconductivity in Pure and Doped $YBa_2Cu_3O_{6+x}$.[1]

H.F. Poulsen[&], N.H. Andersen[&], B. Lebech[&],
J.V. Andersen[#], H. Bohr[#], O.G. Mouritsen[#],
T. Zeiske[*], R. Sonntag[+], D. Hohlwein[*+], and T. Wolf[%].

[&] *Physics Department. Riso National Laboratory, DK-4000 Roskilde.*
[#] *Institute for Physical Chemistry. DTH. DK-2800 Lyngby.*
[*] *Hahn-Meitner-Institut Berlin, Glienicker Strasse 100. W-1000 Berlin 39.*
[+] *Institut Fur Krystallographie der Universitat Tubingen, Germany.*
[%] *Kernforschungscentrum Karlsruhe. ITP, Germany.*

The oxygen stoichiometry of the High T_c superconductor $YBa_2Cu_3O_{6+x}$ is variable over a wide range: $0 < x < 1$, corresponding to the possibility of intercalating oxygens into sites in a specific CuO_x mirror-plane in the material. It has been experimentally proven that the superconducting transition temperature T_c for this material depends not only on the average oxygen stoichiometry, but also explicitly on the configuration of oxygens in the CuO_x plane. The ordering process of the oxygens have in turn been found to comprise a rich variety of structural phenomena. The combination of these properties makes $YBa_2Cu_3O_{6+x}$ a unique choice for studying relations between structure, electrostatics and superconductivity in High T_c materials.

First we present a series of experiments on the static and dynamical structural features, including single crystal- and powder- neutron diffraction work as well as thermodynamic measurements[2]. A major point is the observation of diffuse peaks in a $YBa_2Cu_3O_{6.4}$ crystal. proving the existence of the low-temperature orthorhombic Ortho-II phase. Performing Monte Carlo simulations we show that the majority of our experimental data can be expained within the framework of the most simple two-dimensional lattice gas model for the oxygen ordering process, that is consistent with the existence of the Ortho-II phase (the ASYNNNI model). The interaction potentials are determined and the complete phase diagram established. Extensions to take into consideration the dependence of the interaction potentials on the electrons and the internal elastic forces will be discussed.

Next, we present results from a systematic study of the relationship between the static and dynamic variation of T_c and the corresponding variations of the oxygen configuration in the CuO_x plane. The configurations are generated by Monte Carlo simulations based on the ASYNNNI model. We have earlier demonstrated that within a charge transfer model the relationship between structure and superconductivity can only be rationalized if the description is based on the extended coherently ordered domains of the prevalent types of structural phases[3]. Emphasis will be put on very recent results where we extend these findings to the the case of $YBa_2Cu_{3-y}M_yO_{6+x}$. where metal-ions $M = Al, Co, Fe$ are partially substituted for Cu in the CuO_x plane.

---

[1] Work supported by the Danish Ministry of Energy and the Danish Natural Science Research Council.

[2] T. Zeiske. R. Sonntag. D. Hohlwein. N.H. Andersen, and T. Wolf, Nature **353**. 542 (1991); N.H. Andersen, B. Lebech, and H.F. Poulsen. Physica C **172**, 31 (1991); H.F. Poulsen. N.H. Andersen and B. Lebech Physica C **173**. 387 (1991).

[3] H.F. Poulsen. N.H. Andersen, J.V. Andersen. H. Bohr and O.G. Mouritsen. Phys. Rev. Lett. **66**. 465 (1991); H.F. Poulsen. N.H. Andersen, J.V. Andersen, H. Bohr and O.G. Mouritsen, Nature **349**, 594 (1991).

ClSu1

SUPERCONDUCTIVITY IN THIN FILM MULTILAYERS.

Ø. Fischer, J.-M. Triscone, L. Antognazza, O. Brunner, L. Miéville and E. Koller.

Département de Physique de la Matière Condensée, Université de Genève,
24, Quai E. Ansermet, 1211 Genève 4, Switzerland.

We shall report on the fabrication of epitaxially grown superlattices and ultrathin films made from high temperature superconductors. This approach has allowed a systematic study of certain properties of this class of materials. It is for instance possible to modify the anisotropy in a controlled manner and thus investigate the role of the reduced dimensionality of the high temperature superconductors on the superconducting properties. In the first part of the presentation we shall give an overview of results obtained on the critical temperature of such structures. In the second part we shall discuss in more detail the results related to the behaviour of the flux line lattice in these materials. In particular, we have investigated the thermally activated flux flow as observed in the resistive tails of the superconducting transition. We find in $YBa_2Cu_3O_7$/ $PrBa_2Cu_3O_7$ superlattices that the activation energies varies proportional to the thickness of the individual YBCO layers when the PrBCO thickness is large enough to decouple the superconducting layers (< 36Å). We thus find that the pancake vortices in the individual CuO_2 layers in YBCO are strongly coupled and that the flux line lattice is 2D in the individual YBCO layers up to layer thicknesses of more than 200Å [1]. We have also carried out an analysis of the zero field resistive transition in terms of coulomb gas scaling confirming this result. We find that the systematic broadening of the zero field resistive transition with decreasing YBCO thickness can be understood as a result of enhanced 2D fluctuations [2]. We have recently started investigating the properties of multilayers where the insulating PrBCO layers have been replaced by $Y_{1-x}Pr_xBCO$ metallic alloys. In this case we observe evidence for a proximity coupling across relatively thick normal state layers.

[1] O. Brunner, L. Antognazza, J.-M. Triscone, L. Miéville, and Ø. Fischer.
Phys. Rev. Letters 67, 1354, (1991)

[2] Ø. Fischer, O. Brunner, L. Antognazza, L. Miéville and J. -M. Triscone
To appear in Physica Scripta.

CISu2

SQUIDs

J. Flokstra

University of Twente, Faculty of Applied Physics, P.O.Box 217, 7500 AE Enschede, The Netherlands

The Superconducting QUantum Interference Device has proven to be a very successful tool for sensing very small signals. For example, the very weak (down to 10 fT) magnetic fields, originating from human brains activity (spontaneous or evoked), are presently detected by multichannel neuromagnetometers with low T_c dc SQUIDs. These sensors are often built with the favourable Nb/Al,AlO_x/Nb Josephson tunnel junctions, that are resistively shunted for eliminating the hysteretic behaviour. Noise levels are typically 10^{-6} $\phi_0/\sqrt{Hz}$ and the 1/f-noise onset is below 1 Hz. Further reduction of the 1/f-noise can be obtained by applying adequate modulation techniques. Design criteria for SQUIDs, properties of Nb/Al,AlO_x/Nb tunnel junctions, noise characteristics and improved SQUID read-out will be discussed.

High T_c dc SQUIDs differ in several aspects from the low T_c version. The higher operation temperature (77 K) has consequences for the various SQUID design parameters. The junctions are of SNS-type and may be of different origin. Ramp-type YBaCuO/(PrBaCuO)YBaCuO junctions and grain boundary junctions on bicrystal substrates or templates will be treated. Attention will be paid to the noise properties (white noise and 1/f noise) of the SQUIDs.

Two applications of high T_c SQUIDs will be discussed. The first is a small system for magneto-cardiography. The second application is a superconducting gravity gradiometer, being developed in a combined effort by Danish, Swedish and Dutch research groups.

CISu3

Material Properties and Critical Current Densities in HTSC Superconductors

R. Flükiger

Dépt. Phys. Mat. Condensée, 24 quai Ernest Ansermet, 1211 Genève 4, Switzerland(Fax: +41-22.781.2192)

From the present knowledge, it is probable that the first application of HTSC materials at a large scale will be the construction of superconducting magnets. The reported behavior of the transport critical current data at various temperatures and magnetic fields suggest that this development could happen in two steps, the first one being the construction of small high field magnets operating at 4.2 K producing magnetic fields exceeding 25 T, the next step consisting in raising the operation temperature to 77 K. At this temperature, the expected fields are considerably lower than those at 4.2 K, but 1 Tesla can be considered as realistic in a mean-term time scale. Very recent developments on the Thallium based compound Tl(1223) show that this value could be further enhanced.

The present talk gives an overview of the various problems encountered on the way of the development of superconducting HTSC tapes to be used in magnets. The fields to be treated are: a) the choice of the adequate superconductor, b) the preparation of textured tapes, c) the thermodynamics of phase formation, d) the characterization of the tapes by microstructural analysis and e) the measurement of the transport j_c in the range 4.2 to 77 K as a function of the applied field and its orientation with respect to the tape surface, i.e. perpendicular to the c axis.

The most promising materials known so far are based on Y, Bi and Tl, the superconducting phases being denominated by Y(123), Bi(2212), Bi(2223), Tl(1223) and Tl(2223). The anisotropy of j_c with respect to the field orientation is smallest in theY based system, but the poor mechanical properties of this compound render its deformation to tapes very difficult: so far only bulk samples have been prepared, by means of the melt-texturing technique. The Bi and Tl based superconductors are mechanically softer than the Y-based oxide and can be easily brought into a textured configuration by chosing the correct sequence of pressing and annealing steps for the Powder-In Tube preparation technique. This technique is actually under development in many laboratories.

The mechanical and physical properties of the phases Bi(2223) and Tl(2223) are quite similar, but a substantial difference resides in the formation mechanism. The Tl based phase can be formed by a melting process while Bi(2223) requires a reaction of the solid Bi(2212) with a liquid phase mixture and is stabilized by the addition of Pb. Most data on tapes to be used at 77K have so far been obtai-

ned on Bi(2223) which will be discussed in detail. The Powder-In-Tube technique commonly used for preparing Bi(2223) tapes consists in introducing the appropriate amounts of calcined precursors in Ag tubes which are cold deformed to tapes of 0.1 mm thickness and then submitted to one or more pressing/heat treatment cycles at 837 - 844°C. The thermodynamics of the Bi(2223) phase formation inside the Ag tapes is quite complex. This phase is formed by a reaction of the solid Bi(2212) phase with a liquid phase mixture containing an excess of Pb, Ca and Cu. The simultaneous Bi(2223) grain growth parallel to the tape surface will eventually lead to a contact between neighbouring platelets, a necessary condition for the conduction of transport currents. A small quantity of the Ag originating from the sheath is dissolved into the liquid phase and lowers its melting point by 15 to 20°C, thus enhancing the the Bi(2223) grain growth.

For Ag sheathed, Pb stabilized Bi(2223) tapes (0.1 mm thick), Sato et al.(1) have reached the value of $j_c(77K,0T) = 5.3 \cdot 10^4$ A/cm^2; values up to $4.0 \cdot 10^4$ A/cm^2 have been achieved in our laboratory on 40 mm long tapes (2). Attempts to reach similar values on long tapes deformed by rolling steps alone show that the correct deformation of metal/oxyde composites still constitutes a major problem. Indeed, the known j_c values on tapes with lengths > 1 m are a factor 3 and more below the short sample values. Nevertheless, the highest values for tapes longer than 10 m required to wind small laboratory magnets exceed $1 \cdot 10^4$ A/cm^2. Small superconducting magnets producing 0.1 T at 77K have already been produced in Japan by Sato et al. (1). The variation of j_c with the applied magnetic field parallel to the tape surface (as in wound magnet solenoid) at 77K is fairly strong, the value at 1 T being almost 20% of its value at zero field. For the orientation $B||c$, j_c shows a much stronger dependence, decreasing to 10 % at 0.5 T.

A possible solution to the anisotropy problem has been recently presented by Liu et al. (3), who investigated the compound Tl(1223), where 50% of the Tl are replaced by Pb. For this compound, these authors reported a more 3D behavior than in the phase Bi(2223) and Tl(2223), resulting in a reduced anisotropy in j_c. This exciting result is not yet fully understood, but indicates that there are still unknown mechanisms which may lead to a further enhancement of j_c, even in the unfavourable field orientation, thus fulfilling a necessary condition for the development of the first industrial 77 K magnets.

---

(1) K. Sato, N. Shibuta, H. Mukai, T. Hikata, M. Ueyama, T. Kato, J. Appl. Phys., 70(1991)6484
(2) R. Flükiger, B. Hensel, A. Jeremie, M. Decroux, H. Küpfer, W. Jahn, E. Seibt, W. Goldacker, Y. Yamada, J.Q. Xu, Supercond. Sci. Technol. 5(1992)S61
(3) R.S. Liu, D.N. Zheng, J.W. Loram, K.A. Mirza, A.M. Campbell, P.P. Edwards, Appl. Phys. Lett., 60(1992)1019.

CISu4

Applications[1]

Jarl-Thure Eriksson

Laboratory of Electricity and Magnetism, Tampere University of Technology, P.O.Box 527, SF-33101 TAMPERE, Finland
[Fax +358 31 162160]

The history of superconductivity is flavered with a rich supply of stories almost legends about the personalities struggling with the obstacles of this mysterious, promising and almost always in the end disappointing phenomenon. The first story tells about Kamerling Onnes' reluctancy to accept his assistant's, G. Holst's claim that the resistance of mercury dissappears at 4.2 K[1]. Another story from the early 50s tells us that the nowadays well-famed Russian physicist A.A. Abrikosov put aside his theory of the magnetic vortex lattice because his mentor Lev Landau did not accept it. Not until Landau learnt about Faynmans analog ideas of superfluid vortices, Abrikosov was given the opportunity to publish his results[2].

From the beginning it was apparent that superconductivity could be very beneficial in many senses. Kamerling Onnes wrote in a paper presented at a Chicago conference in 1913: "The solution of the problem of obtaining a field of 100.000 Gauss (10 T) could then be obtained by a coil of say 30 centimeters in diameter and the cooling with helium would require a plant which could be realised at Leiden with a relatively modest financial support." But alas! In February 1914 Kamerling had to admit: "It will be seen that the transition from the supra-conducting condition to the ordinary condition through the magnetic field takes place fairly suddenly."

It was not until 1961, 50 years after the discovery, that real progress was achieved. By that time the first high-flux high-current conductor, the niobium-tin compound was investigated. Somewhat later niobium alloys with zirconium and titanium were developed to the first commercial conductors. Along with the material question mechanical and thermodynamic problems had to be solved. By the end of the 60s the situation had developed in a very positive direction. The first impressive magnets for high energy physics had been constructed. It is therefore not surprising that the optimistic views of 1972-73, Table 1, forecasted a general commercial breakthrough in the mid 80s. But as we all know low temperature superconductors never - with a couple of exceptions; high energy physics and MRI-tomography - came to shot.

In 1986 at the Applied Superconductivity Conference in Baltimore the 75 anniversary of Onnes discovery was held. In spite of the highly appreciated contributions of Bardeen, Cooper and Pippard, the general spirits where to be compared to those at a funeral. Practically nobody at the conference knew that in the same month, September 1986, a paper was published, a paper that should revol utionize the community. The HiTc era was to begin.

[1] The activities related to the application of superconductivity at Tampere University of Technology have during a course of 10 years been sponsored by Imatran Voima Oy, ABB Strömberg, Huurre Cleanroom Oy, The Electric Power Pool, The NEMO (New Energy MethOds) project from Finland and ABB Corporate Research, AGA AB, Statens Vattenfallsverk, Scanditronix AB and University of Lund from Sweden. The support is acknowledged with the deepest gratitude. Many thanks to my students.

One of the first questions that arose was: Where can these tricky materials be used? Table 2 shows an early forecast of the industrialists' view of the most promising application areas. Transportation is high-ranked, because the Japanese industry sees a future in ground transportation (levitated trains as well as in MHD-propulsion of cargo and military ships). Electronics also form a strong option, SQUIDs are supposed to form the basic logic element of future supercomputers.

High temperature superconductors offer very interesting capabilities to the electric power engineering sector. Generator, motor and transformer losses will decrease by, say, 50 %. At the same time crucial savings can be made in weight and volume. Power cable costs will be reduced by 30 % compared to conventional high voltage oil impregnated cables. Superconducting magnetic energy storage (SMES) has received an increasing amount of interest during the last years. In large power networks, of the order of whole Scandinavia Finland included, SMES units of say 5000 MWh capability will have an energy and hence money saving function by levelling out the fluctuations between night and day electric power consumption. According to rough calculations superconductive technology in a network of Sweden's size could have an impact worth 1450 million SEK per annum, a more moderate evaluation based on a 10 - 50 % replacement of conventional equipment results in savings of 300 million SEK per annum[3].

A rather new application area is offered by synchrotron radiation. So far light and x-ray illumination from synchrotron sources have been used in physics research. But in not a too far away future synchrotron x-rays may have a great impact on the production of integrated circuits (x-ray lithography) and on different diagnostic procedures in medicine and microbiology. The coherent and highly quantized radiation can be used for tissue imaging and enzyme identification. The last mentioned option is important for instance in the determination of virus infection or in the follow up of cancer treatment.

In summary. It is a fact that superconductivity is sustained up to 130...150 K. The technology of manufacturing wires for high currant and high magnetic fields has made great progress during the six years since the discovery in 1986. We are still emotionally confined to conventional applications, which might "come in from the cold". However, we must also have an open mind for completely new directions in the development. Conventional technology can handle conventional problems. Superconductivity will bring completely new application areas into focus. MRI-tomography and synchrotron radiation are examples of the unpredictable nature of technical development.

References

1. R. de bruyn Ouboter, IEEE Trans on Magn, MAG-23, No 2, March 1987, pp.355-370
2. Ted G. Berlincourt, IEEE Trans on Magn, MAG-23, No 2, March 1987, pp. 403-412
3. J.-T. Eriksson, Superconductivity to enhance the efficiency of power networks. Vattenfall Report U(E) 1991/16, p. 41 (In Swedish)

Table 1. Large scale applications by 1972-73 (J. Powell, 1973)

Item	Year of introduction
Fusion	2000
MHD	1985
SMES	1980
Generators and motors	1980
Power cables	1990
Levitated trains	1980
Space craft accelerators	1980
Magnetic separators	1980

Table 2. Estimated HiTc breakthrough before 1998 (Nikkei 1988)

Item	Probability %	Comm. volume MSEK/a
MRI	100	1.800
Wigglers	90	3.150
Separators	75	750
SMES	70	13.500
Generators	56	230
Cables	52	120
Levitated trains	100	25.500
Electric motors	52	360
MHD ship prop.	30	7.500
Rocket accelerat.	95	53

CP1

EPITAXIAL GROWTH OF HIGH-T_c SUPERCONDUCTING $Bi_2Sr_2CaCu_2O_{8+x}$ THIN FILMS ON MgO(001), $LaAlO_3$(001), AND $NdGaO_3$(001)

R. de Reus*, R. Seemann†, M. Nielsen*, A. Sewing†, and R.L. Johnson†

*Department of Solid State Physics, Risø National Laboratory
DK – 4000 Roskilde, Denmark

†II Institut für Experimentalphysik, Universität Hamburg, Luruper Chaussee 149
D – 2000 Hamburg, Federal Republic of Germany

Superconducting $Bi_2Sr_2Ca_1Cu_2O_{8+x}$ (BSCCO) thin films prepared by pulsed laser ablation were investigated by a variety of analysis techniques. The films were deposited on the various types of single-crystalline substrates at 500 °C in 0.2 mbar O_2 and subsequently annealed in air for 5 min at 852 °C. By this method BSCCO films were obtained exhibiting superconducting transition temperatures of 80 K or higher. X-ray diffraction, using a four-axis diffractometer, shows an almost 100% *c*-axis orientation for all samples. Although deposited under almost identical conditions, a remarkable difference between the various types of subtrates is noticed. Whereas the BSCCO films deposited onto $LaAlO_3$(001) and $NdGaO_3$(001) appear to be fully epitaxial (*i.e.*, complete alignment of film and substrate in the *ab*-plane), the films deposited onto MgO appear to consist of both oriented regions and domains randomly rotated in the plane of the substrate surface. The oriented parts of the films deposited onto MgO consist of fully oriented regions, meaning that crystallographically the fundamental in-plane symmetry directions of film and substrate are parallel, of regions with a misorientation of 45 degrees, and of regions with an in-plane rotation of 11.5 degrees. Glancing incidence x-ray diffraction showed that the oriented parts of the film are located at the deeper regions of the film. Moreover, the relative amount of randomly in-plane oriented material increases with increasing film thickness. The difference in epitaxy is attributed to the poor lattice match between BSCCO and MgO on the one hand, and the very good lattice match between BSCCO and $LaAlO_3$ or $NdGaO_3$ on the other.

Cooling of the samples to room temperature before the post annealing step at 852 °C results in a different surface morphology. Scanning electron micrographs and scanning tunneling microscopy show that the surfaces of the samples cooled to room temperature before post annealing are significantly less smooth compared to the surfaces of samples directly heated to 852 °C after deposition of the film. Despite these differences no significant changes in the structure of the films could be detected by x-ray diffraction.

BSCCO films deposited at 500 °C, which were not subjected to the post annealing, appear amorphous according to x-ray diffraction analysis. Both as-deposited as well as post-annealed films contain a considerable amount of solidified droplets with diameters up to 0.5 μm. These results indicate that crystallization of the amorphous BSCCO alloy and hence the epitaxial growth takes place during the heat treatment at 852 °C in air.

CP2

Raman Scattering Background as an Evidence of Acoustic Plasmons in High-T_c Superconductors

A. Kallio and V. Apaja

Department of Theoretical Physics, University of Oulu, Linnanmaa
SF-90570 Oulu, Finland, [Fax: 358 81 561 278], [E-mail: vap@jussi.oulu.fi]

Raman scattering of the high-T_c superconductors has revealed an electronic intensity background[1]. In contrast to the weak coupling BCS theory, this background has a linear rise at small energies. We propose a new interpretation for the background based on the SFS model[2]. The SFS model has two mobile components, a light effective mass non-pairing fermion component and a heavier component that pairs into point bosons. We argue that only the lighter component shows in Raman spectra, and thus a direct evaluation of 2Δ from the intensity distribution is not possible. Instead of an energy gap $\Delta(T)$ the Raman background is parametrized with a T-dependent sound velocity $u(T)$.

The Raman intensity is proportional to the dynamic structure factor, for which we use the single mode approximation $S(q,\omega) \propto q\delta(\omega - uq)$. For small ω we get the Raman intensity

$$I(\omega) = [1 + n(\omega,T)]\frac{\gamma}{u^2}\omega.$$

Slakey *et al.*[3] has removed the Bose factor $[1 + n(\omega,T)]$ from their measured spectra and found that the remaining intensity rise is linear both below and above T_c. From the experimental slopes the T-dependence of the sound velocity can be deduced: $u(T)$ has a minimum at T_c and has equal values at $T = 0$ and $T \approx 300\ K$ for YBCO. The value of the sound velocity is expected to be close to the Fermi velocity, $u(T) \sim 10^6\ m/s$. The measurement also proves that the T-dependence of the excitation spectrum is roughly symmetric with respect to T_c, which rules out any attempts to explain the spectra using a gap $\Delta(T)$ that goes to zero at T_c.

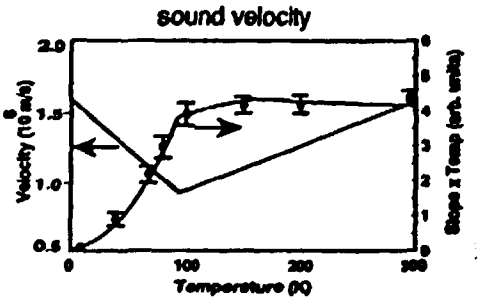

[1] S. L. Cooper, M. V. Klein, B. G. Bazol, J. P. Rice, and D. M. Ginsberg, Phys. Rev. B37, 5920 (1988).

[2] A. Kallio and X. Xiong, Phys. Rev. B41,2530 (1990); Phys. Rev. B43, 5564 (1991).

[3] F. Slakey, M. V. Klein, J. P. Rice, and D. M. Ginsberg, Phys. Rev. B43,3764 (1991)

CP3

The Pressure Effect for Electron- and Hole-Doped Superconductors

A. Kallio, and X. Xiong

Department of Theoretical Physics, University of Oulu, Linnanmaa
SF-90570 Oulu, Finland, [Fax: 358 81 561 278], [E-mail: xix@jussi.oulu.fi]

We show that the pressure dependence of T_c and the pressure asymmetry for the hole-doped and electron-doped superconductors[1] can be explained within a generalized electron-hole liquid model called spectator fermion superfluid (SFS) model[2]. In both cases the experimental pressure gradients of T_c are fitted well if the spectator component has much smaller effective mass than the bosons.

The SFS model so far passes the stringent test of predicting the pressure dependence of many different quantities such as T_c, $\gamma(0)$, $c_p(T_c)$, $R_H(T)$ and $\rho_a(T)$ both for the superconducting and the normal states for a variety of high Tc superconductors (HTS) and heavy fermion superconductor (HFS). We have presented strong evidence that all superconductors with short coherence length can be assigned to belong to one of the four spectator fermion categories (e^-, B^{++}), (h^+, B^{--}), (e^-, B^{--}) and (h^+, B^{++}) on the bases of the pressure dependence of their T_c and the Hall measurements. This in turn is possible only if the rest of the SFS model predictions are true: the existence of at least two accoustic plasmon modes with sound velocities $u_1 < u_2$. The lower mode, associated with pair breaking, determines the superfluid and normal fractions through the bosonic and fermionic excitations. We believe that pair breaking function $f(T)$ is a more fundamental quatity than the density of states of quasiparticles which is needed for theoretical calculation of $f(T)$. Besides the density of states such a calculation needs as input a detailed band structure and knowledge of possible disorder. On the other hand we have shown that many experimental quantities can be expressed in terms of $f(T)$. The higher sound mode predicted by the present model shows up in Raman scattering as continuous back ground which we have previously used to determine the temperature dependence of the corresponding sound mode. The theory predicts an increase of the specific heat linear term with pressure for all four spectator categories. The pressure dependence of T_c and $c_p(T_c)$ for the HFS-compounds UBe_{13} and UPt_3 come out correctly if we assume the structure (h^+, B^{++}) for them. We show that the pressure dependence of the Hall coefficient and the Hall resistance agree with experiments for HTS-compounds for $T > T_c$[3].

---

[1] J.T. Markert, J. Beille, J.J. Neumeier, E.A. Early, C.L. Seaman, T. Moran, and M.B. Maple, Phys. Rev. Lett. 64, 80 (1990); N. Tanahashi, Y. Iye, T. Tamegai, C. Murayama, N. Mori, S. Yomo, N. Okazaki, and K. Kitazawa, Jpn. J. Appl. Phys. 28, L762 (1989).

[2] A. Kallio, and X. Xiong, Phys. Rev. B41, 2530 (1990); A. Kallio, and X. Xiong, Phys. Rev. B43, 5564 (1991); A. Kallio, V. Apaja, and X. Xiong, Physica C (1992) (in print).

[3] C. Murayama, Y. Iye, T. Enomoto, N. Mori, Y. Yamada, T. Matsumoto, Y. Kubo, Y. Shimakawa, and T. Manako, Physica C 183, 277 (1991).

CP4

Josephson Soliton Oscillators coupled to a Superconducting Thin Film Resonator

J. Holm*, Paola Barbara§, N.F. Pedersen, A. Davidson++ and J. Mygind

Physics Laboratory I, The Technical University of Denmark
DK-2800 Lyngby [Fax: +45 45931669] [E-mail: Fyl1jeh@vm.uni-c.dk]

*also: Danish Institute of Fundamental Metrology, DK-2800 Lyngby

§Department of Physics, University of Salerno, I-84100 Salerno

++IBM T.J. Watson Research Center, Yorktown Heights, NY 10598, USA

A Josephson soliton oscillator integrated in a superconducting coupled microstrip resonator [1] has been investigated experimentally. The junctions are trilayer niobium-aluminum oxide-niobium structure with a critical current density of around 1000 A/cm^2. The even and an odd mode half-wave resonances of the thin-film resonator impose different magnetic field configurations at the one junction boundary. The dc IV-characteristic shows Zero-Field Steps containing a large number of self-induced substeps. Their origin is analysed by comparing to steps induced by phase-locking of the soliton motion to an external rf-source.

By investigating these steps as function of applied power, different couplings schemes between the soliton and the microwaves has been verified. It is suggested how these couplings can be separated [2] and be interpreted as either a coupling to the microwave field at the boundaries, or as a more homogeneous coupling over the whole junction length. The results are compared to numerical simulations [3].

[1] A. Davidson, N. Groenbech-Jensen and N.F. Pedersen, IEEE Trans on Magn. MAG-27, 3347 (1991).

[2] Paola Barbara, A. Davidson, G. Filatrella, J. Holm, J.Mygind and N.F. Pedersen, *submitted for publication.*

[3] J.C. Fernandez, G. Filatrella and G. Reinisch, Phys. Lett. A 153, 446 (1991).

CP5
Synthesis of Bi-Pb-Sr-Ca-Cu Oxide Powders for Superconducting Wires[1]

Hans Aage Hjuler and Karen Brodersen
NKT Research Center A/S, Sognevej 11, DK-2605 Brøndby, Denmark

After the discovery[2] of superconductivity in the Bi-Pb-Sr-Ca-Cu-O-system, a large number of methods of synthesis has been examined by researchers all over the world.

In the present study, four methods have been evaluated for the synthesis of the high-T_c phase $Bi_{1.8}Pb_{0.4}Ca_2Sr_2Cu_3O_x$ (Bi-2223) with a T_c of 105-110 K.

Of the selected methods, reproducible results have been obtained with an improved version of the traditional ceramic method based on ball-milling of oxides and carbonates of the constituent metals. The improvement was obtained by using a dispersive agent in the ball-milling procedure. After calcination and sintering, the results show T_c values close to 105 K from AC-magnetic susceptibility measurements and X-ray data show that the powders had a relatively high phase purity with respect to the high-T_c phase.

Also spray drying of nitrate solutions of approx. the same composition gives reprocible results with T_c above 105 K. X-ray data show very high phase purity.

The powders are well-suited for the manufacture of superconducting wires.

Further, a number of inorganic additives to the Bi-2223 superconductor have been tested. These results together with experimental details of the powder synthesis will be presented.

---

1. Work supported by the electricity boards ELSAM and ELKRAFT, Denmark
2. H. Maeda, Y. Tanaka, M. Fukutomi, and T. Asano, Jap. J. Appl. Phys. 27, L. 209 (1988)

CP6

Fabrication of Ag-Sheathed Bi-2223 Superconducting Tapes[1]

Q. Li, K. Brodersen, H.A. Hjuler, and T. Freltoft
NKT Research Center, Sognevej 11, DK-2605 Brøndby, Denmark

Superconducting Ag-sheathed (BiPb)SrCaCuO (2223) tapes were produced using the "powder-in-tube" technique. The Bi-2223 powders with critical temperature, T_c, better than 105 K were prepared by both spray-drying and solid state oxide-carbonate methods and packed into Ag tubes in their calcinated or sintered states. In order to remove adsorbed gases (CO_2, H_2O) from the powders, they were calcinated again under vacuum atmosphere. This calcination process is found to be of central importance for obtaining tapes with critical current densities, J_c, in excess of 5000 A/cm² at 77 K. In addition, repeated cold working processes (rolling or pressing) together with intermediate sintering processes are required for further improvement of J_c. The relation between microstructure and J_c was investigated by SEM and by XRD.

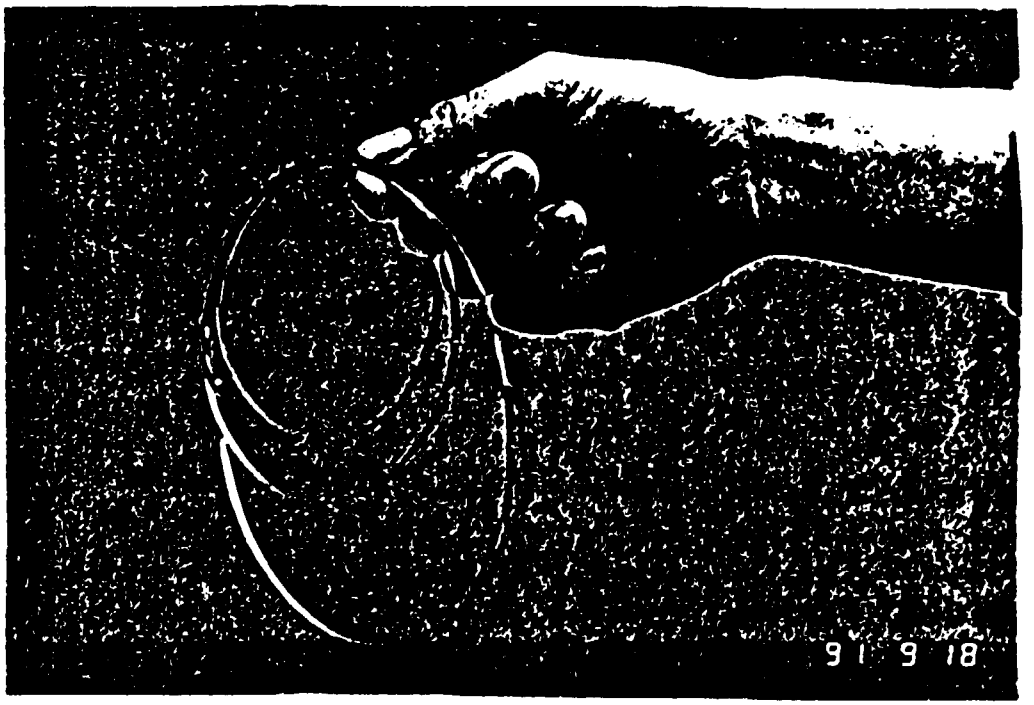

1 Work supported by the electricity boards ELSAM and ELKRAFT, Denmark

CP7

Investigation of Magnetic Flux Noise in Thin-Films of High-Temperature Superconductors[1]

A.Kühle, J. Bindslev Hansen*, C. Schelde Jacobsen and J. Mygind,
Physics Laboratory I,III, The Technical University of Denmark, Lyngby.
* Presently at NKT Research Center, Brøndby, Denmark.

The aim of this work is to measure the spectral density of the flux noise generated by thermally activated flux motion (jumps or creep) in high-T_c thin-films, in particular the excess low frequency noise in the 1/f regime (typically from 10^{-3} to 10 Hz). The fluctuations of magnetic flux are studied as a function of temperature, applied static magnetic field, and thin-film surface roughness (i.e. the density of *droplets* and *outgrowths*) in order to determine the influence of the thin-film quality on flux pinning.

The reason for the investigations is to understand the intrinsic noise mechanisms in high-T_c thin-films which may be related directly to slow flux motion[2] and thereby to find the limiting sensitivity of High-T_c SQUIDs. Apart from the noise contribution of the Josephson junctions[3], the excess low frequency flux noise stemming from the thin-film *pick-up and input coils (the flux transformer)* and the SQUID loop itself sets the limit of the performance of SQUID magnetometers and derived instruments, e.g. superconducting gravitational gradiometers. The investigations will, hopefully, also contribute to the basic understanding of flux behavior in high-T_c thin-films.

The measurements are carried out by means of a low-noise 4.2 K niobium SQUID mounted in a vacuum can immersed in a liquid helium bath. The low-T_c SQUID is bonded to a 1"x1" sapphire substrate mounted on a cold table in good thermal contact with the helium bath. The sapphire substrate contains a niobium pick-up coil which matches the geometry of the high-T_c sample.

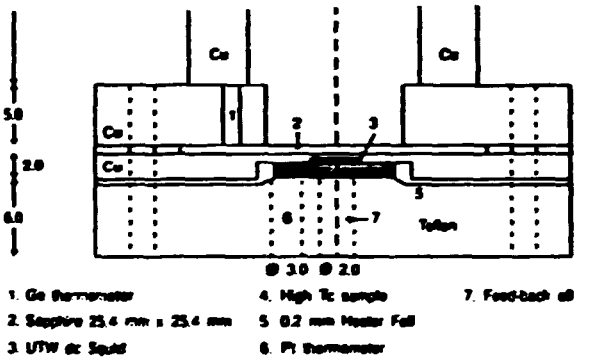

The sample is placed on a heated stage only 200-500μm from the pick-up coil. The temperature-regulated heated stage is in weak thermal contact with the rest of the setup. The setup is electrically and magnetically shielded by a superconducting lead shield and two mu-metal shields.

We report on our experimental set-up and techniques and on the status of our on-going measurements.

---

1 Research is carried out in collaboration with the University of Twente (the Netherlands), Chalmers University of Technology and NKT Research Center, sponsored by European Space Agency.

2 M.J. Ferrari, M. Johnson, F.C. Wellstood, J. Clarke, P.A. Rosenthal, R.H. Hammond and M.R. Beasley, IEEE Trans. Magn. MAG-25, p806, 1989.

3 R.H. Koch, W. Eidelloth, B. Oh, R.P. Robertazzi, S.A. Andrek and W.J. Callagher, Appl. Phys. Lett. 60, p507, 1992.

CP8

Y-Ba-Cu-O Thin Films Produced by Laser Ablation and by Co-Evaporation Techniques[1]

A.Kühle, S. Hjort, I. Rasmussen, J.L. Skov and J. Bindslev Hansen*,
Physics Laboratory I, The Technical University of Denmark, Lyngby.
* Presently at NKT Research Center, Brøndby, Denmark.

We report the progress in the effort at DTH to prepare high-T_c YBCO thin films on MgO by two routes: laser ablation and co-evaporation.

Co-evaporation takes place in a dedicated MBE-system (VG Special System) from two electron beam sources (Y and Cu) and one Knudsen cell (BaF_2). The three materials are deposited at a total rate of about 0.03 nm/s on a room temperature crystalline MgO substrate at 10^{-7} mbar. The amorphous thin film is annealed ex-situ in a flow of wet oxygen, thereby forming YBaCuO. The deposition rates are controlled by quartz crystal microbalances. MBE co-evaporation is an attractive metod because it allows good control of interfaces in multi-layer structures (e.g. for hetero-junctions). The main difficulty with the method appears to lie in the control of the stoichiometry at the required 1 % level.

Laser ablation is done by focussing the beam from a pulsed Questek excimer laser (KrF, 248 nm, max. 0.7 J per 30 ns pulse, 10 Hz) on a hard sintered YBaCuO target in a 1 mbar oxygen atmosphere. A YBaCuO thin film (with the same stoichiometry as the target) grows epitaxially on a heated MgO substrate placed about 4 cm from the target. The deposition rate is around 2 nm/s. The thin film is cooled down slowly in 1000 mbar dry oxygen. The laser ablated thin films exhibit rough surfaces (*droplets* and *outgrowths*) but good electrical characteristics, T_{co} = 91.3 K, Jc(77 K) > 10^6 A/cm^2.

Work is under way to fabricate microwave components from the YBaCuO thin films. We report on the techniques used, particularly co-evaporation, and on the quality (surface, electrical) on the produced films.

1 Work supported by Brdr. Hartmann Foundation, DanninFoundation, ELSAM, Fisker and Nielsen Foundation, Brite/Euram and the Danish Natural Science and Technical Research Councils (MUP Programme).

CP9
MELT-TEXTURED AND DOPED $YBa_2Cu_3O_{7-x}$ PLATES WITH HIGH CRITICAL CURRENT DENSITIES

J. G. Larsen#, N. E. Dam*, C. S. Jacobsen*, H. D. Bærendtsen# & J. G. Sommerschield#.

#: Haldor Topsøe A/S, Nymøllevej 55, 2800 Lyngby, Denmark.
*: Physical Laboratory 3, Building 309, The Technical Univer- sity of Denmark, 2800 Lyngby, Denmark.

Melt texturing of up to 20x2x0.1 cm^3 sized plates of $YBa_2Cu_3O_{7-x}$ doped with Y_2BaCuO_5 has been performed at temperatures somewhat above 1025°C and crystallization rates of 1-5 mm/h. The direction of the crystal growth has been controlled by the temperature gradient so that up to 10x1 cm^2 sized crystals have been formed growing parallel to the sides of the tapes. The crystals contain inclusions of Y_2BaCuO_5 needle-shaped crystallites measuring approx. < 1-5 μm x 1-10 μm. The crystallographic orientation of the $YBa_2Cu_3O_{7-x}$ crystals is varying but in many cases the c-axis is lying close to the plate plane. In most cases, for the slowly grown crystals, with oblique angles to the plate sides. The crystals contain closely spaced (approx. 2 μm) microcracks after the (001) face formed during the oxidation. The orientation of the twins may be affected by the green phase inclusions. In addition the microcracks may also act as barriers which may change the orientation of the twinnings either gradually or discontinously. Oxidation and sintering of silver contacts have been performed in one cycle at 850°C with prolonged oxidation in O_2-flow at 450°C, giving samples with T_C = 88-90 K and δT < 0.3 K and contact resistances down to 0.1 μohm·cm^2. Characterization of up to 10 cm long samples has been performed with an ac pulsed low voltage source and up to 7500 A/cm^2 without exceeding the critical current density, J_C (77K and 0 B-field). Peak currents of up to 3000 A have been employed. In all measurements where the superconductor appeared to go normal it fractured along the (001) cleavage plane.

In addition to direct transport measurements we have investigated a number of samples by magnetization measurements. An external field is varied in order to introduce a state where the sample everywhere carries J_C. The field dependent J_C can be deduced from the change in magnetic moment with field sweep direction (i.e. the hysteresis). The figure shows representative magnetization loops for a sample at four temperatures: 1 = 83.4 K, 2 = 77.4 K, 3 = 71.4 K, and 4 = 65.4 K. At $T < \approx T_C$ (1) J_C is vanishing, while at the lowest temperature J_C is of order $5 \cdot 10^4$ A/cm^2. J_C's up to $9 \cdot 10^4$ A/cm^2 at 77 K have been measured on these samples.

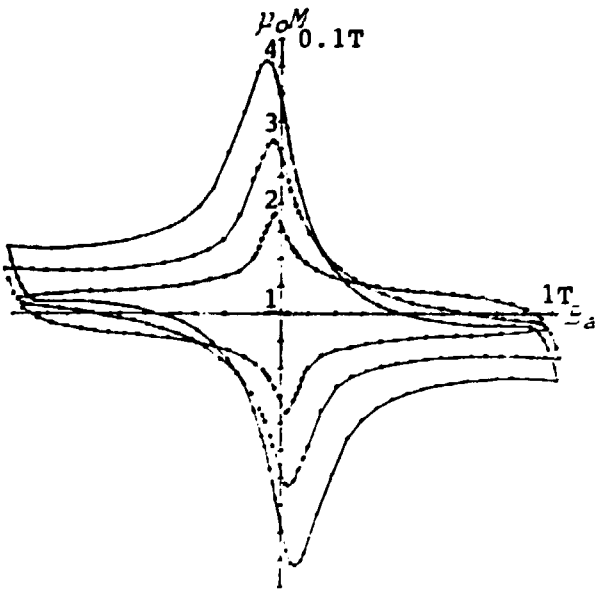

CP10

INVESTIGATIONS OF NEW SYSTEMS USING AN ANALYTICAL TEM

I. Bryntse and A. L. Kharlanov*

Department of Inorganic Chemistry, Arrhenius Laboratory, Stockholm University, S-106 91 STOCKHOLM, Sweden. [Fax: +46 8 152187], [email: Ingridb@inorg.su.se].

*Chemical Department, Moscow State University, Leninskie Gory, 119899, Moscow, Russia. [Fax: +97 95 9390171], [email: bip@mch.chem.msu.su].

Traditional X-ray powder diffraction methods give a quick average analysis of new synthesized bulk materials. One disadvantage is that impurities (<5%) and amorphous parts cannot be detected. The combination of X-ray diffraction and analytical transmission electron microscopy (TEM) is very powerful. It is possible to investigate the samples in detail with respect to:

monophasic or polyphasic nature;
quantitative element analysis of small particles (<50Å);
amorphous parts in the bulk sample;
superstructure of unit cell;
space group;
stacking faults or clusters;
reaction between crucible and mixture during synthesis.

As an example we present the results of structure analysis of the brownmillerite type compound $LaSrCuGaO_5$ (a=5.3515(1)Å, b=5.5205(1)Å and c=16.5216(4)Å) and phase analysis in the $La_{1-x}M_xSrCuGaO_{5-\delta}$ system (M=Sr, Ba, Na). The samples have been prepared by ordinary solid state synthesis followed by high pressure treatments. In some cases the mixtures were pretreated by means of freeze drying technique, which gave a different result. Using that technique it was possible to prepare compounds with a formal valence of the copper ions (determined by iodometric titrations) approximately 2.3.

All these compounds have so far been semiconductors but the samples with a copper valence >2 showed a more metallic resistance behaviour.

CP11

The Evidence for In-Plane Elastic Instability at T_c in Single-Crystalline $La_{1.86}Sr_{0.14}CuO_4$

Takashi Suzuki[1], M. Nohara, Y. Maeno and T. Fujita

Department of Physics, Hiroshima University,
Higashi-Hiroshima 724, Japan, [Fax: +81-824-24-0716]

I. Tanaka and H. Kojima

Institute of Inorganic Synthesis, Yamanashi University,
Kofu 400, Japan

From high-precision ultrasonic measurements in a 16T superconducting magnet on good quality $La_{1.86}Sr_{0.14}CuO_4$ (LSCO) single crystal, we found a remarkable anomaly of the in-plane elastic constant[2] $(C_{11}-C_{12})/2$ (hereafter C_T) around T_c (=36K), which is not directly related to the superconducting transition but indicates that there exists an elastic instability in the Cu-O plane below T_c.

Figure 1 shows the temperature dependence of C_T measured in magnetic fields up to 14T parallel to <001> direction with sound propagation vector k parallel to <110> and displacement u ($\perp$H) parallel to <1-10>. The elastic constant C_T at 0T, which is the responce function to shear strain e_{xx}-e_{yy} in the Cu-O plane, reveals substantial softening from about 45K. The softening increases strongly with increasing magnetic fields without shifting the maximum that occurs around 45K. The change in temperature at which C_T shows a minimum in each field almost coincided with the temperature dependence H_{c2} determined from magnetoresistance of this sample. Therefore these elastic softenings should originate in a lattice instability in the Cu-O plane in the normal conducting state of LSCO. The most plausible mechanism of the lattice instability is proposed to be a structural fluctuation from the orthorhombic (Bmab) phase at mid-temperature (OMT) to anther orthorhombic (Pccn) phase at low temperature (OLT), which has been reported by Crawford et al.[3] in their paper on $La_{1.88-x}Nd_xSr_{0.12}CuO_4$. The elastic stiffening after the softening is considered to arise from quenching of the lattice instability due to the appearance of the superconducting state in analogy with the A15-compond V_3Si. Additional stiffness of flux line lattice below the irreversibility temperature is very small in case of H$\perp$u$\perp$k and thus does not contribute to the stiffening very much.

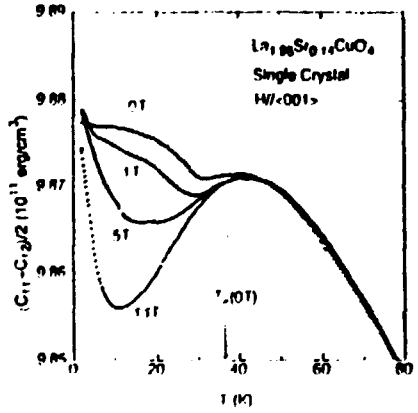

Figure 1

[1]Present address: Division of Physics, The Norwegian Institute of Technology, N-7034 Trondheim, Norway, [Fax: +47-7-593695], [E-mail: takashi@phys.unit.no].

[2]Here we use a crystalline coordinate in I4/mmm phase. It's worth noting that the $(C_{11}-C_{12})/2$ mode is purely shear mode both in I4/mmm and Bmab phases.

[3]M.K.Crawford, R.L.Harlow, E.M.McCarron, W.E.Farneth, J.D.Axe, H.Chou and Q.Huang, Phys. Rev. B44 (1991) 7749.

CP12
TOWARDS A HIGH Tc DC-SQUID MAGNETOMETER

J.W.M. Hilgenkamp, R.P.J. IJsselsteijn, A.J.H.M. Rijnders, W. Jaszczuk, P. van de Riet, J. Flokstra and H. Rogalla

University of Twente, Faculty of Applied Physics, P.O. Box 217, 7500 AE Enschede, The Netherlands.

Two key elements of a high Tc DC-SQUID magnetometer are the superconducting ring interrupted by two Josephson junctions (DC-SQUID) and a flux transformer consisting of a pick-up coil and a (multi-turn) input structure. In this contribution we report on results obtained in the fabrication of both elements.

The characteristics of $YBa_2Cu_3O_{7-d}/PrBa_2Cu_3O_{7-d}/YBa_2Cu_3O_{7-d}$ ramp type junctions and DC-SQUIDs based on these junctions produced in our group have been reported extensively lately.[1] Results obtained with Josephson junctions produced in the same way as the previously mentioned junctions, but without the thin $PrBa_2Cu_3O_{7-d}$ barrier layer, will be presented here. Since the critical current density of these junctions is dependent on the used etching procedure we believe that the barrier is formed by a thin amorphized $YBa_2Cu_3O_{7-d}$ layer rather than by a grain boundary. Voltage modulation as a function of the bias current of a DC-SQUID based on these junctions measured at 4.2K is shown in the figure. IV-characteristics, voltage modulation and noise properties as a function of temperature will be presented.

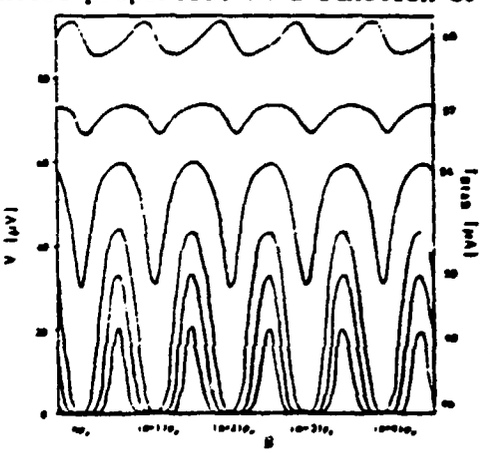

Using Ar-ion etching under an angle high quality cross-overs and via-contact have been fabricated.[2] These are the necessary ingredients for a multi-turn input coil. By combining two chips, one of them containing the DC-SQUID and the other containing the flux transformer, it is possible to form a high Tc DC-SQUID magnetometer. Results on this will be reported.

[1] J. Gao, *Preparation and characterization of high Tc superconducting thin films and devices.* PhD-thesis, University of Twente (1991).

[2] J. Flokstra, R.P.J. IJsselsteijn, J.W.M. Hilgenkamp, *Basic elements for photodeposited high Tc thin film devices.* Subm. to Thin Solid Film.

CP13

Trapping and Motion of Magnetic Flux in Y-Ba-Cu-O powders and ceramics

E. Lähderanta[a], L. Vlasenko[b], V. Fleisher[b], R. Laiho[a], E. Blinov[b]

[a]Wihuri Physical Laboratory, University of Turku, 20500 Turku, Finland
[Fax:+358-21-319836], [E-mail: ERLAH@kontu.cc.utu.fi]
[b]A. F. Ioffe Physico-Tecnical Institute, Academy of Sciences of the USSR, 195021 St. Petersburg, Russia

Remanent, low-field and high-field magnetization has been investigated in Y-Ba-Cu-O powders and ceramics. Measurement of the thermoremanent magnetization $M_R(T)$ reveal a threshold field H_{th} corresponding to trapping of a single flux quantum ϕ_o in a grain[1]: $H_{th} = (1.1 \pm 0.2)\phi_o/d^2$. The temperature dependence of the thermoremanent magnetization of powders cooled in weak fields turned out to be reversible[2] when the samples were heated up and cooled down again in the field H = 0. For d comparable with the London penetration depth λ the reversible part of $M_R(T)$ can be described by $\lambda(T)$ (Fig.1, broken line).

Values of $M_R(T)$ were measured for both powders and ceramics after cooling in strong magnetic field. When the density of vortices in the grains is high, $M_R(T)$ can be described by an exponential law based on a flux-creep model with an activation energy[3] $U_o \approx 7.5$ K or 0.65 meV (Fig. 2, solid line). By using the formula $S = kT/U_o = (dM_R/d\ln t)/M_R$ based on the Bean's critical state model we obtain values of U_o three orders of magnitude larger ($U_o \sim 1$ eV) for the same samples.

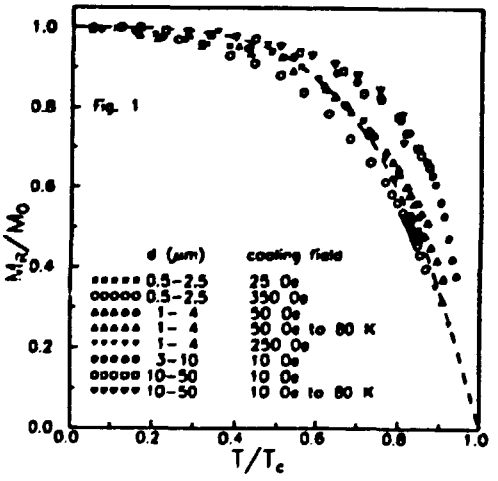

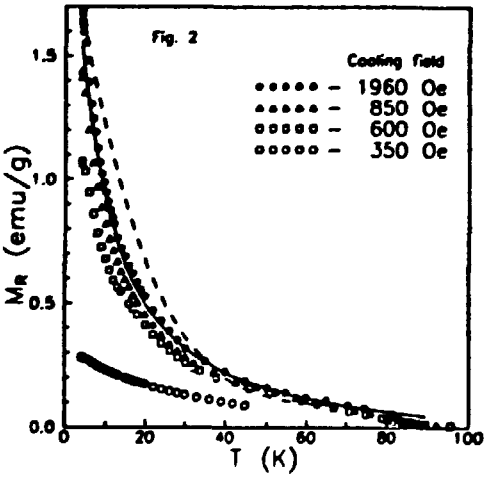

[1] V. Fleisher et al., Physica C 170, 161 (1990).
[2] E. Lähderanta et al., Physica C 190, 497 (1992).
[3] E. Lähderanta et al., Physica C (submitted).

CP14

Ca-Th SUBSTITUTION IN $YBa_2Cu_3O_{7-\delta}$: RAMAN SCATTERING AND CALCULATION OF THE ELECTRON-PHONON INTERACTION

L. BÖRJESSON, H.V. PHUONG., T. JARLBORG#, M. ANDERSSON*, AND Ö. RAPP*

Physics Dept, Chalmers Univ. Techn. S-412 96, Göteborg, Sweden, #Dépt. de Physique de la Matière Condensée, Univ. de Genève, 24 Quai Ernest Ansermet, CH-1211 Genève, Switzerland, and *Solid State Physics, The Royal Inst. Techn. S-10044 Stockholm, Sweden.

Ca and Th can be substituted for Y up to x≈0.1 in $Y_{1-2x}Ca_xTh_xBa_2Cu_3O_{7-\delta}$ in the orthorhombic phase.[1] This substitution is iso-electronic with small changes in lattice parameters and preserved oxygen concentration. Yet the superconducting T_c decreases by $dT_c/dx \approx -130$ K, which is a surprisingly large depression rate. We have investigated this substitution by neutron diffraction,[2] Raman scattering and calculations of the electron phonon interaction.

The atomic distance between chain Cu(1) and apex oxygen O(4) and the vibration frequency of the ≈ 500 cm^{-1} Raman mode associated with O(4), both increase slightly with Ca-Th substitution. Both these changes are unusual and opposite in sign to those usually observed in substitutions in 1:2:3 compounds depressing T_c. The electronic part of the electron phonon interaction η, shows a strong sensitivity to small changes in the Cu(1)-O(4) distance, as anticipated by previous observations.[3] A sizeable decrease of η is calculated for increased Cu(1)- O(4) distance. We thus find shifts both in a characteristic phonon frequency and in η in the directions consistent with the observed decrease of T_c.

1. M. Andersson, Z. Hegedüs, M. Nygren, and Ö. Rapp, Physica C160, 65 (1989).
2. M. Andersson, Ö. Rapp, and R. Tellgren, Solid State Commun. 81 (1991) (in press).
3. T. Jarlborg, Solid State Commun. 71, 669 (1989).

CP15

(Ca,Pr) SUBSTITUTIONS IN Y- AND Sm-BASED 1:2:3 SUPERCONDUCTORS

M.Andersson[1], Z.Hegedüs[2], T.Hörlin[2], M.Nygren[2], Ö.Rapp[1] and T.L.Wen[2]

[1] Department of Solid State Physics, The Royal Institute of Technology, S-100 44 Stockholm, Sweden

[2] Department of Inorganic Chemistry, Arrhenius Laboratory, Stockholm University S-106 91 Stockholm, Sweden

In contrast to other 1:2:3 compounds ($MBa_2Cu_3O_{7-\delta}$ with M = Y or a rare earth element except Tb or Ce), which are all superconductors with a superconducting $T_c \approx 90$ K, $PrBa_2Cu_3O_{7-\delta}$ is an anti-ferromagnetic semiconductor. Several interpretations of the T_c decrease with increasing Pr content in Pr doped 1:2:3 compounds have been discussed: i) if Pr is four-valent in these compounds, the excess electrons fill the crucial holes in the superconducting CuO_2 planes and destroy superconductivity, ii) the magnetic moment of the Pr ions may give rise to magnetic pair-breaking or iii) the Pr ions may localize the holes in the CuO_2 planes.

We have studied co-substitutions of (Ca,Pr) in the Y- and Sm-based 1:2:3 superconductors. If hole-filling or hole localization is important in the case of Pr substitutions, the two-valent Ca ions will add holes and compensate for this effect. For $Y_{1-2x}Ca_xPr_xBa_2Cu_3O_{7-\delta}$[1] and for $Sm_{1-2x}Ca_xPr_xBa_2Cu_3O_{7-\delta}$,[2] a co-solubility limit at $x \approx 0.25$ is observed, while for higher nominal compositions only Pr enters into the 1:2:3 structure. The oxygen deficiency δ is close to zero in all samples. Within the co-solubility limit, we observe a smaller decrease in T_c than for samples doped with Pr only, while outside this limit the T_c depression rate is comparable to the one of the Pr-doped samples, consistent with the interpretation that only Pr enters into the structure.

With increasing doping concentration, an almost linear decrease in T_c is observed for the (Ca,Pr)-doped samples in both of the series, with a larger T_c decrease for the (Ca,Pr)-doped Sm-1:2:3 samples. Such a linear relation may be indicative of a pair-breaking mechanism. Furthermore, the T_c decrease is larger for the $Sm_{1-x}Pr_xBa_2Cu_3O_{7-\delta}$ than for the $Y_{1-x}Pr_xBa_2Cu_3O_{7-\delta}$ system, in accordance with a recently discovered ion size effect of T_c in Pr-doped 1:2:3 materials.[3]

In addition, upper critical magnetic field data, $H_{c2}(T)$, of these samples will be presented.

---

1. M.Andersson, Ö.Rapp, Z.Hegedüs, T.L.Wen and M.Nygren, Physica C 190 (1992), 255

2. T.L.Wen, T.Hörlin, M.Nygren, M.Andersson and Ö.Rapp, Proc. of Int. Workshop in Chemistry and Technology of High-Temperature Superconductors, Moscow, 1991 (in press)

3. Y.Xu and W.Guan, Solid State Comm. 80 (1991), 105

CP16

Preparation of Textured Bi-based Superconducting Wires[1]

J. Sarkaniemi[a], T.Mäntylä[a] and L.Laakso[b]
[a]Institute of Materials Science, Tampere University of Technology
P.O.Box 589,SF-33101 Tampere, Finland, [Fax: +358 31 162330]

[b]Outokumpu Poricopper Oy, P.O.Box 60,SF-28101Pori, [Fax: +358-39-827314]

The processing-structure-properties relationships in superconducting Ag-sheated Bi-based conductor wires have been studied. The wires were prepared by the powder in silver tube method. The processing procedures were optimized to obtain highly textured microstructure in order to maximize the current density. The preparation procedures have been developed aiming either to 2212 structure or 2223 structure in the wire. The starting powder for 2212 phase was prepared by the conventional solid state reaction method and for 2223 phase by precipitation process. For further processing the starting powders were packed into silver tube.

The packed tubes were further processed by mechanical deformation combined with intermediate annealing treatments. In princible, two main approaches were used; the modification of the melt growth (MG) technique and the cold swaging and annealing method (SA). Starting from original diameter of silver tube of 6 mm the final dimensions of the wires after processing cycles were: thickess in the range of 0.5 - 0.2 mm and width 3-5 mm. The reduction in one swaging cycle was 10% for 2223 phase and 25-75% for 2212 phase structures. The MG-method gave the best textured microstructure for 2212 phase structure. The procedure included short annealing at 900 °C, slow cooling to 850 °C at which temperature they were annealed for 1-10 h, and the cooling to room temperature. The SA-method gave better alignment for 2223 grains than the MG-method. This procedure includes several cycles of cold swaging followed by immediate annealing at 850 °C. All heat treatments were done in air.

The MG-method yielded an oriented microstructure with parallel 2212 grains. High degree of orientation was confirmed by XRD. The superconducting properties of these wires were measured by AC susceptibility technique. The T_c temperature was 88 K. The critical current density was as high as 240 x 10^3 A/cm^2 at 4.2 K and in zero magnetic field. The SA-technique seems to be better for orientation of 2223 phase, although it is difficult to obtain uniform phase composition due to the thermodynamic instability of the phase structure. However, considerable increase in textured structures have been obtained as confirmed by XRD. The electrical measurements will be done in near future.

---

1. Work was supported by TEKES and Outokumpu Poricopper Oy

CP17

Anisotropy in the transport measurements of $YBa_2Cu_3O_7$ with Y_2BaCuO_5 inclusions in applied magnetic field.

P. Tuset, M.G. Karkut, L.K. Heill, K. Fossheim.

Division of Physics, The Norwegian Institute of Technology and SINTEF Applied Physics, N-7034 Trondheim, Norway, Fax: +47 7 593695, E-mail: tuset@phys.unit.no

We will present ρ(T) and I-V data as a function of applied magnetic field and crystalline orientation on thin film $YBa_2Cu_3O_7$ and on bulk, melt-processed-melt-grown $YBa_2Cu_3O_7$ with Y_2BaCuO_5 inclusions (MPMG). The later material has larger pinning force then single crystal $YBa_2Cu_3O_7$, and our group has performed an extensive study of the flux dynamics and irreversibility of MPMG by using ac magnetic permeability[1].

Our resistive measurements should complement the ac measurements on MPMG, and enhance our understanding of the improved pinning due to the Y_2BaCuO_5 inclusions in the material. We have developed a measuring probe which can continously vary the angle between the crystalline axis and the applied magnetic field, with a resolution of about 0.004 degrees. This will permit us to study in detail the reduced anisotropy as seen in the ac measurements, of this technologically promising material.

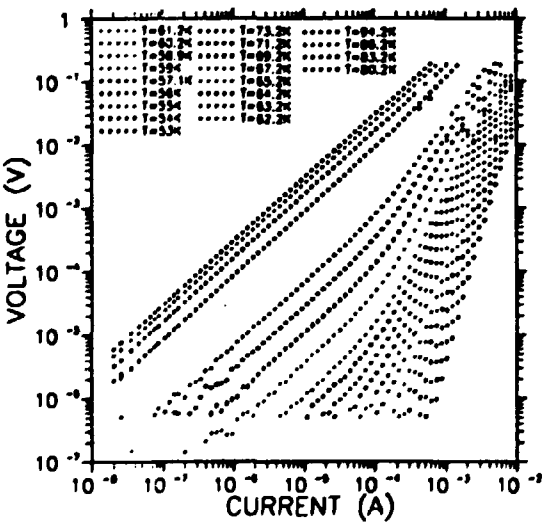

The figure shows I-V curves for a patterned $YBa_2Cu_3O_7$ thin film. As one goes from the lower right corner towards the upper left corner the temperature increases. The I-V curves shows non-linear behaviour for low temperatures and high currents. When the temperature increases one sees a crossover to linear I-V curves. This set of I-V curves can be interpreted in the vortex glass to vortex liquid picture also used to interpret the ac magnetic permeability measurements mentioned above.

[1]K. Fossheim, M.G. Karkut, L.K. Heill, M. Slaski, L.T. Sagdahl, V.M. Vinokur, M. Murakami, H. Fujimoto, N.Koshizuka, S. Tanaka, F. Gencer, J.S. Abell, C.E. Gough, to appear in Physica Scripta, and contributions to this symposium.

CP18

AC permeability as a probe of vortex glass- to -liquid transition in $YBa_2Cu_3O_7$ with Y_2BaCuO_5 inclusions

Ellen D. Tuset, L.K. Heill, L.T. Sagdahl, M.G. Karkut and K. Fossheim
Division of Physics, The Norwegian Institute of Technology and *SINTEF Applied Physics*,
N-7034 Trondheim, Norway, Fax: 47-7-593695, E-mail: ellen@phys.unit.no

We present a study[1] of the ac magnetic permeability $\mu = \mu' + i\mu''$ in two samples: a single crystal of $YBa_2Cu_3O_7$ (*SC*) and a single crystal of $YBa_2Cu_3O_7$ with Y_2BaCuO_5 (Y211) inclusions. We refer to the latter as the MPMG sample after the process used in growing it (melt-powder-melt-growth). Using a home made susceptometer and an 8 Tesla superconducting magnet, the ac response of the two samples is mapped out as a function of temperature, frequency, ac field amplitude, dc applied field and field orientation.

The flux dynamics near the irreversibility line can be probed by investigating the width and position of the loss peak in μ''. We interpret our results by comparing them with expectations for a vortex glass- to -liquid transition. In this picture one would expect the loss peak temperature to depend strongly on H_{ac} and weakly on frequency well below the melting line. This is precisely what we observe when the magnetic field is parallel to the CuO_2 planes. Above the melting line, there should be no H_{ac} dependence but strong frequency dependence. Our results with the field along the c-axis show weak, but still finite H_{ac} dependence together with strong frequency dependence. In other words: within our range of parameters so far, the loss peak seems to occur below the melting line in both configurations. However, in the H⊥c case we are in the strongly non-linear regime, while we are closer to the melting line in the less non-linear regime for H∥c. In our presentation we will describe further attempts to move the loss peak line across the melting line by expanding the range of frequencies and ac-fields. In figure 1 we present the loss peak lines $H^*(T)$ for our two samples in the two different field configurations as determined from the peaks in μ''. Using a low H_{ac} amplitude as here (10^{-4}T) the loss peak line reflects the melting line to a good approximation. Notice the strong anisotropy. The H⊥c lines lie at considerably higher T and H values than the H∥c lines indicating a more stable vortex structure. However, comparing the MPMG results with the single crystal behaviour we observe reduced anisotropy of $H^*(T)$ in the MPMG sample. This indicates increased stability of the vortex structure in the H∥c configuration, presumably caused by the non superconducting Y211 inclusions in MPMG.

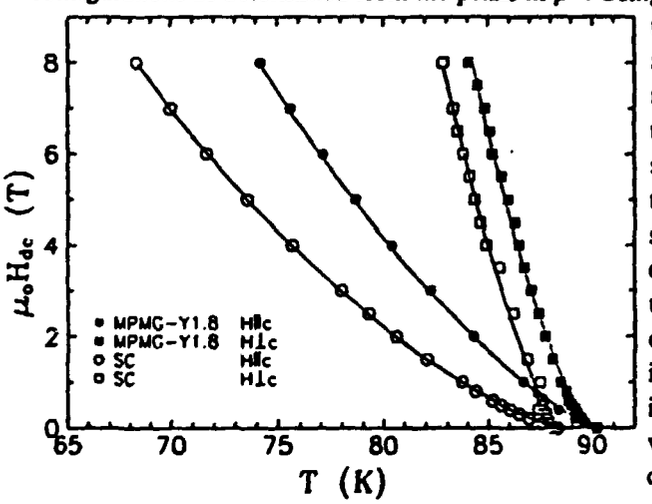

Figure 1. Loss peak μ'' as a function of H_{dc} and T. $H_{ac}=10^{-4}$T and frequency=121Hz

[1] K.Fossheim, M.G.Karkut, L.K.Heill, M.Slaski, L.T.Sagdahl, V.M.Vinokur, M.Murakami, H.Fujimoto, N.Koshizuka, S.Tanaka, F.Gencer J.S.Abell and C.E.Gough. Invited paper at the Nobel Jubilee Symposium, Gothenburg, Sweden, December 4-7, 1991, Low dimensional properties of solids. To appear in Physica Scripta.

CP19

Interfacial structure of Ag contacts to a- and c-axis oriented thin films of $YBa_2Cu_3O_{7-\delta}$

Z.H. Gong, R. Fagerberg, F. Vassenden, J.K. Grepstad and R. Hoier[1]

Institute of Physical Electronics, University of Trondheim - NTH and
SINTEF DELAB, N-7034 Trondheim, Norway

[1]Institute of Physics, University of Trondheim - NTH and
SINTEF, Division of Applied Physics, N-7034 Trondheim, Norway

Proximity coupled SNS (superconductor/normal metal/superconductor) junctions are considered as one alternative to SIS (superconductor/insulator/superconductor) junctions in high-T_c Josephson devices[1]. Strong electronic anisotropy has been observed in SNS junctions fabricated from $YBa_2Cu_3O_{7-\delta}$ (YBCO) thin films of different growth directions and a low-T_c superconducting counter-electrode. A supercurrent was found only for junctions prepared with the CuO_2 planes perpendicular to the YBCO/metal interface[2], i.e. a-axis oriented films.

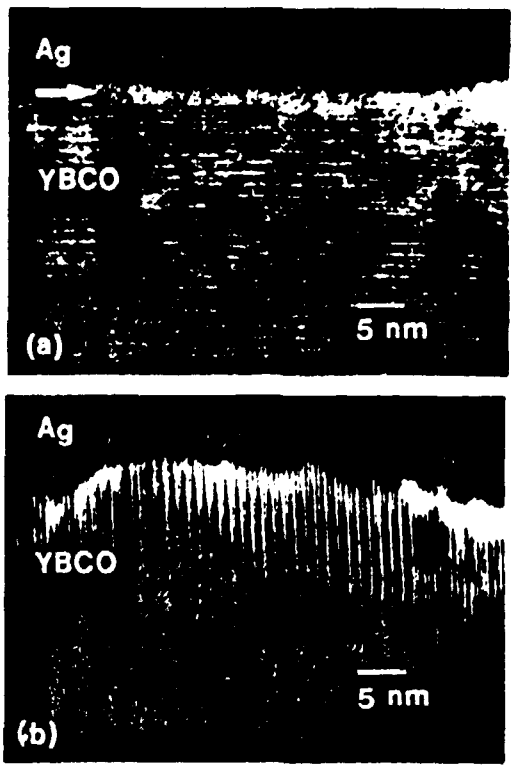

Figure 1: Cross-section TEM images of the YBCO(001)/Ag (a) and the YBCO(100)/Ag interfaces (b)

In the present study, the interface atomic structure of *in situ* sputter deposited Ag contacts to a- and c-axis oriented thin films of YBCO was examined with cross-section transmission electron microscopy (TEM). A structurally disordered interface layer, ~25 Å thick, was found for Ag contacts to c-axis films, see Fig.1a. The layer is taken to be non-superconducting, and will thus strongly suppress proximity effects at this interface, which is attributed to reactions with residual impurity gases during YBCO film deposition and subsequent oxygen loading. Interface reactions between Ag and YBCO appear to be negligible, when silver is deposited at room temperature.

In contrast to this data, cross-section TEM images of Ag contacts to a-axis films, Fig.1b, unveil a clean interface with intimate contact between cuprate and silver. The absence of a disordered interface zone suggests that the YBCO(100) surface is less reactive to gaseous impurities in the sputter chamber. This finding may have important bearing on fabrication of proximity coupled SNS Josephson devices.

[1]J. Talvacchio, IEEE Trans.Comp.Hybrids Manuf.Technol. 12, 21 (1989)
[2]M. Lee, D. Lew, C.B. Eom, T.H. Geballe, and M.R. Beasley, Appl.Phys.Lett. 57, 1152 (1990)

CP20

Negative magnetoresistance in $YBa_2Cu_3O_{7-\delta}$ thin films

[a] W. Holm, [a] M. Andersson, [a] Ö. Rapp, [b] Z. G. Ivanov and [b] T. Claeson

[a] Department of Solid State Physics, The Royal Institute of Technology, S-100 44 Stockholm, Sweden

[b] Physics Department, Chalmers Institute of Technology, S-412 96 Göteborg, Sweden

Abstract

The magnetoresistance of thin c-axis oriented $YBa_2Cu_3O_{7-\delta}$ films has been measured. The magnetic field was perpendicular to the basal plane and the current in these measurements. In one sample the magnetoresistance consisted of the expected positive contribution, and in addition a negative contribution. The negative contribution was found to be dominant over all other contributions at temperatures from 120 up to 300 K and in magnetic fields up to 12 T. It was well described by an expression linear in both temperature and magnetic field. After compensating the low temperature data for this effect the remaining magnetoresistance was strictly positive. This is suggested to originate from superconducting fluctuations. Such fluctuations are described by the Aronov-Hikami-Larkin theory. A fit to the data was made and the following values were obtained: $\xi_{ab} = 13.3$ Å, $\xi_c = 2.0$ Å, $\tau_\phi = 2 \cdot 10^{-14}$ s. It is suggested that the negative effect might originate from a magnetic impurity of very low concentration since the superconducting transition indicates a sample of high quality.

CP21

Measurements of the upper critical magnetic field in superconducting disordered metals.

Anders Nordström and Östen Rapp

Department of Solid State Physics, The Royal Institute of Technology, S-100 44 Stockholm, Sweden

Ulf Dahlborg

Department of Neutron and Reactor Physics, The Royal Institute of Technology, S-100 44 Stockholm, Sweden

An overwiev is given of the usefulness of upper critical field measurements of amorphous superconductors and the application of such measurements in different problems studied by us in recent years. By studying amorphous metals with superconducting transition temperatures of a few K, one gains the important advantage that the full critical field curve can be studied in a dilution refrigerator with magnetic fields of a few Teslas.

Four projects are briefly described

(i) By fitting the Werthamer-Helfand-Hohenberg (WHH) theory to critical field data in a series of $Zr_{1-x}Cu_x$ samples we derived the density of states at the Fermi level, $N(E_F)$, and the spin-orbit relaxation time τ_{so}.

(ii) We have studied H_{C2} in two $Zr_{50}Cu_{50}$ samples doped with such an amount of magnetic impurities that T_C was depressed to about 50 % of the undoped value. From a comparison with critical field data in pure samples the temperature dependence of the magnetic impurity pair breaking parameter could be investigated.

(iii) Deviations from WHH theory have been strongly debated. Two examples from our measurements are $Hf_{67}Co_{33}$ and $Hf_{67}Ni_{33}$ where physically reasonable parameters in the fits of WHH theory could not be obtained. Such deviations have been attributed to both inhomogeneities and weak localization effects.

(iv) Weak localization and interaction effects are expected in the critical magnetic field even at the level where the critical field curve is inseparable from the WHH theory. Our critical field data for the density of states in $Zr_{1-x}Cu_x$ confirm a small enhancement of about 5-10 % as compared to data from specific heat measurements. This problem is further studied by investigating how increased disorder from high energy neutron irradiation influences the upper critical field.

CP22

d-wave pairing in tetragonal superconductors

Fabian Wenger and Stellan Östlund
Department of Theoretical Physics, Chalmers Institute of Technology,
41296 Gothenburg, Sweden
Fax: 46/31/72 32 04 , E-mail: tfyfw@fy.chalmers.se

Using group theoretical methods, we classify into 11 symmetry classes all translationally invariant singlet paired superconducting gap functions whose quasiparticle energy spectrum preserves the symmetry of a tetragonal crystal.

We show that for the gap function of symmetry $\Delta^{d^2}(\cos k_x - \cos k_y)$ *two peaks* generically occur in the density of states $n(E)$ as a function of energy. The peaks are associated with topological changes of the lines of constant quasiparticle energy and the peak at lower energy can be associated with the gap Δ^{d^2} . In the strictly two-dimensional case we get logarithmic singularities and at low energies we see the usual linear dependence of the density of states.

Removing the node in this gap function by adding an imaginary component of symmetry $\Delta^{d^{2'}} \sin k_x \sin k_y$ results in the *only* possible nodeless gap function that does not involve s-wave pairing. We compare our results with tunneling studies on $Bi_2Sr_2CaCu_2O_8$ which seems to show similar behaviour.

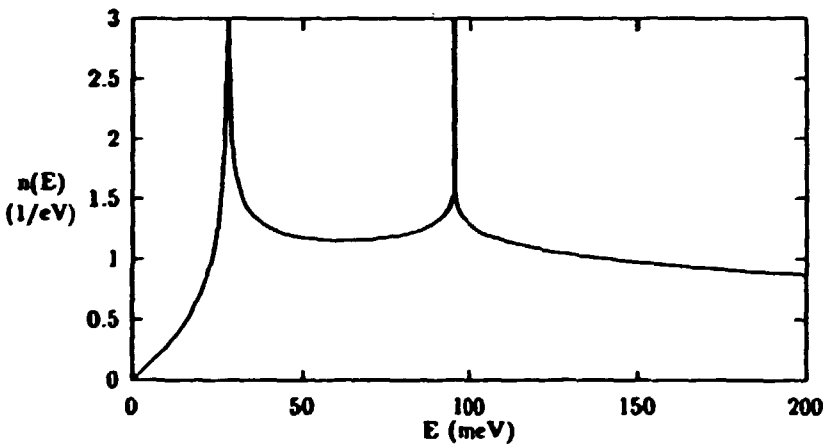

Figure 0.1: generic density of states for d-wave pairing

CP23

MAGNETIC FLUX DISTRIBUTION AND MAGNETIC RELAXATION IN POLYCRYSTALLINE Bi,Pb-Sr-Ca-Cu-O SUPERCONDUCTORS [1]

J. Paasi, M. Polák [a)], M. Lahtinen, V. Plecháček [b)], and L. Söderlund

Tampere University of Technology, Lab. of Electricity and Magnetism
P.O. Box 692, SF-33101 Tampere, Finland [Fax: 358 31 162 160]

a) Institute of Electrical Engineering, Slovak Academy of Sciences,
CS-842 39 Bratislava, Czecho-Slovakia [Fax: 42 7 375 816]

b) Permanent address: Institute of Physics, Czechoslovak Academy of Sciences,
CS-162 00 Prague 6, Czecho-Slovakia [Fax: 42 2 312 3184]

We have studied magnetic flux distribution and magnetic relaxation in polycrystalline $(Bi,Pb)_2Sr_2Ca_2Cu_3O_{10+x}$ superconductors at 77 K using a miniature Hall sensor (size 50 μm x 100 μm). The Hall sensor was placed in a small air gap between two identical cylindrical superconductors. By moving the Hall sensor the magnetic field profile in the air gap due to screening currents was measured.

The reasons to study the magnetic field profiles in the air gap are:
1. The validity of assumptions of homogeneity and constant J_c of the specimens can be tested by comparing the measured profiles to calculated ones.
2. The effects of inter- and intragranular screening currents on flux distribution can be seen and distinguished.
3. The J_c of the specimens can be calculated from the profile.
4. To see the effect of magnetic relaxation on flux distribution.

The measured relaxed and nonrelaxed magnetic field profiles are presented and discussed taking into account the results of the calculations.[2]

---

[1] Work supported by Finnish Development Pool for Electric Power Technology.

[2] J. Paasi, M. Polák, M. Lahtinen, V. Plecháček, and L. Söderlund, in *Critical Currents in High Tc Superconductors*, Vienna, Austria, 22-24 April 1992.

CP24

Superfluidity in the negative-U Hubbard model.

Mats Nylén

Department of Theoretical Physics, University of Umeå, S-901 87 Umeå, Sweden,
[Fax: +46 90 166673], [E-mail: nylen@tp.umu.se]

The density of superconducting particles in the two-dimensional negative-U Hubbard model is calculated using a Quantum Monte-Carlo method. Away from half-filling the model undergoes a Kosterlitz-Thouless phase transition to a superconducting state at low temperature. The calculated behaviour of the density of the superconducting particles at the phase transition is in agreement with the universal jump prediction.

CP25

Fabrication of Superconducting Bi(Pb)-Sr-(Ca,Y)-Cu-O Thick Films by Melt Quenching Method

G.Grigėnaitė, B.Vengalis, V.Jasutis

Lab.of HTC Supercond., Semiconductor Physics Institute, Goštauto 11, Vilnius, 2600, Lithuania, [Fax: +7-0122-627123],
[E-mail: ulbikas%ib.pfi.lt@gateway.uninett.no]

We report the results on preparation of thick oriented Bi(Pb)-Sr-(Ca,Y)-Cu-O films having both 2212 and 2223 crystal structures with zero resistance temperatures of 85 K and 105 K, respectively.

The corresponding composition precursor powder coatings were screen printed on MgO (100) substrates.Subsequently they were melted in air at (950-1050)^{o}C, quenched to room temperature and annealed at (820-860)^{o}C. The as prepared films were characterised by X-Ray diffraction, X-Ray microanalysis and electron microscopy. Resistance and critical current measurements have been performed.

We succeeded in obtaining films with dominating 2223 structure when Bi was partially substituted by Pb. It was determined that both fast cooling from the annealing temperatures and Ca substitution by Y (up to 5%) increase T_c of the 2212 composition films.

Attempts were undertaken to reduce the film composition changes due to evaporation of volatile Bi oxides during heat treatment at melting and annealing temperatures. Additionally it was found that all the precursor materials used by us showed incongruent melting and phase separation in their liquid states. In order to improve film homogeneity and to avoid formation of impurity phases such as $(Ca,Sr)_2CuO_3$ and the 2201-phase, two different possibilities have been proved. According to X-Ray investigations an increase of the heat treatment temperature up to 1000-1050^{o}C and decrease of the melting process time down to 1 min or less promoted synthesis of single phase superconducting material.

Secondly, combinated method using chemical reaction between previously formed Ca_2CuO_3 buffer layer and the melt containing Bi and Sr oxides only was found to be rather successful.

CP26

Hydrogen Induced Oxygen Nonstoichiometry of the Y_2BaCuO_5

A.Jukna, B.Vengalis, A.Vailionis, V.Lisauskas, V.Jasutis

Lab. of HTC Supercond. Semiconductor Physics Institute, Goštauto 11, 2600 Vilnius, Lithuania, [Fax: +7-0122-627123],
[E-mail:ulbikas%ib.pfi.lt@{ -way.uninett.no]

The dielectric compound Y_2BaCuO_5 usually known as the "green phase" is more stable than that of $YBa_2Cu_3O_7$. The relative stability of the material is caused by the crystal structure containing just one type of Cu sites fivefold coordinated by oxygen atoms. Recently the compound was shown to be a good substrate (buffer or interlayer) for $YBa_2Cu_3O_7$ thin film growth due to formation of thermodynamically stable interphase boundary.

Up to now it was assumed that oxygen content in Y_2BaCuO_5 is almost fixed. In this work we report new XRD and optical transmittance data both indicating oxygen nonstoichiometry of the "green phase". We argue that oxygen content in Y_2BaCuO_5 can be reduced and controlled in a predictable way by heat treatment at 200-300°C in hydrogen atmosphere.

Both thin films and bulk ceramic samples have been used for investigations. The Y_2BaCuO_5 films were RF sputtered on MgO (100) substrates from the targets of the same composition and subsequently postannealed in O_2 atmosphere at 950°C. The XRD results showed single phase state and orthorhombic lattice (a=12.15 Å, b=7.12 Å, c=5.64 Å). It is worth noting that after additional anneal at 300°C in H_2 atmosphere the a, b and c values increased up to 12.17 Å, 7.14 Å and 5.65 Å, respectively. Similar lattice expansion have been obtained for H_2 annealed Y_2BaCuO_5 ceramic samples. The changes of XRD line positions were found to be reversible if subsequent annealing in air at 400°C was undertaken. However, when annealing temperature in H_2 exceeded 350°C the Y_2BaCuO_5 phase splitting have been indicated from XRD.

In addition very interesting changes in optical transmittance spectra were observed for the Y_2BaCuO_5 thin films with induced oxygen deficiency. We point out increased absorption in the visible region, slight shift to higher energies of the characteristic 1.8 eV absorption band and appearance of the new absorption band in the near infrared region at 0.9 eV. The low energy absorption band is supposed to be related to the fourfold Cu coordination by oxygen. Then it can be attributed to the d-d electron transitions between crystal field splitted d-levels of copper ions.

CP27

The MBE Grown BiSrCaCuO Thin Films for the S-N Electrical Switches

B.Vengalis*, A.Flodström+, A.Brazdeikis+, S.Balevičius*

*Lab. of HTC Supercond., Semiconductor Physics Institute, Goštauto 11, 2600 Vilnius, Lithuania, [Fax: +7-0122-627123]

+Materials Science, Royal Institute of Technology, S-10044 Stockholm, Sweden, [Fax: 46-8-249131], [E-mail: audrius@theophys.kth.se]

Highly oriented thin BiSrCaCuO films with dominating 2212 crystal structure have been grown on MgO (100) substrates by Molecular Beam Epitaxy and subsequent postannealing of the evaporated Bi, Sr, Ca and Cu metal alloy films in air atmosphere. The best superconducting properties, surface morphology and crystal structure of the as prepared films were obtained after annealing at 820°C for 1.0 h. Fast cooling (≈52°C/min) from the annealing temperature was found to increase films T_c up to 94 K[1]. The film compositions yielding the highest T_c values (T_c>90 K) had higher Bi and Cu contents compared to the nominal 2212.

The microstrips (0.5<l<3.0 mm, 0.1<w<0.01 mm) have been prepared by conventional photolithography technique and chemical etching in phosphoric acid water solution. Switching dynamics for the microstrips from superconducting to normal state (S-N) under the influence of high voltage (1000 V) nanosecond single electrical pulses were investigated. Resistance versus current dependencies for different samples and different measuring temperatures were examined. We had found that very fast electronic S-N switching mechanism (τ<0.1 ns) dominated up to current densities ≈10^7A/cm^2. A slow thermal switching component was clearly seen only for the highest current densities before nonreversible destruction of the samples appeared.

---

[1]B.Vengalis, A.Flodström, A.Brazdeikis, Physica C, 1992, (in press).

CP28
CELL TRIPLED STRUCTURE IN THE PHASE DIAGRAM OF $YBa_2Cu_3O_{6+x}$

Vladimir E. Zubkus[#], Saulius Lapinskas[&] and Evaldas E.Tornau[*1]

[#] Institute of Chemical Physics, Russian Academy of Sciences, Kosygina 4, 117977 Moscow, Russia

[&] Department of Physics, Vilnius University, Sauletekio 9, 2054 Vilnius, Lithuania

[*] Department of Theoretical Physics, Royal Institute of Technology S-100 44 Stockholm, Sweden [Fax: 46 8 104876]

Recently it was shown[2] that the orthorhombic phase O_{III} with reduced wave vector (1/3,0,0) occurs on the phase diagram of $YBa_2Cu_3O_{6+x}$ when the repulsive interaction of the next-nearest oxygen chains is taken into account in Wille et al model[3] of oxygen atoms interaction in the basal CuO plane. However the obtained phase diagram displayed the peculiarity of O_I phase intruding between the phase regions of the O_{II} and O_{III} phases down to zero temperatures and x>0.5 . The peculiarity was caused by the degeneracy of ground states in the chosen 2D ANNNI model in a field. A simple model considering weak long-range attractive interaction of deformative nature as an addition to our previous model[2] allows to remove the degeneracy. The new interaction is taken into account by molecular field approximation. The phase diagram (see fig.) is found to be similar to that obtained by the 3D model[4]. However we avoid the inclusion of inter-planar interaction. The number of independent parameters of cluster method in our model is less almost by an order than that of the 3D case.

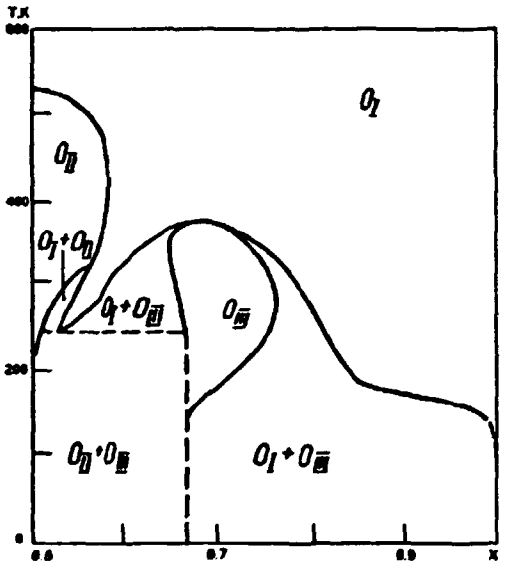

[1] On leave from Institute of Semiconductor Physics, Goštauto 11, 2600 Vilnius, Lithuania [Fax: 7 0122 627123]

[2] V. E. Zubkus, S. Lapinskas, E. E. Tornau, Physica C 166, 427 (1990).

[3] L. T. Wille, A. Berera, D. de Fontaine, Phys. Rev. Lett. 60, 1065 (1988).

[4] G. Ceder, M. Asta, D. de Fontaine, Physica C 177, 106 (1991).

CP29
OXYGEN ORDERING AND SUPERCONDUCTING TEMPERATURE OF $YBa_2Cu_3O_{6+x}$

Saulius Lapinskas[#] and Evaldas E. Tornau[&1]

[#] Department of Physics, Vilnius University, Saulėtekio 9, 2054 Vilnius, Lithuania
[&] Department of Theoretical Physics, Royal Institute of Technology S-100 44 Stockholm, Sweden
[Fax: 46 8 104876]

Determination of the relation between the oxygen ordering in the basal CuO planes and superconducting temperature T_c is performed assuming that the superconductivity in the CuO_2 planes of nonstoichiometric $YBa_2Cu_3O_{6+x}$ appears locally just in the regions located above sufficient amount of O-Cu-O chains. The compound is macroscopically superconducting when such regions form a percolating network which is characterized by the minimal width of a percolation path d, corresponding to the number of neighboring chains in the narrowest place of the network. As x decreases so does the d. Microregions of the CuO_2 plane located above ordered microregions of the CuO plane are supposed to be superconducting when d exceeds the correlation length ξ of the superconducting carriers. For small d the $T_c(d)$ of nonstoichiometric compound is lower than that of stoichiometric. The dependence $T_c(d)$ is obtained from the condition $d = \xi$ and ξ depends on T in accordance with Ginzburg-Landau theory. The calculation of d values is performed by the modified cluster field method[2] in 2D ANNNI model with the interaction constants taken from the first principles total energy calculations. Our results shown by solid line in fig. are in a close agreement with experiments[3] and Monte Carlo results[4].

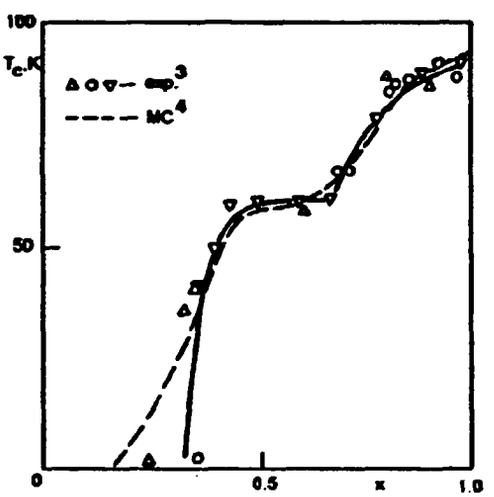

[1] On leave from Institute of Semiconductors Physics, Goštauto 11, 2600 Vilnius, Lithuania [Fax: 7 0122 627123].
[2] V. E. Zubkus, S. Lapinskas, E. E. Tornau, Physica C 159, 501 (1989); 166, 427 (1990).
[3] R. J. Cava B. Battlogg, K. M. Rabe, E. A. Rietman, P. K. Gallagher, L. W. Rupp, Physica C 156, 523 (1988); 165, 419 (1990).
[4] H. F. Poulsen, N. H. Andersen, J. V. Andersen, H. Bohr, O. G. Mouritsen, Letters to Nature 349, 594, (1991).

CP30

Thermal Diffusivity and Thermal Conductivity of $YBa_2Cu_3O_{7-\delta}$ and $YBa_2Cu_4O_8$ between 20 and 300 K

Britt M. Andersson and Bertil Sundqvist

Department of Experimental Physics, Umeå University, S-90187 Umeå, Sweden
Fax: +46 90 16 66 73

The thermal conductivities of dense ceramic samples of $YBa_2Cu_3O_{7-\delta}$ and $YBa_2Cu_4O_8$ have been measured in the range 20 to 300 K. The materials studied were produced at Luleå Technical University, Sweden, by either sintering pure commercial $YBa_2Cu_3O_{7-\delta}$ powder or hot pressing the same material together with a stoichiometric amount of CuO powder to produce $YBa_2Cu_4O_8$.

In order to obtain the best possible accuracy two different methods were used. Between approximately 60 K and 300 K we have calculated the thermal conductivity $\lambda = a(dc_p)^{-1}$ from measured data for the thermal diffusivity a and the density d, and from literature data for the specific heat capacity c_p of the material. a was measured by the classical periodic Ångström method, which gives very accurate values even when heat losses from the specimen are large. Below 100 K the accuracy of the diffusivity measurements was limited by the necessity to use a very low heater power. In this range λ was measured directly, using a linear steady state heat flow method. In the range of overlap, the data obtained by the two methods agreed to within the combined experimental errors.

In spite of the similarity between the structures of the two materials, there were surprisingly large differences between the measured thermal conductivities. For $YBa_2Cu_3O_{7-\delta}$, the thermal conductivity in the normal state was found to be practically independent of T above the critical temperature T_c, with a rapid increase below this, in excellent agreement with literature data. For $YBa_2Cu_4O_8$, on the other hand, the thermal conductivity decreases almost linearly with increasing T above T_c, with only a small additional increase below T_c. The room temperature value of λ for our ceramic polycrystalline sample of $YBa_2Cu_4O_8$ is 5 $Wm^{-1}K^{-1}$, very similar to the in-plane value for single crystal $YBa_2Cu_3O_{7-\delta}$.

Analyzing the results for $YBa_2Cu_4O_8$ in terms of standard models we find that the thermal conductivity in the normal state is almost completely dominated by phonon heat transport limited by phonon-phonon interactions, just like in any "normal" ceramic or dielectric material. This is very different from the behaviour of $YBa_2Cu_3O_{7-\delta}$, or indeed all other high T_c superconductors, for which the thermal conductivity is assumed to be limited by electron-phonon interactions or point defect scattering.

CP31

A.C. Susceptibility and X-Ray Diffraction: Two Compatible Methods in Monitoring the Volume Fraction of High T_c Superconducting Phases in Powder Samples.

G. K.Nicolaides, M. Pissas, V. Psycharis and D. Niarchos.

Institute of Materials Science, N.C.S.R. "Demokritos"
153 10 Ag. Paraskevi, Attiki, Greece,[Fax:+30-1-6519430].

The transformation of the $Bi_2Sr_2Ca_1Cu_2O_y$ (2212) phase to the $Bi_2Sr_2Ca_2Cu_3O_y$ (2223) phase at a constant reaction temperature of 850 ^oC in air for 73 days using as a nominal initial composition the $Bi_{1.7}Pb_{0.3}Sr_2Ca_2Cu_3O_y$, has been studied qualitatively and quantitatively by means of X-ray diffraction (Rietveld analysis) and ac-susceptibility techniques. The quantitative analysis of the X-ray powder diffraction patterns revealed the coexistence of the (2212), (2223) and $Ca_{2-z}Sr_zCuO_3$ phases through out the reaction. It is found that the percentage of the (2223) phase increases in accordance with the relation $w=w_0(1-e^{-kt})$ and reaches an upper level of 80 wt % of the final sample. This in fact, is in very good agreement with the results obtained from the ac-susceptibility studies on the same samples. A repetition of the experiment at a higher temperature (i.e. 865^oC) showed that the reaction kinetics improved, while the $Bi_2Sr_2CuO_y$ (2201) phase is found to be present in addition to the above phases. We have found that the quantitative analysis performed using the Rietveld method and the ac-susceptibility technique has given results in very good mutual agreement and therefore both methods are excellent in studying such phase transformations and usefulll to the preparation of these superconducting materials.

CP32

COMPATIBILITY OF $BaZrO_3$ AND PARTIALLY MELTED YBCO

Xiandong Wang and John Engell

Institute of Mineral Industry, Technical University of Denmark, DK-2800 Lyngby, Denmark. [Fax 4545934886]

The partially melting routes used for texturing YBCO superconductor materials can be classified into two groups according to the top temperature used. The high temperature routes (Y_2O_3+melt) involves heating to ca. 1400°C, whereas the low temperature routes (Y_2BaCuO_5+melt) involves heating to ca. 1050°C. In both cases the melts formed are highly corrosive, and react seriously with all common crucible materials. Finding an appropriate crucible material is therefore of considerable importance.

Here the interaction between partially melted YBCO and dense $BaZrO_3$ crucibles has been studied in the temperature range 1000°-1480°C using XRD and SEM/EDAX. No obvious reaction were observed after 5 min. at 1400°C, the interface between the melt and $BaZrO_3$ is sharp and well defined (Fig. 1). After heating to 1100°C for 2 h, recrystallization occurs in a 20-50 μ thick layer, but no new phases were detected. Thus, $BaZrO_3$ appears to be superior to YSZ, Al_2O_3 and Pt as crucible material for the present purpose.

The growth behaviour of Y_2BaCuO_5 and Y_2O_3 crystallites formed by partial melting of $YBa_2Cu_3O_x$ has also been studied. After 2 h at 1100°C the Y_2BaCuO_5 formed had grown to irregular shaped grains 5-30 μ in diameter. Whereas 3 min. at 1480°C results in equidimensional crystals of Y_2O_3 5-8 μ in diameter (Fig. 2).

It is concluded that it is possible to use $BaZrO_3$ as container material for manufacturing of YBCO superconductor or as a sieve to isolate 123 crystals from an YBCO-flux.

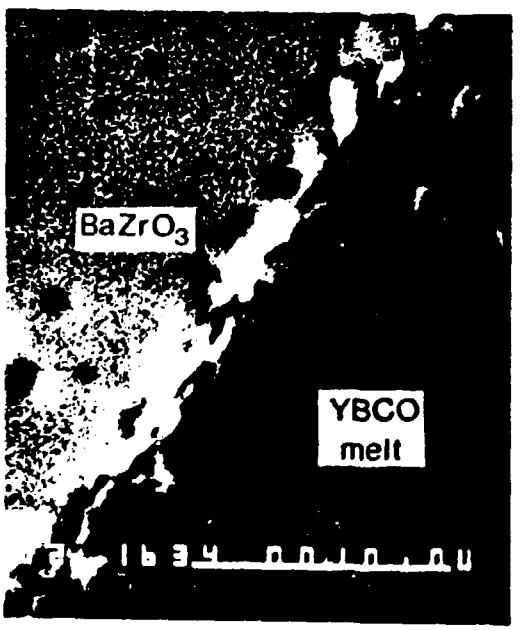

Fig. 1. $BaZrO_3$/123 interface 1400°C/5 min quenched in liquid N_2.

Fig. 2. Partially melted 123 phase quenched in air after 3 min. at 1480°C.

CP33

Microwave Absorption and Luminescence of Defects in $Ba_{1-x}K_xBiO_3$-type Superconductors

E. Feldbach and T. Kärner

Institute of Physics, Estonian Acad. Sci., 142 Riia St., 202400 Tartu, Replublic of Estonia, Fax: SU(01434)72227, E-mail:EEDU@IOP. TARTU.EW.SU

We have found earlier that the subthreshold irradiation of Y- and Bi-type Cu-containing high-T_c superconductors leads to Frenkel-type defects formation [1]. This process is well-known in wide-band-gap ionic crystals as non radiative decay of electronic excitations with creation of defects [2]. The efficiency of this mechanism may be low and needs sensitive methods as luminescence and microwave absorption. The investigation of Cu-free compound enable us to study the creation of defects mainly in oxygen sublattice.

Fig. 1. shows the changes in microwave absorption (a) and captured flux (b), which is determined by the nature and quantity of pinning centers, before (1) and after (2) the X-irradiation.It can be assumed that oxygen vacancies and interstitials have been created. The concentration of oxygen vacancie- of the order of $10^{13} - 10^{14}$ cm^{-3} may be enough to explain the pinning related effects [3]. Luminescence spectra at Fig. 2 (irradiation by 6 keV electrons) support this result. Increased band (2.85 eV) can be originated from O_2 molecules [4] created e.g. by non radiative decay of oxygen excited states ($2s2p \Rightarrow 2s^2$), which have enough energy (15-20 eV) to kick oxygen out of its lattice site with further associating into molecules.

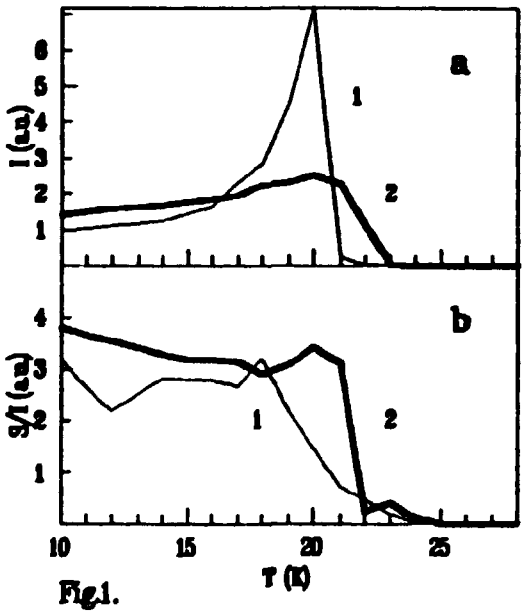

Fig.1.

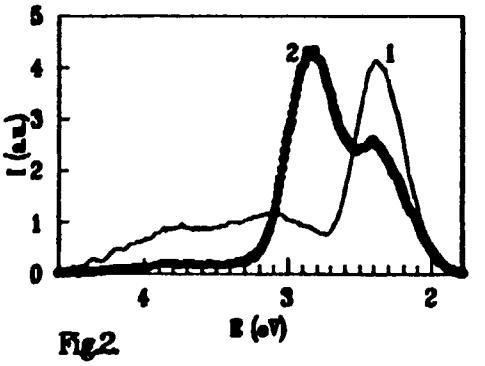

Fig.2.

[1] Ch. Lushchik et al, Proc. Intern. Workshop: Effects of strong disordering in HTSC, Zarechny, USSR (1990), p. 185-193.

[2] Ch. Lushchik, in: Physics of Radiation Effects in Crystals (ed. by R.A. Johnson and A.N. Orlov) Elsevier (1986).

[3] E.H. Chudnowsky, Phys. Rev. Lett. 45, 3060 (1990).

[4] V. G. Stankevich et al., J. Luminescence 48 & 49, 845 (1991).

CP34

Calculated Raman Frequencies in $YBa_2Cu_3O_7$

Kenneth Holmlund and Uno Yxklinten

Institute of Theoretical Physics, Chalmers University of Technology
and University of Göteborg

S-412 96 Göteborg, Sweden, [Fax: +46-(0)31-416984],
[E-mail: tfykh@fy.chalmers.se and tfyuy@fy.chalmers.se]

We present calculations and results for the lattice dynamics of $YBa_2Cu_3O_7$. The vibrational modes that we are interested in are the five Raman active A_g-modes. Vibrational frequencies and their corresponding polarization vectors are computed using the frozen-phonon approximation. To calculate the total energy we use the simple version of the Effective-Medium Theory, EMT [1], in the respect that contributions from the so called one-electron energy term are neglected.

Although we believe this term to be important for the system of interest, we conclude that EMT works surprisingly well already without these corrections. A simple model for the cohesive energy, like EMT, can give reasonable results for the overall geometry of the structure. In order to describe local bonds, correction terms such as the so called one-electron energy needs to be included. Higher order correction terms give a rather small contribution to the total energy, but are crucial to get the bond length and to describe the local interaction correct.

In our calculation we minimize the total energy with respect to the static structure parameters of the unit cell, that is the lattice parameters and the individual positions of the atoms in the unit cell. We supplement a discussion of the importance and the nature of the different chemical bonds and how to explicitly account for them in EMT. The results are compared with other theoretical [2] and experimental [3] results.

---

[1] K.W. Jacobsen, J.K. Nørskov and M.J. Puska, Phys. Rev. B35, 7423, (1987).

[2] C.O. Rodriguez, A.I. Liechtenstein, I.I. Mazin, O. Jepsen, O.K. Anderson and M. Methfessel, Phys. Rev. B42, , (1990)

[3] C. Thomsen and M. Cardona, in *Physical Properties of High Temperature Superconductors I*, page 411, (ed. D.M. Ginsberg), World Scientific, Singapore (1989).

CP35

In-situ Preparation of Y-Ba-Cu-O Thin Films Using Mass-spectrometer Rate Control and Atomic Oxygen

J. Hudner, H. Ohlsén*, P. Nordblad*, T. Larsson*, M. Ottoson[#] and L.-D. Wernlund[#]

Dep. of Solid State Electronics, KTH-Electrum, Box 1298, 164 28 Kista, Sweden

* Swedish Institute of Microelectronics, Box 1084, 164 21 Kista, Sweden

* Dep. of Solid State Physics, University of Uppsala, Box 534, 751 21 Uppsala, Sweden

[#] Dep. of Inorganic Surface Chemistry, University of Uppsala, Box 531
751 21 Uppsala, Sweden

[x] National Defence Research Establishment, Box 1165, 581 11 Linköping, Sweden

In-situ thin films of $YBa_2Cu_3O_7$ (YBCO) have been prepared using a mass-spectrometer controlled coevaporation process[1] with two electron beam guns (Y and Cu) and one effusion source (Ba). Oxygen was incorporated during growth using a commercially availible atomic oxygen beam source (Oxford Applied Research, MPD21). The background pressure during growth was $3 \cdot 10^{-5}$ mbar and the heater temperature was 740°C. During cool down the oxygen pressure is raised to 10^{-3} mbar.

Results from electric and magnetic properties of films fabricated on single crystal low loss substrates such as $LaAlO_3$, $NdGaO_3$ and Al_2O_3 will be presented. Structures for I_c and noise measurements, and coplanar resonators have been made by patterning films on $LaAlO_3$. A standard lithographic technique and wet etch was used for patterning. Results of microwave properties of a reflection coupled resonator and a transmission coupled ring resonator will be reported.

There are several advantages of using Y_2O_3 as a barrier material. Yttria has a stable phase and can be deposited at the deposition conditions for YBCO. There is a small lattice mismatch between Y_2O_3 and YBCO, it has a low dielectric constant and high dielectric strength. Finally, yttria is straightforward to prepare in a coevaporation process of YBCO. Double layers of YBCO and Y_2O_3 have been prepared on $LaAlO_3$ substrates ($LaAlO_3$-Y_2O_3-YBCO and $LaAlO_3$-YBCO-Y_2O_3), as well as a sandwich structure consisting of YBCO-Y_2O_3-YBCO. The layers were deposited without breaking vacuum and have been studied regarding epitaxy, T_c and J_c.

---

[1] J. Hudner, M. Östling, H. Ohlsén and L. Stolt, J. Vac Sci. Technol. A9, 2636 (1991)

CP36

Crystal Structure and Charge Localization in $Pb_2Sr_2Y_{1-x}Ca_xCu_3O_8$ for x= 0.0-0.5

J.-E. Jørgensen[§] and N. Hessel Andersen[•]

[§]Department of Chemistry, Aarhus University, DK-8000 Århus C, Denmark,
Fax: 86 196199, E--mail: JENSERIK@KEMI:AAU.DK

[•]Physics Department, Risø National Laboratory, P. O. Box 49,
DK-4000 Roskilde, Denmark, Fax: 42 370115

Compounds with formula $Pb_2Sr_2La_{1-x}Ca_xCu_3O_8$ where La represents a lanthanide were synthesized and shown to be high T_c superconductors with critical temperatures close to 70 K by Cava et al.[1] in 1988. These compounds are pseudo-tetragonal but orthorhombic and they are having the stacking sequence is La-CuO_2-SrO-PbO-Cu-PbO-SrO-CuO_2-. The lanthanide ions are in this compound sandwiched between two CuO_2 layers, and a similar arrangement is found in $YBa_2Cu_3O_7$ as well as in several of the Bi and Tl based high T_c superconducting compounds. The CuO_2 layers are of importance for high T_c superconductivity and the aim of the present neutron powder diffraction study was to determine the structural changes induced by Ca-doping of $Pb_2Sr_2YCu_3O_8$. Special attention was to paid to changes in the axial Cu-O bond length. This bond is perpendicular to the CuO_2 layers and the equivalent bond in $YBa_2Cu_3O_7$[2] has been shown to be a sensitive probe of the charge state of the copper ions in the CuO_2 layers.

Powder diffraction patterns of $Pb_2Sr_2Y_{1-x}Ca_xCu_3O_8$ were recorded for x= 0.0 to 0.5 and atomic positions were determined by Rietveld refinements while lattice parameters were determined from X-ray Guinier films. Bond valencies for all cations were calculated from the inter atomic distances. The axial Cu-O bond length and the bond valency of the copper ions in the CuO_2 layers are shown in Fig. 1 and 2 respectively. Ca-doping causes the axial Cu-O bond length to go through a maximum at x= 0.4 while the copper bond valency increase with the level of doping. The bond valency of the lead ions increases up to x= 0.4 and then saturates. In conclusion Ca-doping of these compounds oxidizes copper in the CuO_2 layers but the oxidation state of lead is also affected by the doping.

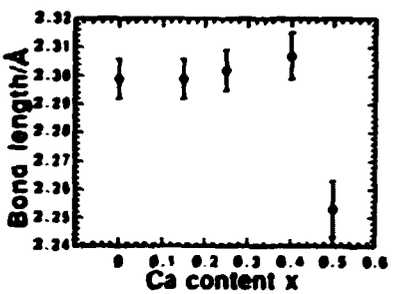

Fig. 1. Axial Cu-O bond length as a function of Ca-doping level.

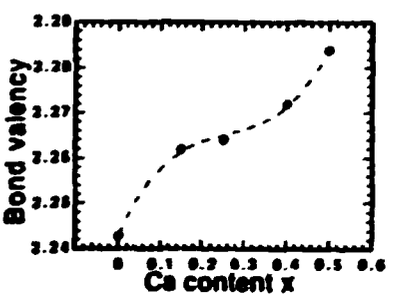

Fig. 2. Bond valency of the copper ions in the CuO_2 layers.

---

[1] R. J. Cava et. al., Nature (London) 336, 211 (1988).

[2] J. D. Jorgensen, Phys. Rev. B41, 1863 (1990).

CP37

Raman scattering study of the effects of Tl and O stochiometry on the phonon spectrum of $Tl_2Ba_2CuO_6$

Mikael Käll, Carin Ström#, Lars Börjesson and Lars -Gunnar Johansson#

Dept. of Physics, #Dept. of Inorganic Chemistry, Chalmers University of Technology, S-412 96 Göteborg, Sweden

The effects of Tl and O stochiometry on the physical properties of the Tl based superconductors are of considerable interest since the Tl content is hard to control due to evaporation problems and small changes in O content have great impact on T_c. Here we report on a Raman scattering study of ceramic $Tl_2Ba_2CuO_6$ high T_c superconductors with nominal Tl contents varying between 1.75 and 2.0 and with two different oxygen contents.

The Raman spectra were taken on small crystallites in the pellets using microprobe optics with a spatial resolution of about 2 μm. Data were taken in two different scattering configurations, namely x(zz)x and z(xx)z, were z is along the c and x along the a or b axis of the crystallites. Data for the oxygen vibrational region, 300-700 cm^{-1}, are presented in this poster.

In the zz spectra two strong phonon lines are visible, the O(2) apical oxygen $A1_g$ mode at ~485 cm^{-1} and the $A1_g$ mode of the O(3) oxygen atom in the TlO layer at ~605 cm^{-1}. The xx spectra show, apart from the apical oxygen mode, strong electronic continuum scattering [1].

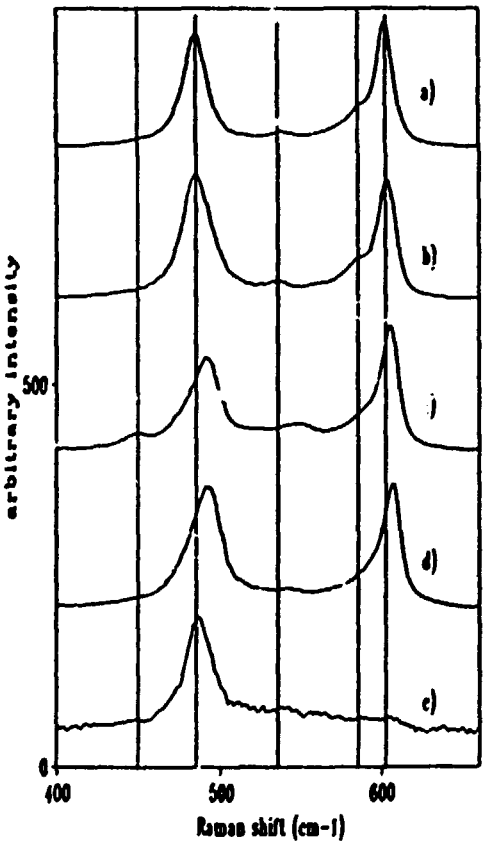

When the Tl content was increased both $A1_g$ modes decreased abruptly by ~6 cm^{-1} between a Tl content of 1.85 and 1.95. This change coincide with a tetragonal to orthorombic phase transition. It seems reasonable that the frequency decrease is connected to changes in Tl coordination occuring at the phase transition.

Increased oxygen content led to a decrease by ~2 cm^{-1} for both $A1_g$ modes irrespective of Tl content. This effect is opposite to what is observed in Y123[1]. The increased oxygen content also led to an slight increase of the electronic background irrespective of Tl content. This change is probably connected with a higher hole concentration at the CuO_2 planes for the oxygen rich samples.

In the samples with low Tl content (1.75 and 1.85 nominal) and high oxygen content we observe an additional peak at ~450 cm^{-1} which is almost absent in the other samples. This peak might be associated with extra oxygen entering O(3) sites which are weakly coordinated to Tl.

In all zz spectra weak peaks are observed around 540 and 585 cm^{-1} which we tentatively ascribe to $A2_u$ oxygen modes made Raman allowed through defect induced symmetry breaking.

T_c and structural measurements made on the same samples will be presented at the conference in another poster.

Figure caption

From top to bottom: a) zz spectra, Tl content 1.95, high O content. b) zz spectra, Tl content 2.0, low O content. c) zz spectra, Tl content 1.75, high O content. d) zz spectra, Tl content 1.75, low O content. e) xx spectra, Tl content 2.0, low O content. Baseline indicate zero intensity for e) spectrum only. Vertical lines indicate phonon modes mentioned in the text.

1) see for example C. Thomsen, M. Cardona in Physical Properties of High Temperature Superconductors 1, ed. D M Ginsberg (World Scientific, Singapore, 1989) p. 409-507

CP38

Characterization of Pr doped $Y_1Ba_2Cu_4O_8$ samples

Pedro Berastegui[$], Mikael Käll[#], Lars-Gunnar Johansson[$] and Lars Börjesson[#]

[$]Dept. of Inorganic Chem., [#]Dept. of Physics, Chalmers University of Technology, S-412 96 Göteborg, Sweden (FAX: 31 167194)

The effects of Pr doping for RE on the superconducting properties of the RE-Ba-Cu-O class of high T_c superconductors has been given a lot of attention since Pr is the only rare earth (RE) atom severely depressing T_c. The reason for this is not clear but suggested explanations include filling of mobile holes, hole localisation and magnetic pair breaking. Here we study the effects of substituting Pr for Y on the structure and superconducting properties of the high T_c superconductor $Y_1Ba_2Cu_4O_8$ (Y-124) using X-ray diffraction, Raman scattering and resistivity measurements.

A series of ceramic samples with nominal composition $Y_{1-x}Pr_xBa_2Cu_4O_8$, where x was varied between 0.0 and 1.0, were synthesized using a sol-gel technique based on citric acid and ethyleneglycol. The precursors were sintered at 830°C for two weeks at one atmosphere oxygen pressure. The purity of the samples and lattice parameters were determined using the Guinier technique. Only small amounts of impurities (<1% of CuO and $BaCuO_2$) could be detected. The sample with x=1.0 however, contained only $PrBaO_3$, CuO and $BaCuO_2$. As can be seen in figure 1) the lattice constants increase linearly with increasing Pr content reflecting the larger radius of Pr. The orthorombicity decreases only slightly. Structural considerations suggest an average Pr valency between 3+ and 4+.

T_c was measured with the usual four-probe resistivity technique. In figure 2) T_c,onset is plotted as a function of Pr content x for the Y/Pr124 samples used in this study and for Y/Pr123 from ref. 1). The transition widths were beetween 5 and 20K, (10%-90%), increasing slowly with Pr content. As can be seen in figure 2) the 124 phase retains superconductivity to a higher Pr doping level than the 123 structure.

Raman measurements were performed in backscattering geometry using microprobe optics. In this poster only the oxygen vibrational region, ~300-700 cm^{-1} is covered. The four observed phonon peaks are, from left to right in figure 3), O(1)/O(2) B_{1g} out-of-phase mode at ~340 cm^{-1}, O(1)/O(2) A_{1g} in-phase mode at ~430 cm^{-1}, O(4) A_{1g} mode at ~495 cm^{-1} and O(3) A_{1g} mode at ~595 cm^{-1}(2). All phonon displacements are in the c-axis direction. The changes in the phonon line positions seen in figure 3) may be explained as follows: the increasing average diameter of the Y/Pr site leads to an increasing CuO_2 plane-plane distance leading to a decreasing frequency for the 340 cm^{-1} mode; the increasing CuO_2 plane-plane distance is to some extent compensated by a decreasing CuO_2-CuO plane-chain and CuO-CuO chain-chain c-axis distance leading to increasing frequencies for the 495 and 595 cm^{-1} modes. The 430 cm^{-1} mode is more or less unaffected by the substitution. It is interesting to note that the shape of the 595 cm^{-1} chain oxygen mode does not change with substitution thus confirming that the 124 double-chain structure is conserved. Structural data from neutron diffraction on the same samples will be presented at the conference.

Acknowledgments: We wish to thank P. Norling for his assistance with the resistivity measurements.

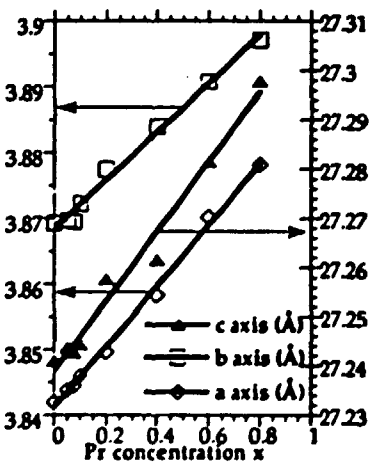

Figure 1

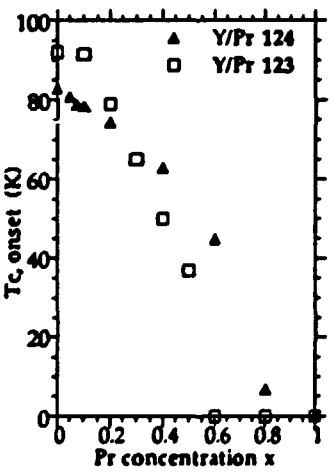

Figure 2

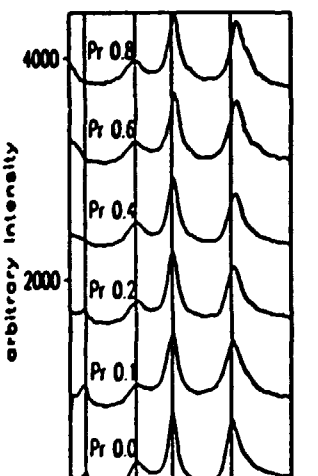

Figure 3

1) L. Soderholm et al, Nature 328, 604 (1987).
2) H.B Radousky et al, Phys. Rev. B 39, 12383 (1989).

CP39

A neutron diffraction study of $Y_1Ba_{2-y}Sr_yCu_{3-x}Me_xO_{7-d}$ (Me=Co, Al, Fe); Structural changes related to charge transfer and compression effects.

S.-G. Eriksson[$,#], C. Ström[$], L.-G. Johansson[$], A. Simon[#] and Hj. Mattausch[#]

[$]Dept. of Inorganic Chem., S-412 96 Göteborg, SWEDEN (FAX 46 31 167194)

[#]MPI fur Festkörperforschung, 7000 Stuttgart 80, GERMANY (FAX 49 7116874371)

The superconducting properties of most high-T_c materials can be related to the number of positive charge carriers in the CuO_2-planes. By introducing dopant atoms or by changing the oxygen content the carrier concentration in the CuO_2-planes can be altered. This is reflected in structural changes and changes in T_c.

The POLARIS instrument at ISIS, RAL, England has been used for the collection of high quality TOF neutron powder diffraction data. In all cases solid state sintered single phase samples of doped Y-123 have been analysed by the Rietveld method. The structural changes caused by the various substitutions have been correlated to changes in e.g. T_c (cf. table 1). We have shown that compression effects (Sr^{2+}) can be separated from charge transfer effects (Co^{3+}, Al^{3+}, Fe^{3+})[1,2] and that the two effects seems to be additive[3]. In figure 1 the two effects are schematically illustrated.

x/y	$(Cu2\text{-}O2,3)_z$	$(Ba\text{-}O4)_z$	Cu1-O4	Cu2-O4	T_c
0.00/0.00	0.269	0.299	1.853(2)	2.291(5)	92
0.00/0.20	0.270	0.297	1.847(3)	2.282(3)	39
0.00/0.40	0.267	0.300	1.845(2)	2.270(3)	87
0.00/0.60	0.269	0.295	1.846(2)	2.250(3)	86
0.00/0.80	0.270	0.300	1.844(3)	2.237(4)	85
0.00/1.00	0.267	0.299	1.843(3)	2.224(3)	81
0.05/0.00	0.259	0.304	1.854(5)	2.306(6)	89
0.15/0.00	0.228	0.343	1.836(5)	2.345(6)	76
0.30/0.00	0.216	0.349	1.838(6)	2.352(7)	30

Table 1. Some characteristic distances in $Y_1Ba_{2-y}Sr_yCu_{3-x}Co_xO_{7-d}$. Cu1 is the chain copper, Cu2 the plane copper, O2 and O3 the plane oxygens and O4 the apex oxygen.

A large number of doped materials have been investigated such as $Y_1Ba_2Cu_{3-x}Me_xO_{7-d}$, $Y_1Ba_{1.6}Sr_{0.4}Cu_{3-x}Me_xO_{7-d}$ and $Y_1BaSrCu_{3-x}Me_xO_{7-d}$ where Me=Co, Al, Fe. A series $YBa_{2-y}Sr_yCu_3O_{7-d}$ has also been characterised. We have found that there exists no simple relation between T_c and the Cu-O distances as has been indicated in the literature. However, T_c and the charge distribution are more directly related to other structural features i.e. the $(Cu2\text{-}O2,3)_z$ and the $(Ba\text{-}O4)_z$ distances.

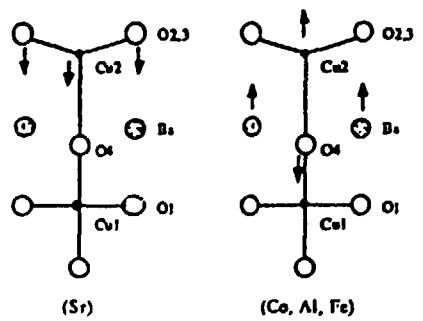

Figure 1. Atomic displacements in the z-direction, caused by compression of the structure (Sr) and by a transfer of holes from the CuO_2-planes to the CuO_x-chains(Co, Al, Fe).

From the large amount of data evaluated we have been able to obtain a firm understanding for the structure - property relations in Y-123.

1) S.-G. Eriksson, Thesis, Göteborg (1990)
2) M. Kakihana, S.-G. Eriksson, L. Börjesson, L.-G. Johansson and C. Ström, Submitted to Phys. Rev. B.
3) S.-G. Eriksson, C. Ström, A. Simon and Hj. Mattausch. To be publ. in JSSC.

CP40

Neutron powder diffraction study of structural changes in $Tl_{2-x}Ba_2CuO_{6-d}$ and $Tl_{2-x}Ba_2CaCu_2O_{8-d}$ related to oxygen and thallium stoichiometry.

C. Ström*, S.-G. Eriksson*¤ and L.-G. Johansson*.
*Dept. of Inorg. Chem., S-412 96 Göteborg, SWEDEN (FAX 46 31 167194)
¤MPI für Festkörperforschung, 7000 Stuttgart 80, GERMANY (FAX 49 711 6874371).

All thallium based high T_c superconductors with double Tl-O layers have tetragonal symmetry except $Tl_2Ba_2CuO_{6-d}$ (Tl-2201) which exists in both tetragonal and orthorhombic forms. Tl-2201 has a remarkably wide range of T_c (0-90K) depending on the preparative conditions[1,2]. T_c and cell parameters are known to be correlated to changes in oxygen content. In the homologous $Tl_{2-x}Ba_2CaCu_2O_{8-d}$ (Tl-2212) only a tetragonal phase is known. However, it does show a large variation in the c axis length depending on the method of preparation.

In this investigation we have used neutron diffraction to study the structural perturbations induced by changing the thallium and oxygen stoichiometry. High quality neutron diffraction data were collected at the spallation source ISIS, RAL, UK, using the high flux, medium resolution powder diffractometer POLARIS. Data were collected from twelve solid state sintered single phase samples of $Tl_{2-x}Ba_2CuO_{6-d}$ and $Tl_{2-x}Ba_2CaCu_2O_{8-d}$ with different x and d, and analysed by the Rietveld method.

Results from the analysis show that the tetragonal-orthorhombic phase transition in Tl-2201 is a function of both the oxygen and the thallium content. Samples with high thallium deficiency are tetragonal and tetragonal thallium deficient samples become orthorhombic after oxygen annealing. This implies that the degree of disorder in the Tl-O double layer region is closely related to thallium and oxygen substoichiometry The cell-parameters are plotted as a function of thallium and oxygen content in figure 1. In Tl-2212 increasing thallium and oxygen content both result in a shortening of the c axis. The changes in coordination induced by changing the thallium and oxygen stoichiometry are not identical in the two related systems. Thus, increasing the thallium and oxygen content results in decreasing Tl-Tl intralayer distance in Tl-2212 while the corresponding distance is not affected in Tl-2201. Structural data and T_c measurements will be presented for Tl-2201 and Tl-2212.

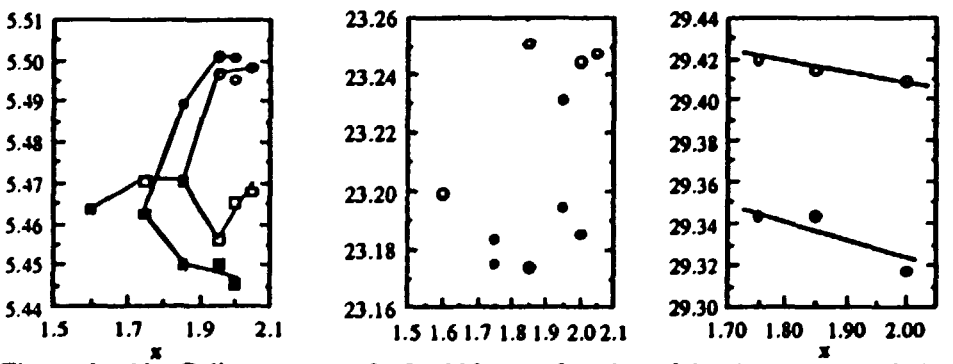

Figure 1a, b) Cell parameters for Tl-2201 as a function of thallium content (Guinier data) c) c axis as a function of thallium content for Tl-2212 (Neutron data). Filled symbols designate oxygen annealed samples.

1. T. C. Huang et al, Mat. Res. Bull., Vol 23, 1307-1314, 1988.
2. A. Maignan et al, Physica C 170 (1990) 350-360

CP41

Correlation Between Crystalline and Optical Anisotropy in High-T_c Superconductors

R.Dagys*, G.-J.Babonas*, E.L.Belokoneva#, L.I.Leonyuk#, G.Pukinskas*

*Semiconductor Physics Institute, Goštauto 11, 2600 Vilnius, Lithuania,
[Fax: +7-0122-627123], [E-mail: ULBIKAS%IB.PFI.LT@gateway.uninett.no]
#Geological Department, Moscow State University, 119899 Moscow, Russia

The cuprate-type high-T_c superconductors (HTSC) are strongly anisotropic with respect to the c-axis. In addition, in superconducting state most of cuprates show anisotropy of the physical properties in the basal (ab)- plane. In this work it has been shown that optical investigations provide an information about the peculiarities of both electronic and crystalline structure of HTSC.

Single crystals of HTSC were grown from the melt by a slow cooling method. The samples prepared for investigations have dimensions 3-5 × 3-5 × 0.1-1.0 mm^3. According to crystallographic data, the obtained crystals were (2212)-, (1212)- and (123)- type for Bi-, Pb- and Y-based compounds, respectively. The dielectric function was measured in the range 1.2-4.5 eV using ellipsometer with rotating analyzer and photoelastic modulator of polarization.

The optical spectra were analyzed considering the excitation of structural units in the elementary cell of HTSC. The features in the range 1.5-2.5 eV were shown to be due to the electronic excitation in Cu(2)-O pyramid, a common unit in cuprates. In the 3-4 eV region the excitations in Bi-O and Pb-O planes manifest themselves in (2212) and (1212)-type compounds.

Optical anisotropy was studied in the (ab) plane of HTSC single crystals. In Pb-based compounds the optical anisotropy was shown to be related with an ordering of oxygen vacancies. In Bi-based (2212)- type compounds the correlation of optical anisotropy with parameter modulation and Pb concentration has been observed. The optical spectra of rare earth (123)-type HTSC has been also discussed taking into account the peculiarities of the crystal structure of the samples containing excess rare earth ions.

CP42

Ion Beam Stimulated Bi-epitaxial Josephson Junctions

Jaime Ramos, Zdravko G. Ivanov and Tord Claeson

Department of Physics, Chalmers University of Technology, S-412 96 Gothenburg, Sweden, [Fax: 031 16 51 76], [E-mail:F4ATC@SECTHF51]

The Artificial grain boundary Josephson junctions grown on Y-ZrO_2 bi-crystal substrates have shown excellent performance at 77K.[1] The adoption of this type of junctions to integrated circuits led to the bi-epitaxial technology developed by the Conductus group.[2] A seed layer was used to create a 45° grain boundary in the junction area. Another possible technology is to modify the surface of the substrate in order to change the conditions for the in-plane epitaxy. It has recently been shown that chemical or mechanical treatment[3] or ion milling[4] of MgO substrates create conditions for 45° in-plane epitaxy on MgO.

We have investigated the possibility to control the in-plane epitaxy by ion beam etching of MgO substrate and to develop Josephson junctions and dc SQUIDs. One half of the substrate was ion beam milled ~ 5-15 nm depth and an YBaCuO film was deposited on top by using pulsed laser deposition. A 45° degree grain boundary was formed between the two halves of the substrate. Microbridges which include the grain boundary were patterned and studied.

Three substrates were processed to different stepheights, 5, 10 and 15 nm. In all cases ,the grain boundary weak links showed Josephson effects and most of them worked above 77K. The critical current density at the grain boundary was depressed about four orders of magnitude compared to the film. We observed a tendency in the critical current decreasing by increasing the step height. However, we are confident that the influence of the step itself on current transport is minimal. The critical current vs. temperature dependence, $I_c(T)$, showed a behavior typical for S-N-S Josephson junctions, some junctions ,however, showed a nonmonotonic $I_c(t)$ dependence with a well developed maximum at temperatures of 4-30 K, typical for an S-SemiC-S weak link, see for example the abstract: *Z.G.Ivanov et al.* at this conference (where S-superconductor, N-normal metal and SemiC-semiconductor). For the substrate with a 15 nm step several maxima were observed and we speculate that there are several weak links in parallel with different critical currents. For smaller steps there was mainly one maximum indicating a single junction with misorientaion of 45°.An S-N-S behavior might be explained by a low angle grain boundary. Further investigations are in progress to optimize the conditions for uniform in-plane epitaxy.

---

[1] Z.G.Ivanov, P.Å.Nilsson, J.A.Alarco, D.Winkler, T.Claeson, E.A.Stepantsov, and A.Ya.Tzalenchuk, Appl. Phys. Lett., 59, 3030 (1991).

[2] K.Char, M.S.Colclough, L.P.Lee, and G.Zaharchuk, Appl.Phys.Lett.,59,2177 (1991).

[3] B.H.Moeckly, S.E.Russek, D.K.Lathrop, R.A.Buhrman, Jian Li, and J.W.Mayer, Appl.Phys.Lett.,57,1687(1990).

[4] N.G.Chew, S.W.Goodyear, R.G.Humphreys, J.S.Satchell, J.A.Edwards, and M.N.Keene, submitted to Appl.Phys.Lett.

CP43

Growth and Properties of a-axis Oriented YBaCuO Films

Jaime Ramos, Tord Claeson, Zdravko G. Ivanov, Eva Olsson, and Evgeniy Stepantsov*

Department of Physics, Chalmers University of Technology, S-412 96 Gothenburg, Sweden, [Fax: +46 31 16 51 76, E-mail: F4ATC@SECTHF51]
*Institut of Crystallography, Russian Academy of Sciences

Development of YBaCuO (YBCO) thin films with a axis perpendicular to the substrate is an important issue in understanding the anisotropy of transport properties of YBCO materials and creating Josephson junctions based on tri-layer technology.[1] We have grown a-axis oriented YBCO thin films on a variety of substrates: $SrTiO_3$ (STO), MgO and Y-ZrO_2 (YSZ) using the pulsed laser deposition technique.[2] The films were characterized by transport measurements, X-ray diffraction, scanning and transmission electron microscopy. A thin PrBaCuO (PBCO) template layer was used to promote the a-axis growth of YBCO films. Both layers , PBCO and YBCO, were deposited in one vacuum cycle with varying substrate temperature T_{sub}. The optimum temperature for the a-axis growth of PBCO was determined to be 630°C and 680°C on MgO and STO correspondingly. No good a-axis PBCO films were grown on YSZ even at temperatures of 600°C. The TEM study indicated that template layers with different thicknesses are required for the a-axis YBCO growth on different substrates. The dependences of the transition temperature to the superconducting state T_c and the lattice parameter a were studied as function of the T_{sub} (see Fig.1 for STO and Fig.2 for MgO). The highest measured Tc's were 84K and and 81K for STO and MgO substrates.The films were patterned to 4 µm wide microbridges and critical current densities of up to $4x10^4$ A/cm^2 were measured at 4.2 K in the plane of the film. The SEM study showed that at optimal deposition parameters the films were extremely smooth.

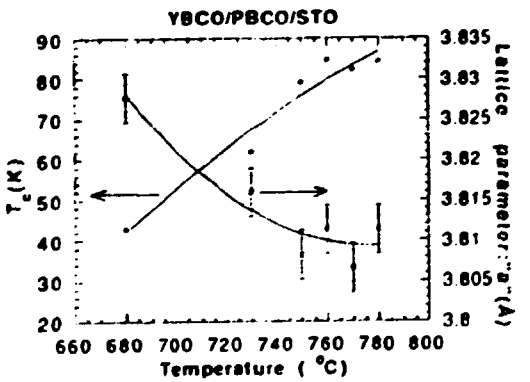

Fig. 1

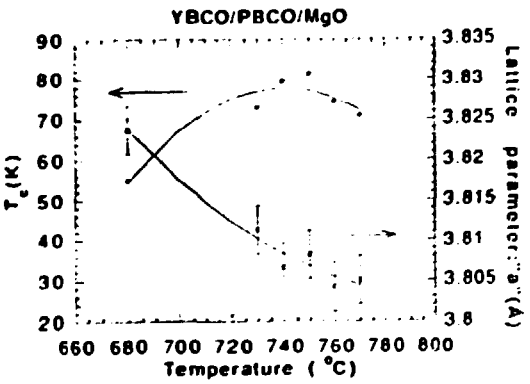

Fig. 2

---

[1] J.B.Barner, C.T.Rogers, A.Inam, R.Ramesh, and S.Bersey, Appl. Phys. Lett., 59,742 (1991).

[2] G.Brorsson, Z.Ivanov, P.Å.Nilsson, Proc. of the Conf. on the Science and Technology of Thin-Film Superconductors, April 30-May 4,1990,Denver,Colorado, USA.

CP44

Superconductivity in the two-band model with the pure repulsive interaction in the low density limit

M.A.Baranov

Chalmers University of Technology, Göteborg, Sweden*

[Fax: +46 31 416984, E-mail: WENDIN@FY.CHALMERS.SE]

M.Yu.Kagan

Institute for Physical Problems, Moscow, Russia

*Permanent address: Moscow Engineering Physics Institute, Moscow, Russia

We consider the two-band model with a pure repulsive interaction in the limit of small one-particle hybridization and weak coupling constant for both two-dimensional and three-dimensional cases. The limit of the weak coupling constant indeed describes two different situations: one of a weak interaction and arbitrary density and another of a strong interaction but small density. In both cases the gas-parameter - the unique parameter, characterizing a Fermi system - is small. Under these conditions possible mechanisms of superconductivity were analyzed and it was found that the leading one is the pairing in one band through the polarization in another band. However the details are different for 2D or 3D cases and for electron-electron or electron-hole bands. In any case the resulting superconductivity has the p-type pairing and the corresponding critical temperature is determined by the second order of the perturbation theory. We also discuss the possibility of the s-wave pairing in such systems and argue that it seems to be unlikely to obtain it, but the strong suppression of the bare Coulomb repulsion, preventing the s-pairing, can take place. This makes it easier to obtain the s-wave pairing when other degrees of freedom (lattice, spin, etc) are taken into account.

CP45

Diamagnetic Response of Bi-based Superconductor Carrying Transport Current[1]

A.N.Ulyanov[#+], V.N.Korenivski[#+], K.V.Rao[#], A.M.Grishin[+]

[#]Royal Institute of Technology, S-100 44 Stockholm, Sweden
[+]Donetsk Physico-Technical Institute, 340114, Donetsk, Ukraine

The magnetic response of granular superconductors over a wide temperature range has been studied experimentally and described to some extent theoretically. From application point of view it is interest to study the magnetic response of superconductors in the presence of a transport current (ac or dc). The galvanomagnetic properties in such situation have not been explored. This paper is an attempt in this direction.

We present here our studies of the real $\chi'(T)$ and imaginary $\chi''(T)$ components of ac susceptibility of a slab carrying dc-transport current I in a direction normal to the magnetic field H_{ac}. We observe a strong suppression of both intra- and intergranular properties by the transport current.

The investigated single-phase $Bi_2Sr_2Ca_2Cu_3O_y$ ceramic sample had the dimensions of 8·8·0.8 mm^3.The susceptibility was measured using inductive technique at 2.45 kHz. Geometry of experiment is shown in the inset to Figure.

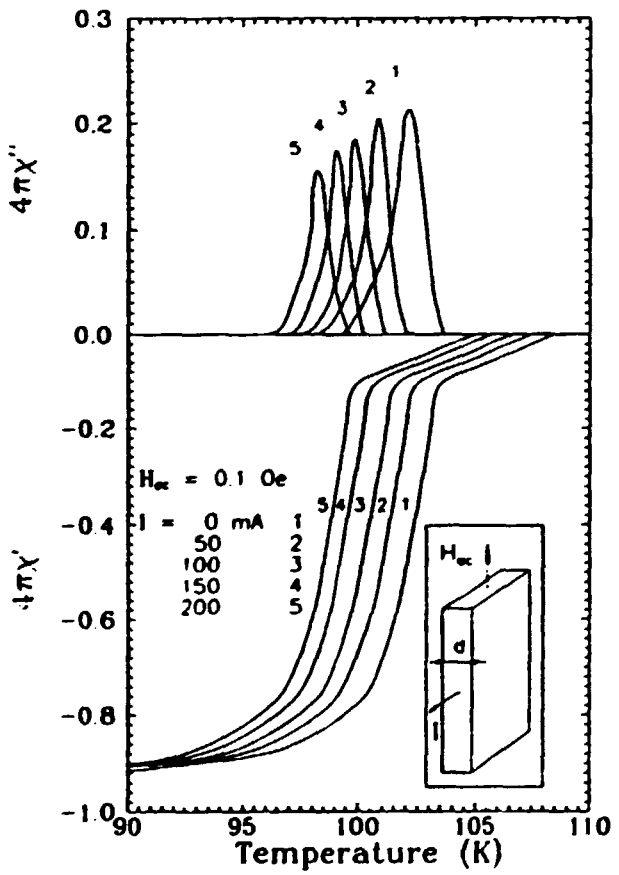

Temperature dependencies of χ' and χ'' obtained at H_{ac} = 0.1 Oe and different values of transport current are shown in the Figure.

The shift of the diamagnetic response onset temperature $T_{on\chi'}$ of $\chi'(T)$ dependencies witnesses about the suppression of intragrain superconductivity by transport current.

Suppression of intergranular susceptibility by the transport current is displayed in the decrease of $\chi''(T)$ maximum value and the shift of χ'' onset temperature with increasing I. The peak of the lossy component also shifts to low temperatures as I increases at a rate $\delta T/\delta j \approx 1.3$ K/(A/cm^2). The increase of I, in the contrary to increase of exciting magnetic field H_{ac}, does not broaden the $\chi'(T)$ and $\chi''(T)$ curves.

We discuss in detail the observed phenomenon and its potential for applications as novel sensors, superconducting switches, ets.

[1]Work supported by the Swedish Royal Academy of Sciences under the Swedish-USSR exchange program.

CP46

High T_c SQUID's and magnetometers

R. Kromann[1], J. J. Kingston, A. H. Miklich, L. T. Sagdahl, Y. Saito and J. Clarke

Department of Physics, University of California, Berkeley, CA 94720, USA

We report on our efforts to fabricate thin film SQUID's and integrated magnetometers based on YBCO grain boundary junctions. The junctions and SQUID's are fabricated by pulsed laser deposition on MgO substrates using a bi-epitaxial process. Initially the substrate is covered with a $SrTiO_3$ buffer layer followed by two very thin seed layers of MgO and CeO_2. The seed layers are removed from parts of the substrate by ion milling, leaving the $SrTiO_3$ layer exposed. Subsequently a second CeO_2 layer is deposited followed by the YBCO layer. Because the lattice parameter of CeO_2 is close to $\sqrt{2}$ times larger than that of $SrTiO_3$, the in-plane orientation of the second CeO_2 layer will unde · a 45° rotation along the edge defined by the ion milling step, and this in-plane rotation will be imposed on the YBCO layer.
The integrated magnetometer is fabricated by combining the SQUID with a flux transformer on the same substrate. The flux transformer consists of a 1 turn pick-up coil in series with a 5 turn input coil. The area of the pick-up coil is made as large as possible given the substrate size, whereas the input coil is designed to match the size of the SQUID body which is 250 μm × 250 μm. The flux transformer and the SQUID are separated by a thick insulating layer of $SrTiO_3$.

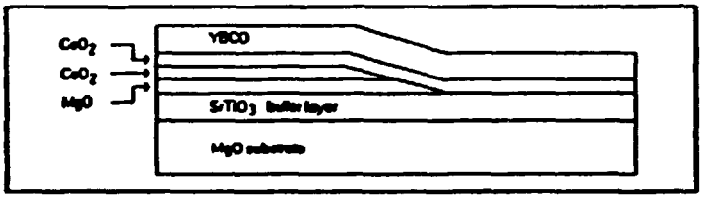

Sketch showing the sequence of epitaxial layers that goes into the fabrication of a grain boundary junction.

Typical values for the critical current and normal state resistance for our junctions are 100 μA and 1 Ω, measured at 4.2 K. The SQUID's exhibit voltage modulation up to 78 K. For the magnetometer samples we measure a gain of about 60, defined as the effective area of the magnetometer relative to the effective area of the bare SQUID. The magnetometers work up to 73 K.
Noise measurements indicate that grain boundary SQUIDS's compare unfavorably with other competing SQUID technologies. Currently we are developing processes for grain boundary junctions on YSZ and for YBCO/Ag/YBCO tunnel junctions.

---

[1]Permanent address: Physics Department, Risø National Laboratory, P.O. Box 49, 4000 Roskilde, Denmark

CP47

ELECTRONIC STRUCTURE CALCULATION OF La_2CuO_4 IN THE SELF-INTERACTION CORRECTED LOCAL-SPIN-DENSITY FUNCTIONAL FORMALISM

A. Svane

IFA, Aarhus University, DK-8000 Aarhus C

[Fax: (+45) 12 07 40], [E--mail: svane@dfi.aau.dk]

The electronic structure of tetragonal La_2CuO_4 as calculated in the self-interaction corrected (SIC) local-spin-density (LSD) approximation is presented and compared to results of the LSD approximation and to experiments. In contrast to LSD calculations, the SIC-LSD approach reveals the experimentally observed antiferromagnetic and semiconducting ground state of La_2CuO_4 . The energy gap is calculated to be 1.04 eV and of indirect charge transfer character, and the Cu moment to be 0.47 μ_B. Analysis of the highest occupied states show these to reside on the O atoms with about equal weight on the in-plane and out-of-plane O atoms. The valence band top region is dominated by O states not coupling to the Cu d-states, but a significant component of O states with Cu d-like symmetry is found.

CP48

Diamagnetic Response of Bi-based Superconductor Carrying Transport Current[1]

A.N.Ulyanov*+, V.N.Korenivski*+, K.V.Rao*, A.M.Grishin+

*Royal Institute of Technology, S-100 44 Stockholm, Sweden
+Donetsk Physico-Technical Institute, 340114, Donetsk, Ukraine

The magnetic response of granular superconductors over a wide temperature range has been studied experimentally and described to some extent theoretically. From application point of view it is interest to study the magnetic response of superconductors in the presence of a transport current (ac or dc). The galvanomagnetic properties in such situation have not been explored. This paper is an attempt in this direction.

We present here our studies of the real $\chi'(T)$ and imaginary $\chi''(T)$ components of ac susceptibility of a slab carrying dc-transport current I in a direction normal to the magnetic field $\vec{H}_{ac}$. We observe a strong suppression of both intra- and intergranular properties by the transport current.

The investigated single-phase $Bi_2Sr_2Ca_2Cu_3O_y$ ceramic sample had the dimensions of 8·8·0.8 mm³.The susceptibility was measured using inductive technique at 2.45 kHz. Geometry of experiment is shown in the inset to Figure.

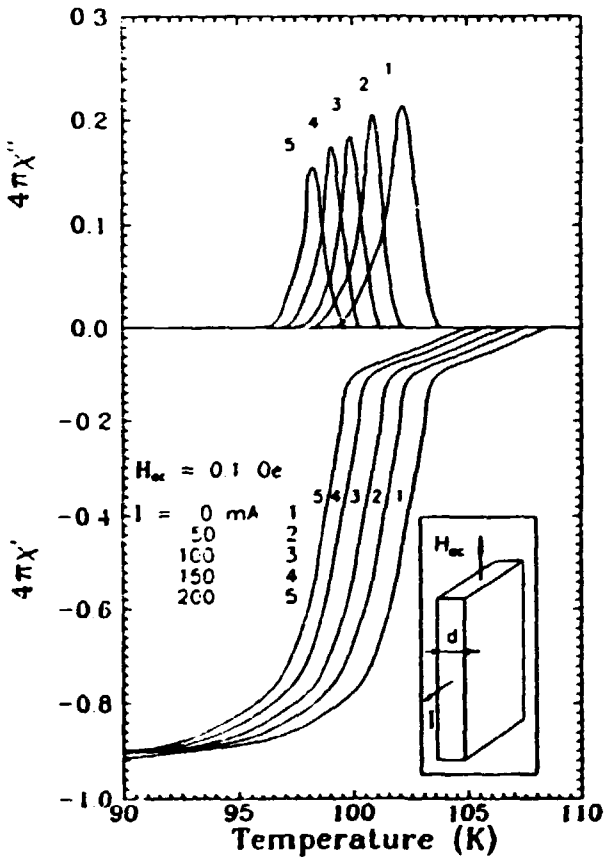

Temperature dependencies of χ' and χ'' obtained at H_{ac} = 0.1 Oe and different values of transport current are shown in the Figure.

The shift of the diamagnetic response onset temperature $T_{on\chi'}$ of $\chi'(T)$ dependencies witnesses about the suppression of intragrain superconductivity by transport current.

Suppression of intergranular susceptibility by the transport current is displayed in the decrease of $\chi''(T)$ maximum value and the shift of χ'' onset temperature with increasing I. The peak of the lossy component also shifts to low temperatures as I increases at a rate $\delta T/\delta j \approx 1.3$ K/(A/cm²). The increase of I, in the contrary to increase of exciting magnetic field H_{ac}, does not broaden the $\chi'(T)$ and $\chi''(T)$ curves.

We discuss in detail the observed phenomenon and its potential for applications as novel sensors, superconducting switches, ets.

[1]Work supported by the Swedish Royal Academy of Sciences under the Swedish-USSR exchange program.

CP49

Interaction of High and Low T_c-Phases in Thin Multiphase Bi-Sr-Ca-Cu-O Films

A.M.Grishin[#], G.V.Gusakov[#], A.B.Mukhin[#], B.Vengalis[*] and A.Flodström[&]

[#]Donetsk Physical-Technical Institute, 340114, Donetsk, Ukraine
[*]Lab. of HTC Supercond., Semiconductor Physics Institute, 2600 Goštauto 11, Vilnius, Lithuania, [Fax: +7-0122-627123]
[&]Materials science, Royal Institute of Technology, S-10044, Stockholm, Sweden, [Fax: +46-8-7908482]

Thin superconducting films of $Bi_2Sr_xCa_yCu_zO_N$ with x=1.5-2.2, y=1.0-2.1 and z=1.8-3.5 have been prepared on MgO(100) substrates using MBE and subsequent postannealing of the as grown metal alloy films at 820°C in air. Further the films were cooled down rapidly to room temperature. Auger electron spectroscopy and electron beam excited X-ray analysis have been used for the composition control. Different phases were analyzed by X-ray (CuK_α) diffraction.

It was found that the 2212-like structure dominated for all the prepared films. When the films were multiphase both high (2212) and low T_c (2201) phases as well as Ca and Cu oxide impurities have been indicated. However, because of relatively low anneal temperature no traces of the highest T_c (2223) phase have been found. In this work we represent composition mapping in respect to amount of the 2212)like phase for the Bi-Sr-Ca-Cu-O films. According to our X-ray data the highest amount of the phase including single phase state corresponds to compositions which are close to the nominal 2212 and 2223 ones. Both the 2212 and 2201 structures were found to be highly oriented with their c axes's directed perpendicular to the film surface. Rocking curves for the (00*m*) reflections showed just the same misorientation of a and b vectors for both 2201 and 2212 crystallites.

Interesting peculiarities of the diffraction spectra for the multiphase films appeared when the amount of (2201)-phase increased. We stress on substantial broadening of the (00*m*) diffraction lines. Further there were unusual shifts of several (00*m*) 2212 lines to the side of closest (00*m*) 2201 line positions. However, direction of the shift for the (008) 2212 reflex was found to be opposite to that of the (0012) 2212 one. We came to a conclusion that the multiphase films contain intergrowths of perfect 2201-phase and the distorted 2212 regions. Furthermore, the low T_c-phase tends to interact with the high T_c one. In order to explain interaction of such kind we assume cation vacancies formed in CuO and CaO planes of the 2212-phase.

Electrical properties of the films depended on their composition. Decrease of zero resistance temperature, broadening of superconducting transition and strengthening of semiconductor behaviour were determined for the multiphase films.

CP50

Instabilities and Correlations of an Elastic Lattice in a Random Potential.

Henrik Jeldtoft Jensen[1], Yves Brechet[2], Benoit Doucot[3], and Andrew Brass[4]

[1]The Niels Bohr Institute, Blegdamsvej 17,DK-2100 Copenhagen, Denmark.
E-mail: JENSEN@nbivax.nbi.dk
[2]LTPCM, ENSEEG, BP 75 Domaine Universitaire de Grenoble,
F-38402 St. Martin d'Heres, France
[3]CRTBT, CNRS, BP 166, F-38042 Grenoble Cedex 9, France,
[4] Dep. of Biochemistry and Molecular Biology,
University of Manchester, Manchester M13 9PT, United Kingdom.

Since the discovery of the high temperature superconductors in 1986 the interest for vortex lattices has been renewed. Many detailed experimental as well as theoretical studies of the structure and possible phases of the vortex system have been performed. Among experiments the Bitter patterns are the most pictorial indication that various regimes for the spatial correlations of the vortices can exist. Motivated by these remarkable results we have made model studies of one and two dimensional elastic lattices in a random background potential.

The study of the two dimensional case is focused on the breakdown of adiabatic continuation between the ideal lattice and the ground state as the random potential is gradually switched on. For a finite system a region exists in which the deformed lattice is analytically connected to the ideal lattice configuration. This region *vanishes* as the inverse square root of the number of particles. When the amplitude of the pinning potential is increased non-linear elastic instabilities occur as particles jump towards local minima of the background potential. As soon as the elastic instabilities occur the sequence of ground states obtained by the gradual change of the pinning strength is no longer reversible. The probability for a particle to undergo an instability grows rapidly with A_p. As A_p is further increased above a certain threshold topological defects are nucleated.

We have studied the spatial correlations of the lattice as it is adiabatically relaxed to the pinning potential. Although the random background induces elastic instabilities as well as mis-coordinated particles the long range order of the lattice is *preserved* when the random potential is switched on adiabatically. This finding contrasts previous investigations.

In order to gain a deeper understanding of the onset of instabilities and their effect on the properties of the system we also studied a linear harmonic chain which is pulled through a random potential. The chain undergoes instabilities connected with the jump from one metastable state to another. The energy released in such a process is found to be a random variable with a power law distribution: $D(E) \propto E^{-b}$, where $b \approx 0.8$. This model can be considered as a microscopic description of the phenomenological friction force included in earthquake models. Furthermore, the pinning force as function of position (or time) is measured and the power spectrum is found to behave as $1/f^2$. These properties are in qualitative agreement with experiments on solid friction.

CP51

Oxygen Ordering in YBCOx and GdBCOx A Study by Copper NQR and NMR[1]

Ivo Heinmaa[1] and Hans Lütgemeier[2]

[1] Institute of Chem. Physics and Biophysics, 10 Rävala pst, 200001, Tallinn, Estonia, [Fax:007-0142-440640],[E-mail:ivo@kbfi.tll.cw.su]

[2] IFF, Forschungszentrum Jülich, D-5170, Germany, [Fax:2461-61-2410],[E-mail:IFF021@DJUKFA11.bitnet].

The experimental determination of the oxygen order in the Cu(1) layer of the oxygen depleted YBCOx is a difficult task unless the local order of oxygen is a long range order. We have studied the copper NQR/NMR spectra at 4.2K and 1.2K in the series of YBCOx and GdBCOx ($6.0<x<7.0$) samples with the aim to investigate the oxygen ordering in these compounds[2].

The copper NQR spectra in oxygen deficient YBCOx have reported to be extremely complicated[3,4], for the overlapping of the lines from ^{63}Cu and ^{65}Cu isotopes from several sites in Cu(1) and Cu(2) layer. To separate the lines from the two copper layers we have used the GdBCOx compound, where the magnetic Gd^{3+} ions cause a rapid transverse relaxation of the copper nuclei in Cu(2) sites. This effect suppresses the Cu(2) lines in the spectra. The comparison of the Cu NQR and NMR spectra in YBCOx and GdBCOx and their development with the oxygen content enabled us to assign the different peaks in the spectra to the particular oxygen configurations in the Cu(1) layer.

In both systems the spectra show the existence of the ordered structure with alternating full and empty chains (ortho-II) in the oxygen concentration region $6.55<x<6.65$. At higher x the spectra do not show the presence of the domains with alternating of two full and one empty chain, instead, the spectra of the samples with $6.7<x<6.8$ indicate the coexistence of the ortho-II and 'diluted' ortho-I structure, proposed recently to explain the '60K plateau' on the Tc vs x curve[5]. The different preparation and annealing procedures show up only in the size of the ordered domains. The Cu(2) lines disappear in the spectra of the superconducting samples with Tc below the '60K plateau' values. This is attributed to the slowing down of the spin fluctuation at the Cu(2) sites. The sharp Cu(1) lines in these samples, however, prove that no magnetic order or spin glas state exists.

The quantitative analysis of the relative intensities of the Cu(1) lines allows us to estimate the average number of the oxygens per one Cu-O chain, n, shown in Figure. We found that in the '60K plateau' region the chains are comparatively short, hardly exceeding 10 oxygen atoms. As the condition for the onset of superconductivity we obtained that the filled chain fragments with a length about 6 are attached to filled fragments at the next nearest chain.

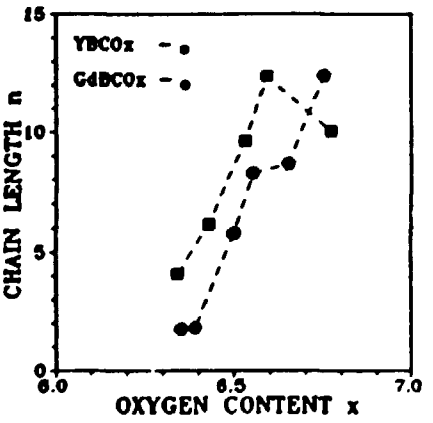

Fig. 1 Average chain length n in YBCOx and GdBCOx depending on the oxygen content x.

[1]This work has been supported by the DAAD financial aid.

[2]I.Heinmaa, H.Lütgemeier, A.Jánossy, S.Pekker, G.Krabbes and M.Buchgeister, J. Appl. Magn. Resonance, submitted.

[3]H.Yasuoka et al. Hyperfine Int. 49, 167 (1989).

[4]A.J.Vega et al. Phys. Rev.B39, 2322 (1989).

[5]C.F.Poulsen et al. Nature, 349, 594 (1991).

CP52

Y-Ba-Cu-O High T_c Superconductor Thin Film Preparation by RF Sputtering and Electron Beam Irradiation

J. Klavins, P. Cikmach, I. Eglitis, D. Klavins, A. Liepins, J. Pinnis and V. Purvinskis

Institute of Solid State Physics, University of Latvia, 8 Kengaraga St., 226063 Riga, Latvia

This paper reviews our investigations in the field of preparation and characterizing $YBa_2Cu_3O_{7-x}$ (YBCO) superconducting thin films. The films were prepared by two different methods - electron beam irradiation and RF sputtering. The substrate used were (100) oriented MgO wafers 10 x 10 x 0.5 mm size. The films were characterized from the structural, electrical and optical point of view. Standard 4-point technique was employed to measure the resistivity vs. temperature curves.

In the first method YBCO multilayer films were prepared in a HV-chamber using electron beam evaporation sources for Cu, Y and BaF_2. The quartz crystal film thickness and deposition rate meter controlled the evaporation rates of the components. The process parameters were as follows: target - substrate distance 25 cm, pressure in the vacuum chamber 8×10^{-3} Pa, substrate temperature 500 °C, average deposition rate 10 nm/min., film thickness 200 - 400 nm.

By RF sputtering the film growth has been performed from mosaic target of Y, Cu and BaF_2 with square ratio 1:2.47:3.42 or 1:1.5:2 in an Ar atmosphere at 7×10^{-1} Pa. The target diameter was 120 mm. In the process of sputtering the substrate heats to 100-170 °C. The target - substrate distance was 140 mm. The film thickness was between 400 and 900 nm and the growing rate was from 4 to 8 nm/min. Optical plasma monitoring of RF sputtering processes took place.

In order to improve crystallinity and to take away fluorine, the films were post annealed in the flow of humid oxygen at 850 °C for half an hour and after that half an hour in the pure oxygen to stabilize the equilibrium of oxygen concentration in the sample. This process was followed by cooling down with rate 5 °C/min and annealing at 450 °C to reach stoichiometric oxygen amount in the films. Such the films had 89 K temperature of the beginning of superconducting phase transition.

CP53

The Electron-phonon Coupling and Structural Phasetransitions in the Cuprate Superconductor

Anders Smith and Per Hedegård

Physics Laboratory, H. C. Ørsted Institute, University of Copenhagen,
Universitetsparken 5, DK-2100 Copenhagen Ø, Denmark
Fax: 45 31 35 06 28, Email: hedegard@nbivax.nbi.dk

All high-T_c superconductors are orthorhombic in the superconducting phase and several of them undergo a tetragonal to orthorhombic phasetransition when the chemical composition or the temperature is varied. To try to account for this in terms of a strongly-correlated Hubbard model used to describe the CuO_2-planes, we study a generalised Hubbard model including the lattice dyanmics.

We construct a general framework for calculating the dynamical matrix. Using an electronic mean-field approximation we identify two different mechanisms for phonon-driven structural instabilities in a strongly correlated electron gas, corresponding to fermionic and bosonic quasiparticles. For fermions the mechanism is a generalised Peierls-instability—nesting in a low-dimensional Fermi surface, while for bosons we find the analogue is scattering between two minima in the energy giving rise to a self-consistently determined deformationpotential.

While the nesting properties of the fermions are more or less destroyed away from half-filling, the bosons remain effectively one-dimensional. This means that to explain the structural phasetransitions that in e.g. $(La,Ba)_2CuO_4$ occur over a wide range of doping away from half-filling the present model indicates that the quasiparticles in the CuO_2-planes should be bosons (or more precisely: the spinons should be bosons and the holons fermions).

Calculations in both fermionic and bosonic mean field states are presented, and we show that the structural instabilities are present using realistic values of the parameters.

CP54

Functional properties of single crystals and Laser deposited thin films of cubic BKBO superconductors.[#]

J. Nogués, B.M. Moon, K.V. Rao

Department of Condensed Matter Physics
Royal Institute of Technology
100 44 STOCKHOLM, SWEDEN

Cubic bismuthate $Ba_{1-x}K_xBiO_3$ has been identified as a potentially attractive new class of "high T_c" superconductor. Although their T_c's are around 30 K, their cubic symmetry and the demonstrated SIS junction characteristics are found to be attractive for applications.

We present magnetic measurements on a 2x2x1 mm^3 single crystal of BKBO, from which the temperature and field dependence of the intrinsic critical currents have been determined. Low field magnetic data confirm the single crystal character of these samples. At helium temperatures we obtain J_c to be 1.8×10^4 A/cm^2. The functional character of the temperature and field dependence of Jc will be discussed. In addition, possible anisotropy effects in J_c studied from the angular dependence of magnetization measurements will be presented.

The thin films of BKBO were obtained by pulsed laser deposition from a stoichiometric target. The films exhibit rather sharp transition temperatures around 28 K and are highly oriented in the (100) or (110) direction on MgO, $SrTiO_3$, and $LaAlO_3$ substrates. The characteristics of the SIS (superconductor-insulator-superconductor) tunnel junctions obtained from two BKBO films as well as point contact tunneling data will be presented. From the tunneling data the energy gap is determined to be about 4.5 meV, giving a BCS-type gap value of $2\Delta/k_BT_c$ of 3.8-4.0. The current-voltage curve exhibits extremely low subgap conductance and is found to increase sharply at $2\Delta = 9$ meV. AC susceptibility analyses and SEM micrographs for some of the films will also be presented.

[#] This work is supported by Swedish funding agencies NFR-STU.

CP55

'IN-SITU' SUPERCONDUCTING Y-Ba-Cu-O THIN FILMS BY 'ON-AXIS' OBLIQUE INCIDENT RF MAGNETRON SPUTTERING.

Junhao Xu, B.M.Moon, Y.L. Zhou, Guo-Guang Zheng*, K.V.Rao,*

Department of Condensed Matter Physics
Royal Institute of Technology,
S-100 44 Stockholm, Sweden,

(*) Institute of Physics,Chinese Academy of Sciences
Beijing 100080, P.R. China.

High-quality superconducting $Y_1Ba_2Cu_3O_{7-x}$ thin films have been fabricated 'in situ' by on-axis reactive rf magnetron sputtering from a single planar stoichiometric 1-2-3 target at Ar-25% O_2 sputtering pressures as low as 2×10^{-2} mbars. By placing a grounded metallic mask between the target and the substrate during sputter deposition, negative oxygen ion sputtering is nearly eliminated and high quality c-axis oriented YBCuO thin films on $SrTiO_3$(100), and $LaAlO_3$ (100) substrates are routinely obtained with excellent reproducibility. The zero resistance superconducting transition temperatures Tc_0's of these films are as high as 91.5K with transition width ΔTc's (90-10%) of about 1K. A possible mechanism for the elimination of the resputtering effects in our technique is proposed. In addition, we present a modified geometry of the substrate, mask, and the target for growing large area YBCuO films. The transport properties of the on-axis deposited films described above have been studied by means of Hall effect and magnetoresistance measurements over a wide temperature range and especially in the vicinity of the superconducting transition. The non-linear magnetic properties of these films will be discussed along with the field and temperature dependence of the determined critical currents.

D : JOINT NORDIC SPRING MEETING '92

DFr : PHYSICS OF SMALL CLUSTERS WORKSHOP

DFrI

Experimental Investigations of Small Metal Clusters

S. Bjørnholm[§]

The Niels Bohr Institute, Blegdamsvej 17, Dk-2100 Copenhagen

A number of the basic insights and problems encountered in nuclear physics reappears in a new guise with other small systems composed of Fermi paritcles. Recent experimental progress in the study of alkali metal clusters will be presented and discussed in relation with the Balian-Bloch theory of shell and supershell structures.

[§] *Work done in collaboration with J. Pedersen, J. Borggreen, K. Hansen, B. Mottelson, H. Nishioka*

DFr2

NON-SPHERICAL SODIUM DROPLETS.

L.Lundsberg-Nielsen*), K.Lützenkirchen**), J.Pedersen, M.B.Nielsen, S.Bjørnholm, J.Borggreen and H.D.Rasmussen.

Niels Bohr Institute, Risø, 4000 Roskilde, Denmark.

Molten sodium drops form spheres due to the surface tension. For sufficiently small droplets, however the quantized valence electrons are able to break the symmetry and produce spheroidal shapes 1). The shape of the droplet - or cluster can be probed by measuring the splitting of the plasmon resonance peak.

The plasmon mode in a Na(N) cluster is described as a density wave excitation of the N valence electrons in the potential of the positive ions. In the classical , Drude formulation the resonance frequency is proportional to the density of excited electrons, which is a constant- to first order - for varying shape and size. For spheroidal (ellipsoidal) distortions there will be a polarizability for each of the three axes and the resonance peak will split into two (or three) peaks.

In a series of measurements at the Niels Bohr Institute the plasmon resonances are mapped for sizes $8 < N < 40$ in a frequency interval of 1.5 - 5 eV. Preliminary data indicate the existence of one or two resonance peaks for spherical and spheroidal clusters, repectively. The relative intensity in the case of two peaks shows whether the shape is oblate or prolate.

The figure shows the resonance of the Na(20)+ with 19 electrons, which is one off the closed N=20 shell 2). The two Lorentzian shapes fitted indicate a small oblate distortion.

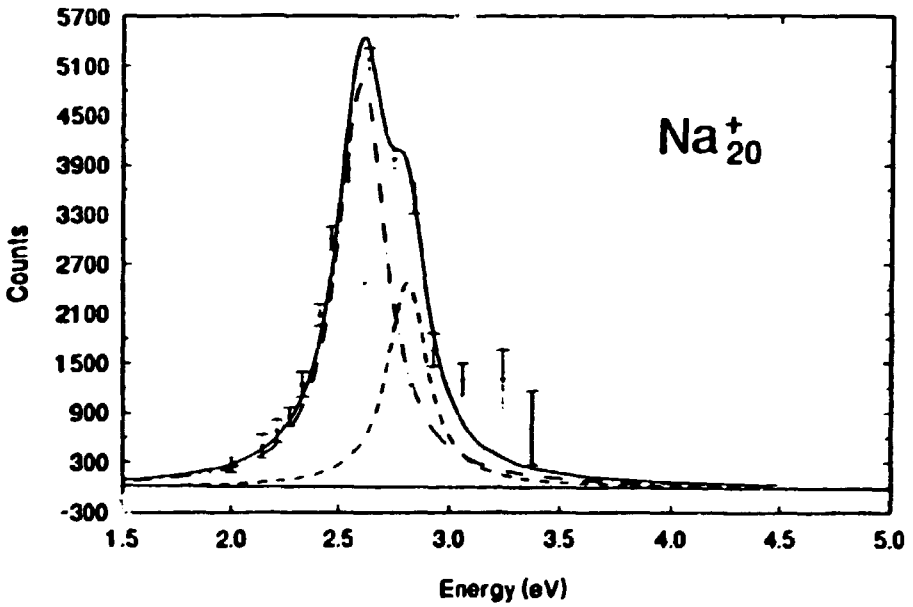

*) Danish Institute af Fundamental Metrology, 2800 Lyngby, Denmark.
**) Institute for Nuclear Chemistry, Univ. of Mainz, 6500 Mainz, Germany.

1) W.A.de Heer, W.D.Knight, M.Y.Chou and M.L.Cohen, Sol.State Phys. 40(1987)93.
2) J.Pedersen, S.Bjørnholm, J.Borggreen, K.Hansen, T.P.Martin and K.Hansen, NATURE 353(1991)733.

DF-1

On the electronic structure and geometry of metal clusters

J. Mansikka-aho, S. Valkealahti, M. Koskinen
M. Manninen, J. Timonen, E. Hammarén, P. O. Lipas
Department of Physics, University of Jyväskylä
P.O. Box 35, SF-40351 Jyväskylä, Finland

An outline of the cluster research in Jyväskylä is given. The work on cluster magnetism is described in an separate abstract.

1. *Electronic structure of large nonspherical clusters* is studied using two simple models, the tight binding (Hückel) model and the free electron model[1]. The results show that the icosahedral cluster has the same shell structure as spherical cluster when the cluster has less than about 1000 atoms. By studying the quadrupole deformations we have shown that surface waves in spherical liquid clusters have only a minor effect on the shell structure.

2. *The effect of the surface roughness on the level spacing* close to the Fermi energy has been studied using a tight binding model (with s and p-electrons in each atom) and an fcc lattice gas model for the cluster[2]. A Monte Carlo sampling was used to create the cluster ensemble at different temperatures. Above the melting temperature a Wigner distribution was found for the level spacing. The width of the distribution increases with cluster size and approaches the asymptotic limit $4\epsilon_F/3N$. No shell structure has been found close to the Fermi level of the spherical clusters in the lattice gas model.

3. *Molecular dynamics* using many-atom potentials of the effective medium theory is used to study the equilibrium geometry and dynamics of large copper clusters. Cuboctahedral clusters are found to be unstable, and they spontaneously transform to icosahedra[3]. The melting temperature of the clusters has been found to follow the simple rule $T_N = C_N T_m / C_0$, where T_m is the bulk melting temperature, and C_N and C_0 are the average coordination numbers of the clusters and of the bulk, respectively.

4. *The nuclear shell model* is used to study the electronic structure of spherical jellium clusters[4]. It seems that only for clusters with less than nine atoms the exact ground state energies can be obtained. The results for the smallest clusters indicate that the local spin density approximation is very accurate for the ground state. Calculation of the photoabsorption spectra show that the the two-peak structure of the 9 and 10 atom clusters can result directly from many-body effects and no deformation of the spherical shape is needed.

1. J. Mansikka-aho, M. Manninen and E. Hammarén, Z. Phys. D 21, 271 (1991), and Preprint JYFL 29 (1991).
2. J. Mansikka-aho, M. Manninen and E. Hammarén, to be published.
3. S. Valkealahti and M. Manninen, Phys. Rev. B (in press).
4. M. Koskinen, P. O. Lipas, E. Hammarén and M. Manninen, Preprint JYFL 6 (1992).

DFt4

Theory of the Structure of Clusters

J. Norskov

Laboratory of Applid Physics, The Technical University of Denmark, 2800 Lyngby

DFr5

Atomic Imaging in Real Time of Small Metal Clusters

L.R. Wallenberg

Nat. Center for High Resolution Electron Microscopy, Inorganic Chemistry 2, Chemical Center, Box 124, S-221 00 Lund, Sweden [Fax: +46-46 10 45 25]

When small metal particles (50-500 atoms) are heated, e.g. by inelastic scattering of the incident electron beam in a high resolution electron microscope, they undergo rapid structural rearrangements even well below the melting point. This was first discovered for gold[1], but has subsequently been shown for other fcc and hcp metals, such as Pt, Rh, Ru and Cd.

The rate at which the series of abrupt transformations occur can be controlled by changing the beam current density. Normally, 10-80 A/cm^2 was sufficient to go from atom hopping only at the surface, to a complete rearrangement involving all atoms. To confirm the temperature as the main cause of motion and shape changes, complementary experiments were performed in a 100 kV electron microscope equipped with a heating holder[2]. The beam current density was kept as low as approx. 1 A/cm^2 and an onset of particle motion was found at 470°C for gold.

Fig. 1 shows a series of single-frame images of a gold particle, recorded in a dedicated 400 kV high resolution electron microscope (0.16 nm resolution limit). The images were selected with a few seconds interval from a real-time video tape, recorded with an image intensified TV-camera, attached to the microscope.

A short video, highlighting events like surface column hopping, shape and structure changes, surface cloud formation and coalescence will be shown during the lecture.

Fig. 1. a) 20 Å gold par..le,on amorphous carbon support, with an outline and structure image corresponding to a cubeoctahedron of ccp, viewed along <110>. Some asymmetric truncation propable.
b) {111} surfaces has grown at the expence of {100} surfaces, giving a shape close to the "equilibrium" shape, obtained from Curie-Wulff construction. Each black dot represents atomic columns, projected along the beam direction and separated by 2.5 Å.
c) The particle has rotated to the <100> projection. d_{200}= 2.0 Å (orthogonal fringes)
d) Twin planes have been introduced to give a decahedral multiply twinned particle with close to pentagonal symmetry.

---

[1]L.R. Wallenberg, J.-O. Bovin and G. Schmid, Surface Sci. 156, 256 (1985).
[2]D.J. Smith, A.K. Petford-Long, L.R. Wallenberg and J.-O. Bovin, Science, 233, 872 (1986)

DFt6

Cluster magnetism

J. Merikoski, E. Viitala, M. Manninen and J. Timonen

Department of Physics, University of Jyväskylä

P.O.Box 35, SF-40351 Jyväskylä, Finland

We give a brief review of the observed properties of ferromagnetic Fe and Ni clusters. Generic properties of the various theoretical models which have been proposed will be discussed, and we shall give a qualitative argument for why Ising model[1,2] can be used in this context.

We have also determined[3] the exact magnetization of antiferromagnetic Ising clusters for up to 27 spins. There is a clear distinction between frustrated and unfrustrated antiferromagnetic structures, and we shall make a number of predictions which may be subjected to experimental verification (provided frustrated antiferromagnetic clusters can be produced).

1. J. Merikoski, J. Timonen, M. Manninen and P. Jena, Phys. Rev. Lett. 66, 938 (1991)
2. J. Merikoski, M. Manninen and J. Timonen, in *Physics and Chemistry of Finite Systems: From Clusters to Crystals*, P. Jena, S.N. Khanna and B.K. Rao (eds.), Kluwer Academic Publs., Boston (in press)
3. J. Merikoski, E. Viitala, M. Manninen and J. Timonen, to be published

DFr7

Magnetic properties of clusters

P.V. Hendriksen[a], S. Linderoth[a] and P.-A. Lindgård[b]

[a]Laboratory of Applied Physics, Technical University of Denmark, DK-2800 Lyngby, Denmark, [Fax: 45932399], [e-mail: Hendrik@ltf.dth.dk]

[b] Risø National Laboratory, DK-4000 Roskilde, Denmark, [Fax 42370115], [e-mail: PAL@risoe.dk]

The magnetic properties of clusters have recieved much interest lately - experimentally [1] as well as theoretically [2 3 4]. We have evaluated the effects of the finite size on magnetic properties such as the temperature dependence of the magnetization and the Curie temperature. The exchange interaction is modelled with the Heisenberg model, and the spin-wave spectrum is found by a direct diagonalization of the equation of motion of the spin deviation, S^+.

In the case of a bulk material the translational invariance allows the equation of motion to be diagonalized by a Fourier transformation. In the case of a finite system, however, q is no longer a good quantum number and the equation of motion must be solved in the real space. This is illustrated in the figure. To the left the scattering intensity $S(q,E)$ for q along the [111] direction for a 55 fcc spin cluster is given, demonstrating the discrete energy levels and the distribution in the q-space. On the right is shown the corresponding δ-function dispersion curve for the bulk.

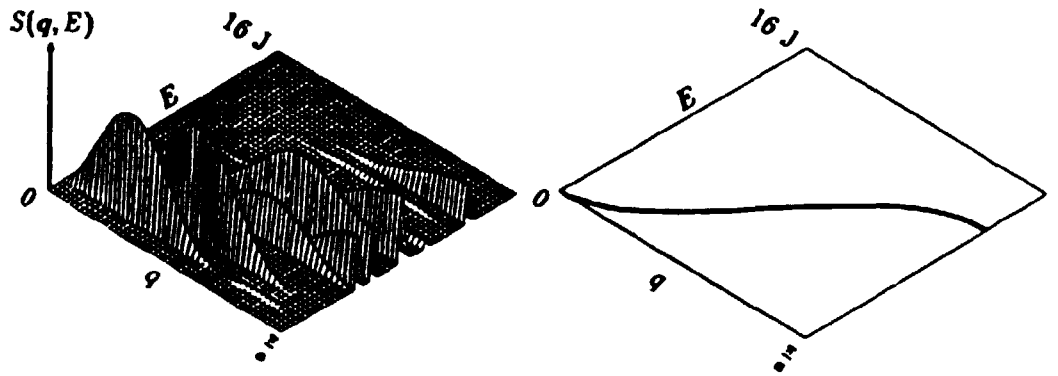

As the size of the cluster increases the energy spacing between the eigenstates decreases, the energy gap between the first state and 0 becomes smaller, and the distribution in the q-space narrows approaching the bulk dispersion curve.

The finite size is found to cause the magnetic properties of clusters to be markedly different from those of the bulk. The temperature dependence of the magnetization of the clusters deviate substantially from the bulk $T^{3/2}$-law yielding an exponential behaviour at low temperature and approximately a T^2 dependence at higher temperature. This is due to the energy gap in the spin wave spectrum (caused by the finite size limiting the number of degrees of freedom) and due to the lack of coordination at the surface. This also leads to a lowering of the Curie temperature. The effects have been studied as a function of size for fcc and bcc structured clusters ranging in size from 9 to 749 spins.

[1] W.A. de Heer, P. Milani, and A. Chatelain, Phys Rev. Lett. 65, 488 (1990)
[2] J. Meioksi J. Timonen, M. Manninen, and P. Jena, Phys Rev. Lett. 66, 938 (1991)
[3] S. N. Khana, S. Linderoth, Phys. Rev. Lett. 67, 742 (1991)
[4] P. V. Hendriksen, S. Linderoth, and P.-A. Lindgård, J. Magn. Magn. Mater. (in press)

DFr8

Superparamagnetic clusters and particles[1]

Søren Linderoth

Laboratory of Applied Physics, Technical University of Denmark, DK-2800 Lyngby, Denmark, [Fax: (+45) 4593 2399], [E—mail: linderot@ltf.dth.dk].

The direction of the magnetization vector in ferromagnetically ordered single-domain clusters will, at sufficiently high temperatures, fluctuate between easy directions, i.e., the clusters may be viewed as paramagnetic atoms having very large (super) magnetic moments (equal the number of atoms in the particle times the magnetic moment per atom). The superparamagnetic relaxation can be descibed by an Arrhenius law with a relaxation time given by $\tau = \tau_0 e^{KV/k_B T}$, where $\tau_0 \approx 10^{-10} - 10^{-13}$ s and KV is the magnetic anisotropy energy. When τ is shorter than the 'measuring' time (τ_m) the clusters act superparamagnetically. We will discuss different studies, performed by Mössbauer spectroscopy and magnetization measurements (Stern-Gerlach and SQUID set-ups), where superparamagnetic relaxation phenomena have been observed recently. The three techniques above have τ_m's of about 10^{-9} s, 10^{-4} s, and 10^{+2} s, respectively.

For free clusters of Fe_N and Co_N (N = 10–300) the magnetic moment *per atom* have in Stern-Gerlach measurements been observed to increase linearly with size and applied magnetic field (H)[2,3]. The measured moment per atom were found to be much below the bulk value. The results can be explained[4] if the clusters are assumed to behave superparamagnetically. From an analysis of published experimental data the true magnetic moment per atom in Fe_N and Co_N clusters can be deduced to be 10–50 % larger than for bulk.

For Fe clusters the magnetic moment per atom has been observed to *increase* with increasing temperature[1], which may seem somewhat surprising. However, a similar behaviour can be observed when studying magnetic particles in a SQUID magnetometer[5]. This will demonstrated for ultrasmall Fe-C particles where the magnetization is seen to increase with temperature at the lowest measuring temperatures. Above the blocking temperature for superparamagnetic relaxation the magnetization decreases following a Langevin function. The same particles also reveal superparamagnetic relaxation in Mössbauer studies, but at somewhat higher temperatures — a consequence of the difference in τ_m. Combination of the Mössbauer and the magnetization measurements allows an estimate of τ_0 and KV to be given.

---

[1] Part of work done in collaboration with groups in USA, Spain and Denmark.

[2] W.A. de Heer, p. Milani, and A. Chatelain, Phys. Rev. Lett. 65, 488 (1990).

[3] J.P. Bucher, D.C. Douglass, and L.A. Bloomfield, Phys. Rev. Lett. 66, 3052 (1991).

[4] S.N. Khanna and S. Linderoth, Phys. Rev. Lett. 67, 742 (1991).

[5] S. Linderoth et al., to be published

DFr10

Structural investigations of C_{60}

Jakob Bohr

Department of Solid State Physics, Riso National Laboratory, DK-4000 Roskilde, Denmark, [Fax +45-42370115], [E-mail: BOHR@RISOE.DK]

An introduction is given to C_{60}, also called Buckminsterfullerene. This exiting new material has already lead to the discovery of novel high transition superconductors such as K_3C_{60}. Synchrotron x-ray diffraction of single crystals of C_{60} will be presented[1]; the type of crystalline order as well as the structure of the C_{60} cluster will be discussed. The x-ray experiment agrees with nuclear magnetic resonance data and theoretical calculations. A list of references of overview's are to be find below[2345,6]. Likewise, references to two important (original) papers are given[7,8]. The figure depict the geometrical structure of C_{60} as adapted from Ajie et al[9]

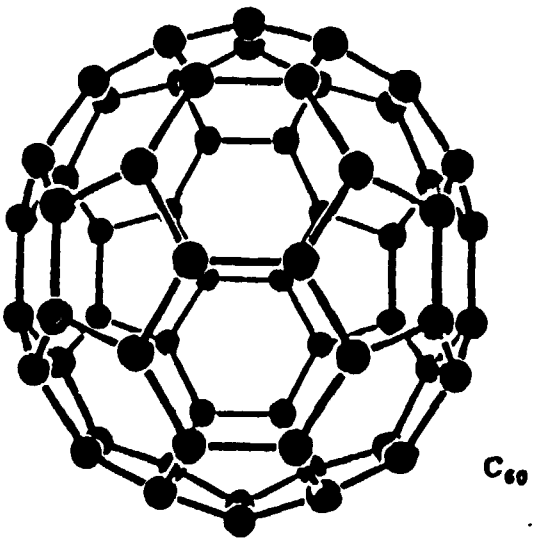

C_{60}

[1]Order, Di. order and Structure of Crystals of C_{60}/C_{70}, J. Bohr, D. Gibbs, S.K. Sinha, W. Krätschmer, G. Van Tendeloo, E. Larsen, H. Egsgaard and L.E. Berman, Europhys. Lett. 17, pp. 327 (1992).

[2]Fullerenes, R.F. Curl and R.E. Smalley, Scientific American, pp. 32, October (1991).

[3]C_{60}:Buckminsterfullerene, H.W. Kroto, A.W. Allaf, and S.P. Balm, Chemical Reviews, vol. 91, pp. 1213 (1991).

[4]Space, Stars, C_{60}, and Soot, H. Kroto, Science, vol. 242, pp. 1139 (1988).

[5]Great balls of carbon, J. Baggott, New Scientist, pp. 34 (1991).

[6]Solid C_{60}, D.R. Huffman, Physics Today, pp. 22, November (1991).

[7]C_{60}:Buckminsterfullerene, H.W. Kroto, J.R. Heath, S.C. O'Brien, R.F. Curl and R.E. Smalley, Nature, vol. 318, pp. 162 (1985).

[8]Solid C_{60}:a new form of carbon, W. Krätschmer, L.D. Lamb, K. Fostiropoulos and D.R. Huffman, Nature, vol. 347, pp. 354 (1990).

[9]Characterization of the Soluble All-Carbon Molecules C_{60} and C_{70}, H. Ajie, M.M. Alvarez, S.J. Anz, R.D. Beck, F. Diederich, K. Fostiropoulos, D.R. Huffman, W. Krätschmer, Y. Rubin, K.E. Schriver, D. Sensharma and R.L. Whetten, J. Phys. Chem. 94 pp. 8630 (1990).

DFr11

Many-electron Effects in Models of C_{60} and M-C_{60}, M=Cs,Ba,La: Collective Response and Molecular Effects in Optical Conductivity.[1]

Göran Wendin

Institute of Theoretical Physics,
Chalmers University of Technology, S-412 96 Göteborg, Sweden,
Fax: -46-31-416984, E-mail: wendin@fy.chalmers.se

In the present work we model the C_{60} molecule as a spherical shell with a spherical-well potential. This should be a reasonable approximation for describing the main features of the electronic single-particle and collective excitation spectrum, e.g. optical conductivity, photoionization[2] and EELS[3]. In this way we lose the detailed atomic structure but we retain essential features of σ, π, δ etc. electrons in the radial node structure across the well. In contrast, the angular node structure will not be commensurate with the lattice structure of C_{60} but will represent free electrons.

So far calculations have been performed for the inner-shell 4d-photoionization cross section of a spherical-shell C_{60} molecule with a Ba or La atom at the centre, using a modification of the local-density-random-phase-approximation (LDRPA) approach described in Ref. 4. The 4d-*f* giant dipole resonance, which is resonant in the Ba inner-well potential, now also shows pronounced modulation effects (NEXAFS) over a wide energy range due to resonant behaviour and multiple scattering of the f-continuum wave in the C_{60} ligand outer-well region.

The work is now being extended to inclusion of the dielectric response of the valence shell of C_{60} and M-C_{60} in order to model the optical conductivity and EELS in the 0-50 eV region. Preliminary results will be presented at the Conference.

---

1. Work supported by the Swedish Natural Science Research Council.
2. J.H. Weaver et al., Phys. Rev. Lett 66, 1741 (1991).
3. E. Sohmen, J. Fink and W. Krätschmer, Z. Phys. B 86, 87 (1992).
4. G. Wendin, Phys. Rev. Lett. 53, 725 (1985).

DSa : SOFT CONDENSED MATTER PHYSICS

WORKSHOP

DSa1

Computer Simulation of Langmuir-Blodgett films

D.J. Tildesley[§], K.S. Kim[§], and N. Quirke[‡]

[§] Department of Chemistry, The University of Southampton, S09 5NH, U.K., [Fax: +44 703 593781], [Email: D.J.Tildesley @ mail.soton.ac.uk]

[‡] N.Quirke, BP Research Centre, Chertsey Road, Sunbury on Thames, Middlesex TW16 7LN, U.K.,
[Fax: +44 932 763959]

Molecular dynamics and energy minimisation calculations have been performed to calculate the structure and thermodynamic properties of Langmuir-Blodgett monolayers and bilayers of stearic acid adsorbed on a graphite surface[1,2] at room temperature and a variety of head-group areas per molecule (A_m).

The energy minimisation calculations show that compressing the adsorbed layer causes a change in the molecular tilt. The united-atom model does not reproduce this phase transition at a reasonable head-group area per molecule as observed in the surface pressure-area isotherm. The united-atom model with $\sigma = 3.923$Å and $\epsilon/k_B = 72.0$K, which has been used in the studies of liquid alkanes, and lipid bilayers, predicts that the molecular tilt occurs at $A_m = 17.6$Å^2 which is higher than the normal solid densities of all forms of crystalline stearic acid. An explicit-hydrogen model, with methylene groups represented by three interactions sites, predicts the phase transition observed in the surface pressure-area isotherm at a molecular area of approximately 21Å^2. The monolayer exhibited a molecular tilt of about 30° with respect to the surface normal at $A_m > 21$Å^2. On further compression the layer changes its molecular tilt from 30° to 0° over a small range of density. The inclusion of the electrostatic interactions between the head-groups in the all-atom model does not have a significant influence on the minimum energy structure since the configurational energy of the film is dominated by the intermolecular Van der Waals interactions which account for more than 90% of the total energy of the layer. The minimisation calculation using the all-atom model shows a molecular tilt transition at $A_m = 20.7$Å^2. The energy minimisation of the bilayer with a head-to-head structure shows that there is a strong correlation in the translational and orientational structure of the two layers. The detailed structure of each layer in the bilayer is quite similar to the minimum energy structure of the monolayer at the same density.

We have performed molecular dynamics simulations of the monolayers at $A_m = 20.79$Å^2 and $A_m = 21.2$Å^2 to predict the structure and dynamics of the layer at 300K using the explicit-hydrogen model. These simulations also predict a change in the molecular tilt at a molecular area of around $A_m = 21$Å^2. The layer shows no tilt at $A_m = 20.79$Å^2 and a tilt of approximately 9° at $A_m = 21.2$Å^2 with the molecules pointing to their next-nearest-neighbours in a triangular solid structure. The molecular tilt of 9° at $A_m = 21.2$Å^2 is significantly smaller than the value of 32° obtained from the energy minimisation. The difference in the molecular tilt is predominantly due to the increase in the effective density of the layer caused by the lateral thermal vibrations of the molecules in the plane of the surface. The radial distribution function of the centres of masses of the molecules is solid-like while the densities at which we performed the simulation are normally labelled as a liquid regime in the surface pressure-area isotherm

of the Langmuir monolayer of stearic acid[1]. The stearic acid molecules in the layer exhibit conformational defects at 300K. The defects are located mainly at the top and bottom of the layer and exhibit significant intermolecular and intramolecular correlations. The layer also shows long lived co-operative motions involving simultaneous changes in the molecular tilt and the azimuthal orientation, which arise because of the relatively small molecular tilt in the layer.

We have also performed molecular dynamics simulations of the explicit hydrogen model with an additional electrostatic interactions between the dipoles of the head-groups and between the head-group diploe and the surface (the all-atom model)[3]. The layers exhibit well-ordered structures with similar orientational properties to those obtained from the monolayer using the explicit-hydrogen model. The radial distribution functions of the centres of masses of molecules are solid-like and the centres of masses of molecules have well-ordered in-plane hexagonal structure (hexatic order parameter = 0.8±0.02). The layers show significant conformational disorder at the C-C bond connecting the carboxylic acid group and alkyl tail group even in the layer with A_m = 20.6Å^2. Such a gauche defect is found in the stearic acid crystal form B, which has a head-group area of 20.7Å^2. The layer with A_m=20.6Å^2 has a negligible molecular tilt of 2.4° but the layer with A_m=21.2Å^2 has a molecular tilt of 18.8°, which is more than twice the molecular tilt obtained using the explicit-hydrogen model at the same density. The structure factor S(k) for the monolayer is dependent on the size of the tilt, the rotation around the long axes of the molecule and the direction of the molecular tilt in the layer. The structure factor for the layer with A_m=20.6Å^2 shows two strong and four weak peaks while the structure factor for the layer with A_m=21.2Å^2 shows four strong and two weak peaks due to the tilting towards next-nearest-neighbour in the layer. The dipolar interactions in the layer have an effect on the precise orientation of the molecules although the overall orientation of the layer is controlled by the inter-chain non-bonded interactions. The dipoles are aligned head-to-head in a plane parallel to the surface. A study of the dynamics of the layer shows that the broad peak in the density of states in the region of $0<\omega<150$ cm^{-1} is due to the translational motion of the molecules and that sharp peaks in the range 200 cm^{-1} to 500 cm^{-1} are mainly due to valence angle flexing.

Finally, we report the results of the molecular dynamics simulation of a bilayer film of stearic acid. The most important feature of the bilayer is the very strong correlation of the orientational and translational structure and the dynamics of molecules in the two layers because of the strong electrostatic interactions between the head-groups in this geometry. As in the monolayer the radial distribution function of the centres of masses is solid-like while the distributions of head and tail groups are liquid-like, because of the conformational disordering at the top and bottom of the molecule. The dipoles are oriented parallel to the surface in a two-sublattice structure, which changes to a one-sublattice structure at lower densities.

---

[1] R.A. Hann, *Langmuir-Blodgett Films*, Edited by G. Roberts, 1990 Plenum Press, New York.
[2] M.A. Moller, D.J.Tildesley, K.S. Kim, and N. Quirke, J. chem. Phys, 94, 8390 (1991).
[3] K.S. Kim, M.A. Moller, D.J. Tildesley, and N.Quirke, Molec. Phys, *submitted for publication*, (1992).

DSa2

A GINZBURG-LANDAU MODEL FOR TERNARY MIXTURES CONTAINING SURFACTANTS

M. Laradji, H. Guo, M. Grant, and M.J. Zuckermann

Centre for the Physics of Materials and Physics Department, McGill University, Rutherford Building, 3600 University Street, Montréal, Quebec, Canada H3A 2T8

The phase behavior of ternary systems containing surfactants was investigated by means of a Ginzburg-Landau model. The free energy functional for the model is given in terms of two scalar fields representing the local difference in concentration between water and oil and the local surfactant concentration. A term describing the interfacial curvature due to the surfactants is explicitely included. We have investigated this model using mean field theory for the equilibrium phase behavior and Langevin simulations to examine the effect of fluctuations. From mean field theory, we found an oil-water coexistence region, a lamellar phase and a micro-emulsion region in the disordered phase. The same phases were found in the Langevin simulations. The micro-emulsion region was characterized by the appropriate structure factor. We have also investigated the tricritcal behavior of this system and we have discovered that a Lifschitz tricritical point occurs for certain parameters of the model. When fluctuations were included, we used the method of Toner and Nelson to locate the transition from the micro-emulsion region to the lamellar phase in two dimensions. The result was found to agree with Langevin simulations of the model. We also discuss the effect of spontaneous curvature on the micro-emulsion structure in two dimensions.

General
Oral

DSa3

NEUTRON SCATTERING FROM CRITICAL FLUCTUATIONS IN A NEMATIC LIQUID CRYSTAL

T. Riste and K. Otnes
Institutt for energiteknikk, N-2007 Kjeller, Norway

In a seminal paper in 1969, de Gennes showed that the strong scattering of light from a nematic liquid crystal is due to critical, long-wavelength thermal fluctuations of orientation. The fluctuations are strongly damped by viscuous terms, and are predicted to be relaxational. We have performed some neutron scattering experiments in order to (a) characterize the nematic phase relative to the adjoining solid and isotropic liquid phases, and to (b) search for oscillatory orientational fluctuations, not contained in the de Gennes theory.

(a) Several time series of the neutron scattering intensity from a nematogenic sample in its different thermodynamic phases (solid, nematic, isotropic liquid) and hydrodynamic conditions (quiescent, convecting) have been analyzed by the rescaled-range method to give the Hurst exponent H for the temporal dependence of the variance and the β-exponent for the frequency dependence of the power specrum. In the nematic phase, in zero external field, we find[1] $H = 0.74$ and $\beta = 2.47$, satisfying the scaling relation $\beta = 2H + 1$. In the solid and isotropic liquid phases we find $H \sim 0.5$ and $\beta \sim 2$, indicating that only the nematic state is selforganized critical.

(b) In an initially aligned nematic sample we have studied the distortions after the aligning field had been reduced. The time series reveals a set of persistent, oscillatory modes whose periods are of the order of the relaxational times predicted by the de Gennes theory. In order to be able to draw any definite conclusion as to the origin of these oscillations, more experiments are being performed.

---

[1] K. Otnes and T. Riste, Physica Scripta (in press)

DSa4

Block Polymer in Aqueous Solution: Micelle Formation and Crystallization.

Kell Mortensen[a], Jan Skov Pedersen[a], and Wyn Brown[b]

[a] Physics Department, Risø National Laboratory,
DK 4000 Roskilde, Denmark
(Fax: +4542370115, E-mail: mortensen@risoe.dk)

[b] Inst. Phys. Chem. Uppsala University
Uppsala, Sweden

The structural properties of PEO-PPO-PEO block copolymers dissolved in water have been studied by small-angle neutron scattering. [1] Three different phases appear. At low-temperature (T<15°C) the block-copolymers are dissolved as individual Gaussian chains (unimers). At intermediate temperatures, the hydrophobic nature of PPO cause aggregation into a liquid of micelles. At even higher temperature (T>36.5°C) the micellar liquid 'freezes' into a crystalline powder. The structure factor of the micellar liquid follows that of interacting hard spheres, with a volumen fraction which increases linearly in temperature untill it reaches a critical value, ϕ_c, at which the micellar liquid crystallizes in a body-centered cubic structure. The bond correlation length of this crystal is, however, only of quasi-long range order. Application of shear to the crystalline powder abruptly transforms the powder into a single crystal, with macroscopic orientational order. These findings strongly indicate that the crystalline state is cubatic.

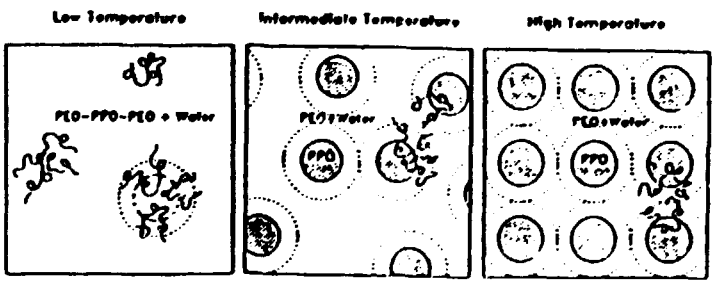

[1] K. Mortensen, W. Brown, and B. Nordén, submitted for publication

DSa5

Theoretical modelling of structure in charged micellar solutions with applications to SANS.

Per Linse

Physical Chemistry 1, Chemical Center, University of Lund,
P.O. Box 124, S-221 00 Lund, Sweden
Fax: Int+ 46 46104413,
E-mail: FK1PLI@KANDINSKY.FKEM2.LTH.SE

The structure of an asymmetric electrolyte has been calculated by means of molecular dynamics simulations and integral equation techniques.[1,2] The charge asymmetry of the electrolyte is 1:20 which corresponds to small micelles formed by ionic amphiphiles. The structure has been used to assess the accuracy of approximative statistical methods as the mean spherical approximation (MSA), the hypernetted-chain (HNC), and the Rogers-Young (RY) equations as well as more simplified models like the one-component model with an electrostatically screened micelle-micelle interaction.[3]

An important conclusion is that the inherent approximations of the MSA and HNC theories cause the micellar charge currently extracted from small-angle neutron scattering (SANS) experiments to be smaller than the nominal one. Thus, the extracted micellar charge should be viewed as a purely fitting parameter and a value smaller than the nominal one does not necessarily imply an incomplete ionization of the counterions from the micelle, as previously suggested in the literature.

1. J. P. Hansen and I. R. McDonald "Theory of Simple Liquids", Academic Press, London, 1976.
2. P. Linse, J. Chem. Phys. 94, 3817-3828 (1991).
3. P. Linse, J. Chem. Phys. 94, 8227-8233 (1991).

DSa6

Hydrophobic Aggregation in Aqueous Solutions

Anders Wallqvist

Physical Chemistry 2, Chemical Center, POB 124
S-22100 Lund, Sweden, [Fax: int+46 46 104543],[E--mail:fk2awe@beckmann.fkem2.lth.se]

Computer simulations of an initially disordered molecular fluid composed of water and methane exhibits a phase-separation into a cylindrical core of methane molecules surrounded by an aqueous phase[1]. Earlier studies of the potential of mean force between two methane particles in aqueous solutions have never revealed any tendency for hydrophobic aggregation. Thus the systems studied here confirms the importance of many-body effects in hydrophobic assemblies[2]. Properties of the solution indicate only minor perturbances of the interfacial water relative to the bulk water, belying the notion of any specific character of bound water associated with hydrophobic hydration. Instead the remarkable property of water is just the ability of being "liquid" water everywhere. Water does not penetrate into the hydrophobic part of the system, and only a few hydrocarbon molecules are solvated in the aqueous phase.

A water/methane/methanol system[3] also supports two phases, with only a weak preferential solvation of the methyl part of methanol into the hydrocarbon core region. The solvation of methanol in the hydrocarbon core is enhanced by increased pressure, i.e. the hydrogen bonded network of water becomes a less flexible for the only partially polar alcohol molecules and expells them into the hydrocarbon phase. For pressures below ≈10 kbar water retains its tetrahedral structure and it is only for these systems that we observe the phase separation of hydrophobic and hydrophilic molecules. At sufficiently high pressure the phase separation is inhibited by a formation of small methane clusters into water cavities or clathrates.

---

[1] A. Wallqvist, J. Phys.Chem. 95, 8921 (1991).

[2] A. Ben-Naim, *Hydrophobic Interactions*; Plenum Press, New York, (1980).

[3] A. Wallqvist, Chem. Phys. Lett. 182, 239 (1991).

DSa7

On the Origin of Complex Phase Behaviour in Block Copolymer Melts

[1]K. Almdal, [2]K. Mortensen, [3]K.A. Koppi and [3]F.S. Bates

[1]Materials Department, [2]Solid State Physics Department, Risø National Laboratory, Denmark

[3]Department of Chemical Engioneering and Materials Scinece, University of Minnesota, USA

In a recent publication[1] we have identified a complex phase behaviour in a poly(ethylene-propylene)-poly(ethylethylene) (PEP-PEE) diblock copolymer where the volume fraction of PEP, f, is 0.65. Four distinct phases exist as a function of temperature. These findings are inconsistent with the generally accepted concept of universal block copolymer phase behaviour based on f and χN alone, where χ and N are the Flory-Huggins interaction parameter and degree of polymerization, respectively. A prominent feature of the PEP-PEE block copolymer system is the asymmetry in block coil dimensions (i.e the difference in the statistical segment length between the blocks). For equal molar mass the radius of gyration of a PEP homopolymer is 44% larger than a corresponding PEE homopolymer. As the volume of the domains in a microstructure is fixed by the overall composition the packing problem presented by the asymmetry in block coil dimension cannot easily be relieved. For example, a compositionally symmetric (f=0.5) lammelar morphology may not accommodate a molecule highly asymmetric with respect to block coil dimension, leading to the development of alternative morphologies.

In this paper we examine the robustness of the complexity in the phase behaviour in the PEP EE system at f=0.65. The value of M_w/M_n is increased by mixing two f=0.65 PEP-PEE samples with different molar mass. Differences in the block length distribution are another possible perturbation of the system which is introduced by mixing two PEP-PEE block copolymers of equal molar mass but with f=0.53 and f=0.75, respectively in such a manner that the overall composition is f=0.65. A third sample in which both M_w/M_n is increased and the block length distribution is modified is obtained by mixing two PEP-PEE samples with different composition and molar mass to obtain the overall composition f=0.65. These samples were investigated using small-angle neutron scattering (SANS) and rheological measurements. The evaluation of ordered phase structure was facilitated by the introduction of long range order using a shear orientation technique. The order-disorder and order-order transitions were identified based on discontinuities in the dynamic elastic modulus and SANS pattern symmetries. At the lowest temperature all these samples exhibit a lamellar phase. At intermediate temperatures the behaviour differs between the samples. At the highest temperature a fluctuating disordered state exists in all the samples. A general result is that perturbations of the block length distribution decrease the complexity in the phase behaviour whereas increasing the overall M_w/M_n does not.

1: K. Almdal, K.A. Koppi, F.S. Bates, K. Mortensen, *Macromolecules*, 25, 1743 (1992)

DSa8

Monolayers at Liquid Surfaces: 2D Systems on a Smooth Substrate

K. Kjær

Physics Department, Risø National Laboratory, DK-4000 Roskilde, Denmark

Amphiphilic organic molecules (which have one hydrophilic and one hydrophobic end) may form socalled *Langmuir films*: Monolayers at the air-water interface[1]. The physics of such quasi-2D systems may be influenced by variation of surface density, surface pressure, temperature, surface charge etc.

We report on X-ray and neutron scattering studies[2] of structures and phase transformations in Langmuir films at the water surface.

Information on the z-variation of the monolayer structure results from specular X-ray reflectivity measurements (vertical scattering vector $\mathbf{Q} = (0,0,Q_z)$). The reflectivity can be measured on an absolute scale and then compared to calculations based on model structures. Further, comparison of neutron and X-ray reflectivity data allows the use of *contrast variation* techniques (H_2O/D_2O; $(CH_2)_n/(CD_2)_n$; and X-rays/neutrons). Also, in some cases, the measured signal can be directly inverted to give an un-biased estimate of the vertical monolayer structure.[3]

The lateral positional order in the film can be characterized by measurement of the horizontal scattering. For a monolayer, Bragg peaks seen at horizontal scattering vectors $\mathbf{Q}$ extend as *Bragg rods* in the Q_z-direction. The intensity variation along the Bragg rods gives information about the z-distribution of the laterally ordered part of the monolayer and allow to deduce the orientation of the linear molecules. Again, the X-ray optics are simple enough that it is feasible to compare experiment and theory on an absolute scale[4].

X-ray results for *fatty acids on pure water* give us detailed information about the structures throughout the phase diagram[5]: At high temperature we find two distinct *distorted-hexagonal (DH)* phases with uniform molecular tilt in symmetry directions (towards nearest and next-nearest neighbours, respectively) and positional correlation lengths ≤ 50 spacings. At low temperature and high surface pressure has vertical molecules in a tight, nearly incompressible *DH* crystal structure with correlation lengths $\gg 100$ spacings, while on increase of temperature there first occurs another vertical *DH* phase with shorter correlations, and finally a *hexagonal* vertical structure.

For a *charged monolayer on an ionic subphase* (eicosanoic acid $CH_3(CH_2)_{18}COOH$ on a $CdCl_2$ solution[6]) a strong interaction between the Langmuir film and the dissolved Cd^{++} ions is observed. At low temperature ($T \simeq 10$ °C), high *pH* $\simeq 8.8$ and surface pressure $\simeq 0$, the monolayer molecules form an oblique 2D lattice and tilt uniformly by 11°, approximately in a next-nearest neighbour direction, while a stoichiometric layer of Cd^{++} counter ions form just below. The ions order in a commensurate 2×3 super-structure. The positional correlations are of long range ($\gg 100$ spacings).

---

[1] A. Ulman, *Introduction to Ultra-Thin Organic Films*, Academic Press (1991).

[2] J. Als-Nielsen and K. Kjær, in *Phase Transitions in Soft Condensed Matter*, (T. Riste and D. Sherrington, eds.) Plenum Press (1989), p. 113.

[3] J. Skov Pedersen, in press, J. Appl. Cryst. (1992).

[4] K. Kjær, to be published.

[5] R. M. Kenn, C. Bohm, A. M. Bibo, I. R. Peterson, H. Möhwald, J. Als-Nielsen, and K. Kjær, J. Phys. Chem. 95, 2092 (1991).

[6] F. Leveiller, D. Jacquemain, M. Lahav, L. Leiserowitz, M. Deutsch, K. Kjær, and J. Als-Nielsen, Science, 252, 1532 (1991).

DSa9

Structural Studies of Y-type LB-films of Octadecyl-thiobenzoquinone[1]

N. B. Larsen[¤], T. Bjørnholm[¤], F. Christensen[§],
T. Skettrup[*], M. Jørgensen[¤], P. Sommer-Larsen[¤]

[¤]CISMI, Univ. of Copenhagen, Blegdamsvej 21, 2100 Ø, Denmark
[§]Danish Space Research Institute, Gammel Lundtoftevej 7, 2800 Lyngby, Denmark
[*]Fys. Lab. III, Technical Univ. of Denmark, Lundtoftevej 100, 2800 Lyngby, Denmark

Low angle X-ray diffraction of 25 double layers of octadecylthio-benzoquinone show an intense 1. order Bragg peak corresponding to an interlayer separation of 47 Å. This spacing is in agreement with ellipsometric measurements and spacefilling properties of the molecule, assuming an all trans configuration of the alkyl chain. By spectroscopic studies the direction of the electronic dipole transition of the main chromophore has been found. In combination with molecular orbital calculations this gives additional structural information indicating that the molecules are oriented along the dipping direction.

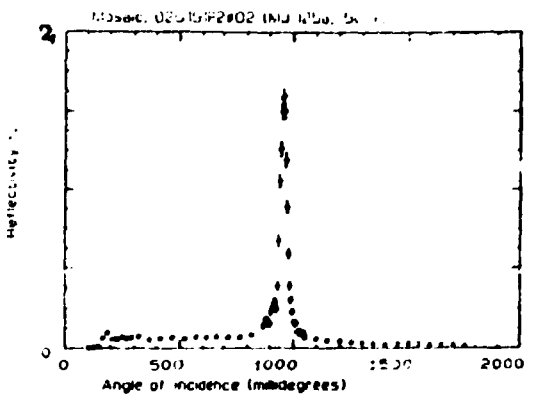

1. order Bragg peak (Cu K_α)

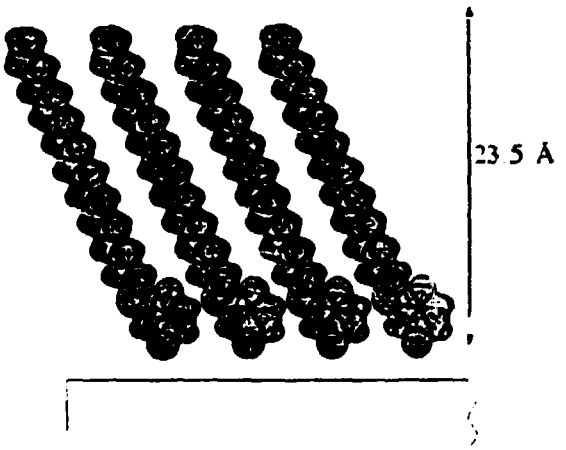

Schematic representation of structure in LB-films of octadecyl-thiobenzoquinone

[1] This work was supported by the Danish Materials Research programme.

DSa10

Tilt Transitions in Langmuir Monolayers of Long–Chain molecules.

S. Karaborni*[1] and S. Toxvaerd

Department of Chemistry

H. C. Ørsted Institute

Molecular dynamics simulations have been used to investigate tilt transitions in a monolayer model of amphiphilic molecules at an air–water interface. Eight simulations were performed at 300 K on monolayers in the density range of 18.5 to 25Å^2/molecule. The model amphiphilic molecules contained 19 pseudoatoms each representing a methyl or a methylene and a head group representing a carboxylate group. Amphiphile–amphiphile interactions are modeled using a new anisotropic united atom model that accounts implicitly for the presence of hydrogen atoms in alkanes, and water-amphiphile interactions are modeled using two external potentials that do not constrain the head groups to the interface, allow methylene segments to enter the water, and provide a finite size interface of the same order of magnitude as the size of the experimental water-air interface. The tilt behavior of the monolayer is monitored as a function of molecular area. Tilt angle results and structure factor analysis point to the occurrence of a transition between 20 and 21Å^2/molecule from an almost upright to a tilted monolayer. At 21 and 22Å^2/molecule the monolayer is divided into sections in which molecules are tilted over their nearest neighbors, and sections in which molecules are tilted over their next nearest neighbors. Upon monolayer expansion to 23Å^2/molecule, the molecules become tilted over their nearest neighbors.

DSu : ELECTRONIC PROPERTIES WORKSHOP

DSu1

Electronic and optical properties of strained Ge/Si superlattices

U. Schmid and N.E. Christensen*

Max-Planck Institut für Festkörperforschung, D-7000 Stuttgart 80

* and IFA, Aarhus University, DK-8000 Aarhus C

[Fax: (+45) 12 07 40], [E--mail: nec@dfi.aau.dk]

We present a comprehensive theoretical study of short period $(Ge)_n/(Si)_m$ strained-layer superlattices (SLS's) on Si and Ge [001] substrates, and the "free-standing" cased, based on *ab initio* calculations. Special emphasis is placed on the orthorhombic nature of the SLS's with both n and m even, as reflected in both the energy-band structure and the dielectric response $\varepsilon_2(\omega)$, which is different for all three polarizations along the main axes. The effects of various substrates are examined for the occurring interband transition, and in some cases reduced to a simple deformation-potential ansatz. A similar approach is taken for the splitting of the top of the valence band due to the internal uniaxial strain, which obeys a simple Vegard-type law; it is shown that confinement effects are negligible up to the values considered, i.e. $n+m=12$. The SLS's with a period of $n+m=10$ and sufficiently large strain in the Si layers have a direct gap; the transition from the top of the valence band to the lowest zone-folded conduction band at k= 0, however, is only dipole allowed for special cases, such as the superlattices with n, m odd, i.e., for systems with no inversion symmetry. The $(Ge)_5/(Si)_5$ SLS is predicted to be a good candidate for optoelectronic devices. A reversal of the two lowest folded conduction states (dipole allowed and forbidden, respectively is obtained when going from the n=4 to the n=6 case (see also the figure).

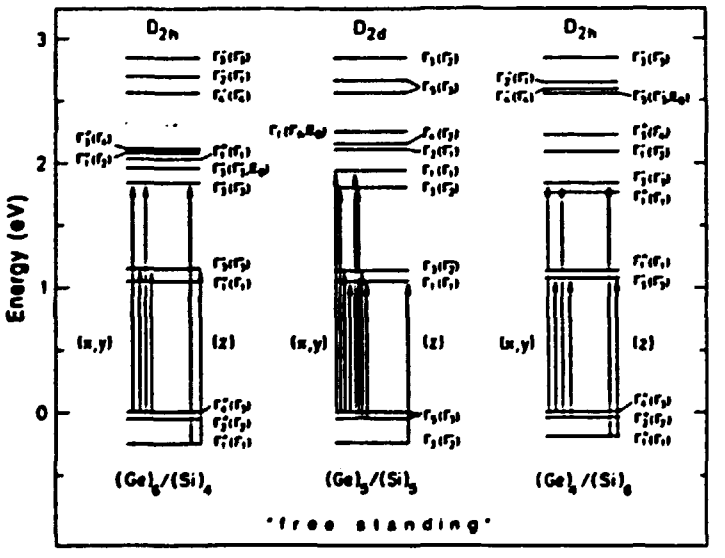

Symmetry and order of the energy levels at the Γ point of the three 10-ML SLS's covered in the text. Note that we use Koster's notation for symmetry labeling, with the BSW notation added parentheses. The dipole allowed transitions are given for clarity only for the four lowest states. Further details in Ref. 1.

[1] U. Schmid, N.E. Christensen, M. Alouani, and M. Cardona, Phys.Rev. B 43, 14597 (1991); Phys.Rev.Lett. 65, 2610 (1990).

DSu1

Calculated electronic properties of $NiSi_2$, $CoSi_2$ and $FeSi_2$

N.E. Christensen
IFA, Aarhus University, DK-8000 Aarhus C
[Fax: (+45) 12 07 40], [E--mail: nec@dfi.aau.dk]

$NiSi_2$ and $CoSi_2$ assume under normal conditions the fluorite structure, and they are metallic. $FeSi_2$ has a stable phase (β-$FeSi_2$) with a complex orthorhombic structure and β-$FeSi_2$ is a semiconductor. The fluorite form of $FeSi_2$ can be grown by epitaxy. The formation of the gap in β-$FeSi_2$ is resulting from a Jahn-Teller-like distortion, and it is shown that the gap states couple strongly to the phonon system. Consequences of this for the transport properties and the applicability of β-$FeSi_2$ in electronic devices are discussed.

Ferromagnetism in Fe_3Si and Fe_3Al under pressure

N.E. Christensen
IFA, Aarhus University, DK-8000 Aarhus C
[Fax: (+45) 12 07 40], [E--mail: nec@dfi.aau.dk]6

The electronic properties of Fe_3Si and Fe_3Al are calculated within the spin-density-functional formalism. Particular attention is paid to the pressure dependence of the magnetic moments on the 'A-C' and 'B' Fe-sites in the DO_3 structure.[1] The A-C-site moment undergoes transitions between various spin states and even relatively small pressures can cause a dramatic change of the magnetization. This is similar to the metamagnetic behaviour of fcc iron, but in this latter case theory predicts this to occur at large expansions of the lattice.

[1] See also the abstract (N.E. Christensen and J. Kudrnovsky)

DSu1

Magnetic properties of disordered transition-metal silicides

N.E. Christensen[§] and J. Kudrnovsky[‡]
[§]IFA, Aarhus University, DK-8000 Aarhus C
[Fax: (+45) 12 07 40], [E--mail: nec@dfi.aau.dk]
[‡]Institute of Physics CSAV, Praha, Czechoslovakia

The spin-density functional formalism in conjunction with the linear muffin-tin-orbital method and the coherent-potential-approximation (LMTO-CPA) is used to derive[1] electronic and magnetic properties of $Fe_{3-y}Si_{1-y}$ and $Fe_{3-x}V_xSi$ alloys as functions of composition. The crystal structures of these are all derived from the cubic DO_3 structure. The moments on the B-sites ('bcc like') remain essentially unaffected by changes in x and y, whereas the A-C sites ('tetrahedral') have moments that vary strongly. Excellent agreement with experiment and semi-empirical models[2] are obtained.
Also, a simple explanation of the site preference of substitutional transition-metal impurities in Fe_3Si is given.

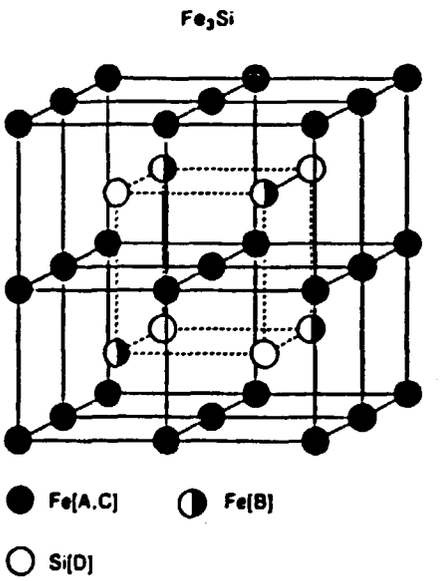

Sketch of the DO_3 structure (Fe_3Si taken as an example). Solid circles, ●, Fe[A,C]; open circles, ○, Si[D]; half-solid circles, ◑, Fe[B].

[1] J. Kudrnovsky, N.E. Christensen, and O.K. Andersen, Phys.Rev. B 43, 5924 (1991).
[2] V.A. Niculescu, T.J. Burch, and J.I. Budnik, J.Magn. Mater. 39, 223 (1983).

DSu2

A first-principles potential for solids

N. Chetty, K. Stokbro, K.W. Jacobsen and J.K. Nørskov

Laboratory of Applied Physics, Technical University of Denmark, DK 2800, Lyngby, Denmark

e-mail chetty@ltf.dth.dk, FAX (+45) 45 93 23 99

Metallic systems are very efficient in screening local perturbations, and there is a perception that many physical properties are determined by the local environment despite the inherent nonlocality of quantum mechanics. Density functional theory [1] relates the total energy of a system to the local density function but in solving for the eigenstates of the system, which is the time-consuming step in any solid state program, one apparently seeks to derive more information than is needed.

We present here a theory that relates the total energy directly to the physical variable of relevance, namely the density, and we emphasize the local nature of the screened ionic system. The idea is to associate each atom in the system under investigation with a corresponding reference system where the atom is in similar surroundings but where the symmetry is higher so that the total energy calculation is simpler: the quantum kinetic interactions are taken into account to good measure in the reference calculation which is done just once and for all times. The differences we treat in perturbation theory, and the eigenvalue problem is reduced to determining a first-order correction.

Our theory consists of a succession of approximations. At the most accurate level, the theory consists of a systematic derivation of an ansatz for the electron density, which is best suited for the Harris functional [2]. At the most approximate level, the theory is equivalent to the usual effective medium theory [3]. At all levels of approximation, every term in the total energy expression can be calculated *ab initio*, that is, without any fitting to experiment or to other calculations. The theory is applied to calculations of the surface energies and vacancy formation energy of Al. At the most accurate level, the theory gives results that are in almost complete agreement with selfconsistent calculations. At the more approximate, but also computationally much less demanding level, the theory gives results that are still in excellent agreement with the selfconsistent results, e.g. the surface energies are calculated to better than 0.1 eV.

[1] P. Hohenberg and W. Kohn, Phys. Rev. 136, 3864 (1964)

[2] J. Harris, Phys. Rev. B31 (4), 1770 (1985)

[3] K.W. Jacobsen, J.K. Nørskov and M.J. Puska, Phys. Rev. B35 (14), 7423 (1987)

DSu3

A theoretical study of surface magnetism, surface energies and work functions for the magnetic 3d-elements

Magnus Aldén*, H.L.Skriver+, Susanne Mirbt* and B.Johansson*
*Condensed Matter Theory Group, Department of Physics,
University of Uppsala, Box 530, Uppsala, Sweden
+Laboratory of Applied Physics
Technical University of Denmark, DK-2800 Lyngby, Denmark

Fax : +46 18-18 35 24, E-mail : magnusa at anna.fysik.uu.se

We have implemented a spin-polarized version of the tight-binding (TB) LMTO Green's function technique for surfaces and interfaces, where the local spin-density approximation (LSDA) is used for the exchange and correlation energy. The technique, as developed for the paramagnetic case by Skriver and Rosengaard[1], is based on the work by Andersen and co-workers [2,3]. An essential aspect is the ability, within the atomic sphere approximation (ASA) and in the TB representation, to generate the Green's function matrices for a real, two-dimensional surface by a simple and efficient procedure. The extremely short range of the TB structure constants is here an important ingredience.

Earlier theoretical work on surface magnetism have stressed the importance of accurate representations of the charge density and potential, i.e. all-electron and full-potential calculations. We stay within the ASA as far as the potential is concerned, but for the charge density we include the dipole moments. It is then of interest to investigate the reliabilty of these approximations for studying surface magnetism.

We calcululated magnetic moments, work functions and surface energies for several of the most close-packed surfaces of iron, cobalt and nickel. Studies on manganese and chromium have also been carried out. All of these elements give rise to enhanced spin moments at the surfaces considered except for Ni fcc(111) where the moment at the surface reverts to its bulk value. This is in close agreement with earlier slab-calculations. In addition, we find that the calculated work functions and surface energies agree with experimental values to within 10 % which may be considered most satisfactory in view of the computational efficiency of the Green's function technique.

It is seen that the calculated surface energies and the work functions are substantially lowered by the spin-polarization. The magnetic effects on the surface energies are discussed in terms of a simple model describing the d-band filling.

---

[1] H.L.Skriver and N.M.Rosengaard, Phys. Rev. B **43**, 9538 (1991).

[2] O.Jepsen, J. Madsen, and O.K.Andersen, Phys. Rev. B **26**, 2790 (1982)

[3] O. K. Andersen and O. Jepsen, Phys. Rev. Lett. **53**, 2571 (1984)

DP1

"Over-scattering from Expanded Gels (PDMS)". Swelling from Dry State to Maximum Swelling.

A.N. Falcão[1] , J. Skov Pedersen, K. Mortensen and [§]F. Boué

Department of Solid State Physics, Riso National Laboratory, Denmark.
Fax: 42370115.E-mail: falcao@risoe.dk
§ Lab. Léon-Brillouin, C.E.N. Saclay, France

PDMS in bulk state, at room temperature, is a liquid of polymer chains (melt). Irradiating the melt with high energy electrons randomly creates radicals that, after diffusion processes, react forming essentially chemical links. Above a certain radiation threshold a macroscopic network is formed. In contact with an excess of a good solvent for the polymer, the network will absorb it, expanding progressively from its original volume V_0, to a maximum saturation value $V_{max} = Q_{max}V_0$. The use of deuterated solvent enables scattering techiques to probe the local structure of the polymer chains.

We measured the intensity scattered at small angles by samples irradiated to 5 different doses. Their saturation swelling ratios, Q_{max}, were $Q_{i,max}$=15.0, 10.3, 7.1, 4.8 and 3.4. Each sample was measured at all possible Q values belonging to the above set (*i.e* all those lower than its saturation Q_{max}). In the range of low scattering vector, q, we observe, for each sample, an increase in the intensity scattered with increasing swelling ratio Q.This suggests that large scale heterogeneities in polymer concentration are present in the system, and that they span larger distances in space with increasing dilution (increasing Q). The characteristic length, ξ_L associated with these heterogeneities increases fast in the early stages of solvent absortion and saturates at the maximum swelling. We also observe that, at the same swelling ratio, samples more cross-linked scatter more. In the range of the high scattering vector q limit, the scattered intensity has a shape close to the one produced by an equivalent semi-dilute solution of the same polymer concentration. (The characteristic length ξ_s obtained from the gels is close to the one characteristic of the equivalent solution). At the largest q, $q > 1/\xi_s$, the slope is close to the one of the solution ($-5/3$, self-avoiding walk), but slightly reduced with increasing Q. We discuss the results in the framework of different models that describe the structure of gels, in particular its heterogeneity [2] and how this plays a role in accomodating the isotropic swelling.

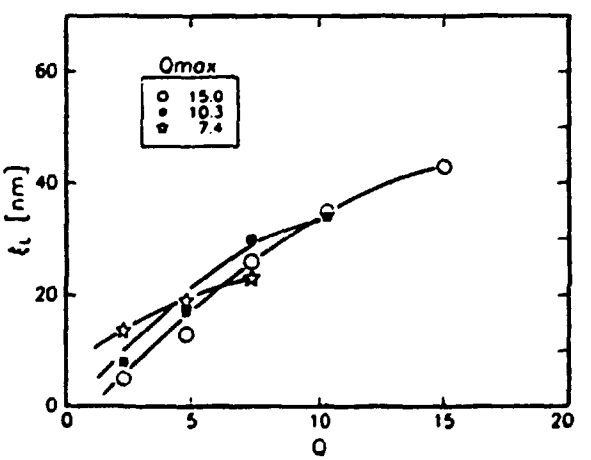

Fig. 1. ξ_L versus swelling degree Q, for the samples whose saturation swelling ratio, Q_{max} is 7.1,10.3 and 15.0, obtained by fitting the low q scattering part with the scattering law of a fractal system. The lines are guides to the eye.

[1]Supported by an EEC bursary (contract BREU-CT900378)

[2] J. Bastide, E. Mendes, F. Boué, M. Buzier and P. Lindner (1990). Makromolecular Chemie 40, 81

DP2

Size distributions and melting/solidification behaviour of nm-size metal inclusions

B. Schmidt, K. Hjemsted, E. Johnson, K. K. Bourdelle, H. H. Andersen, A. Johansen and L. Sarholt-Kristensen

Physics Laboratory, H. C. Ørsted Institute, Universitetsparken 5,
DK-2100 Copenhagen Ø, Denmark, [Fax: +45 31 35 06 28]

Ion implantation of Pb or In into Al results in spontaneous phase separation and formation of small Pb or In inclusions. The inclusions grow in topotactical alignment with the matrix with a cube/cube orientation relationship [1]. Differences in the lattice parameters together with this topotaxy causes TEM images characterised by moiré fringes (see the figure). All the Pb inclusions and the small In inclusions show well-defined facetting with predominant {111} facets and less prominent {100} facets, indicating a truncated octahedral shape.

The size distributions for In and Pb inclusions formed during room temperature implantation are quite narrow, and the average size of the inclusions increases gradually from 2 nm to 5 nm as the fluence increases from $2 \cdot 10^{19}$ m^{-2} to $5 \cdot 10^{20}$ m^{-2}. The areal density of the inclusions increases markedly with fluence, showing that nucleation still takes place at the lower fluences. At higher implantation temperatures the size distributions broadens out and the average size increases [2].

Melting and solidification of the inclusions have been studied by in-situ TEM heating and cooling experiments. The Pb inclusions exhibit superheating up to ≈ 75 K above the bulk melting point, and there is a clear tendency for large inclusions to melt first. Melting is associated with only partial loss of facetting of the largest inclusions. The mobility of both solid and liquid inclusions increases strongly with temperature, and growth probably occurs by coalescence of neighbouring liquid inclusions. Solidification is accompanied by a strong supercooling ≈ 45 K below the bulk melting point. Surprisingly, the smallest inclusions are the first to solidify during cooling.

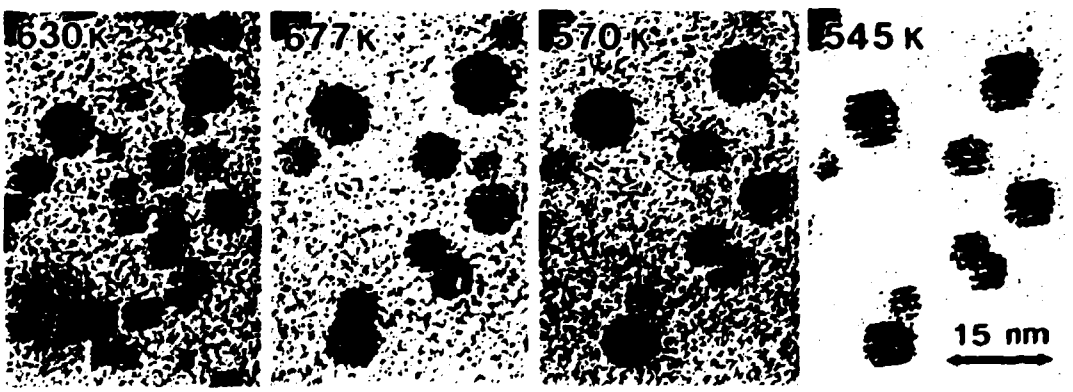

Melting and solidification of Pb inclusions in Al. T_m (bulk) = 600 K.

[1] L. Gråbæk et al., Phys. Rev., Vol. 45 (1992) in press.

[2] E. Johnson et al., Material Research Society, Symp. Proc. Vol. 235 (1992) in press.

DP3

Bismuth Inclusions in Aluminium

N. B. Thoft[§], J. Bohr[§], E. Johnson[†],
H. H. Andersen[†], A. Johansen[†] and L. Sarholt-Kristensen[†]

[§]Department of Solid State Physics, Risø National Laboratory, DK-4000 Roskilde, Denmark, Fax: 42 37 01 15, E-mail: thoft@risoe.dk

[†]Physics Laboratory, H. C. Ørsted Institute, Universitetsparken 5, DK-2100 Copenhagen Ø, Denmark.

Mixing two immiscible elements can lead to formation of inclusions in the host material. Examples of this are seen in aluminium single crystals implanted with bismuth or lead. The main concern for our present studies will be the melting, solidification and growth of bismuth inclusions.

In earlier X-ray diffraction studies[1] of lead inclusions in aluminium, large superheating (up to 67K) and large supercooling (at least 18K) were observed. It was concluded that the most important single factor contributing to the superheating is the lack of free surface where the melting can nucleate, as the lead lattice expands faster with temperature than the aluminium host lattice. The observed supercooling is believed to be caused by the inclusions being too small to solidify at higher temperatures by homogeneous nucleation.

In contrast to lead, bismuth expands more slowly than aluminium, and furthermore bismuth contracts when melting (like ice). These differences make it interesting to compare the melting and solidification behaviour of bismuth inclusions in aluminium. Prelimenary results indicate no superheating, but large supercooling, and this marks the difference between the two systems. An example of the preliminary data is shown in the figure below; the dashed lines should only be taken as guides for the eye.

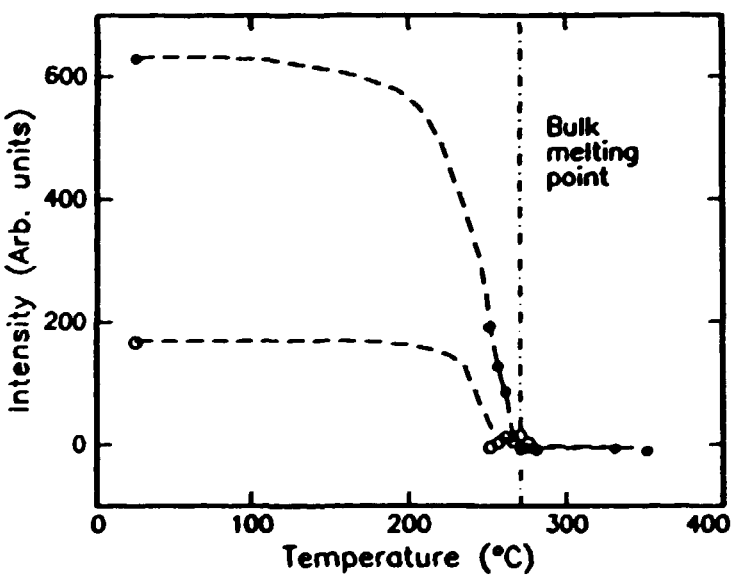

[1] L. Gråbæk, J. Bohr, E. Johnson, A. Johansen, L. Sarholt-Kristensen and H. H. Andersen, Phys. Rev Lett. 64, 934 (1990).

DP4

Second Harmonic Generation at Donor-Acceptor Interfaces in Langmuir-Blodgett Films[1]

T. Bjørnholm,[§] T. Geisler,[*] M. Jørgensen,[§] J. Larsen,[§] K. Schaumburg,[§] K. Brunfeldt,[§] K. Bechgaard[§]

[§]CISMI, University of Copenhagen, Blegdamsvej 21, DK-2100, Copenhagen Ø, Denmark [Fax: +45 31 42 60 62]

[*]Danish Institute of Fundamental Metrology, Lundtoftevej 100, DK-2800, Lyngby, Denmark [Fax: +45 93 11 37]

Langmuir-Blodgett films consisting of 2-dimensional interfaces between electron donor and acceptor molecules show a significant second harmonic generation which may be attributed to the intermolecular contact between donor and acceptor molecules across the interface (fig. 1). Current experimental results on such films will be presented and discussed and particular emphasis will be given to the question of how nonlinear optical properties may be improved in organic thin films by way of intermolecular charge transfer.

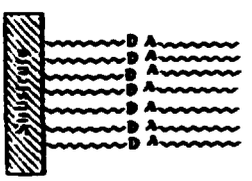

Fig. 1. Donor-acceptor interface in LB-film.

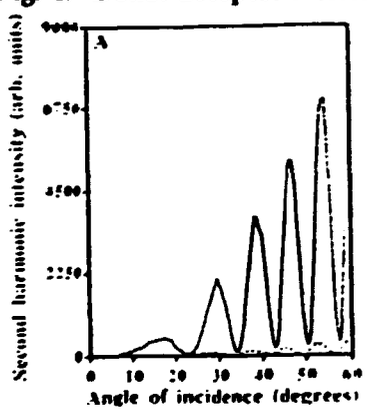

Fig. 2. Second harmonic generation of 20 alternating layers of donor and acceptor molecules

Fig. 3. Isotherms of donor and acceptor on water

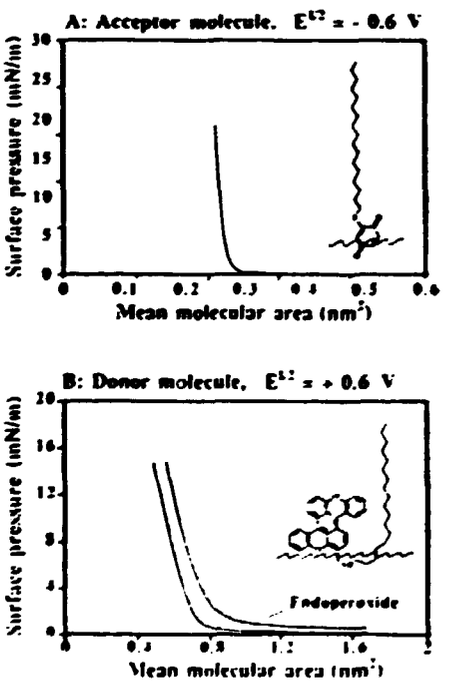

[1]This work was supported by the Danish Materials Research Programme.

DP5

Conductivity of Cementite[1]

Johan Helsing

Department of Theoretical Physics, The Royal Institute of Technology
s-100 44 STOCKHOLM, Sweden, [Fax: +46-8104879], [E-mail: joh@theophys.kth.se]

Cementite, Fe_3C, is only metastable below 1200 C. Rapidly cooled and, e.g., in the form of pearlite it is still very stable at room temperature. Pearlite is a lamellar mixture of 12 % cementite and 88 % ferrite that is a common constituent of various cast irons. In free form cementite rapidly decomposes into ferrite and graphite making direct measurements of its room temperature electric and thermal conductivities impossible.

We want to calculate the conductivity of cementite indirectly from data of overall conductivities of cast iron samples. Such calculations are possible if the detailed component geometries and the conductivities of all components of a sample, except cementite, are known. The component geometries of a cast iron sample is prohibitively complicated. Different idealized cast iron models, parametrizing salient features, are therefore defined to facilitate calculations. Gray cast iron, for example, is modeled as a composite material consisting of random, space filling aggregate of highly anisotropic spheroidal graphite flakes, weakly anisotropic spherical pearlite grains and isotropic spherical cementite grains. Possible alloying elements are assumed to form solid solutions in the ferrite and affect its conductivity in a known way[2].

The conductivities of the idealized composite materials are calculated withtin an Average Field Approximation.[3] Different grains in a sample are treated as if they were surrounded by a homogeneous medium with conductivity to be determined by self-consistent averaging. There are various formulations of Average Field Approximations. They differ in terms of over what field quantity the averaging is done and they predict different percolation thresholds for the components. We choose the formulations which most accurately predicts the percolations threshold for the components in our idealized systems. This involves calculation of the percolation threshold for the number density of two-dimensional disks of radius unity in a three-dimensional continuous medium.

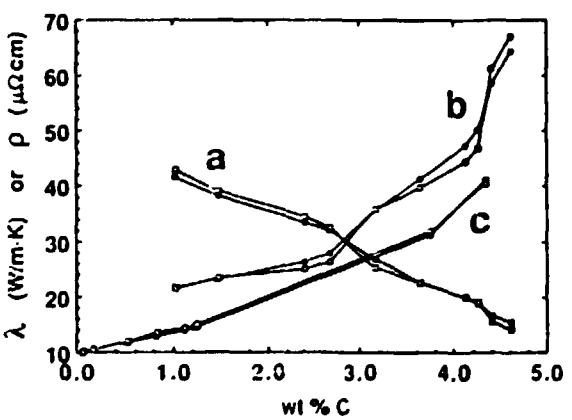

The Figure shows the best fit[4] of calculated (open squares) to measured (filled squares) values of thermal conductivity λ (curve a) and electric resistivity ρ (curve b,c) for the alloyed steels and cast irons of two references. The conductivity and resistivity of cementite used in this best fit was λ = 8.6W/(m K) and ρ = 107$\mu\Omega$cm. Previous estimates of these two quantities have varied considerably.

[1] Work partly supported by the Swedish Board for Technical Development
[2] R.K. Williams, D.W. Yarbrough, J.W. Masey, T.K. Holder, J. Appl. Phys. 62, 2778 (1987)
[3] J. Helsing and A. Helte, J. Appl. Phys. 69, 3583 (1991).
[4] J. Helsing, G. Grimvall, J. Appl. Phys. 70, 1198 (1991).

DP6

LMTO calculations of IV-IV heterostructures[1]

Troels Brander Nielsen and Axel Svane

Institute of Physics and Astronomy, Aarhus University
DK-8000 Aarhus C, Denmark
E-mail: troels@dfi.aau.dk

We study some macroscopic properties of superlattices of silicon and germanium. We do this by performing bandstructure calculations, which give the electronic properties of a given crystal from first principles.

Our calculations are based on the local density approximation to the density functional theory.[2] Specifically, we are using Linear Muffin-Tin Orbitals[3] to perform the desired bandstructure calculations of different configurations of silicon and germanium in a supercell. Our version of a LMTO calculation is especially suited for large systems, because we omit the time-consuming diagonalization of the Hamiltonian matrix. The system converges to its self-consistent ground state by the use of a Steepest Descent algorithm.

Some of the macroscopic properties studied are Bulk Modulus, Cohesive Energy and Lattice Constants, the latter found to be in agreement with Vegards law, which states that the lattice constant varies linearly with the abundancy of the two kinds of atoms in the lattice, between the two extremes of pure silicon and pure germanium. The variation in total energy for different systems is interpreted in terms of simple nearest neighbour interactions.

[1] The calculations will be part of TBN's Master Thesis
[2] R.O.Jones and O.Gunnarsson, *Rev. Mod. Phys.* 61, 701 (1989)
[3] H.L.Skriver, The LMTO Method Springer series in Solid State Sciences Vol.41 (Berlin, 1984)

DP7

GaAs/GaAlAs superlattice with a basis

Anders Kristensen[1&2], Poul Erik Lindelof[1], Henrik Smith[1],
Erling Veje[1], Peer Tidemand Pettersson[3], and Claus B. Sørensen[1]

[1]Physics Laboratory, H.C. Ørsted Institute, Universitetsparken 5, DK-2100 Copenhagen
[2]Danish Institute of Fundamental Metrology, Bldg. 307, Lundtoftevej 100, DK-2800 Lyngby
[3]Telecommunications Laboratory, Lyngsø Allé 2, 2970 Hørsholm

Transport properties of GaAs/GaAlAs superlattices (S.L.) are studied experimentally. Three GaAs/GaAlAs heterostructures with a 1.1 μm thick superlattice sandwiched between two metallic GaAs contact layers were grown by MBE on a semi-insulating GaAs substrate. In the first structure, the superlattice is a simple Kronig-Penney potential with a period of 39 Å. The S.L. period is doubled in the second structure, and each primitive cell contains two potential wells - a 2-point basis. In the third structure the S.L. period is tripled having a 3-point basis. The S.L. period and total thickness is measured by high-resolution X-ray diffraction. The X-ray spectra clearly reveal the 1-, 2- and 3-point basis of the superlattices.

The miniband structure can easily be calculated for the first superlattice, using a Kronig-Penney model. The lowest miniband has a width of 230 meV and an effective mass $m^* = 0.08\ m_0$ in $k = 0$. The minibands of the S.L.s with 2- and 3-point basis are calculated in a tight-binding model. For the second S.L. the minizone is halved and the lowest miniband is split in two. Simikar for the third S.L., the minizone is 1/3 of the first and the lowest miniband is split into three. These predictions concerning the minibands are confirmed by photoluminescence measurements in the temperature range from 10 to 300 K.

For electrical measurements, small area - 20 x 20 μm to 100 x 100 μm - devices are mesa etched and contacted, whereby an electrical current can be passed through the S.L. Current-voltage characteristics of the S.L.s are measured at temperatures from 0.3 K to 300 K. At low electric fields the miniband-properties of the S.L. transport are present, while localization phenomena are possible at high fields.

DP8

The bandgap energy of $Ga_{(1-x)}Al_xAs$ versus x and T

M. El Allali, C.B. Sørensen, and E. Veje

Physics Laboratory, H.C. Ørsted Institute,
Universitetsparken 5, DK-2100 Copenhagen, Denmark
Telefax: +45 31 35 06 28

P. Tidemand-Petersson

TFL, Telecommunications Research Laboratory,
Lyngsø Alle 2, DK-2970 Hørsholm, Denmark
Telefax: +45 45 76 63 36

The precise height of the bandgap of $Ga_{(1-x)}Al_xAs$ is of importance for practical purposes ("bandgap engineering") as well as in basic research in which GaAs/GaAlAs junctions are involved. Although the bandgap has been studied as a function of the mole fraction, x, at room temperature and also at low temperatures, the variation of the bandgap with temperature, T, and for different values of x is not well established. Therefore, we have initiated a systematic study, in which we measure the bandgap energy of $Ga_{(1-x)}Al_xAs$, lightly doped with Si (n-type) with the use of photoluminescence, as a function of x and from 10 K to 300 K. At the same time, we determine energies of the Si donor level, the C acceptor level (the samples are unintentionally doped with carbon), and the bulk GaAlAs exciton.

The samples were produced at the MBE-center at the Ørsted Institute. The mole fraction, x, was determined from RHEED oscillations observed during growth on special, stationary test-wafers, carried out prior to growth on rotating wafers, from which the samples were cut. Therefore, we felt it desirable to measure x in an independent way, namely by applying high-resolution, X-ray crystallography. Small differences between the results of the two methods re seen, and this is being investigated further.

DP9

Characterization of GaAs irradiated with 80 keV He^+ ions

A. Kristensen, C.B. Sørensen, and E. Veje

Physics Laboratory, H.C. Ørsted Institute
Universitetsparken 5, DK-2100 Copenhagen, Denmark
Telefax: +45 31 35 06 28

It is well known that irradiation of GaAs or other semiconductor materials with neutrons, electrons, or atomic ions produces damage in that part of the sample, which is exposed to the bombardment. This has often been used as a technique to create electrically insulating regions in semiconductor devices like, e.g., diode lasers. Recently, also bombardment of GaAs/GaAlAs quantum Hall samples with quite low fluences of He^+ ions has shown to be usefull in the production of quantum Hall samples by introducing an adequate density of scattering centers in the samples, without changing the carrier density noticeably.

However, whereas ion bombardment of semiconductor materials thus is a versatile tool for sample modification, the more detailed properties of the radiation-induced defects are not well known. Therefore, we are carrying out a more systematic work in which GaAs and GaAlAs samples are bombarded with various fluences of 80 keV He^+ ions, and are subsequently characterized with electrical and photoluminescence methods.

DP10

Neutron diffraction study of the magnetic phase diagram of MnSi close to the critical temperature.

B. Lebech*, P. Harris*, C. Gregory†, N. Bernhoeft†, J. Skov Pedersen* and K. Mortensen*

*Department of Solid State Physics, Risø National Laboratory, Denmark

†Physics Department, University of Durham, Durham, UK.

The cubic intermetallic compounds MnSi and FeGe belongs to a class of magnetic metals that crystallize in the tetrahedrally coordinated cubic structure ($P2_13$) of FeSi. Therefore, they lack inversion symmetry and are according to present theory capable[1,2] of supporting a static spin density wave corresponding to a long range magnetic spiral structure. This is a consequence of the Dzyaloshinskii instability. If B_2 is the second order gradient in the free energy expansion, it is shown, that for $B_2 < 0$ the spirals will propagate along the (111) directions and for $B_2 > 0$ the spirals will propagate along the (001) directions.

MnSi has a critical temperature of 29.5 K below which a helix with a period of 180 Å propagates along equivalent (111) directions.

FeGe has a critical temperature of 278.7 K below which a helix of periodicity 700 Å propagates along equivalent (100) directions. Below 211 K the helix turns and propagates along equivalent (111) directions.

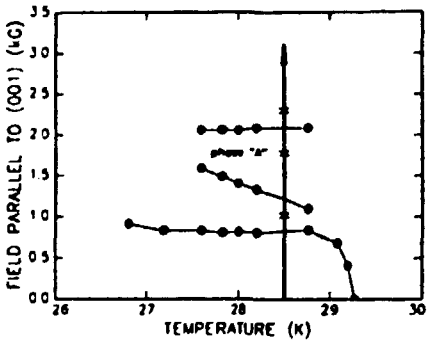

A detailed magnetization study of MnSi close to the critical temperature showed the socalled 'phase A' which we investigated by neutron scattering on a SANS instrument, using incident neutrons with a wavelength of 7 Å.

Neutron scattering data was collected on a cylindrical single crystal of MnSi (1.5 mm in diameter and 4 mm long) cut with the (001) axis parallel to the cylinder axis. The crystal was mounted in a vertical field 5 T split coil superconducting magnet with the field applied in the (001) direction. The measurements were done as a function of magnetic field just below the magnetic ordering temperature. This were done for two different crystal settings. From the data we conclude:

1. For fields just below the 'phase A', but above the domain reorientation the helix has rotated to propagate along equivalent (100) directions.
2. In 'phase A' the symmetry breaks and the helix propagates only perpendicular to the fiels along the (100) and (010) directions.
3. At fields above 'phase A' the helix propagates along the field direction ((001)).

[1] O. Nakanishi, A. Yanase, A. Hasegawa and M. Kataoka, (1980) Solid State Commun. 35, 995.
[2] P. Bak and M.H. Jensen, (1980) J. Phys. C: Solid State Phys. 13, 1881.

DP11

Diffraction Study of the Nuclear and Magnetic Ordering of the Layered Perovskite PAMC

P. Harris*, B. Lebech* and N. Achiwa†

*Department of Solid State Physics, Risø National Laboratory, Denmark

†Department of Physics, Kyusho University, Fukuoka, Japan

The layered perovskite $(CH_3CH_2CH_2NH_2)_2MnCl_4$ (PAMC) has been investigated by neutron diffraction and an X-ray study is in preparation. PAMC is known to undergo several phase transitions on cooling from 441 K to 5 K. Our attention has been focussed on the transition at 111.5 K, where it transforms from an orthorhombic phase with an incommensurate modulation of wave vector $(\delta + \frac{1}{3})a^*$ to a monoclinic phase with a commensurate modulation of wavevector $\frac{1}{3}(a^* \pm b^*)$, and on the transition at 39 K where it orders into an antiferromagnetic phase with a small ferromagnetic contribution in the a-direction.

The chemical structure of the monoclinic phase is not known, but NMR results show[1]. that the transformation from the orthorhombic to the monoclinic structure is caused by increasing order of the hydrogen bondings between the NH_3-groups and the chloride ions, and that the change in modulation vector is caused by a change of the tilting of the system of rigid carbon chains and $MnCl_6$ octahedra. The antiferromagnetic phase is a quasi 2d Heisenberg antiferromagnet, with a small ferromagnetic contribution. The magnetic structure gives rise to magnetic satellites, that turns out to be superimposed on the nuclear satellites[2] which indicates that the space groups of the tilted chemical system and the spacegroup of the antiferromagnetic system are the same

In order to understand the interaction between the magnetic and chemical structure. we have measured the monoclinic angle as a function of temperature. This has been done by measuring the splitting of the single strong (040) orthorhombic reflection into the two monoclinic reflections along the c^*-axis. After a small increase the angle decreases on cooling until it locks in to an almost constant value below 40 K. This lock-in transition might be caused by the magnetic order

Also the intensities of selected magnetic Bragg reflections and satellites have been measured as a function of temperature. The magnetic satellites are very weak and in addition they are superimposed on the nuclear satellites. Very good statistics are needed to determine the magnetic intensity. To get this a new neutron diffraction study on a very big (thickness 3 mm, width and length 2 cm) virgin crystal has started.

An X-ray study on a 4-circle diffractometer will be done in the near future. With the determination of the chemical structure of the low temperature phase. the interaction between the magnetic and nucleic tilting system will hopefully be understood

[1] P. Muralt, R. Kind and W. Bührer (1988) Phys. Rev. B 38, 666

[2] N. Achiwa, T. Matsuyama and T. Yoshinari (1990) In Phase Transitions 28, 79

DP12

MAGNETIC PROPERTIES OF BARIUM FERRITE

Anna Ruokolainen, Yngve Bergström, Jonte Bernhard and Peter Harström
Materialscentre - HTM, University College of Falun/Borlänge, S-781 27
Borlänge, Sweden [Fax +46 243 73402]

Hard ferrites, also known as ceramic magnets, are in widespread use in motors, generators, loudspeakers and various holding or clamping devices. The most common hard ferrites are the hexagonal (magnetoplumbite structure) barium or strontium ferrite ($BaO{\cdot}6Fe_2O_3$ or $SrO{\cdot}6Fe_2O_3$).

Ceramic materials like barium ferrite have properties such as: high hardness, high Young modulus, low density, very small reduction in mechanical strength at elevated temperatures, high electric resistivity, low fracture tension, good stability and high corrosion resistance in oxidating and reducing environments (even at high temperatures), raw materials are in ample supply, energy use at production is lower than that used by metals.

Hematite (α-Fe_2O_3) is produced in large quantities as a residual product from the pickling acid at the SSAB Domnarvet steelplant in Borlänge, Sweden. The hematite raw material is obtained as a very fine sized powder (particle size 0,3±0,05 μm) with 99,3–99,4 wt% Fe_2O_3. We have used the hematite raw material and barium carbonate ($BaCO_3$) for preparation of barium ferrite $BaO{\cdot}nFe_2O_3$ (n = 5,5 in this work). The powder mixture was calcinated at different temperatures (1000–1300 °C) and at different holding times (2 and 4 h). During calcination the ferrite formation reaction ($nFe_2O_3 + BaCO_3 \rightarrow BaO{\cdot}nFe_2O_3 + CO_2$) is initiated. After calcination the material was wet milled and after drying briquettes were pressed and sintered at different temperatures (1000–1300 °C) and times (1–4 h). The objective was to investigate the influence of variations in processing parameters on magnetic, mechanical ant other properties of bariumferrite and to investigate the feasibility of the residual hematite raw material for production of ceramic magnets. Depending on the process parameters most ferrites obtained, hitherto, had remanence B_r = 0,18–0,23 T, coercitivity H_c = 170–260 kA/m and energy product $(BH)_{max}$ = 6–8 kJ/m^3.

DP13

Magnetic properties of $ErRh_3B_2$

J Bernhard[a], P Granberg[b], I Higashi[c], T Shishido[d], H Takei[e] and T Fukuda[d]

[a]University College of Falun/Borlänge, S-781 10 Borlänge, Sweden (Fax +46 243 73402); [b]Institute of Technology, Uppsala University, S-751 21 Uppsala, Sweden; [c]The Institute of Physical and Chemical Research (RIKEN), Wako-shi, Saitama, 351-01, Japan; [d]The Institute for Materials Research, Tohoku University, Sendai, 980, Japan; [e]The Institute for Solid State Physics, The University of Tokyo, Roppongi, Minatoku, Tokyo, 106, Japan

The ternary system RE-Rh-B (RE = Rare earth elements) have attracted much interest since the discovery of reentrant superconductivity and coexistence of ferromagnetism and superconductivity in $ErRh_4B_4$[1,2] and because of unusual magnetic properties in the $RERh_3B_2$ system[3,4].

The compounds in the ternary $RERh_3B_2$ system crystallizes either in the hexagonal $CeCo_3B_2$ type structure (RE = La–Gd) or in the $ErIr_3B_2$ type structure (RE = Tb–Lu), which is a base-centered monoclinic structure with space group *C2/m*[5]. The $CeCo_3B_2$ structure (*P6/mmm*) is derived from the binary $CaCu_5$ type structure (*P6/mmm*) and the $ErIr_3B_2$ type structure is pseudohexagonal with a small distortion from the hexagonal symmetry of the $CeCo_3B_2$ structure. The crystal structure of $ErRh_3B_2$ belongs to the monoclinic system with a crystal lattice of $ErIr_3B_2$ type[5,6,7].

Magnetic measurements have been carried out on single crystals which were grown using natural boron or isotopically enriched boron (99,3% ^{11}B). Susceptibility measurements in low magnetic field (B_{appl} = 10 mT (100 Gauss)) indicates that the magnetic properties of $ErRh_3B_2$ are highly anisotropic, and that $ErRh_3B_2$ is ferromagnetic with $T_c \approx 27$ K. The highly anisotropic magnetic properties of $ErRh_3B_2$ are probably due to the Er-chains along the c-axis. The saturation moment at 10 K ($B \parallel c$) is 1,0 MA/m (8,4 μ_B/Er) for $ErRh_3{}^{11}B_2$.

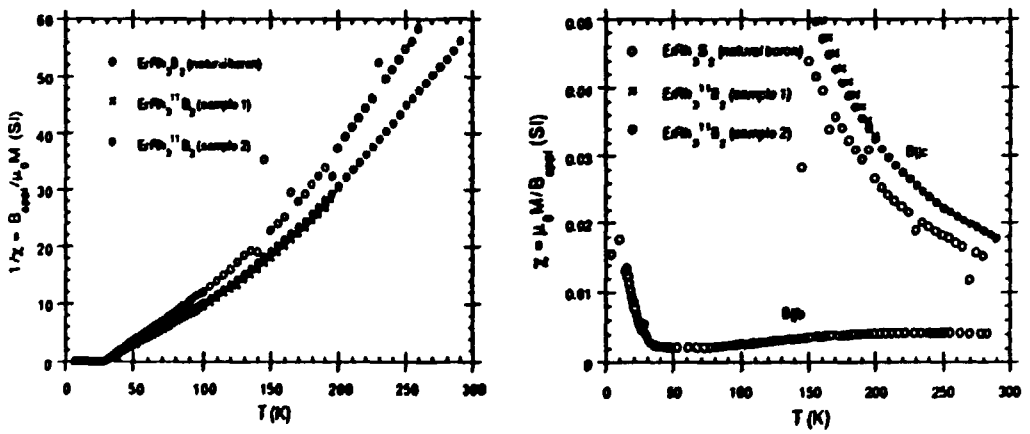

Fig 1. Magnetic data for $ErRh_3B_2$. The inverse susceptibility $1/\chi = B_{appl}/\mu_0 M$ are shown in (a) and the susceptibility $\chi = \mu_0 M/B_{appl}$ in low magnetic field are shown in (b).

[1]W A Fertig, D C Johnston, L E DeLong, R W McCallum, M B Maple and B T Matthias, Phys Rev Lett, 38, 987 (1977).

[2]D C Johnston and H F Braun, Superconductivity in Ternary Compounds II, eds M B Maple and Ø Fischer (Springer-Verlag, Berlin, 1982) p 11.

[3]S K Dhar, S K Malik and R Vijayaraghavan, J Phys C: Solid State Phys, 14, L321 (1981)

[4]S A Shaheen, J S Schilling and R N Shelton, Phys Rev B, 31, 656 (1985); E V Sampathkumaran, G Kaindl, C Laubschat, W Krone and G Wortmann, Phys Rev B, 31, 3185 (1985) and references therein.

[5]H C Ku and G P Meisner, J Less-Common Metals, 78, 99 (1981)

[6]Bernhard J, Kitazawa H, Higashi I, Shishido T, Fukuda T and Takei H, in D Emin et al (Eds), AIP Conference Proceedings 231 (American Institute of Physics, New York, 1991) p 201

[7]J Bernhard, I Higashi, P Granberg, L-E Tergenius, T Lundström, T Shishido, A Ruokolainen, H Takei and T Fukuda. To be published.

DP14

Phonon scattering at a twin boundary[1]

Sune Pettersson

Department of Theoretical Physics, University of Umeå, S-901 87 Umeå, Sweden,
Fax: +46 90 166673, E-mail: pettersson@tp.umu.se

A lattice dynamical theory has been used to describe phonon scattering at a twin boundary in a face centered tetragonal indium-thalium alloy. Many experiment indicate a strong scattering of phonons from such a boundary but approximate calculations suggest that the scattering should be weak[2].

A phonon that is incident on an interface between two materials has a certain probability of being reflected or transmitted. Most theoretical estimates of this phenomena have been based on the acoustic mismatch model[3], in which the two media are regarded as two elastic continua and a perfect juntion between the two is assumed, i.e., the interface is "welded". The boundary conditions allow three different phonons to be reflected and transmitted, respectively.

In a lattice dynamical theory you solve the equations of motion for atoms at the interface and the actual forces that act across the interface must be taken into account. A weak bonding at the interface will give a low probability for transmission of phonons. We have previously shown[4] that a lattice dynamical theory requires more than three phonons to be reflected and transmitted, respectively, when the two materials have different structures or different lattice constants. This is due to the need of a larger interface unit cell in order to include all different interactions across the interface.

At a twin boundary, we have identical lattices on both sides of the interface but the lattices do not have the same orientation. This gives an increased interface unit cell and we find that, in our case, six phonons will be reflected and transmitted, respectively. We present results for the phonon transmission coefficient for low frequency phonons.

[1] Work supported by the Swedish Natural Science Research Council.

[2] A. C. Anderson, private communication.

[3] E.T.Swartz and R.O Pohl, Rev. Mod. Phys. 61, 605 (1989).

[4] Sune Pettersson and G. D. Mahan, Phys. Rev. B 42, 7386 (1990).

DP15

Charge-Density Wave Phases in TaS_2

David B. Pengra and Jakob Bohr

Department of Solid State Physics, Risø National Laboratory
DK-4000 Roskilde, Denmark
[Fax: +45 42 37 01 15], [e-mail: pengra@risoe.dk]

It has long been known that charge-density wave (CDW) phases are present in crystalline TaS_2, a hexagonal crystal which has a layered structure[1]. These CDW phases induce a modulation of the atomic lattice, and hence, produce satellite reflections near the principal Bragg peaks seen in diffraction experiments. In the octahedral (1T) polytype of this crystal, which is metastable below 550 K, the CDW phases can exist in three different forms, as evinced by different patterns of diffraction satellites. Below 190 K, the CDW phase is commensurate, and forms a $\sqrt{13} \times \sqrt{13}$ R13.51° superlattice relative to the atomic lattice. From about 190 K to 340 K, the CDW state rotates about the *c*-axis away from this commensurate state to about 12°, and the satellite *q*-vector increases from $a^*/\sqrt{13}$ by about 4 percent. Finally, above 340 K, the rotation angle drops to 0°. In the two higher temperature forms, the superlattice has a repeat period along the *c*-axis of 3 molecular layers, but in the lowest temperature form, this increases to about 13 layers.

Our experiments, now in progress, are designed to measure the rotation angles and correlation lengths of the CDW phases as the system passes through the lower temperature transition, by means of x-ray diffraction. In particular, we seek to understand whether the rotation angle correlates with the shapes and sizes of the CDW domains, and whether the phase transition occurs in two steps: a preliminary loss of order between successive layers in the crystal followed by a continuous rotation of the CDW state. Earlier investigations have reported a loss of *c*-axis order in the low-temperature phase[2], and a continuous rotation of the CDW state as the crystal cools toward the transition[3], but a detailed understanding of this is still lacking. If our hypothesis proves correct, it would suggest that the rotation angle of the CDW state is controlled by finite-size effects of the CDW domains—a phenomenon recently suggested as one of several mechanisms governing epitaxial rotations[4].

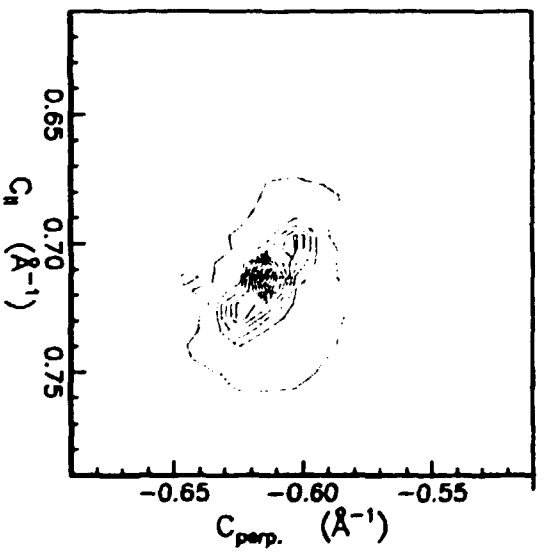

Preliminary results have confirmed the different rotation angles of the CDW state: we measure a rotation of 11.8° at room temperature and 13.8° at 12 K. At left is a room-temperature satellite of the (001) Bragg peak. We are currently investigating the slight anisotropy in spot shape.

---

[1] J. A. Wilson, F. J. Di Salvo, and S. Mahajan, Adv. in Phys. bf 24, 117 (1975)

[2] R. L. Withers and J. W. Steeds, J. Phys. C 20, 4019 (1987)

[3] C. B. Scruby, P. M. Williams and G. S. Parry, Philos. Mag. 31, 225 (1974)

[4] J. Bohr and F. Grey, *Condensed Matter News*, Vol. 1, No. 3, p. 12 (1992)

DP16

First principles determination of static and dynamical properties of Sn and Sn-O compounds

E.L. Peltzer y Blancá[*], A. Svane[§], N.E. Christensen[§]
C.O. Rodriguez[†], O.M. Cappannini[†], M.S. Moreno[‡], and M. Methfessel[¤]
[*] on leave from Instituto de Física de Líquidos y Sistemas Biológicos (IFLYSIB)
– Universidad Nacional de La Plata (UNLP) –
Consejo Nacional de Investigaciones Científicas y Técnicas (CONICET), Argentina
[Fax: (+45) 12 07 40], [E--mail: eitek@dfi.aau.dk]
[§]IFA, Aarhus University, DK-8000 Aarhus C
[Fax: (+45) 12 07 40], [E--mail: svane@dfi.aau.dk]
[†]IFLYSIB-UNLP-CONICET
[‡]Dep. de Física - UNLP
[¤]Fritz-Haber Institut, Berlin, BRD

We have studied the static and dynamical properties including high pressure phases of Sn, SnO, and SnO_2 using the Full-Potential-LMTO method, which gives a very accurate description of these properties. In addition, dynamical properties (phonon frequencies and Grüneisen parameters) were obtained for SnO and SnO_2 within the same approach. In the literature several aspects of these compounds, from the theoretical and experimental points of view, are undetermined. The experimental data on dynamical properties are sparse. For those properties that are experimentally determined, very good agreement is found with our calculation, and for the quantities which have not yet been measured, our calculations give predictions.

DP17

Pressure studies of GaN and AlN: Electronic structures and structural phase transitions

N.E. Christensen[§], I. Gorczyca[‡], P. Perlin[‡], I.Grzegory[‡], H. Teisseyre[‡], and T. Suski[‡]
[§]IFA, Aarhus University, DK-8000 Aarhus C
[Fax: (+45) 12 07 40], [E--mail: nec@dfi.aau.dk]
[‡]High Pressure Research Centre, Polish Academy of Sciences, PL - Warsaw

GaN, AlN, and BN form an interesting subgroup of the III-V semiconductor family. They have large gaps (E_g>3eV) and physical properties that in many respects are similar to those of diamond (hardness, high thermal conductivity). Therefore, these compounds are becoming interesting for technological applications. The growth of single crystals (performed in Warsaw) requires a complicated high pressure technique. Experimental optical data are compared to theoretical first-principles calculations. Further, using the density-functional theory, we derive pressure-induced phase transitions. In some cases (wurtzite and NiAs structures) this requires a detailed optimization of internal structural parameters.

DP18

Simulations of 2D vortex dynamics

Olof Westman

Department of Theoretical Physics, University of Umeå, S-901 87 Umeå, Sweden,
[Fax: +46 90 166673], [E--mail: westman@tp.umu.se]

A model describing a two-dimensional array of resistively shunted Josephson-junctions is investigated by aid of computer simulations. By adding Langevin noise for finite temperatures one gets information on vortex dynamics close to the phase-transition. It can also be viewed as a model for superconducting films.

The complex impedence Z is calculated for this model and the real and imaginary parts are used to calculate ϵ^{-1}. In particular the peak ratio predicted by Minnhagens dynamical theory[1] is put to test.

[1] P. Minnhagen, Rev. of Mod. Phys. B59, 1001 (1987).

DP19

The magnetic susceptibility of 9,10-di(2-(ferrocenyl)-vinyl)anthracen in different oxidation states

Dorthe Posselt*, Wolfgang Badur and Michael Steiner

Inst. für Physik, Johannes-Gutenberg Universität, D-6500 Mainz, Germany
*Present address: IMFUFA, Roskilde University Center, DK-4000 Roskilde, Danmark

With the ultimate aim of constructing a macromolecular ferromagnet, systematic studies of candidate building block molecules are important in order to learn about both intra- and intermolecular coupling mechanisms. The requirement of high spin molecules might be satisfied using both organometallic compounds and purely organic compounds forming stable radicals.

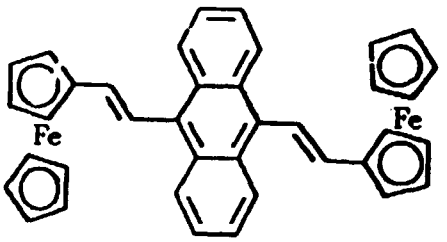

The structure of the organometallic compound 9,10-di(2-(ferrocenyl)-vinyl)anthracen is shown on the figure. The molecule contains two iron atoms which in the unoxidized state have valence +2. By adding a controlled amount of I_3, the valence state of the two iron atoms can be varied systematically.

We have measured the magnetic susceptibility of powder samples in the temperature range from 1.9 to 310 K. The figure to the left shows the data for the unoxidized sample, which is diamagnetic. The data for the mixed valence sample (Fe^{2+}, Fe^{3+}) and the sample with both iron atoms having valence +3, are shown to the right. The effective moment pr. molecular unit, $\sqrt{(3k_B\chi(T-\theta)/N)}$, is plotted against temperature. Here N is the number density of molecules, χ is the measured susceptibility and θ is the Curie-Weiss temperature, found by fitting $1/\chi$ at high temperatures to the Curie-Weiss law, $1/\chi \propto (T-\theta)$. θ is negative for both samples, indicating that the exchange interaction is antiferromagnetic. At high temperatures where the oxidized samples are paramagnetic, the effective moment of the two-spin molecule is roughly twice the effective moment of the one-spin molecule. The data shown were measured at a field of 500G; application of a 1 kG field result in a drastic change in the high temperature effctive moment, which we at the moment pursue for further understanding.

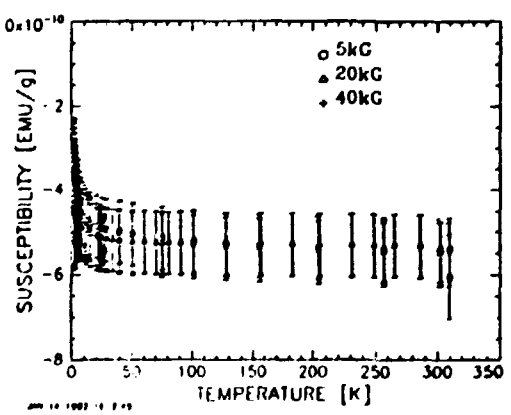

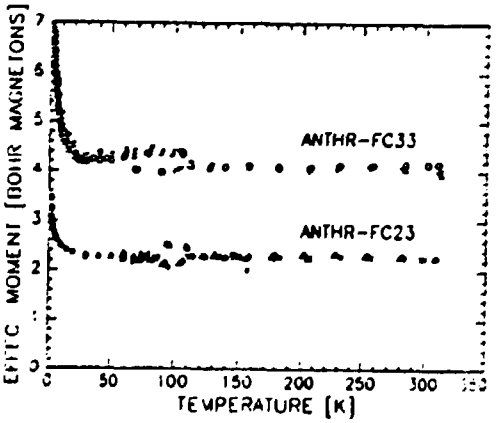

Acknowledgement: We thank Martin Baumgarten, Max-Planck Inst. für Polymerforschung, Mainz, for providing us with the samples.

DP20

Self association of zinc free insulin

Kadima W.[§], Øgendal L.[*], Bauer R.[*], Kaarsholm N.[°], Hansen J[°] and Irlind P[*].

[*]Department of Mathematics and Physics, Royal Veterinary and Agricultural University, Thorvaldsensvej 40, DK 1871 Frederiksberg , Denmark (Fax: 35282350)

[§]Present adress: Department of Biochemistry, University of California, Riverside, California 92521 USA

[°]Novo Research Institute, NOVO Allé, DK-2880 Bagsvaerd, Denmark

Insulin is stored in the β cells of the pancreas in the form of two-zinc hexamers. In the blood stream however, insulin circulates as a monomer, which is the physiologically active species binding to the insulin receptors. In solutions of zinc free insulin there exist equilibrium species of other association states with a distribution governed by ionic strength, pH and insulin concentration.

Static and dynamic light scattering[1] has been used to investigate the influence of these factors on the self association of zinc free insulin. The concentration of sodium chloride was varied between 10 and 100 mM and the pH between 7.5 and 10.5. The measured homodyne autocorrelation function was used to asses the mean hydrodynamic diameter as well as the weight averaged molar weight of the insulin species in solution. The average molar weight as a function of ionic strength and pH has been interpreted in terms of a simple thermodynamic model with only four fitting parameters. The model describes the self association as a result of two terms in Gibbs free energy: One attractive term that is independent of all other parameters and one repulsive term due to electrostatic interaction. The latter is assumed to be determined by the pH dependent degree of ionisation of the insulin residues and the ionic strength dependent screening effect of the sodium ions. Figure 1 shows the measured apparent molar weights as a function of the effective charge (ionisation charge reduced by screening) of the insulin monomer together with the fitted molar weights. Figure 2 shows the molar concentration of the various oligomers (1 to 10 monomeric units) as a function of the effective charge.

The good agreement between observations and model fit suggests that it should be possible to predict aggregational properties of various insulin mutants.

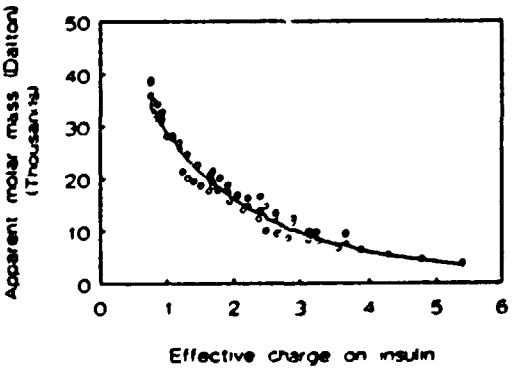

Figure 1

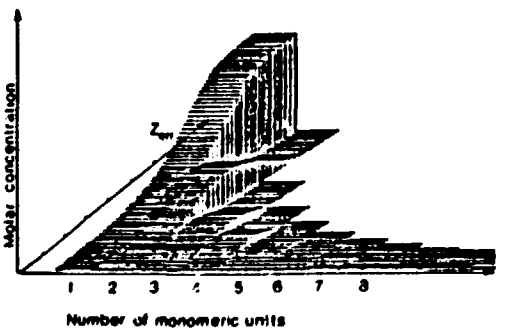

Figure 2

[1]Victor Bloomfield, Dynamic Light Scattering (R. Pecora ed.), 1985, Plenum Press N.Y.

DP21

Modeling of the Charge Separation in the Photoactive Molecular Devices

A. Tamulis[1)] and L. Bazhan[2)]

[1)]Institute of Theoretical Physics and Astronomy, Goštauto 12, Vilnius, 2600, The Republic of Lithuania, [E-mail: itpa.ma@ma-mii.lt.su]

[2)]Polytechnic Institute of Nizhnii Novgorod, Nizhnii Novgorod, Russia

We have used the quantum chemical MNDO method for the investigations of the electronic structure of the carbazole (Cz) - photodonor, insulator, photoacceptor molecules, as well as for investigations of the designed photoactive charge transfer supermolecules and supramolecules - molecular photodiodes[1-3]. The modeling of the photoinduced charge separation in the Cz, and in the photoacceptor molecules: 2,4,7-trinitro-9-fluorenone,2,4,5,7-tetranitro-9-fluorenone, 7,7,8,8/tetracyanoquinodimethane, 2,4,7-trinbitro-9-dicianofluorene, 2,4,5,7-tetranitro-9-dicianok fluorene, 1,2,4,5-tetracyanobenzene, 2,3 dichloro-5,6-dicyanobenzoquinone, tetra-fluoro-7,7,8,8/tetracyanoquinodimethane was done. The localization of the additional electrone hole in the Cz and additional electron in the acceptor molecules has been found. We offer to use these local charge distribution regions in the construction of the radiation solar energy cells as well as in the basic elements of the molecular computers.

1. A. Tamulis, S. Janušonis, L. Bažan, Macromol. Chem. Macromol. Symp., v. 46, 181-185 (1991).

2. A. Tamulis, L. Bažan, "Charge Photogeneration in Carbazole Containing Compounds and Valency Bands of Oligomers", Proceedings of the 29 Europhysics Conference on Macromolecular Physics "Physics of Polymer Networks", Alexisbad, Germany, 9 to 14 September 1991 (in press).

3. A. Tamulis, L. Bažan, "Electronic Structure of the Supermolecules and Supramolecules Constructed from Carbazole and Acceptor Molecules", Proceedings of the "5 International Conference on Photoactive Solids. Symposium on Molecular Systems", Okazaki, Japan, 13 to 17 October, 1991. To be published in journal "Molecular Crystals and Liquid Crystals".

List of Exhibitors

The following companies presented an exhibition at the meeeting

Aage Christensen A/S
Skelmosevej 10
Postbox 399
2500 Valby, Denmark

Bodenseewerk Perkin-Elmer GmbH
Physical Electronics
Bruckmannring 40
D-8042 Oberschl·issheim, Germany

Caburn - MDC Ltd.
The Old Dairy, The Street, Glynde,
East Sussex, BN86SJ, England

Cryophysics LtD
Unit 4, Avenue Two
Station Lane Ind Est
Witney OXON
OX8 SYD Denmark

Convex Computer
Struergade 22
2630 Tåstrup, Denmark

DME - Danish Micro Engineering A/S
Transformervej 12
2730 Herlev, Denmark

Elsevier Science
Publishers
P.O. Box 103
1000 AC Amsterdam, The
Netherlands

Fison Instrum. Nordic AB
Box 1211
S-17123, Sweden

Leybold Aps
Roskildevej 342 A
2820 Gentofte, Denmark

Nordiska Balzers AB
Box 10412
S-434 24 Kungsbacka, Sweden

Oxford Instruments
Scientific Research Division
Old Station Way, Eynsham Witney,
Oxon, OX8 1TL, England

List of Participants
(according to country and institution)

DENMARK

CISMI
University of Copenhagen
Blegdamsvej 21
2100 Copenhagen Ø, Denmark

Bechgaard, Klaus
Bjørnholm, Thomas
Larsen, Niels Bent

DANISH INSTITUTE OF FUNDAMENTAL METROLOGY
Lundtoftevej 100
2800 Lyngby, Denmark

Carneiro, Kim
Geisler, Tommy
Lundsberg-Nielsen, Line
Madsen, Lars

HALDOR TOPSØE A/S
Nymøllevej 55
2800 Lyngby, Denmark

Alstrup, Ib
Clausen, Bjerne S.
Larsen, Jørgen Gutzon
Törnqvist, Eric

H.C. ØRSTED INSTITUTTET
University of Copenhagen
Universitetsparken 5
2100 Copenhagen Ø, Denmark

Binau, Karina
Ge, Qingfeng
Hedegård, Per
Mackintosh A.R.
Mikkelsen, Kurt V.
Møller, Preben Juul
Neergaard, Hanne
Nielsen, Mads
Padilla, Paz
Peters, Günther
Schmidt, Bjarne
Smith, Anders
Toxværd, Søren
Veje, Erling
Velasco, Enrique
Wang, Lichang
Yu, Liangdeng
Younas, Irfan

NIELS BOHR INSTITUTET
Blegdamsvej 17
2100 Copenhagen Ø, Denmark

Bjørnholm, S.
Bohr, Thomas
Borggreen, Jørn
Flyvbjerg, Henrik
Jensen, Henrik Jeldtoft
Nielsen, Mek Buhl

NIELS BOHR INSTITUTET
Tandem Accelerator Laboratoriet
Risø, DK-4000 Roskilde

Rasmussen, Henrik

NKT RESEARCH CENTER
Sognevej 11
2605 Brøndby, Denmark

Li, Qi
Shen, Yueqiang
Freltoft, Torsten
Hansen, Jørn Bindslev
Hjuler, Hans Aage
Vase, Per

NORDITA
Blegdamsvej 17
2100 Copenhagen Ø, Denmark

Hertz, John
Schwarze, Holm
Wulff, Niels Holger

NOVO NORDISK A/S
Biostructure
Novo Allé
2800 Bagsværd, Denmark

Olsen, Ole Hvilsted

RISØ NATIONAL LABORATORY
Department of Solid State Physics
4000 Roskilde, Denmark

Als-Nielsen, J.
Andersen, Niels Hessel
Bohr, Jakob
Falcao, Antonio
Feidenhans'l, Robert
Fiig, Thomas
Findeisen, Eberhard
Foss, Morten
Harris, Pernille
Kjær, Kristian
Kromann, Rasmus
Lebech, Bente
Lefmann, Kim
Lindgård, Per-Anker
Mason, Thomas
Mortensen, Kell
Nielsen, Mourits
Pedersen, Jan Skov
Pengra, David
Reus, Roger de
Schou, Jørgen
Thoft, Nina Bjørn
Vives, Eduard

ROSKILDE UNIVERSITY CENTER
IMFUFA, RUC
P.O. Box 260
4000 Roskilde, Denmark

Dyre, Jeppe
Posselt, Dorthe

ROYAL SCHOOL OF PHARMACY
Universitetsparken 2
2100 Copenhagen Ø, Denmark

Bjørnholm, Berith

ROYAL VETERINARY AND
AGRICULTURAL UNIVERSITY
Thorvaldsensvej 40
1871 Frederiksberg C, Denmark

Bauer, Rogert
Danielsen, Eva
Hansen, Steen Laugesen
Ogendal, Lars

THE TECHNICAL UNIVERSITY OF
DENMARK
2800 Lyngby, Denmark

Chetty, N.
Chorkendorff, Ib
Dahl, Jens Peder
Dam, Niels-Ebbe
Engell, John
Hammer, Bjørk
Hansen, Lars Bruno
Hendriksen, Peter Vang
Holm, Jesper
Hønger, Thomas E.R.
Ipsen, John Hjort
Jacobsen, Karsten W.
Jacobsen, Claus Schelde
Kühle, Anders
Linderoth, Søren
Mouritsen, Ole G.
Mørup, Steen
Oxborrow, Carol Anne
Pedersen, Niels Falsig
Rasmussen, Peter Bilde
Sperotto, Maria M.
Stoltze, Per
Sørensen, Steen Aagaard
Sørensen, Mads Peter
Taylor, Patrick A.
Wang, Xiandong

UNI.C
The Technical University of Denmark
2800 Lyngby, Denmark

Moth, Jørgen

UNIVERSITY OF AALBORG
Pontoppidanstræde 103
9220 Alborg Ø, Denmark

Bozhevolnyi, Sergey
Jakobsen, Christian
Keller, Ole
Liu, Ansheng
Pedersen, Kjeld
Sølberg, Carl-Erik
Xiao, Mufei

UNIVERSITY OF AARHUS
8000 Århus C, Denmark

Adams, David L.
Besenbacher, Flemming
Burchhardt, Jeppe
Christensen, N.E.
Fogedby, Hans
Gorczyca, Iza
Jørgensen, Jens-Erik
Klink, Casper
Lauritsen, Kent Bækgaard
Nielsen, Troels Brander
Nielsen, Lars Pleths
Nielsen, Martin Meedom
Peltzer, E. L.
Ruan, Like
Stensgaard, Ivan
Svane, Axel

UNIVERSITY OF ODENSE
Campusvej 55
5230 Odense M, Denmark

Bjørn, Jacob
Ellegaard, Ole
Jansson, Christian
Morgen, Per
Onsgaard, Jens
Scharfschwerdt, Christoph
Sigmund, Peter
Storm, Jesper
Tougaard, Sven
Yubero, Francisco

Petersen, Steen
Griffenfelds Gade 39 B
2200 København N, Denmark

FINLAND

HELSINKI UNIVERSITY OF TECHNOLOGY
Otakaari 1 M
02150 Espoo, Finland

Alatalo, Matti
Boehm, Juhani von
Kaukonen, Harri-Pekka
Mölsä, Heini
Nieminen, Risto
Virkkunen, Riikka

HELSINKI UNIVERSITY
Research Institute for
Theoretical Physics Siltavuorenpenger
20C
SF-00170 Helsinki, Finland

Ala-Nissila Tapio

PAPER SCIENCE CENTRE
KCL, Box 70
SF-02151 ESPOO, Finland

Niskanen, Kaarlo

TAMPERE UNIVERSITY OF TECHNOLOGY
P.O. Box 692,
33101 Tampere, Finland

Kankaala, Kari
Eriksson, Jarl-Thure
Karttunen, Mikko
Kaski, Kimmo
Lindroos, Matti Juhani
Lukkarinen, Ari
Mikkonen, Risto
Nieminen, Jouko Aulis
Paasi, Jaakko
Sarkaniemi, Jyrki

UNIVERSITY OF JYVÄSKYLÄ
P.O. Box 35
SF-40351 Jyväskylä, Finland

Häkkinen, Hannu
Timonen, Jussi

UNIVERSITY OF OULU
Linnanmaa
SF-90570 Oulu, Finland

Apaja, Vesa
Kallio, Alpo J.
Kusmartsev, Feodor
Xiong, Ziaoming

UNIVERSITY OF TURKU
Wihuri Physical Laboratory
University of Turku
20500 Turku, Finland

Lähderanta, Erkki
Mäkinen, Ari

VTT, TECHN. RES. CENTER OF FINLAND
Tietotie 2, P.O. Box 202
SF-02151 Espoo, Finland

Teleman Olle

NORWAY

INSTITUTT FOR ENERGITEKNIKK
Postboks 40
N-2007 Kjeller, Norway

Riste, Tormod
Steinsvoll, Olav

SIT, TELEMARK
Sivilingeniørutdanningen i Telemark
Kjølnes
N-3900 Porsgrunn, Norway

Førrisdahl, Ole Kr.
Holta, Randi Toreskaas

UNIVERSITY OF OSLO
P.O. Box 1048
Blindern
0316 Oslo 3, Norway

Taftø, Johan

UNIVERSITY OF TRONDHEIM
N-7034 Trondheim, Norway

Berg, Cecilie
Bergene, Edvard
Borg, Anne
Fossheim, Kristian
Gong, Zhenghong
Grepstad, Jostein
Hafskjold, Bjørn
Hunderi, Ola
Li, Xiaoyun
Raaen, Steinar
Suzuki, Takashu
Tuset, Pål
Tuset,, Ellen Dahler
Vassenden, Frode

SWEDEN

CHALMERS UNIVERSITY OF TECHNOLOGY
S-412 96 Göteborg, Sweden

Beiastegui, Pedro
Brånander, Jan-Olov
Börjesson, Lars
Engdahl, Christen
Hamawi, Aref
Hansson, Tony
Boldhuis, P.G.
Harada, Yuichi
Holmlund, Kenneth
Ivanov, Zdravko G.
Johansson, Lars Gunnar
Käll, Mikael
Li, Yinggang
Lundqvist, Bengt
Nilsson, Per-Olof
Nyberg, Per-OlofAnna
Persson, Mats
Ramos, Jaime
Rashkeev, Sergey
Setterlind, Carl Johan
Starnberg, Hans
Ström, Carin
Tzalenchuk, Alexander Ya.
Wendin, Göran
Wenger, Fabian
Yxklinten, Uno

KTH-ELECTRUM
Box 1298
S-164 28 Kista, Sweden

Hudner, Jan

LULEÅ UNIVERSITY OF TECHNOLOGY
S-951 87 Luleå, Sweden

Weber, Hans

MANNE SIEGBAHN INSTITUTE OF PHYSICS
Frescativägen 24
S-10405, Sweden

Rubel, Marek

NUTEK
S-11786 Stockholm, Sweden

Agrell, Ingela

STOCKHOLM UNIVERSITY
Arrhenius Laboratory
S-106 91 Stockholm, Sweden

Bryntse, Ingrid
Laaksonen, Aatto
Odelius, Michael

THE ROYAL INSTITUTE OF TECHNOLOGY
S-10044 Stockholm, Sweden

Andersson, Magnus
Brazdeikis, Audrius
Costa, J.L.
Dzugutov, Mikhail
Gothelid, Mats
Grishin, A.M.
Hedman, Fredrik
Helsing, Johan
Holm, William
Koga, Takaaki
Korenivski, V.
Lundqvist, Pieter
Moon, Byung M.
Muhammed, Mamoun
Nogues, Josep
Nordström, Anders
Norin, Martin
Rao, K.V.
Rapp, Öster
Terryl, Kathleen
Wang, Lingna
Xu, Junhao
Zakharchenko, Igor
Zhou, Y.L.

UMEÅ UNIVERSITY
S-901 87 Umeå, Sweden

Andersson, Britt
Fedchenia, Igor
Houlrik, Jens M.
Minnhagen, Petter
Nylén, Mats
Olsson, Peter
Pettersson, Sune
Sundqvist, Bertil
Westman, Olof
Xu, Lifang
Zdunek, Janusz

UNIVERSITY OF FALUN
Materials centre
University College of Falun/Borlänge
Box 764
S-781 27 Borlänge, Sweden

Bernhard, Jonte
Ruokolainen, Anna

UNIVERSITY OF KARLSTAD
Box 9501
S-650 09 Karlstad, Sweden

Magnussen, Kjell

UNIVERSITY OF LINKÖPING
58183 Linköping, Sweden

Håkansson, Lennart
Johansson, Hans
Johansson, Leif
Münger, E. Peter
Mårtensson, Per
Norberg, Petronella
Owman, Fredrik
Severin, Mattias

UNIVERSITY OF LUND
S-223 62 Lund, Sweden

Andersen, Jesper N.
Håkansson, Cecilia
Johansson, Lars
Jönsson, B.
Linse, Per
Lundgren, Edvin
Nyholm, Ralf
Qvarford, Mats
Sjöström, Lena
Ullner, Magnus
Wallenberg, L.R.
Wallqvist, Anders

UPPSALA UNIVERSITY
S-75121 Uppsala, Sweden

Aldén, Magnus
Andersson, Jan-Olov
Bennich, Peter
Brühwiler, Paul
Hernnäs, Bo
Magnusson, Johan
Marelius, Anders,
Mårtensson, Nils
Nilsson,, Anders
Ohno, Masahide
Siegbahn, Hans
Zdansky, Erik O.F.

BALTIC COUNTRIES

Heinmaa, Ivo
Institute of Chemical Physics and Biophysics
Rävala pst. 10
Tallinn EE0001, Estonia

Feldbach, Eduard
Institute of Physics
142 Riia Str.
202400 Tartu Estonia

Klavins, Janis
Institute of Solid State Physics
University of Latvia
8 Kengarage St.
226063 Riga, Latvia

Silin, Andrejs R.
Institute of Solid State Physics
University of Latvia
8 Kengaraga St.,
226063 Riga, Latvia

Tamulis, Arvydas
DIDLAUKIO,
27-40 Vilnius 2057,Lithuania

SEMICONDUCTOR PHYSICS INSTITUTE
Gastauto 11
2600 Vilnius, Lithuania

Dagys, R.
Tornau, Evaldas
Vengalis, B.

BELGIUM

Tendeloo, Gustaaf Van
RUCA
Groenenborgerlaan 171
B-2020 Antwerp, Belgium

CANADA

McGILL UNIVERSITY
Dept. of Physics
3600 University st
Montreal, QVE, Canada H3A 2T8

Grant, M.
Zhang, Z.
Zuckermann, M.

ENGLAND

Slaski, Marcin
Supercond. Res. Group
University of Birmingham
ED6 Baston B15 2TT, England

Tildesley, Dominic
Department of Chemistry
Univ. of Southampton
Highfield
Southampton SO9 5NH, England

FRANCE

Andersen, Jørgen Vitting
LTPCM. INPG, ENSEEG,
Grenoble, B.P. 75
F-38402 Saint-Martin-d'Heres
CEDEX, France

Leibler, S.
Ser. Phys. Theor.
91191 Gif-sur-Yvette, France

Villain, J.
85x, 38041 Grenoble Cedex, France

GERMANY

Behm, R.J.
Institut für Kristallographi und
Mineralogie
Universität München
Theresienstr. 41
D-8000 München 2, Germany

Brandt, Ernst Helmut
Teckstr. 10
W-7252 Weil der Stadt, Germany

Eriksson, Sten
MPI, Abt. Simon
Heisenbergstr. 1
7000 Stuttgart 80 , Germany

Haase, Jochen
Fritz-Haber-Institut der MPG
Faradayweg 4-6
1000 Berlin 33, Germany

Lengeling, Gregor
Aixtron GMbH
Kackerstraß2 15-17
D-5100 Aachen, Germany

Manzke, Recardo
Institut für Experimentalphysik der
Universität Kiel
Olshausenstr. 40
2300 Kiel 1, Germany

Poulsen, Henning Friis
HASYLAB zm. 232
DESY, Notkestr. 85
D-2000 Hamburg 52, Germany

Reif, Jürgen
Inst. f. Experimentalphysik
FU Berlin
Arnimallee 14
W-1000 Berlin 33, Germany

Schmitz, Vera
Forschungszentrum Jülich
Postfach 1913
D-5170 Jülich

UNIVERSITY OF OSNABRÜCK
Fachbereich Physik
D-4500 Osnabrück, Germany

Heiland, W.
Neumann, Manfred
Speller, Silvia
Uhlenbroch, Stephan

GREECE

Nicolaides, George
NCSR, "Demokritos"
Agleia Parasrevi, Greece

POLAND

UNIVERSITY OF WROCLAW
Institute of Experimental Physics
ul. Cybulskiogo 36
50-205 Wroclaw, Poland

Mróz, Stefan
Jurczyszyn, Leszek

SWITZERLAND

Cornell, Stephen
Department de Physique Theorique
Universite de Geneve
24 Quai Ernest Ansermet
CH 1211 Geneve 4, Switzerland

Fischer, Ø. H.,
32 Blv. d'Yvoy
CH-131 Geneve, Switzerland

Flükiger René
Dept. Phys. Mat. Cond. Universite de Geneve
24 Quai Ernest Ansermet
CH 1211 Geneve 4, Switzerland

Gunsteren, W.F. van
ETH, Physical Chemistry
CH-8092 Zürich, Switzerland

THE NETHERLANDS

UNIVERSITY OF TWENTE
Faculty of Applied Physics
P.O. Box 217
7500 AE Enschede, The Netherlands

Flokstra, Jaap
Hilgenkamp, J.W.M.

USA

Banavar, J.R.
Penn. State University
Dept. of Physics
104 Dovey Lab., University Park
PA 16802, USA

Christensen, Kim
Department of Physics
Brookhaven National Laboratory,
Upton
New York 11973, USA

Einstein, T.
University of Maryland
Department of Physics
College park
Maryland 20742-4111, USA

Haight, Richard
IBM
T.J. Watson Research Center
P.O. Box 218
Yorktown Heights
New York 10598, USA

Jorgensen, James
Materials Science Division
Argonne National Laboratory
Building 223
Argonne, IL 60439, USA

Kaiser, William J.
Jet Propulsion Lab.
California Inst. of Technology
MS 302-231
4800 Oak Grove Drive, Passadena
California 91109, USA

Kresin, V.Z.
University of California
Berkeley
Washington D.C., USA

Rikvold, P.A.
Supercomp. Comp. Res. Inst.
Fl. St. University
B-186 Tallahassee
FL-32306-4052, USA

Rettner, Charles T.
IBM Almaden Res. Center
K133/801
650 Harry Road
San Jose
CA 95120-6099, USA

Yates, Jr. John T.
Surface Science Center
Department of Chemistry
University of Pittsburgh
Pa 15260 USA

AT&T BELL LABORATORIES
600 Mountain Ave.,
Murray Hill, NJ 07974, USA

Fleming, Robert M.
Varma, C.M.

USSR

Kharlanov Andrey
Moscow State University
Leninslue Gory
119899 Moscow, USSR

Strocov, Vladimir N.
Int. Inst. of Interphase Interactions
P.O. Box 1146
S. Petersburg 19491, USSR

Markel, Vadim A.
Inst. of Automation and Electrometry
Universitetski Pr. 1
630090 Novosibirsk, USSR

List of Contributors

Code:
(Session), (Inv./Contr./Poster),(week day),(number)

ACKNOWLEDGEMENT

It is a pleasure to acknowledge the help in producing these proceedings. Foremost, a thank to the contributors for submitting interesting and nice extended abstracts closely abiding to the desired format, to Lone Astradsson and Lajla Frederiksen, Margit Kloster, Charlotte Korgaard and Ca Studinski for secretarial assistance and finally Risø REPRO and Risø Library for very efficient printing and handling of this booklet.

Bibliographic Data Sheet Risø-R-628(EN)

Title and author(s)

Proceedings of the Joint Nordic Spring Meeting '92

edited by P.-A. Lindgård

ISBN	ISSN
87-550-1810-6	0106-2840

Dept. or group	Date
Physics Department	May 1992

Groups own reg. number(s)	Project/contract No.

Pages	Tables	Illustrations	References
346	4	187	931

Abstract (Max. 2000 char.)

Proceedings in the form of extended abstracts of the Joint Nordic Spring Meeting '92 including the 3rd Nordic Conference on Surface Science, the Nordic Symposium on Computer Simulation, and 3rd Nordic Symposium on Superconductivity. In addition there are contributions from workshops on the Physics of Small Clusters, on Soft Condensed Matter Physics and from an Electronic Properties Workshop. The proceedings contain over 300 contributions on the mentioned subjects. Further, there are several contributions on general solid state subjects, magnetism, semiconductors etc.

Descriptors INIS/EDB

Available on request from:
Risø Library, Risø National Laboratory (Risø Bibliotek, Forskningscenter Risø)
P.O. Box 49, DK-4000 Roskilde, Denmark
Phone (+45) 42 37 12 12, ext. 2268/2269 · Telex 43 116 · Telefax (+45) 46 75 56 27